

ISSN 1927-0488 (Print)
ISSN 1927-0496 (Online)

Environment and Natural Resources Research

Vol. 6, No. 2 June 2016



CANADIAN CENTER OF SCIENCE AND EDUCATION

Editorial Board

Editor-in-Chief

John James Milledge, University of Greenwich, United Kingdom

Associate Editors

Hary Razafindralambo, University of Liege, Belgium

Rakesh Ghosh, University of California, United States

Sara E. Wagner, University of Georgia, United States

Wei Wang, Vanderbilt University, United States

Editorial Assistant

Joan Lee, Canadian Center of Science and Education, Canada

Editorial Board Members

Abdelazim M. Negm, Egypt

Abdelmageed M. Othman, Egypt

Ademir de Oliveira Ferreira, Brazil

Aggeliki Barberopoulou, New Zealand

Ahmed Shams, UK

Ajay Sharma, USA

Akhilesh Tiwari, India

Alan H. McGowan, United States

Amin Mohebbi, USA

Amin Rasekh, United States

Andrew Lo, Taiwan

Anuluxshy Balasubramaniam, Sri Lanka

Barbara Sladonja, Croatia

Beatrice Hernout, USA

Benkun Qi, China

Bing Ma, United States

Céline Vaneekhaute, Belgium

Chaoxu Wang, China

Charbel Afif, Lebanon

Chenlin Hu, China

David Tsetse, United States

Dilek Bakircioglu, Turkey

Dogus Meric, United States

Duminda Jayaranjan, Thailand & Sri Lanka

Eduardo Saldanha Vogelmann, Brazil

Fahim Hossain, Saudi Arabia

Francis C Bergeron, Switzerland

G. Asadollahfardi, Iran and Canada

Gilbert Ahamer, Austria

Giovanni Ortosecco, Italy

Giuseppe Andrea de Lucia, Italy

Gustavo Mockaitis, Brazil

Harro Stolpe, Germany

Hartmut Meyer, Germany

Hedia Chakroun, Tunisia

Hesham Gehad Ibrahim, Libya

Himayatullah Khan, Pakistan

Huapeng Chen, Canada

Hui Li, USA

Humphrey Zebulun, United States

Ismaila Vela Haruna, Nigeria

Jan David, Czech Republic

João Fernandes, Portugal

João Fernandes, Portugal

Jord J. Warmink, Netherlands

Juan José Villaverde, Spain

Julie M. Kezik, United States

Karam Farrag, Egypt

Koushik Dutta, India

Lei Wu, USA

Liang Yang, Germany

Lin Chen, Japan

Luis Alfonso Sarabia, Chile

Mani Sanjeeva Gandhi, India

Marcus Vinícius Estigoni, Brazil

Mariya V. Konyushkova, Russian Federation

Maurizio Manera, Italy

Mohamed M Gomaa, USA

Mohamed Samer, Egypt

Mohammad Arab Amiri, Iran

Mohammad Valipour, Iran

Mukesh Kumar Sharma, India

Murat Eyvaz, Turkey

Naohiro Matsui, Japan

Nasroallah Moradi Kor, Iran

Nguyen Duc Luong, Vietnam

Nuray Balkis, Turkey

Omoniyi K.I., Nigeria

ÖNER DEMİREL, Turkey

Ovidiu Dima, Romania

Paola Ovando Pol, Spain

Patrícia Gomes Costa, Brazil

Patrik Grahn, Sweden

Prakash Mallappa Munnoli, India

R.K. Singh, India

Raimundo Jimenez Ballesta, Spain

Rakesh Ghosh, USA

Rasoul Yousefpour, Denmark

Renata Valente, Italy

Riccardo Guarino, Italy

Roger Cranswick, Australia

Sachinder Mohan Sharma, India

Shahab Araghinejad, Iran

Shiro Horiuchi, Japan

Silvano Bertoldo, Italy

Srđan Kostić, Serbia

Sunitha N. Seenappa, India

Tamara Zelenovic Vasiljevic, Serbia and Montenegro

Teodorico Alves Sobrinho, Brazil

Tiago Miguel Ferreira, Portugal

Valentina Ferretti, Italy

Victor Sluchyuk, Ukraine

Vinay Kumar, USA

Worku Legesse Mulat, United States

Xiaobo Gu, United States

Xiaobo Liu, China

Xiaokai Chen, China

Xingang Chi, United States

Xiong Xiong, USA

Xuan Li, United States

Yu Wang, United States

Yuan Tian, United States

Zhanbei Liang, United States

Contents

Community Participation in Decentralized Management of Natural Resources in the Southern Region of Mali <i>Clarisse Umutoni, Augustine Ayantunde, Matthew Turner & Germain J. Sawadogo</i>	1
Spatial Variability Modeling of Soil Erodibility Index in Relation to Some Soil Properties at Field Scale <i>C. Gyamfi, J. M. Ndambuki & R.W. Salim</i>	16
Assessment of a Regional-Scale Weather Model for Hydrological Applications in South Korea <i>Yong Jung & Yuh-Lang Lin</i>	28
A Historical Perspective of the Maasai - African Wild Dog Conflict in the Serengeti Ecosystem <i>Richard D Lyamuya, Emmanuel H Masenga, Robert D Fyumagwa, Machoke N Mwita, Craig R Jackson & Eivin Røskaft</i>	42
Study on Changes of Textural and Biochemical Properties of Tuna during Ultra-Low Temperature Storage <i>Yu-ying PAN, Xiao-hua QIU & Jin-sheng YANG</i>	51
COD Removal of Edible Oil Content in Wastewater by Advanced Oxidation Process <i>Aola Hussein Flamarz Tahir, Nagham Obeid Kareim & Shatha Abduljabbar Ibrahim</i>	57
A Simultaneous Model for Simulating the Propagation of Hydraulic Head in Aquifers with Leakage Pathways <i>Seong Jun Lee</i>	65
Orographic Effects on Supercell: Development and Structure, Intensity and Tracking <i>Galen M Smith, Yuh-Lang Lin & Yevgenii Rastigejev</i>	76
Preparation and Antimicrobial Evaluation of Neem Oil Alkyd Resin and Its Application as Binder in Oil-Based Paint <i>Haruna Musa & Sharif N. Usman</i>	92
Water Quality Assessment of <i>Aflaj</i> in the Mountains of Oman <i>Mohammed Saif Al-Kalbani, Martin F. Price, Mushtaque Ahmed, Asma Abahussain & Timothy O'Higgins</i>	99
Flood Risk Assessment of Residential Neighbourhoods in Calabar Metropolis, Cross River State, Nigeria <i>Benedict E. Ojikpong, Bassey E. Ekeng, Ukpali E. Obongha & Samuel I. Emri</i>	115
Valuing Urban Tropical River Recreation Attributes Using Choice Experiments <i>Luis Santiago, John Loomis, Alisa V. Ortiz & Ariam L. Torres</i>	128
Modeling the Geographic Distribution of <i>Prosopis africana</i> (G. and Perr.) Taub. in Niger <i>Laouali Abdou, Abdoulaye Diouf, Maman Maârouhi Inoussa, Boubacar Moussa Mamoudou, Salamataou Abdourahamane Illiassou & Ali Mahamane</i>	136
Evaluating the Competing Claims on the Role of Ownership Regime Models on International Drinking Water Coverage <i>Chadd Stutsman, Kelly Tzoumis & Susan Bennett</i>	145
Reviewer Acknowledgements for Environment and Natural Resources Research, Vol. 6, No. 2 <i>Joan Lee</i>	156

Community Participation in Decentralized Management of Natural Resources in the Southern Region of Mali

Clarisse Umutoni¹, Augustine Ayantunde², Matthew Turner³ & Germain J. Sawadogo⁴

¹International Livestock Research Institute (ILRI), c/o ICRISAT, Bamako, Mali

²International Livestock Research Institute (ILRI), c/o CIFOR, Ouagadougou, Burkina Faso

³Department of Geography, University of Wisconsin, 160 Science Hall, 550Noth Park Street, Madison, USA

⁴Department of Biological Science and Animal Production, Cheikh Anta Diop University, Dakar, Senegal

Correspondence: Clarisse Umutoni, International Livestock Research Institute (ILRI), c/o ICRISAT, B.P. 320 Bamako, Mali. Tel: 223-2070-9200. E-mail: c.umutoni@cgiar.org

Received: February 2, 2016 Accepted: February 15, 2016 Online Published: March 10, 2016

doi:10.5539/enrr.v6n2p1

URL: <http://dx.doi.org/10.5539/enrr.v6n2p1>

Abstract

Decentralized governance of natural resources is considered one of the key strategies for promoting sustainable management of natural resources at local level. Effective decentralized natural resource management requires strong local natural resource institutions. Therefore, strengthening local institutions governing the management of natural resources is one of the core principles of decentralization reforms in Francophone West Africa countries. This study assessed the existing local institutions (rules, norms and or local conventions) governing the management of natural resources and forms of community participation in the development of these natural resource institutions. Our findings showed significant variation within the study sites regarding the level of knowledge of existing local rules and norms governing the management of natural resources by the respondents. Results showed that the level of knowledge of local conventions was significantly ($P < 0.05$) higher in the district of Bougouni than in the district of Koutiala (a score of 3.16 compared to 1.70 on a scale of 0 to 4). This study shows also that participation was dominated by a small group of individuals, often community leaders and elites. The results suggest that women are marginalized. Presently, the big challenge that faces the institutions governing natural resource use in the study area is the system of representativeness in the community in the development of local rules and norms as community leaders and household heads often dominate, which does not encourage active participation of community members. Therefore, for effective implementation of local natural resource institutions, the interest of key natural resource users should be taken into account. It is also important to promote rules and norms that attempt to protect or strengthen women's access to natural resources in the community.

Keywords: decentralization, land use plan, local institutions, Mali, Sudano-Sahelian zone

1. Introduction

In West Africa, as in most of sub-Saharan Africa, natural resources (land, grazing/ rangelands, water, forest) form the basis for livelihoods of rural poor as they depend almost exclusively on agriculture and livestock production (Benjamin, 2004). Many factors, such as the rapid increase in human population, declines in cropland fertility and increase in livestock populations have resulted in growing pressure on the natural resources in the region (Hilhorst, 2008). Given these changing pressures on resource management, these natural resources are facing problem of over-exploitation and degradation, and consequently decline in their quality and productivity (Ribot, Agrawal, & Larson, 2006). Therefore, responsive resource management institutions are much needed. In this sense, decentralization is now put at the center of a good management of natural resources.

In the context of decentralization, local authorities are key actors in the management of natural resources as the state delegates management of community resources to local authorities. Community-based management of natural resources has been advocated by many technical and development practitioners in West Africa (Benjamin, 2008; Ribot, 2002; Gibson, McKean, & Ostrom, 2000) as indispensable for sustainable natural resource management (NRM). According to Benjamin (2008), decentralized management is the key to achieving a more equitable and sustainable natural resource management. Moreover, the same author observed that

decentralized natural resource management in West African Sahel is often characterized by legal pluralism, that is, the coexistence and interaction of several normative orders with different sources of legitimacy and authority. Benjamin (2008), and Agrawal and Ribot (1999) also remarked that the traditional and customary structures are often ignored in the delegation of power over natural resources to local districts and prefecture by the state though the effects of the degradation of natural resources are most apparent at village level. To this end, in recent years, there has been emphasis in the literatures on the local participation in natural resource management in Africa (Kellert, Metha, Ebbin, & Lichtenfeld, 2000; Barrett, Brandon, Gibson, & Gjertsen, 2001; Ribot, 2002). Several of these authors have shown that community participation is an essential component of efforts to bring about positive economic and environmental change in African communities. Strengthening local institutions in the management of their natural resources is therefore essential to maintain a healthy natural resource base for sustainable intensification of crop and livestock production systems.

In this context and to reduce the increasing pressure on natural resources and the associated degradation of ecosystems, in southern region of Mali, some local authorities and village communities have taken initiatives to develop and formalize rules governing the management of natural resources such as local conventions with the support and advice of the national administrative and technical services, and financial partners (Djiré, 2003). However, the ambiguous legal status of local conventions has slowed down the effective implementation of decentralized natural resource management (Benjamin, 2008).

Although significant work has been conducted on natural resource institutions and decentralized natural resource management in Mali, and generally in West African Sahel, for example Ribot's work (Ribot, 2004) on the accountability of local customary authority to community members, participation of community members in the development of these local rules has not been addressed adequately despite the importance of community members as custodians and users of the natural resources. Given that the local populations are directly affected by the implementation of decentralization reform, there is need for adequate representation of the community members in the decentralized natural resource management. Therefore, we included community members in this study in order to know and assess their understanding of the existing natural resources institutions and their level of participation in the elaboration and implementation processes. Then, this study is based on the following strands of argument: A strong representation of the community members is essential for strong local institutions. For these institutions (rules, norms, governing bodies) to be effective, the following basic features are required: (1) Community members who are using the resources are aware of these institutions; and (2) Community members view these institutions as legitimate which is often tied to the community members' level of involvement in their formation. The purpose of this study was to document and analyze the existing natural resource institutions in mixed crop-livestock systems of southern Mali and to examine the factors that influence the level of participation of farmers in elaborations of natural resource institutions.

In addressing the above objective, we looked at the following research questions: What are the type and characteristics of existing natural resource institutions in the study sites? To what extent are community members aware of these institutions? Are community members adequately engaged in the development of these local natural resource institutions, including women? Addressing these questions will help to identify innovative options that will facilitate better participation of community members in the development and enforcement of the local natural resource institutions and consequently, proper use and management of natural resources in Sudano-Sahelian zone of West Africa.

2. Theories and Trends in Decentralized Natural Resource Management (Note 1)

Since the early 1990s, many West African countries have introduced political, economic, and institutional reforms, one of the most important of which is decentralization reform (Manor, 1999; UNCDF, 2000). Through decentralization reform, the government transfers some decision making power and responsibilities to sub-national institution at the provincial, district, city, town and village levels with the objective of promoting public participation in local governance (Crook & Manor, 1998). Basically, the key thrust of decentralization is rooted in democratic principles of representation and accountability that allow constituencies to effectively express their needs and preferences to local government officials and to hold these officials accountable. This accountability was distinguished as downward and upward accountability by Agrawal and Ribot (1999). These authors refer to downward accountability as situations where local bodies can be held to account by the populace through positive or negative sanctions (this is often referred to as true decentralization) while they refer to upward accountability as the case where power is transferred to low level actors who are accountable to their superiors in an hierarchy (this is referred to as deconcentration).

Given the important role that natural resources play in the livelihoods of local population, particular attention has been given to the decentralization of natural resource management. According to Agrawal and Ostrom (2001), decentralized governance of natural resources is considered one of the key strategies for promoting sustainable management of natural resources at local level. The rationale behind decentralization of natural resources is that local populations are both better situated and more highly motivated than outside agencies to manage the resources in an ecologically and economically sustainable manner given the importance of these resources in their daily lives (Benjamin, 2004). The latter stresses again that by moving decision making closer to the local level, decentralization seeks to correspond with the interests and priorities of local population and thereby improve the efficiency and equity of government.

There is a body of literature that has emerged in the past two decades suggesting that decentralization reform has created opportunities for collective actions (Brinkerhoff, 1995; Thomson, 1994; Gibson et al., 2000; Ostrom, 1990; Ostrom, 1999) over natural resource management. In addition, several studies (Agrawal & Gibson, 2001; Ostrom, Gardner, & Walker, 1994) have shown that institutions are a critically important tool for both explaining and influencing human behavior around natural resource use. An important facet of the institutions is the right they confer on those who use, manage and own natural resources. Institutional theory stresses the dynamic nature of institutional arrangements as complex adoptive systems which are continuously adjusted by resource managers in response to contextual changes (Ostrom, 1990; Thomson, 1992; Young, 2002). However, it has to be emphasized that institutions alone cannot ensure the successful outcome of decentralization. Besides, the outcomes of decentralization depend very much on details of what power is transferred to whom, by what means, and how the decisions on natural resource use and management are made (Agrawal & Ribot, 1999; Ribot, 2002). In addition, the effective implementation of decentralization also depends on how well the specific institutional arrangements fit the sociological and ecological environments, and on the interplay of multiple institutions at different scales (Young, 2002).

Though decentralization reform in Mali is often cited as a particularly successful example in West Africa (Charlick, 2001; Clark, 2000; Smith, 2001), Mali is still confronted with many challenges as its Sahelian neighbors such as institutionalizing the balance of power between central and local governments, establishing effective local government with limited technical and financial resources, and reconciling traditional and modern legal traditions, including those related to natural resources. Analysis by Benjamin (2008) shows that while decentralization in Mali has created structures for increasing local participation in governance and natural resource management, it has undermined many of the traditional structures that organize social life in rural communities and the traditional authorities appear to be threatened by the elected "conseils communales", in such way that in some parts of Mali, many rural people perceive decentralization as a threat that may transfer existing power to control their community resources from their hands to the local government ("commune rurale"). Furthermore, some authors have suggested the capture of decision-making mechanisms over the community resources by local elites, which has been reported to derail decentralized natural resource management (Ribot, 2004; Béné et al., 2009). Based on the concerns expressed in the literature above on lack of local participation in development of local natural resource institutions, there is a strong need to understand the awareness and understanding of non-elites about existing institutions. In this regard, Agrawal and Ribot (1999) argue that "downward accountability" is not simply dependent on local election but it depends on the non-elites to engage and demand/expect "downward accountability" and this can only happen if non-elites are aware of local institutions and recognize them as legitimate.

To strengthen local participation in decentralized natural resource management, the importance and pertinence of natural resource institutions have been emphasized (Benjamin, 2008). This author explained that these local rules and norms provide a mechanism for managing local specificities through negotiated rules and management principles and reconciling legal ambiguities not adequately addressed in national legislation. His arguments support the idea that the local conventions and rules governing natural resource management present an opportunity to secure customary right by engaging local government, and state authorities under legally binding constraints.

3. Materials and Methods

3.1 Description of the Study Area

The study was conducted in six communities in Koutiala and Bougouni districts in the Sikasso region of Mali (Figure 1). The two study sites are located in the southern part of Mali with a Sudanian climate characterized by an alternation of dry and rainy seasons that last about six months each. Annual precipitation varies between 750 - 1100 mm and 900 - 1200 mm for Koutiala and Bougouni, respectively. The main ethnic groups in Bougouni are

the Fulani, the Bambara, the Sarakolé, the Malinke, the Dogon and the Bozo with dominance of Bambara and Fulani. Generally, the Bambara are autochthonous populations while others ethnics, especially Fulani ethnic, are immigrant populations who came to settle in the South. Koutiala is a cosmopolitan city with dominance of Minianka which constitutes more than 50% of the population of Koutiala followed by Bambara (20%) and Sarakolé (10%) ethnic groups. Miniankan and Bambara are considered as indigene ethnics. The livelihood strategies of both districts are mainly based on agro-silvo-pastoral activities. Maize, millet, sorghum, groundnut and cowpea are the main food crops and cotton is the main commodity crop in both study sites. In fact, Koutiala is the capital of cotton production in Mali followed by Bougouni. Livestock play an important role in the rural economy, especially through animal traction and income generation to meet household needs. The main livestock species raised in the study sites are cattle, sheep, goats and poultry. Bougouni district is traversed by many rivers which provide opportunities for irrigation and fishing. Forest area in Bougouni is much larger than in Koutiala. Secondary livelihood activities in Bougouni included gold mining and handcrafts. Given the dependence of farmers in both study sites on natural resources for their livelihoods, the demand for these resources are high which lead to over-exploitation and in many times to several conflict among different stakeholders with competing interests.

The two study sites were selected in terms of different current status (availability and the quality) of natural resource base. Whereas the level of natural resource degradation in Koutiala is high due to greater cropping intensity, natural resource is still relatively abundant in Bougouni. As a result of relatively abundant natural resources in Bougouni, there are multiple natural resource users with sometimes conflicting interests. So, by selecting two districts with different natural resource status we are able to test the assumption that local populations tend to be more aware of the rules and norms that govern their natural resources when there are increased pressure through competing multiple users.

3.2 Methods

Surveys on existing local natural resource institutions including local conventions and the level of participation of community members in the development process were conducted using group discussions (Duggleby, 2005) and individual interviews of key stakeholders (Creswell, 2014). Focus group discussions were used to collect information on participants' view and experiences on natural resource institutions while interviews were used to explore the views of individuals on participation in elaboration of NR institutions and to collect quantitative information which will support the qualitative information. Data collection was carried out between November, 2013 and January, 2014, in the dominant local language (Bambara) and French by the survey team including the first author of this paper and five field assistants. The data collection involved three types of informants: crop-livestock farmers (indigenous and immigrant populations), community and traditional authorities as well as administrative authorities and technical services.

3.2.1 Group Discussions

Eight group discussions were carried out, consisting of two group discussions with administrative and technical services (one in each district with 27 participants in total), and six group discussions with community and traditional authorities (one in each community with 53 participants in total). Table 1 outlines the socio-professional profile of the participants in the focus group discussions conducted in the two districts on natural resource institutions including local conventions. During these group discussions we focused on identifying and recording details on existing rules, norms and or local conventions governing natural resource management in the study sites. The level of knowledge of the different groups on these local natural resource institutions was also assessed.

During the focus group discussions, participants were asked to name and describe the existing local rules, norms and or local conventions governing natural resource management in their communities. In addition, the participants were asked to provide the key features of the mentioned local natural resource institutions in terms of the natural resources addressed, the date of establishment (if known), the key elements of the rules/norms and the area of coverage (village, inter-villages or district). Furthermore, the respondents in each group discussion were asked to assess their level of knowledge of the existing local natural resource institutions on a scale of zero (none) to four (well informed of the existing rules and norms). The score was recorded at individual level, and then the average was calculated to get the average score for the whole group.

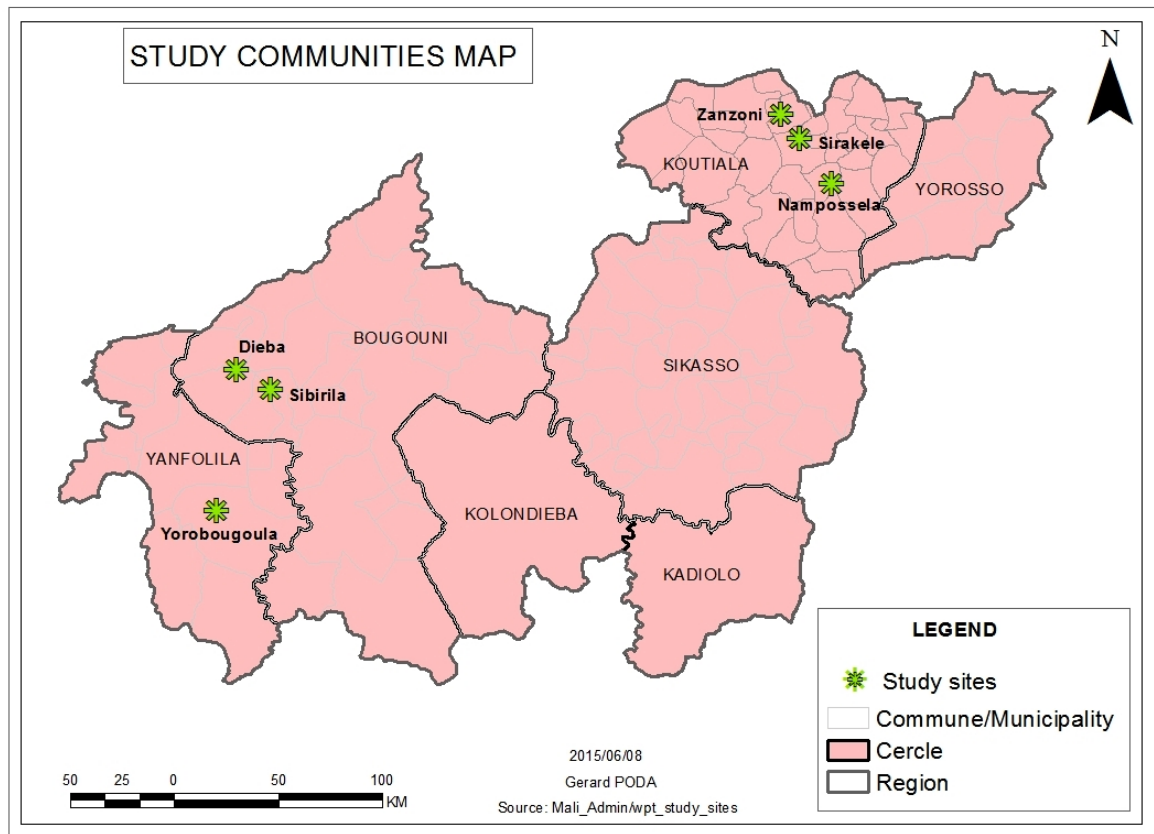


Figure 1. Map of study sites in southern Mali

3.2.2 Individual Interviews

A total of 165 farmers were interviewed on local natural resource institutions in the two districts comprising of 76 (52 men and 24 women) and 89 (59 men and 30 women) crop-livestock farmers in Bougouni and Koutiala, respectively. Stratified random sampling on the basis of gender and status of residence (indigenes and immigrant) in the village was adopted to select the farmers interviewed. Status of residence in the village is important in terms of access, control and use of the community's natural resources.

Information gathered during these interviews included farmers' perception on types of local rules and norms governing NRM, level of knowledge of existing local rules and norms and participation in the development of the local natural resource institutions. To assess the interviewees' knowledge of rules and norms governing the management of natural resources, each interviewee was first asked to mention the natural resources (land, pasture, forest, river etc.) in the community that he/she knows. This was then followed by a question if the interviewee knows rules or agreement between the community members or between community members and outside users for access, use and management of each resource he/she mentioned. If the interviewee answered that he did not know any existing rules and norms, we then mentioned the rules, norms and or local conventions already identified by the community leaders during the focus group discussions and asked if he/she is aware of any of them. Some of the interviewees responded that they are not aware of any existing rules and norms governing NRM while others said yes. Based on this response, we scored the level of knowledge of the interviewees as: 0 = not aware of any of the existing local rules and norms; 1 = aware of the existing local rules and norms but do not know the substance (details); 2 = aware but has limited understanding of some of the local rules or norms governing NRM; 3 = aware of all the existing local rules and norms governing NRM and has a good understanding of most of them; 4 = aware of all the existing local rules and norms governing and know in details their key elements.

Table 1. Socio-professional profile of the participants of the focus group discussions on local rules, norms and or local conventions in the study sites

District	Group	Community	Male	Female	Profile
Bougouni	Local administrative authorities		9	0	Technical services (Agriculture, rural extension agents, animal production and industries, veterinary service, forestry official, social development workers -Local administrative authority (district)
		Local community leaders	Diéba	10	3
		Sibilira	10	2	
		Yorobougoula	6	2	
Koutiala	Local administrative authorities	-	9	1	Technical services (Agriculture, rural extension agents, animal production and industries, veterinary service, forestry official, social development workers) Local administrative authority (district)
		Local community leaders	Namposséla	9	2
		Sirakéle	9	2	
		Zanzoni	9	2	

3.2.3 Data Analysis

Quantitative data were analyzed using SAS software (SAS, 1987). PROC MEANS was used to calculate means and standard errors for each variable. PROC REG was used to perform regression analysis to evaluate the relationship between the independent variables (age; years of residence in the community; sex: female and male; livelihood type: herder, farmer-herder and farmer; education: formal (primary, secondary school), koranic and informal education (adult education) and land owning status and the response variables (level of participation in the development of existing local rules and norms governing NRM). In the regression analysis, variables sex takes 1 if sex is female, and 0 if not; the variable livelihood type takes 1 if the respondent is either herder or farmer-herder, and 0 if not; the variable education takes 1 if level of education is either a formal education or a koranic education and 0, if otherwise and the variable landowning status takes 1 if the respondent is not land owning (non- indigenous), 0 otherwise. T-test of means was used to compare the mean values of different parameters obtained from the two districts. Level of statistical significance was declared at $P < 0.05$.

4. Results

4.1 Variation in the Knowledge of Existing Natural Resource Institution in the Study Areas

In Table 2, we presented a summary of the different types of existing natural resource institutions in the six study communities in Koutiala and Bougouni. Local natural resource institutions existed in all communities studied. Expectedly, most of these local rules and norms existed in an informal or oral form as only three of the over twenty local natural resource institutions we identified in all study communities were formal (formal refers to rules that are generally written and sanctioned/recognized by the state). Formal local conventions tended to cover a very large area even extending to two or more villages and or districts while the main coverage of almost all informal existing rules governing NRM was limited to the village. In addition, our results revealed most informal rules governing NRM were established as far back as the establishment of the villages. They are mostly the initiative of community leaders who decided to set regulations to better manage the resources in their territories and protect them against external users. However, sometimes, with changing demographic and socio-cultural context, the rules are revised or updated by the communities to accommodate the realities of their times.

The level of knowledge of community members differed from one individual to another; and from one community to another depending on sex, age and ethnic group. Overall, the level of knowledge of local rules and norms governing NRM was significantly ($P < 0.05$) higher in Bougouni than in Koutiala. The average score for the level of knowledge (on a scale of 0 to 4) of rules and norms governing NRM was good (3.16 in Bougouni but relatively low in Koutiala, an average of 1.70). Results presented in Figure 2 showed that men had a higher

knowledge of local natural resource institutions compared to women. Specifically, 67% of men as against 38% of women interviewed in Bougouni responded to have a very good knowledge of local rules and norms. This percentage was 12% for men as against 7% for women in Koutiala.

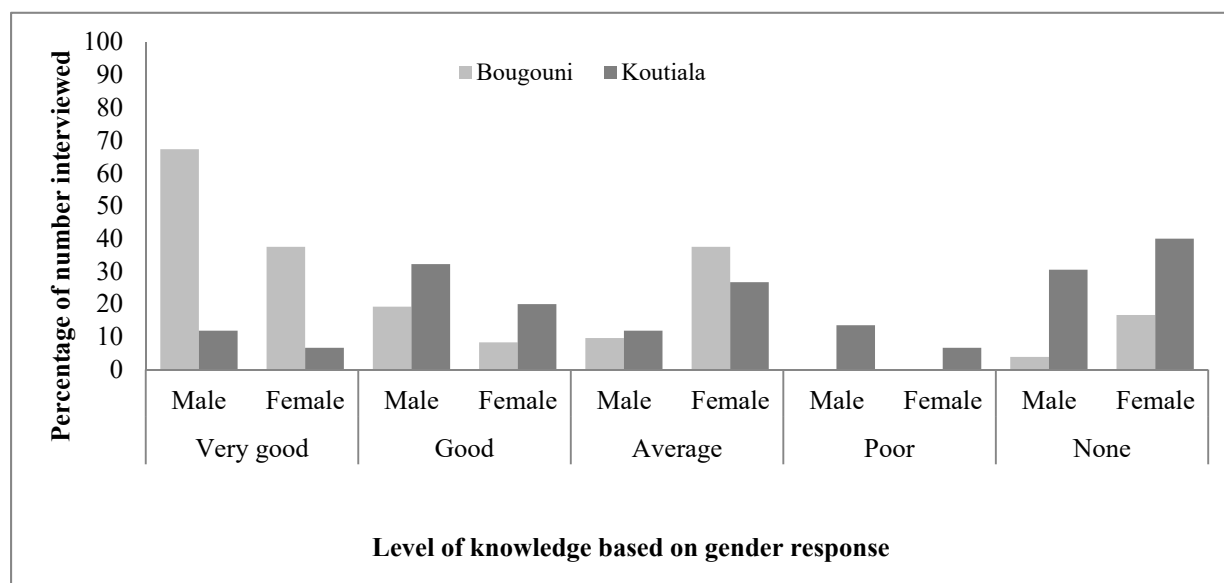


Figure 2. Level of knowledge of local rules or norms governing NRM according to gender in Bougouni and Koutiala

The results of focus group discussions showed that the level of knowledge of local natural resource institutions by administrative authorities and technical services was generally low compared to that of community (traditional) leaders (Figure 3). Generally, the technical services from the government agencies had knowledge of formal (written) natural resource institutions because they were often heavily involved in their establishment. Expectedly, the technical services had almost no knowledge of many existing non-formal rules and norms in the communities as they are largely oral.

Table 2. Summary of the different types of existing natural resource institutions in the study sites

District	Interviewed Group	Name of the local natural resource institutions/ local convention	Written/Oral	Date of establishment	Natural resources addressed and key conventions issues	Coverage
Koutiala	Local administrative authority Sirakelé Community	SIWAA	Written	May 1997 (formalization date)	Land, common pasture, forest, transhumance, conflict management, bush fire, hunting	Inter-District
		CPC	Oral	Since the creation of the village	Forest - protection of sacred trees and community forest, regulation of harvesting of tree products by indigenes and foreigners, rules for harvesting Néré and shea butter, periods for harvesting wild fruits	Village
		CGC	Oral	Since the creation of the village	Conflict over land, pasture, transhumance - processes for mediation and resolution of conflict among the indigenes and foreigners over land, water and grazing, fines and sanctions for the offenders, permission for grazing crop residues after harvesting whether	Village

				for transhumant herders or community members, conditions of accepting transhumant herders in the community, duration of stay of transhumant herders in the territory, period for entering grazing lands, protection of livestock corridors.	
	CGPE	Written	2007	Water – rule of access to the watering point, management of watering point and charges for use by foreigners, processes for conflict mediate over watering point	Village
Namposséla Community	SIWAA	Written	1989	Land - rules of land ownership, rules of access to community land and acquisition by foreigners, protection of sacred land, organization and clearing modalities. Communal pastures – rules of access and use, management of communal pastures, protection from cropping. Forest – rules for cutting and sale of wood, quotas for harvesting forest resources for use as timber and fire wood. Transhumance - Demarcation of livestock routes in the community, arrival date of transhumant herders and duration of stay in the community. Conflict management – processes for mediation and resolution of conflict among the indigenes and foreigners over land, water and grazing. Bush fire - agenda for controlled bush fire and prohibition of uncontrolled bush fire, fine for uncontrolled bush fire Hunting - protection of some wildlife species, precision about species that could be hunted, date for community group hunting	Inter-District
	KOMO	Oral	Since the creation of the village	Fishing: Protection of fish species, restriction of fishing in certain period of the year, fixing of the period of fishing by community leaders and communication to community members	Village
	CAT	Oral	Since the creation of the village	Land use and management - land tenure and security, condition of access to land by foreigners, and transfer of land among the community members	Inter-Village
Zanzoni Community	CGT	Oral	Since the creation of the village	Transhumance – protection of livestock routes in the community, conditions for receiving transhumant herders in the village territory, arrival date and duration of stay in the community, resolution of conflict between herders and the community members, permission to graze crop field by the transhumant herds	Village
	CGC	Oral	Since the creation of the village	Conflict over land use, communal pasture and water - processes for mediation and resolution of conflict among the indigenes and foreigners over land, water and grazing; fines for the offenders and compensation for the victims in case of damage to crops	Village
	CTT	Oral	Since the	Land use and management - land tenure and	Village

				creation of the village	security, condition of access to land by foreigners, and transfer of land among the community members	
		CGF	Oral	2003	Forest - conditions of cutting and sale of fuelwood, rules and roles for monitoring of community forest	Inter-district
Bougouni	Local administrative authority	CGRN	Written	November 2010	Land, common pasture, forestry, water, conflict, bush fire, wild resources (fauna and flora, wild fruit)	Inter-district
		CPC	Oral	Since the creation of the village	Wild fruit harvest	Inter-village
		CAP	Oral	2006	Land use and forest - land tenure and security, condition of access to land by foreigners, protection of sacred forest, rules for cutting of trees in community forest and protection of certain tree species	Inter-Village
	Sibilira Community	CGF	Oral	1993	Forest – rules for cutting trees for fuel-wood and prohibition of sale of fuel-wood	Village
		CGPC	Oral	2011	Pasture - access and use of grazing areas, prohibition of cropping on grazing land conflict management - processes of conflict resolution, precision of sanctions.	Village
	Yorobougoula Community	CGRN	Written	November 2010	Land, pasture, forest – modalities for exploitation of forest resources, protection of pasture for animal, harvesting of forest product, rules for sale of woods, conditions of harvesting wild fruits and fixing of harvesting period of wild fruits. Water, conflict management, bush fire – access to watering points, processes for conflict mediation, rules for controlled bush fire, sanctions for uncontrolled bush fire. Hunting - management modalities: hunting license, fixation of hunting period, and rules for ritual hunting)	Inter-District
		CGF	Oral	2007	Forest - management of protected area. hunting, bush fire – rules for controlled bush fire	Inter-Villager
	Diéba Community	CGF	Oral	Since colonial period	Forest - conditions for cutting of fuel wood	Village
		CGP	Oral	In the 1960s	Pasture - access and use of grazing area	Village
		CGM	Oral	Since the creation of the village	Ponds with various fish species - management system, fixing period for fishing	Village

Acronyms: SIWAA (SIWAA Convention); CGPE: Conventions on management of watering points, CGT: Rules on land allocation - land tenure security, CPC: Rules on the regulation of wild fruits, CGC: Rules on conflicts management, KO-MO: Rules on collective fishing, CGT: Rules on transhumance management, CTT: Rules on land tenure, CGF: Rules on forestry management, CGRN: Convention on natural resource management, CAP: Rules on Protected Areas, CGPC: Rules on rangeland and conflicts management, CGP: Rules on rangeland management, CGM: Rules on standing pools management.

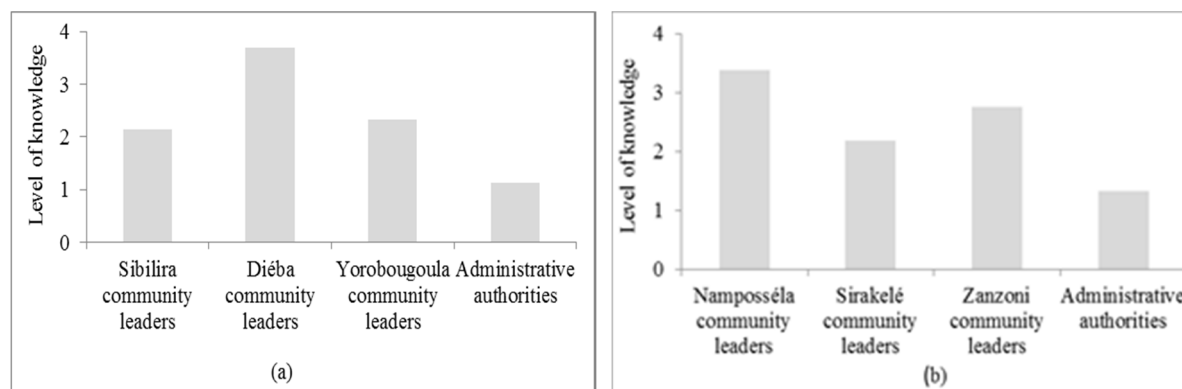


Figure 3. Level of knowledge of local rules, norms and or local conventions governing natural resources use by group interviewed (a) Bougouni, (b) Koutiala.

Level of knowledge: Score: 0= none, 1= low, 2= average, 3 = good, 4= very good

4.2 Local Participation in the Elaboration of Natural Resource Institutions in the Study Sites

There are no standard procedures for the elaboration of rules, norms or local conventions governing NRM as they differ depending on the type of natural resource institutions and strategies adopted by the different stakeholders. The level of community participation in the development of local rules or norms governing NRM was very low in both districts. According to the results, 72% and 77% of the respondents in Bougouni and Koutiala respectively, reported that they have not participated in development of existing local rules or norms governing NRM in their communities, while 21% and 16% had slightly participated, respectively.

Table 3 shows the degree of participation in development of existing local rules and norms by gender. The results showed that women's participation in development of existing local rules and norms in the study sites was generally low despite the fact that women are major users of natural resources in the communities. The lower level of participation by women compared to men suggested a domination of local institutions by men.

Table 3. Participation in the elaboration processes of rules and norms governing natural resource use in the study sites by gender

Factor	Variable	Bougouni		Koutiala	
		Means	s.e	Means	s.e
Gender	Male	0.56 ^a (N=52)	0.12	0.53 ^a (N=59)	0.12
	Female	0.04 ^b (N=24)	0.04	0.07 ^b (N=30)	0.05

The score for the level of participation was 0 = none, 1 = low, 2 = average, 3 = high, 4 = very high. Means in the same column with different superscript letters are statistically different at $P < 0.05$.

Table 4 shows the results of the regression analysis on the effect of independent variables on the level of participation by the respondents in the development of local rules and norms governing NRM in the study sites. The results showed that age, year of residence in the community, gender and formal education appeared to influence the level of participation of community members in the elaboration processes of rules governing natural resources management in Bougouni. The results suggested that a female was less likely to participate in the elaboration of rules governing NRM and that older people were more likely to be involved. Similar but less significant results were obtained in Koutiala where two factors namely female sex and formal education had a significant influence on the stakeholders' level of participation in the formulation of rules and norms governing NRM. A major difference is that the level of formal education had a positive influence in Koutiala while negative one in Bougouni.

Table 4. Results of the regression analysis of the level of participation of community members in the elaboration of rules and norms governing natural resources use in the study sites

Independent variable	Bougouni	Koutiala
Age	0.029***	0.004
Residence	-0.023***	0.010
Female	-0.575***	-0.389**
Herder	-1.098	0.189
Farmer-herder	-0.093	0.026
Formal education	-0.411**	0.340*
Koranic education	0.206	0.035
Non land owning lineage	-0.280	0.282
Constant	0.188	-0.258
R ²	0.317	0.117

*** Significant at the 1 % level, ** significant at the 5 % level, * significant at the 10 % level.

Values are regression coefficients for each independent variable.

5. Discussion

The existence of local natural resource institutions in all communities according to our results agrees with observations by Dicko (2002) and Tutu, Pregernig, and Pokorny (2015) that rural communities often put in place rules and norms to monitor the management of their resources and to protect from overexploitation. In this sense, Granier (2010) argued that local natural resource institutions have always existed in African society and the only difference today is the involvement of the government. With rapidly changing demographic, socio-cultural and institutional contexts in many rural communities, some authors (Tutu et al., 2015) observed that these informal natural resource institutions may no longer be appropriate for the current realities in many communities and this thought has encouraged the tendency to move from a status of informal local rules and norms to that of legal tool in form of formal local conventions (Granier, 2010).

5.1 Knowledge of Existing Local Natural Resource Institutions in the Study Areas

Even though local rules and norms exist in both study sites, the level of knowledge by the community members varied among groups according to their socio-professional profile and gender. Coulibaly and Sanogo (2006) confirm our results that all those involved in the use and management of natural resources do not have the same level of knowledge or the same perception on the local natural resource institutions. In addition, these results suggest a higher level of knowledge of natural resource institutions in Bougouni than in Koutiala. This could be explained by more pressure on natural resources being experienced in Bougouni which might have contributed to greater awareness of the natural resource institutions by the community members.

Despite their expected roles to support better management of natural resources at community level, the local administrative authorities and technical services had almost no knowledge of existing local natural resource institutions in the communities they are supposed to support as shown by our results. This may be an indication of disconnection and mutual distrust between the communities, and the state technical agents and administrative services as reported by Hilhorst (2008). To support this point, one of the community participants in our study sites said at one of the group discussions that: "*Forestry officials are our enemies, they do not mean good for us; what they want is money.*" Another participant added: "*The mayor of the local government came here to sow discord.*"

5.2 Community Participation in the Elaboration of Rules and Norms

The low level of participation in the elaboration of rules of access, use and management of natural resources in the communities reported in this study could be partly attributed to domination of the process by few individuals in the communities who are often the leaders and, elites in the communities (Bachir, Vogt, & Vogt, 2007). These local leaders and elites think that they represent others, and they can decide on their behalf knowing that none can contest their decision. This is closely linked to the concept of elite domination as observed by Poteete and Ribot (2011) in which powerful actors gain, build and maintain positions of dominance. Cases of elite capture in

decision over natural resource management have been reported in many studies on decentralized natural resource management (Shackleton, Campbell, Wollerberg, & Edmunds, 2002; Granier, 2010; Poteete & Ribot, 2011; Platteau, 2004; Béné et al., 2009). Elite capture is often considered as a problem with community based natural resource management as individuals use institutions to take advantage of them in order to further their own gains. Ribot (2004) argued that the incompleteness of recent attempts at decentralizing authority and functions to local and district level has led to strengthening of local elites and increasing vulnerability of the already marginalized rural people. The low participation of community member in decentralized natural resource management has been also reported in others studies (Béné et al., 2009). These authors added that even where participation of legitimate group of end users seem to have been more effectively achieved, a more thorough analysis reveals that the level of participation is often reduced to an instrument for implementation rather than an effective and empowering involvement in decision-making.

The significant different levels of participation of community members found between Bougouni and Koutiala could be partly attributed to the strong interest of the people in Bougouni to protect their resources from external users and this resulted in strong mobilization of the population. Bachir et al. (2007) argue that the biggest motivation for farmers in developing rules and norms governing NRM is the protection of their resources from external users. These authors added that more people tend to be involved in the development of local rules and norms in the areas experiencing a multiplicity and diversity of users of natural resources from outside as was the case in Bougouni.

Despite the fact that women are major users of natural resources, their level of participation in elaboration of local natural resource institutions is generally low in the study sites. This low level of participation by women can be partly explained by socio-cultural factors as in most African traditions including Malian culture where women are not considered responsible for management of natural resources in the community. In general, a man, as the household head, represents his spouse(s) and he is responsible for the actions of his wife (wives). In addition to socio-cultural factors, low level of participation of women can also be attributed to general low level of education among women, and lack of information and awareness of the elaboration processes of the local natural resource institutions. Results from the study by Coulibaly and Sanogo (2006) on the role of women in participatory management of natural resources in Southern Mali support our findings. These authors observed that women are not directly concerned by the management of natural resources and are almost excluded. To highlight the importance of women's active involvement in NRM and the change that can be brought if they are fully engaged in decision making over natural resources use, a recent study in Nepal attributed the success of forest management program to management of the community forest by the women (Tiwari & Joshi, 2015).

The results of regression analysis revealed that the level of participation in the elaboration of rules governing NRM depended on a number of factors and these factors varied between the two study sites. Expectedly age had positive effect suggesting that old people will likely to be engaged in the development of rules and norms governing NRM. This may not be far from the reality on the ground where old people are generally first to be consulted in most decision-making at the community levels. Another important factor reported in Bougouni is year of residence in the community which tends to have negative influence on the likelihood of participation in development of rules and norms. The likely explanation for this is that the people with long years of residence in the community enjoy rights of access and control of resources in the communities and may not be too concerned regarding their participation in the elaboration of local natural resource institutions. The effect of level education on involvement in development of local rules and norms for NRM is location-specific from the results.

The negative effect of being female on the level of participation confirms the argument that men are more likely to participate in decision-making over natural resource use and that women are generally marginalized in NRM in West Africa (Coulibaly & Sanogo, 2006). Livelihood types like being a herder or farmer-herder and having no land-holding status in the community do not play influential role regarding participation in local natural resource institutions elaboration. The lack of influence of livelihood type could be partly attributed to general marginalization of herders in the decision making process by the indigenous farming populations. To support this, leaders in one of the communities where we conduct this study stated in a focus group discussion that: *"herders do not live in our community, why do we have to include them in decision-making regarding the resources available in our community? What we do is to inform them of our decision"*.

6. Conclusion

This paper explores key features of existing local natural resource institutions, level of awareness of these local natural resource institutions by community members and their level of participation in the elaboration processes. Our results demonstrate that the level of knowledge of natural resource institutions by community members

differed from one individual to another; and from one community to another depending on sex, age and social group status. Our results suggest that level of awareness is closely interlinked with the level of participation in the elaboration processes of natural resource institutions and it could be stated that community with high level of awareness of local rules and norms will likely be associated with the high level of participation. This study further shows that natural resources decision-making is still under strong influence of traditional leaders and elites. Findings from this study also show that participation of community members in elaboration of natural resource institutions is low. Factors that influence the level of participation include age, year of residence in the community, gender and education level. For effective implementation of local natural resource institutions, the interest of key natural resource users should be taken into account. It is also important to promote rules and norms that attempt to protect or strengthen women's access to natural resources in the community.

Acknowledgements

The authors acknowledge the strong support of Association Malienne d'Eveil pour le Développement Durable (AMEDD) for the fieldwork. We also appreciate the support and participation by local administrative authorities and technical services as well as community leaders and farmers. This research was funded by United States Agency for International Development (USAID) as a part of Feed the Future Africa RISING project in West Africa. USAID played no role in the design of the study, in the collection, analysis, and interpretation of the data, in the writing of the article, or in the decision to submit the article for publication.

References

- Agrawal, A., & Gibson, C. C. (2001). *Communities and the Environment: Ethnicity, Gender, and the State in Community-Based Conservation*. New Brunswick, NJ: Rutgers University Press.
- Agrawal, A., & Ostrom, E. (2001). Collective action, property rights, and decentralization in resource use in India and Nepal. *Politics and Society*, 29, 485-514. <http://dx.doi.org/10.1177/0032329201029004002>
- Agrawal, A., & Ribot, J. C. (1999). Accountability in Decentralization: A Framework with South Asian and West African Cases. *Journal of Developing Areas*, 33, 473-502. <http://www.jstor.org/stable/4192885>
- Bachir, A., Vogt, G., & Vogt, K. (2007). *Les conventions locales au Niger: L'expérience de la forêt classée de Takieta*. Institut International pour l'Environnement et le Développement (IIED), London. Retrieved from http://www.iedafrique.org/IMG/pdf/CL._Niger.pdf
- Barrett, C., Brandon, K., Gibson, C., & Gjertsen, H. (2001). Conserving tropical biodiversity amid weak institutions. *BioScience*, 51, 497-502.
- Béné, C., Belal, E., Baba, M. O., Ovie, S., Raji, A., Malasha, I., ... Neiland, A. (2009). Power Struggle, Dispute and Alliance Over Local Resources: Analyzing Democratic Decentralization of Natural Resources through the Lenses of Africa Inland Fisheries. *World Development*, 37, 1935-1950. <http://dx.doi.org/10.1016/j.worlddev.2009.05.003>
- Benjamin, C. E. (2004). *Livelihoods and institutional development in the Malian Sahel: A political economy of decentralized natural resource management (Unpublished doctoral dissertation)*. University of Michigan, USA.
- Benjamin, C. E. (2008). Legal Pluralism and Decentralization: Natural Resource Management in Mali. *World Development*, 36, 2255-2276. <http://dx.doi.org/10.1016/j.worlddev.2008.03.005>
- Brinkerhoff, D. (1995). African state-society linkages in transition: the case of forestry policy in Mali. *Canadian Journal of Development Studies*, 16, 201-228. <http://dx.doi.org/10.1080/02255189.1995.9669593>
- Charlick, R. B. (2001). Popular participation and local government reform. *Public Administration and Development*, 21, 149-157. <http://dx.doi.org/10.1002/pad.155>
- Clark, A. F. (2000). From military dictatorship to democracy: the decentralization process in Mali. In R. J. Bingen, D. Robinson, & J. Staats (Eds.), *Democracy and Development in Mali* (pp. 251-264). East Lansing, MI: Michigan State University Press.
- Coulibaly, N'G., & Sanogo, J. L. (2006). Rôle des femmes dans la gestion participative des ressources naturelles en zone Mali-Sud. In J. S. Zoundi, I. Butare, J. Ndikumana & K. Adomefa (Eds), *Intégration agriculture Elevage : Alternative pour une gestion durable des ressources naturelles et une amélioration de l'économie familiale en Afrique de l'Ouest et du Centre* (pp. 314-327). Ouagadougou: INERA, Nairobi: ILRI, Dakar: CORAF /WECARD.

- Creswell, J. W. (2014). *Research design: Qualitative, quantitative and mixed methods approaches*. California, USA: Sage Publication, Inc.
- Crook, R., & Manor, J. (1998). *Democracy and Decentralization in South Asia and West Africa*. United of Kingdom, Cambridge University Press.
- Dicko, A. K. (2002). *Les conventions locales dans la gestion des ressources naturelles au Mali. Programme d'appui aux collectivités territoriales Etudes No.14, Bamako, Mali*. Retrieved November 10, 2014 from <https://rmportal.net/framelib/pact-etudes-n14.pdf>
- Djiré, M. (2003). *Les conventions locales au Mali outils de gestion durable des ressources naturelles. Revue de Littérature. Bamako, Mali: IIED*. Retrieved August 20, 2014 from http://hubrural.org/IMG/pdf/mali_conventions_locales_outils_gestion_rm.pdf
- Duggleby, W. (2005). What about focus group interaction data. *Qualitative Health Research*, 15, 832-840.
- Gibson, C. C., McKean, M. A., & Ostrom, E. (2000). Explaining deforestation: the role of local institutions. In C. C. Gibson, M. A. McKean, & E. Ostrom (Eds), *People and Forests* (pp. 1-26). Cambridge, MA: MIT Press.
- Granier, L. (2010). *Are local conventions effective tools for the joint management of natural resources? Pedagogic factsheets to gain understanding, ask the right questions, and take action on land tenure issues in West Africa. Bamako: "Land Tenure and Development" Technical Committee*. Retrieved June 15, 2014, from http://www.agter.org/bdf/_docs/ctf_granier_local_conventions_en.pdf
- Hilhorst, T. (2008). Local governance institutions for natural resources management in Mali, Burkina Faso and Niger. *KIT Working Paper Series G1. Amsterdam, the Netherlands*. Retrieved from <http://www.bibalex.org/>
- Kellert, S. R., Metha, J. N., Ebbin, S. A., & Lichtenfeld, L. L. (2000). Community natural resource management: promise, rhetoric, and reality. *Society and Natural Resources*, 13, 705–715.
- Manor, J. (1999). *The Political Economy of Democratic Decentralization*. World Bank, Washington, DC. <http://dx.doi.org/10.1596/0-8213-4470-6>
- North, D. C. (1991). Institutions. *Journal of Economic Perspectives*, 5, 97-112.
- North, D. C. (2005). *Understanding the Process of Economic Change*. New Jersey: Princeton University Press.
- Ostrom, E. (1990). *Governing the Commons: The Evolution of Institutions for Collective Action*. Cambridge, Cambridge University Press.
- Ostrom, E. (1999). Coping with the Tragedy of the Commons. *Annual Review of Political Science*, 2, 493-535.
- Ostrom, E., Gardner, R., & Walker, J. (1994). *Rules, Games, and Common-Pool Resources*. Ann Arbor, the University of Michigan Press. Retrieved March 22, 2015 from <https://www.press.umich.edu/pdf/9780472065462-fm.pdf>
- Platteau, J-P. (2004). Monitoring elite capture in community-driven development. *Development and Change*, 35, 223–246. <http://dx.doi.org/10.1111/j.1467-7660.2004.00350.x>
- Poteete, A. R., & Ribot, J. C. (2011). Repertoires of Domination: Decentralization as Process in Botswana and Senegal. *World Development*, 39, 439–449. <http://dx.doi.org/10.1016/j.worlddev.2010.09.013>
- Ribot, J. C. (2002). *Democratic decentralization of natural resources: institutionalizing popular participation*. World Resources Institute, Washington, DC. Retrieved September 10, 2014 from http://pdf.wri.org/ddnr_full_revised.pdf
- Ribot, J. C. (2004). *Waiting for Democracy: The Politics of Choice in Natural Resource Decentralization*. World Resources Institute, Washington, DC
- Ribot, J. C., Agrawal, A., & Larson, A. M. (2006). Recentralizing While Decentralizing: How National Governments Reappropriate Forest Resources. *World Development*, 34, 1864-1886. <http://dx.doi.org/10.1016/j.worlddev.2005.11.020>
- Shackleton, S., Campbell, B., Wollerberg, E., & Edmunds, D. (2002). Devolution and community – based natural resources management: Creating space for local people to participate and benefit? *Natural Resource perspectives*, 76, 6. The Overseas Development Institute (ODI), London. Retrieved March 15, 2015 from <http://www.odi.org/sites/odi.org.uk/files/odi-assets/publications-opinion-files/2811.pdf>
- Smith, Z. K. (2001). Mali's decade of democracy. *Journal of Democracy*, 12, 73-79.
- Statistical Analysis System Institute. (1987). *SAS/STAT for Personal Computers*. SAS Institute, Inc., Cary, NC.

- Thomson, J. T. (1992). *A Framework for Analyzing Institutional Incentives in Community Forestry*. FAO Community Forestry Note. Rome: FAO.
- Thomson, J. T. (1994). Legal Recognition of Community Capacity for Self-Governance: A Key to Improving Renewable Resource Management in the Sahel. *Sahel Decentralization Policy Report. Vol. III, USAID*.
- Tiwari, P. C., & Joshi, B. (2015). Local and regional institutions and environmental governance in Hindu Kush Himalaya. *Environmental Science & Policy, 49*, 66–74. <http://dx.doi.org/10.1016/j.envsci.2014.09.008>
- Tutu, P. O., Pregernig, M., & Pokorny, B. (2015). Interactions between formal and informal institutions in community, private and state forest contexts in Ghana. *Forest Policy and Economics, 54*, 26–35. <http://dx.doi.org/10.1016/j.forpol.2015.01.006>
- UNCDF. (2000). *Local Development and Decentralized Management of Natural Resources*. Cotonou, Benin.
- Young, O. R. (2002). *The Institutional Dimensions of Environmental Change: Fit, Interplay, and Scale*. Cambridge, MA: MIT Press.

Notes

Note 1. This paper focuses mainly on the management of natural resources such as land, forests, pastures, and watersheds. Decentralization is defined as a process by which powers are transferred from the central government to lower levels in a ‘territorial hierarchy’ (Crook & Manor, 1998). The term “institution” as used in this paper is: "A complex of norms and behavior that persist over time by serving collectively values purposes". Benjamin (2008) describes institutions in terms of rules, norms and strategies that emerge in communities from interacting livelihood strategies to structure patterns of collective action. And North (1991, 2005) categorized institutions in formal and informal institutions with formal characterized by written –down and well document principles that guide the affairs of a society. While informal institutions are simply unwritten traditional rules and norms that influence how a people is organized. Our focus on in this study is mainly informal natural resource institutions.

Copyrights

Copyright for this article is retained by the author(s), with first publication rights granted to the journal.

This is an open-access article distributed under the terms and conditions of the Creative Commons Attribution license (<http://creativecommons.org/licenses/by/3.0/>).

Spatial Variability Modeling of Soil Erodibility Index in Relation to Some Soil Properties at Field Scale

C. Gyamfi^{1,2}, J. M. Ndambuki¹ & R.W. Salim¹

¹Department of Civil Engineering, Tshwane University of Technology, Pretoria, South Africa

²School of Bio-resources Engineering, Anglican University College of Technology, Nkoranza, Ghana

Correspondence: Charles Gyamfi, Civil Engineering Department, Tshwane University of Technology, Pretoria, South Africa. Tel: 27-0-834-335-917, 233-0-2432-12413. E-mail: gyamficharles84@yahoo.com

Received: February 2, 2016 Accepted: February 16, 2016 Online Published: March 14, 2016

doi:10.5539/enrr.v6n2p16

URL: <http://dx.doi.org/10.5539/enrr.v6n2p16>

Abstract

Soil erosion is a major land degradation issue affecting various facets of human lives. To curtail soil erosion occurrence requires understanding of soil properties and how they influence soil erosion. To this end, the soil erodibility index which gives an indication of the susceptibility of soils to erosion was examined. In particular, we aimed to determine soil erodibility index at field scale and establish relationships that exist between selected soil properties and soil erodibility index. It was hypothesized that for soil erodibility index to vary spatially, then the existing soil properties should have varying spatial structure. Hundred disturbed and 100 undisturbed soil samples were collected from a 7.3 ha gridded area. The samples were analyzed for particle size distribution, bulk density, particle density, organic matter content and porosity. All soil analyses were conducted following standard procedures. Data were analyzed statistically and geostatistically on the basis of semivariograms. Sandy clay loam was the dominant soil texture in the studied field. Results indicate significant negative relationship between sand content, bulk density, particle density and organic matter with soil erodibility index. Silt correlated significantly with a positive relation with soil erodibility. Estimated erodibility for the sampled field ranged from 0.019 t.ha.hr/ha.MJ.mm to 0.055 t.ha.hr/ha.MJ.mm. The order of dominance of erodibility ranges were 0.038-0.042 t.ha.hr/ha.MJ.mm > 0.036-0.08 t.ha.hr/ha.MJ.mm > 0.032-0.036 t.ha.hr/ha.MJ.mm > 0.019-0.032 t.ha.hr/ha.MJ.mm > 0.042-0.055 t.ha.hr/ha.MJ.mm. Regression analysis revealed silt to be the most significant variable that influences soil erodibility. The best regression of soil properties on soil erodibility index gave an R² of 0.90. A comparison of the regression equation with other studies indicated good performance of the equation developed.

Keywords: Soil erodibility; spatial dependency; erosion; semivariograms.

1. Introduction

Land degradation through soil erosion is considered a natural and geologic phenomenon, and one of the most important components of the global geochemical cycle. Soil erosion is identified as one of the key challenges that impacts on diverse sectors of our human existence ranging from the depletion of top nutrient rich soils, lowering agricultural productivity and volume storage depletion of reservoirs through sedimentation (Meadows 2003; Colombo, 2010; Gupta et al., 2010; Wang et al., 2013). Current increases in global demand for food and fresh water with its attendant land use changes exacerbate the menace of soil erosion with substantial consequences on soil and water resources sustainability. Earlier studies on erosion, reported that about 33% of the total arable land of the world were lost to soil erosion and continues to be lost at a rate of 10M ha/yr (Pimental et al,1995). The alarming rate at which soils are being lost calls for remediation measures in order to safeguard against future food and water security threats. Paramount to tackling the soil erosion menace is the need to take into cognizance the spatially distributed pattern and inherent variations caused by different land use management practices and varying soil types. Other factors equally influencing the soil erosion process are rainfall and erosivity index, slope and length factor, cropping management factor and the practice factor and soil erodibility factor (Breetzke et al., 2013). By far, soil erodibility is considered an essential parameter among these factors since it governs the ease with which soils are detached. The erodibility of soils is documented to be more dependent on both the extrinsic and dynamic properties of soil (Torri et al., 1997). Due to the complex nature of erosion processes coupled with anthropogenic factors, it becomes truly essential to have up to date knowledge that is geared towards conservation

and management planning strategies. According to Gupta et al. (2010) a thorough understanding of soil properties is required in the consideration of remediation measures for land degradation. Toy et al. (2002) also affirms the need to comprehend soil properties in the wake of ensuring the implementation of management strategies. In view of the above, exploring the relationships that exist between soil properties and how these properties influences the erosion processes through the examination of the erodibility factor becomes essential. To this end, the study had as its objectives to determine soil erodibility index at field scale and establish relationships that exist between selected soil properties and soil erodibility index. It was hypothesized that the existing soil types at the study field had varying spatial structure which influences the spatial variability of soil erodibility index.

2. Materials and Methods

2.1 Study Area

The study was conducted in the Steelpoort subcatchment of the Olifants Basin in South Africa (Figure 1). The subcatchment is located within a semi-arid environment and geographically stretches from latitudes 24.43°- 25.81° S and longitudes 29.73°-30.66° E. The area is characterized by Inter-Tropical Convergence Zone (ITCZ) with temperatures ranging 5°C – 34°C (IWMI, 2008). Rainfall is seasonal in the catchment occurring during the months of October to April with appreciable spatio-temporal variability with coefficient of variation of 24% (Gyamfi et al, 2016). Land uses are documented to include agricultural, urban or built up settlements and grasslands among others (CSIR, 2003). The major soil types in the area are namely; cambic arenosols, orthic acrisols, chromic vertisols and chromic luvisols (FAO, 2002; 2005). It must be reiterated that the steelpoort River is an important source of water for a range of economic activities within the catchment.

2.2 Soil Sampling Strategy and Analysis

Soil samples were collected during the month of October, 2015 using systematic grid sampling approach. An area of 7.3 ha under agricultural utilization was gridded with spacing of 30 m interval. Samples were collected at the nodes of each grid. The grid sample method was employed due to its precision and efficiency with which spatial patterns can be determined (Brus & Heuvelink, 2007; Pennock et al., 2008). In total, 100 disturbed and 100 undisturbed soil samples were collected from the top soil (0-20 cm) using a soil auger and soil core sampler, respectively. The dimensions of the soil core sampler were 10 cm × 10 cm. At each station of sampling, coordinates were taken with a hand held Garmin etrex legend HCx GPS to reference the exact location of the sample. Collected samples were subsequently stored in brown paper bags for onward transfer to the laboratory for analysis. Sampled soils were analyzed for particle size distribution, organic carbon content, bulk density, particle density and porosity. Prior to soil analysis, disturbed samples were oven dried and plant residues were removed. The Bouyoucos hydrometer method of particle size analysis (PSA) as described by Kroetsch and Wang (2008) was used in determining three fractions (sand, silt and clay) of sampled soils. Analysis for bulk density of undisturbed soils followed the procedure outlined by Hao et al. (2008). Determination of soil organic content (SOC) was done using the Walkley-Black method (Walkley & Black, 1934). The organic carbon content obtained using the Walkley-Black method was converted to organic matter content using $OM = 1.72OC$ (Brady, 1984; Boyd, 1995; Pansu & Gautheryou, 2006).

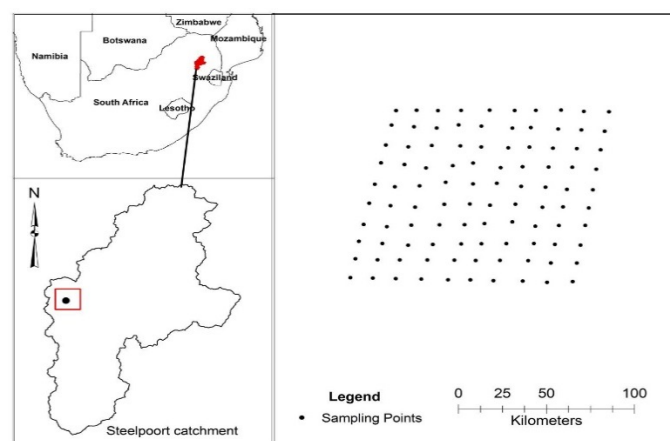


Figure 1. Study location showing soil sampling points

2.3 Soil Erodibility Index Estimation

According to Basson and Di Silvio (2008), the estimation of soil erosion in a semi-arid environment should be based on the Modified Universal Soil Loss Equation (MUSLE) rather than the Universal Soil Loss Equation (USLE). One component of the MUSLE equation, the soil erodibility index which is the subject matter of this study was therefore estimated using measured soil properties following the method outlined by Williams (1995). This approach of soil erodibility index estimation presents advantages of eliminating expensive cost and time involved in direct field measurements. The proposed equation by Williams (1995) is given as;

$$K = f_{csand} \cdot f_{cl-si} \cdot f_{orgc} \cdot f_{hisand} \quad (1)$$

Where; K is erodibility factor (t.ha.hr/ha.MJ.mm), f_{csand} is a factor that gives low soil erodibility factors for soils with high coarse- sand contents and high values for soils with little sand, f_{cl-si} is factor that gives low soil erodibility factors for soils with high clay to silt ratios, f_{orgc} is a factor that reduces soil erodibility for soils with high organic carbon content and f_{hisand} is a factor that reduces soil erodibility for soils with extremely high sand contents.

The individual factors were estimated using the following equations with the measured soil properties as inputs.

$$f_{csand} = \left(0.2 + 0.3 \exp \left[-0.256 m_s \cdot \left(1 - \frac{m_{silt}}{100} \right) \right] \right) \quad (2)$$

$$f_{cl-si} = \left(\frac{m_{silt}}{m_c + m_{silt}} \right)^{0.3} \quad (3)$$

$$f_{orgc} = \left(1 - \frac{0.25 \cdot orgC}{orgC + \exp[3.72 - 2.95 \cdot orgC]} \right) \quad (4)$$

$$f_{hisand} = \left(1 - \frac{0.7 \cdot \left(1 - \frac{m_s}{100} \right)}{\left(1 - \frac{m_s}{100} \right) + \exp[-5.51 + 22.9 \left(1 - \frac{m_s}{100} \right)]} \right) \quad (5)$$

where m_s is the percent sand content, m_{silt} is the percent silt content, m_c is the percent clay content and $orgC$ is the percent organic carbon content.

2.4 Spatial Variability Modeling of Soil Properties and Erodibility Index

Geostatistical methods employing the use of semivariograms were used in exploring the spatial variability and dependency of both soil properties and erodibility index. Semivariograms give a measure of the relation of data points within a particular variable to each other with respect to distance. The theoretical semivariogram as formulated by Matheron (1963) is given by:

$$\gamma(h) = \frac{1}{2N(h)} \sum_{i=1}^{N(h)} \{Z(x_i) - Z(x_i + h)\}^2 \quad (6)$$

Where; $\gamma(h)$ is semi-variance at lag h, h is distance (lag), x is position in one dimensional space, N(h) is Pairwise Euclidean distance

Ordinary Kriging theoretical semivariograms were fitted to the empirical semivariograms by comparing a set of given models. The choice of the best model was made based on statistical measures of the lowest root mean square error (RMSE), largest Pearsons coefficient of determination (R^2) and lowest residual sum of squares (RSS). From the best fitted theoretical models, the spatial structure of each variable (soil property) was determined using the method described by Cambardella et al. (1994).

2.5 Data Analysis

Results of the soil analysis were presented using descriptive statistics inclusive of mean, median, range, standard deviation, skewness coefficient and coefficient of variation. Pearson's correlation coefficient and multiple regression analysis were used to establish relationships between soil properties and estimated soil erodibility index. SPSS 16.0 and MS excel 2010 were used for the statistical analysis whiles ArcGIS 10.1 was used for the geostatistical analysis and surface creation for soil erodibility index.

3. Results and Discussion

3.1 Descriptive Statistics

To establish the relationship between physical properties of soil and soil erodibility, the sampled soils were analyzed and the summary of the results presented in Table 1. All the examined soil properties were found to be normally distributed based on estimated skewness coefficients ranging from -0.76 for particle density to 0.43 for

soil porosity. A dataset is considered to be normally distributed when skewness coefficients are between -1 to 1 (Virgilio et al., 2007; Ortiz et al., 2010). Since all the dataset were normally distributed there was no need for data transformation. The means and medians of the measured parameters were similar with the medians having smaller values than the means. This implies that the measures of central tendency are not dominated by outliers in the distribution. Cambardella et al. (1994) also detected similarities in the mean and median of soil properties and attributed the similarities to the minimal number of outliers found in the soil distribution set. Soil proportions including sand, silt and clay showed wide ranges with mean values of 62.23%, 14.28% and 23.49%, respectively. Conversely, minimal ranges were recorded for soil porosity, organic matter content, bulk density and particle density with corresponding mean values of 42.66 %, 1.91%, 1.47 g/cm³ and 2.56 g/cm³.

There were observed variations in the sampled soil properties as indicated by the coefficient of variation. The coefficient of variation values ranged from a minimum of 2.86% to a maximum of 41.80%. As a means of assessing variability, silt was seen to show the highest variation while particle density indicated a weak variation. Notably, other properties of the sampled soil inclusive of clay, organic matter content and sand all exhibited some degree of variation with coefficient of variation values of 33.28%, 23.56% and 17.44% respectively. The soil properties with the lowest coefficient of variation were bulk density, particle density and soil porosity.

Table 1. Summary statistics of physical properties of soil

Variable	Descriptive statistics ^a							D.T ^b
	Mean	Median	Min-Max	Range	SD	SC	CV (%)	
Sand (%)	62.23	62.22	37.79-83.05	45.26	10.85	-0.14	17.44	N
Silt (%)	14.28	13.57	1.94-30.80	28.86	5.97	0.40	41.80	N
Clay (%)	23.49	23.74	6.92-40.86	33.94	7.82	0.10	33.28	N
BD (g/cm ³)	1.47	1.47	1.31-1.60	0.29	0.07	-0.23	4.86	N
PD (g/cm ³)	2.56	2.58	2.39-2.68	0.29	0.07	-0.76	2.86	N
Pores (%)	42.66	42.25	38.85-47.06	8.21	1.59	0.43	3.72	N
OMC (%)	1.91	1.83	0.83-2.77	1.94	0.45	0.06	23.56	N

^a Min., minimum; Max., maximum; SD., standard deviation; SC., skewness coefficient, CV., coefficient of variation, BD., bulk density; PD., particle density; OM., organic matter content.

^b Distribution type, N; normal distribution.

Textural classification using the USDA textural triangle revealed six main soil textures to characterize the sampled field. The textures were namely; sandy clay loam (57%), sandy loam (29%), clay loam (6%), sandy clay (4%), loamy sand (3%) and clay (1%) of sampled soils. Distribution of bulk density, particle density, porosity and organic matter content at the textural class level is presented in Figure 2 using a boxplot. Evidently, bulk density in sandy loam and loamy sand was higher compared to the remaining soil textures. The lowest bulk density values were recorded in sandy clay and clay loam with mean values of 1.49 g/cm³ and 1.39 g/cm³ respectively. Particle density follows a similar trend as that discovered for bulk density. Porosity and organic matter content were high in sandy clay with corresponding mean values of 43.87% and 2.20%. Sandy loam had the least pores compared to the remaining soil textures. The lowest organic matter content was found to exist in clay loam. Analysis of particle density, porosity and organic matter content on textural levels indicated the presence of outliers most of which were lower than the limit in the distribution. Yet, further examination of these parameters considering all sampled soil but not on textural classes revealed no outliers. This is perhaps so because there is a wider limit of the distribution when all the soil samples are considered together. In view of this, the detected outliers during the textural class analysis were maintained and used in the ensued geostatistical analysis.

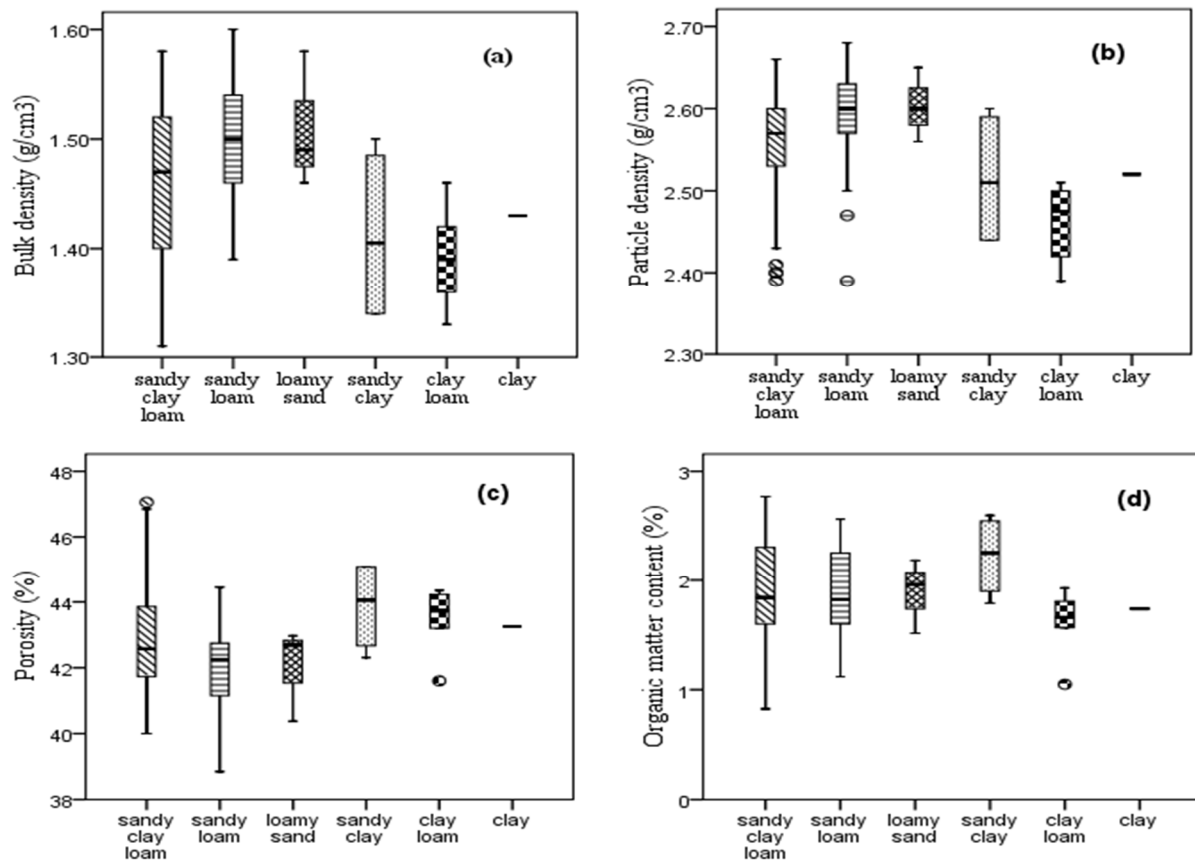


Figure 2. Boxplot of (a) bulk density, (b) particle density, (c) porosity and (d) organic matter content within soil textural classes

3.2 Spatial Analysis of Soil Properties

It was hypothesized that existing soil types at the study field had varying spatial structure which influences the spatial variability of soil erodibility index. To authenticate the veracity of this hypothesis, the spatial distribution and structure of soil properties were investigated by first generating an empirical semivariogram for each of the selected soil properties following which theoretical semivariograms were fitted. An exploration of the soil dataset revealed no trend and anisotropy and hence isotropic semivariograms were fitted. Best fitted isotropic semivariograms were selected based on RMSE, RSS and R^2 (Table 2). With the exception of porosity which was defined by the exponential model, all the other soil parameters including sand, silt, clay, bulk density and organic matter content were defined by the spherical model (Figure 3). From Table 2, it is clear that all the fitted models were able to explain more than 50% of the total variance inherent in the observed data and that the predictions from the model considered to be satisfactory for field predictions of soil properties.

In determining the spatial dependence of soil properties used was made of the nugget/sill ratio as prescribed by Cambardella et al. (1994). This approach of spatial dependency determination has been used by other researchers such as Liu et al. (2014) in the determination of spatial variability of rice yield. The nugget to sill ratio ranged from 45.46 % to 95.60 % putting the soil properties into two major spatial classes of moderate and weak spatial dependency. The three proportions of soil (sand, silt and clay) exhibited weak spatial dependency with nugget/sill range of 93.58% to 95.03 %. Bulk density, organic matter content and porosity constituted the soil properties with moderate spatial dependency with nugget/sill range of 45.46% to 64.50%. The moderately spatially dependent properties may be controlled by intrinsic variation of the soil such as texture and extrinsic factors such as land use activities (Cambardella et al., 1994; Ruth & Lennartz, 2008; Wu et al., 2010; Liu et al., 2013). MacCarthy et al. (2013) also ascribed the low spatial dependency of topsoils to land use and management practices. The spatial dependency determined based on the nugget/sill ratio collaborates the estimates of the coefficient of variation as given in the descriptive statistics section.

Semivariograms (Figure 3) and estimated fitted model parameters (Table 2) revealed most parameters had ranges less than 100 m with the exception of organic matter content and clay which had ranges of 100 m and 190 m respectively. This finding implies samples should be taken at locations not more than 100 m for sand, silt, bulk density, organic matter content and porosity in order to capture the spatial relation between studied properties. For clay, the sampling distances should not exceed 190 m. It thus can be concluded that the spatial structure relations deduced in this work for the studied soil properties are reflective of that on the ground due to the sampling grid distance of 30 m which is far less than the ranges established.

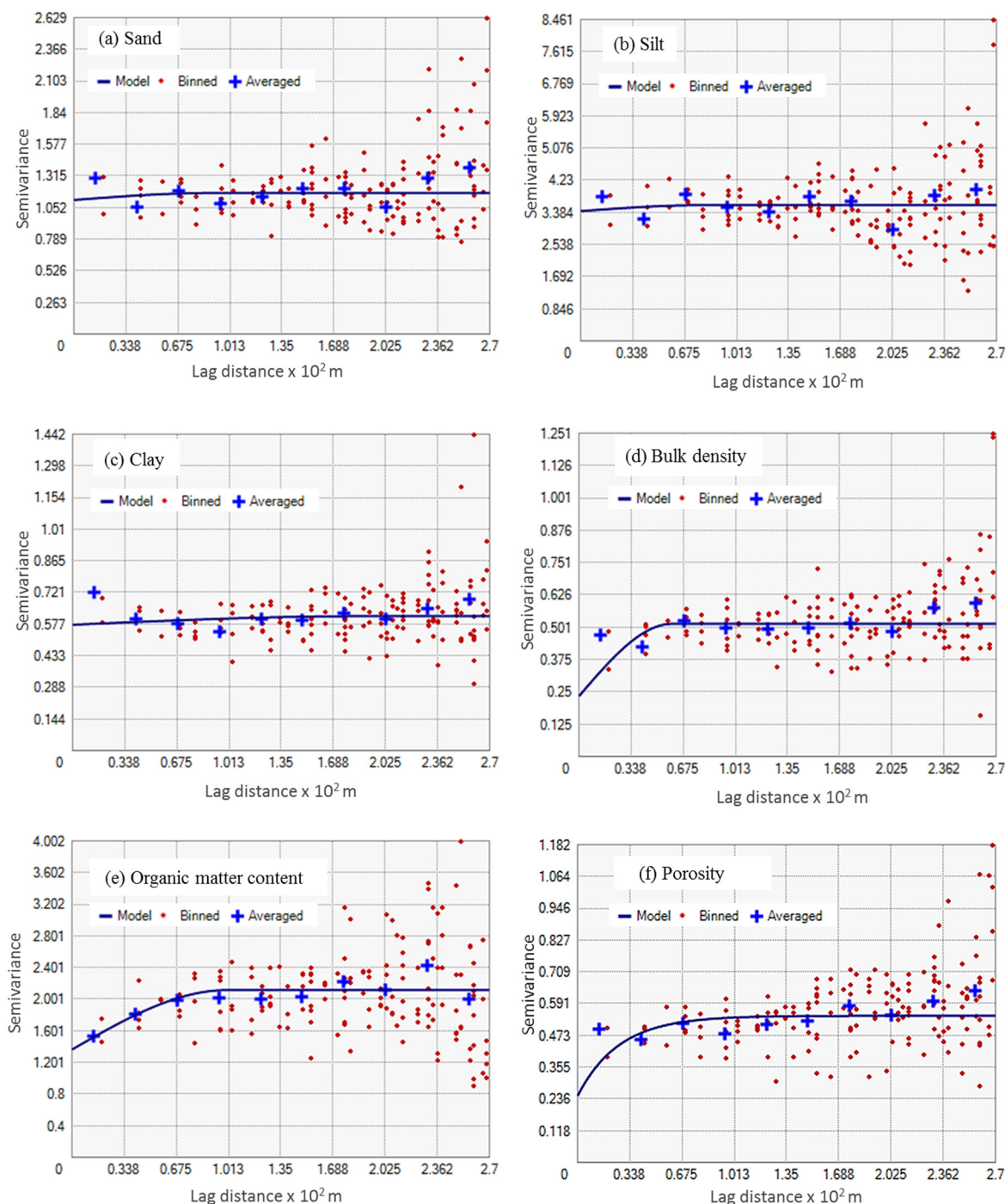


Figure 3. Experimental semivariograms and best fitted models for selected soil properties

Table 2. Parameters of models fitted to experimental variograms of soil properties

Parameter ^a	Model	Semivariance ^b			Range (m)	Class ^c	Diagnostics ^d		
		N	S	(N/S) %			RMSE	RSS	VE (%)
Sand	Spherical	1.11	1.17	95.03	90	W	7.32	5.37E+03	54.96
Silt	Spherical	3.42	3.58	95.60	80	W	3.93	1.55E+03	56.57
Clay	Spherical	0.57	0.61	93.58	190	W	4.87	2.37E+03	64.51
BD	Spherical	0.23	0.51	45.54	60	M	0.04	0.162	67.91
OMC	Spherical	1.37	2.12	64.50	100	M	0.24	5.72	72.14
Porosity	Exponential	0.25	0.55	45.46	80	M	0.04	0.161	71.25

^aBD, bulk density; OMC, organic matter content

^bN, nugget; S, sill; N/S, ratio of nugget to sill.

^cW, weak spatial dependency; M, moderate spatial dependency.

^dRMSE, root mean square error; RSS, lowest residual sum of squares; VE, proportion of total variance of observed data explained by model.

3.3 Spatial Distribution of Soil Erodibility Index at Field Scale

The resulting surface for soil erodibility index is shown in Figure 4 with severity of erodibility captured under five classes. The five class erodibility distinction is to allow for easy identification of most vulnerable areas from least vulnerable areas. Soil erodibility index ranged from 0.019 t.ha.hr/ha.MJ.mm to 0.055 t.ha.hr/ha.MJ.mm with a mean of 0.038 t.ha.hr/ha.MJ.mm. The coefficient of variation for erodibility index was 15.79 % and standard deviation of 0.006 t.ha.hr/ha.MJ.mm. Based on the classification used by Le Roux et al. (2006), the studied field was classified as having low to very high soil erodibility. The estimated soil erodibility for the sampled field was well within range of 0.004 to 0.092 t.ha.hr/ha.MJ.mm stipulated by Le Roux et al. (2006) for South Africa. The order of dominance of erodibility ranges were 0.038-0.042 t.ha.hr/ha.MJ.mm > 0.036-0.038 t.ha.hr/ha.MJ.mm > 0.032-0.036 t.ha.hr/ha.MJ.mm > 0.019-0.032 t.ha.hr/ha.MJ.mm > 0.042-0.055 t.ha.hr/ha.MJ.mm.

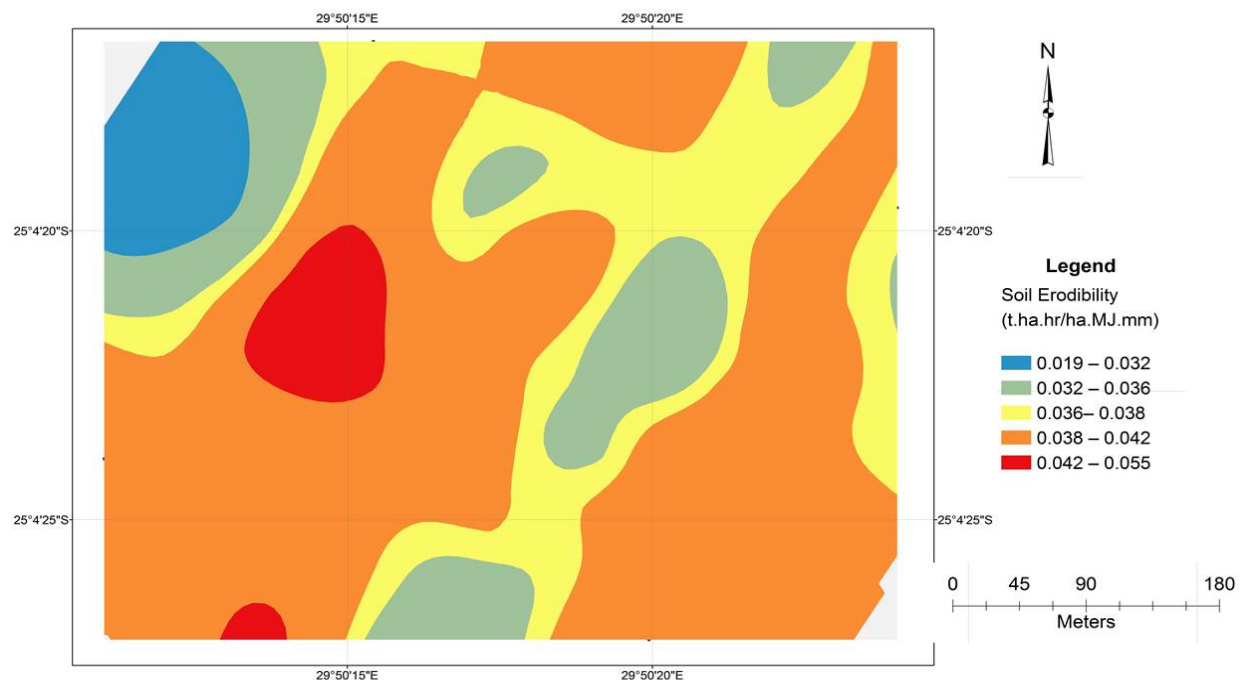


Figure 4. Soil erodibility map for the studied field

3.4 Soil Erodibility Index (K) Correlation with Soil Properties

The characterization of total soil response to a varying number of dynamic soil erosion processes can be achieved using soil erodibility index. These erodibility index are influenced by both intrinsic (e.g. soil texture) and dynamic (e.g. organic matter content) properties of underlying soils (Torri et al., 1997). Here, Pearson's correlation was used to establish the veracity of the relationship existing between soil properties and erodibility factors and the result summarized in Table 3. Results indicate significant negative relationship between sand content, bulk density, particle density and organic matter with soil erodibility index. Soil parameters showing significant positive relationship with soil erodibility were silt content and porosity. Organic matter content is known to increase the stability of soils and subsequently reducing the threat of soils to erosion. The negative relationship between organic matter content and soil erodibility index collaborates the role of organic matter in soil stability. A similar statistically significant relationship was found by Gupta et al. (2010) to exist between organic carbon content (which can be converted to organic matter content) and soil erosion index.

Table 3. Correlation coefficients (Pearson's test) of soil properties and K.

	Sand	Silt	Clay	BD	PD	Porosity	OMC	K _{USLE}
Sand	1							
Silt	-0.713**	1						
Clay	-0.845**	0.226*	1					
BD	0.652**	-0.685**	-0.383**	1				
PD	0.669**	-0.649**	-0.433**	0.866**	1			
Porosity	-0.454**	0.528**	0.228*	-0.860**	-0.490**	1		
OMC	0.005	-0.133	0.095	0.067	0.029	-0.086	1	
K _{USLE}	-0.558**	0.867**	0.113	-0.590**	-0.509**	0.504**	-0.466**	1

** $P < 0.01$; * $P < 0.05$.

A further analysis of the relationship between soil erodibility index and soil parameters was performed using multiple regression analysis and the resulting outcome summarized in Table 4. The analysis revealed sand content alone to account for the 31% of the variation in soil erodibility. Sand and silt together explained approximately 76% of the variation in soil erodibility index. The inclusion of silt increased the variability of soil erodibility index from 31% to 76% indicating the essential role silt plays in the soil erosion process. Wischmeier and Smith (1978) noted similar findings when they ascribed soils with high silt content to be more erodible. Bulk and particle density did not turn to be of much influence on soil erodibility as the addition of these parameters to silt and sand only explained 77% of the variation in soil erodibility. Jointly however, soil parameters inclusive of sand, silt, bulk density, particle density, porosity and organic matter content explained 90% of the variability in soil erodibility index. This finding concurs with previously established facts which alluded to the influential role played by both intrinsic and extrinsic soil properties to the soil erosion processes (Torri et al., 1997).

A study carried out elsewhere indicated bulk density, porosity, water holding capacity, moisture equivalent, silt and sand to account for 59 % of the variation observed in soil erosion index (Gupta et al., 2010). Organic matter content is a crucial dynamic property of soils that ensures soil stability. The exclusion of this property of soil from the regressions developed by Gupta et al., (2010) may have resulted in the low Pearson correlation coefficient recorded for soil erodibility index and soil properties. Mean soil erodibility indexes relatively indicated high values in clay loam, clay and sandy clay loam soils (Figure 5) implying high susceptibility of these soil textures to soil erosion. The low organic matter content and the least pores of these identified soil textures among other factors may account for their high susceptibility to erosion. Diop et al., (2011), also asserts that silts and certain clay textured soils are more susceptible to erosion than other textured soil types. They attributed their reasons to possibly the low infiltration rate, low organic matter content and the lack of soil structure that may be inherent in these soil texture types.

The best regression equation obtained in this study (Equation 6 in Table 4) was compared with findings from other studies (Table 5) whose regression equations were developed using a range of soil properties. It was found out that the regression equation developed in this study with six variables compared well in terms of the coefficient of

determination with regression equations developed in other studies using series of explanatory variables. The most significant variable on soil erodibility in this study was silt as compared to clay/OMC, aggregation index, particle size parameter and slope in other studies (Barnett & Rogers, 1966; Wischmeier & Mannering, 1969; Romkens et al., 1977; Young & Mutchler, 1977). The dissimilarities observed in the most significant variable influencing soil erodibility in the study results of others as compared to that in this study could be attributed to land use and underlying soil types of the study locations. Le Roux et al. (2006) also acknowledged the proneness of soils with high silt content to structural breakdown and consequently erosion. From the ongoing discussions, it presupposes that the estimation of soil erodibility depends on varying number of soil properties, here however being more dependent on silt.

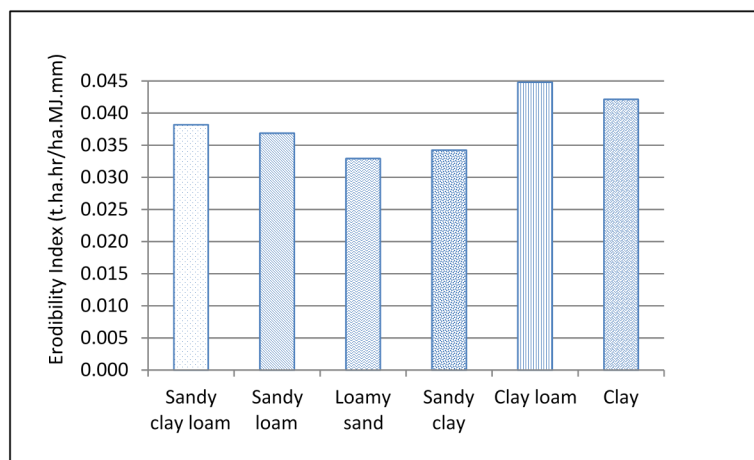


Figure 5. Susceptibility of soil textures to soil erosion

Table 4. Regression analysis of erodibility index (K) in relation to measured soil properties

Eq. No.	Dependent variable	Regression Equation ^a	R ²
1	K	$Y = 0.023 - 0.558\text{Sand}$	0.312
2	K	$Y = 0.151 + 0.121\text{Sand} + 0.95\text{Silt}$	0.758
3	K	$Y = 0.184 + 0.132\text{Sand} + 0.937\text{Silt} - 0.035\text{BD}$	0.759
4	K	$Y = 0.026 + 0.102\text{Sand} + 0.940\text{Silt} - 0.167\text{BD} + 0.178\text{PD}$	0.766
5	K	$Y = 6.584 + 0.087\text{Sand} + 0.893\text{Silt} - 9.097\text{BD} + 5.383\text{PD} - 5.114\text{Pores}$	0.779
6	K	$Y = 7.625 + 0.026\text{Sand} + 0.795\text{Silt} - 10.312\text{BD} + 6.073\text{PD} - 5.828\text{Pores} - 0.355\text{OMC}$	0.90

^a K, soil erodibility index; BD, bulk density; PD, particle density; OMC, organic matter content.

Table 5. Regression data of K values on soil properties

Study ^a	No. of soils	Variables in regression equation	R ²	Most ^b significant variable	Dominant soil texture
1	17	8	0.87	Slope	Sand
2	7	2	0.95	M	Clay
3	13	5	0.90	Agg.	Loam
4	55	24	0.98	Clay/OMC	Silt loam
This study	100	6	0.90	Silt	Sandy clay loam

^a1, Barnett and Rogers, 1966; 2, Romkens et al., 1977; 3, Young and Mutchler, 1977; 4, Wischmeier and Mannering, 1969.

^bM, particle size parameter; Agg., aggregation index; OM, organic matter content

4. Implications of Findings

The high soil erodibility observed in the study area is expected to impact negatively on water resources within the catchment area mainly through sedimentation that may arise from soil erosion. The problem of sedimentation has the tendency to reduce channel capacity of receiving rivers, cause eutrophication as a result of nutrient rich soil deposits and subsequently impact negatively on aquatic life. The cost of treating such waters for domestic water supply and irrigation purposes is expected to be high and perhaps the cost of treatment transferred unto the consumer. From the agricultural perspective, the removal of top rich nutrient soils may result in loss of vital nutrients for plants culminating into low agricultural productivity and turnover.

5. Conclusion

We examined in this study soil erodibility index at field scale and established relations between soil properties and erodibility. Estimated erodibility index for the studied field indicated a greater proportion of the field to be susceptible to erosion with high to very high erodibility index. The predisposition of soil to erosion was found to be significantly dependent on silt content of soil in addition to other soil properties. From the spatial analysis point of view, the spatial variability observed in soil erodibility index can be attributed to the varying spatial structure of studied soil properties. Geostatistical techniques viz-a-viz conventional statistical methods provided a better perspective of the role of soil properties in soil erodibility issues.

Acknowledgement

Financial support for this research was provided by Tshwane University of Technology (TUT), South Africa. The authors would also like to thank the Institute of Soil, Climate and Water of the Agricultural Research Council (ARC-ISCW) for availing their facility for the sample analysis. Mr. Smith O. O. Ojo of TUT and Mr. Simon Mampana of Department of Water Affairs, Hydrology Section are duely acknowledged for their unwavering assistances during the soil sampling phase of this work.

References

- Barnett, A. P., & Rogers, J. (1966). Soil physical properties related to runoff and erosion from artificial rainfall. *Transactions of the American Society of Agricultural Engineers*, 9(1), 123-125.
- Basson, G., & Di Silvio, G. (2008). Erosion and sediment dynamics from catchment to coast; a northern perspective and a southern perspective. Technical Documents in Hydrology No. 82 UNESCO, Paris, 2008.
- Boyd, C. E. (1995). *Bottom Soils, Sediment and Pond Aquaculture*. Chapman & Hall, New York, p. 348.
- Brady, N. C. (1984). *The Nature and Properties of Soils*. Macmillan Publishing Co., New York, p. 750.
- Breetzke, G. D., Koomen, E., & Critchley, W. R. S. (2013). GIS-Assisted modeling of soil erosion in a South African catchment: Evaluating the USLE and SLEMSA approach. In R. Wurbs (Ed.), *Water resources planning, Development and Management* (pp. 53-71). INTECH, Croatia.
- Brus, D. J., & Heuvelink, G. B. M. (2007). Optimization of sample patterns for the universal kriging of environmental variables. *Geoderma*, 138, 86-95. <http://dx.doi.org/10.1016/j.geoderma.2006.10.016>
- Cambardella, C. A., Moorman, T. B., Novak, J. M., Parkin, T. B., Karlen, D. L., Turco, R. F., & Konopka, A. E. (1994). Field-Scale variability of soil properties in Central Iowa Soils. *Soil Science Society of American Journal*, 58, 1501-1511.
- Colombo, C., Palumbo, G., Aucelli, P. P. C., De Angelis, A., & Roskopf, C. M. (2010). Relationship between soil properties, erodibility and hillslope features on central Apennines, Southern Italy. 19th World Congress of Soil Science, Soil solutions for a changing world. 1-6 August 2010, Brisbane, Australia.
- CSIR. (2003). *National Landcover dataset attributes*. Satellite Applications Centre, ICOMTEX, Council for Scientific and Industrial Research, Pretoria.
- Diop, S., Stapelberg, F., Tegegn, K., Ngubelanga, S., & Heath, L. (2011). A review on problems soils in South Africa. Council for Geoscience Report number: 2011-0062, Western cape, South Africa.
- FAO. (2002). Major soils of the world. Land and water digital media series. Food and Agricultural Organization of the United Nations. FAO, Rome.
- FAO. (2005). Digital Soil Map of the world and derived soil properties of the world. Food and Agricultural Organization of the United Nations. FAO, Rome.
- Gupta, R. D., Arora, S., Gupta, G. D., & Sumberia, N. M. (2010). Soil physical variability in relation to soil erodibility under different land uses in foothills of Siwaliks in N-W India. *Tropical Ecology*, 51(2), 183-197.

- Gyamfi, C., Ndambuki, J. M., & Salim, R.W. (2016). A Historical Analysis of Rainfall Trend in the Olifants Basin in South Africa. *Earth Science Research*, 5(1), 129-142.
- Hao, X., Ball, B.C., Culley, J. L. B., Carter, M. R., & Parkin, G. W. (2008). Soil density and porosity. In M. R. Carter, & E. G. Gregorich, (Eds.), *Soil sampling and methods of analysis* (pp. 743-759). CRC Press. New wark.
- IWMI. (2008). Baseline Report Olifants River Basin in South Africa: A contribution to the Challenge Program Project 17 “Integrated Water Resource Management for Improved Rural Livelihoods: Managing risk, mitigating drought and improving water productivity in the water scarce Limpopo Basin”.
- Kroetsch, D., & Wang, C. (2008). Particle size distribution. In M. R. Carter, & E. G. Gregorich (Eds.), *Soil sampling and methods of analysis* (pp. 713-725). CRC Press. New wark.
- Le Roux, J. J., Morgenthal, T. L., Malherbe, J., Smith, H. J., Weepener, H. L., & NEWBY, T. S. (2006). Improving spatial soil erosion indicators in South Africa. ARC-ISCW report no. GW/A/2006/51, Pretoria, South Africa.
- Liu, Z. P., Shao, M. A., & Wang, Y. Q. (2013). Spatial patterns of soil total nitrogen and soil total phosphorus across the entire Loess Plateau region of China. *Geoderma*, 197-198, 67-78.
- Liu, Z., Zhou, W., Shen, J., He, P., Lei, Q., & Liang, G. (2014). A simple assessment on spatial variability of rice yield and selected soil chemical properties of paddy fields in South China. *Geoderma*, 235-236, 39-47.
- MacCarthy, D. S., Agyare, W. A., Vlek, P. L. G., & Adiku, S. G. K. (2013). Spatial variability of some soil chemical and physical properties of an Agricultural landscape. *West African Journal of Applied Ecology*, 21(2), 47-61.
- Matheron, G. (1963). Principles of geostatistics. *Economic Geology*, 58, 1246-1266.
- Meadows, M. E. (2003). Soil erosion in the Swartland, Western Cape Province, South Africa: Implications of past and present policy and practice. *Environmental Science and Pollution*, 6, 17-28.
- Ortiz, B. V., Perry, C., Goovaerts, P., Vellidis, G., & Sullivan, D. (2010). Geostatistical modeling of the spatial variability and risk areas of Southern root-knot nematodes in relation to soil properties. *Geoderma*, 156, 243-252.
- Pansu, M., & Gautheyrou, J. (2006). Handbook of Soil Analysis, Mineralogical, Organic and Inorganic methods. Springer, Berlin Heidelberg New York.
- Pennock, D., Yates, T., & Braidek, J. (2008). Soil sampling designs. In M. R. Carter, & E. G. Gregorich (Eds.), *Soil sampling and methods of analysis* (pp. 1-14). CRC Press. New wark.
- Pimental, D., Harvey, C., Resosudarmo, P., Sinclair, K., Kurz, D., McNair, M.,... Blair, R. (1995). Environmental and economic costs of soil erosion and conservation benefits. *Science*, 267, 1117-1124.
- Römkens, M. J. M., Roth, C. B., & Nelson, D. W. (1977). Erodibility of selected clay subsoils in relation to physical and chemical properties. *Soil Science Society of American Journal*, 41(5), 954-960.
- Ruth, B., & Lennartz, B. (2008). Spatial variability of soil properties and rice yield along two catenas in Southeast China. *Pedosphere*, 18(4), 409-420.
- Torri, D., Poesen, J., & Borselli, L. (1997). Predictability and uncertainty of the soil erodibility factor using a global dataset. *Catena*, 31, 1-22.
- Toy, T. J., Foster, G. R., & Renard, K. G. (2002). Soil erosion: processes, prediction, measurement and control. John Wiley & Sons, Inc. New York. USA.
- Virgilio, N. D., Monti, A., & Venturi, G. (2007). Spatial variability of switchgrass (*Panicum virgatum*L.) yield as related to soil parameters in a smallfield. *Field Crop Research*, 101, 232-239.
- Walkley, A., & Black, I. A. (1934). An examination of Degtjareff method for determining soil organic matter and a proposed modification of the chromic acid titration method. *Soil Science*, 37, 29-37.
- Wang, B., Zheng, F., Romkens, M. J. M., & Darboux, F. (2013). Soil erodibility for water erosion: A perspective and chinese experiences. *Geomorphology*, 187, 1-10.
- Williams, J. R. (1995). The EPIC model. In V. P. Singh (Ed.), *Computer models of watershed hydrology* (pp. 909-1000). Water Resouces publication, Highlands Ranck, CO.
- Wischmeier, W. H., & Mannering, J. V. (1969). Relation of soil properties to its erodibility. *Soil Science Society of American Journal*, 33(1), 131-137.

- Wischmeier, W. H., & Smith, D. D. (1978). Predicting rainfall erosion losses: a guide to conservation planning. Agriculture Handbook 282.USDA-ARS.
- Wu, C. F., Luo, Y. M., & Zhang, L. M. (2010). Variability of copper availability in paddy fields in relation to selected soil properties in southeast China. *Geoderma*, 156, 200-206.
- Young, R. A., & Mutchler, C. K. (1977). Erodibility of some Minnesota soils. *Journal of Soil and Water Conservation*, 32, 180-182.

Copyrights

Copyright for this article is retained by the author(s), with first publication rights granted to the journal.

This is an open-access article distributed under the terms and conditions of the Creative Commons Attribution license (<http://creativecommons.org/licenses/by/3.0/>).

Assessment of a Regional-Scale Weather Model for Hydrological Applications in South Korea

Yong Jung¹ & Yuh-Lang Lin²

¹ Department of Civil and Environmental Engineering, Wonkwang University, Korea

² Department of Energy & Environmental Systems, North Carolina A&T State University, USA

Correspondence: Yuh-Lang Lin, Department of Energy & Environmental Systems, North Carolina A&T State University, USA. E-mail: ylin@ncat.edu

Received: February 22, 2016 Accepted: March 3, 2016 Online Published: March 17, 2016

doi:10.5539/enrr.v6n2p28

URL: <http://dx.doi.org/10.5539/enrr.v6n2p28>

Abstract

In this study, a regional numerical weather prediction (NWP) model known as the Weather Research Forecasting (WRF) model was adopted to improve the quantitative precipitation forecasts (QPF) by optimizing combined microphysics and cumulus parameterization schemes. Four locations in two regions (plain region for Sangkeug and Imsil; mountainous region for Dongchun and Bunchun) in Korean Peninsula were examined for QPF for two heavy rainfall events 2006 and 2008. The maximum Index of Agreement (IOA) was 0.96 at Bunchun in 2006 using the combined Thompson microphysics and the Grell cumulus parameterization schemes. Sensitivity of QPF on domain size at Sangkeug indicated that the localized smaller domain had 55% (from 0.35 to 0.90) improved precipitation accuracy based on IOA of 2008. For the July 2006 Sangkeug event, the sensitivity to cumulus parameterization schemes for precipitation prediction cannot be ignored with finer resolutions. In mountainous region, the combined Thompson microphysics and Grell cumulus parameterization schemes make a better quantitative precipitation forecast, while in plain region, the combined Thompson microphysics and Kain-Frisch cumulus parameterization schemes are the best.

Keywords: regional numerical weather prediction model, quantitative precipitation forecast, localized conditions, mountainous region, hydrology

1. Introduction

Flooding is one of the major natural hazards associated with extreme weather events, such as tropical cyclones and snowstorms, because it accounts for a large proportion (30% in Asia from 1990 to 2011; EM-DAT 2014) of total disasters (Dolcine et al., 2001; Hudson & Colditz, 2003). In the past decade, flood modeling prediction has been improved through the application of various technologies. Having been implemented in the U.S. and other countries, an advanced next generation Doppler weather radar system known as NEXRAD (WSR-88D) has become a popular way of monitoring weather systems. In terms of lead time for QPF, Bedient et al. (2003) asserted that two or three hours were gained when NEXRAD was adopted in the flood warning system. These lead times can be used in the conversion process from the NEXRAD rainfall time series to a flood inundation map, especially for extreme flood events (Knebl et al., 2005). Unfortunately, the lead time of QPF by including NEXRAD in the flood warning system does not apply to mountainous watershed regions due to shorter flow travel times (Anderson et al., 2002; Yoshitani et al., 2009).

As a result, some researchers have adopted numerical weather prediction (NWP) models to extend the lead time to one or two days for flood forecasting at small mountainous watersheds (Anderson et al., 2002; Yoshitani et al., 2009). For example, the Penn State-NCAR fifth generation Mesoscale Model (MM5, see Grell et al., 1995) and the Weather Research Forecast (WRF, see Skamarock et al., 2008) model have been used for QPF in flood prediction. Yu et al. (1999) used MM5 with fixed parameterizations (multi-level Blackadar type planetary boundary layer and Grell cumulus parameterizations) for the Upper West Branch of the Susquehanna River Basin at Williamsport, Pennsylvania. In addition, Westrick et al. (2002) and Anderson et al. (2002) utilized MM5 for rainfall predictions in the western U.S., specifically along the western flanks of the Washington Cascade Mountains and the Calaveras River Basin in central California. These types of NWP models have also been used in Korea (Hong & Lee, 2009) and Japan (Yoshitani et al., 2009).

In regionalized NWP model applications, high spatial and temporal variability in QPF for different regions with diverse climate conditions make a regional-scale NWP model very sensitive to model configurations (Giorgi & Mearns, 1999) such as cumulus and microphysics parameter schemes. In applying the WRF model in a hydrological model, Lowrey and Yang (2008) evaluated both physical parameterization schemes for QPF using a 2002 central Texas storm event in the San Antonio River Basin. Sensitivity tests for combinations of physics parameterization schemes have also been performed for rainfall estimation (Evans et al., 2012) and winter precipitation estimation (Yuan et al., 2012). Both studies found deficiencies in applying the best physics scheme combinations for rainfall estimation (Ji et al., 2013). Based on previous studies, a regional-scale NWP model with selected model configurations can provide acceptable lead time with reasonable accuracy for QPF. However, there have been few applications of regional-scale NWP models, such as WRF, to hydrological aspects of the Korean Peninsula. The major purpose of this study is to investigate the applicability of the WRF model (Skamarock et al., 2008) to the Korean Peninsula using two July storms for years 2006 and 2008 and to present better options for diverse terrain conditions. In addition, comparisons with diverse grid sizes are presented to provide the most favorable resolution for the central Korean Peninsula.

2. Description of the WRF model

In this study, the WRF model v3.1, which is also called the Advanced Research WRF (ARW) model, was used to predict regional-scale precipitation for hydrological applications. WRF v3.1 has been updated for satellite imagery-based land use categories instead of USGS categories, generalized soil moisture and temperature arrays in three dimensions, and fixed interpolation schemes from previous versions. The WRF models have various options in numerical schemes, physics representations and parameterizations, and data assimilation packages for real-time NWP, thus allow parameterization sensitivity tests and idealized numerical simulations to be conducted. In addition, the WRF model conserves mass, momentum, and entropy in prognostic equations to generate spurious oscillations and numerical smoothing, whereas MM5 has no conservational property (Pattanayak & Mohanty, 2008). In various model evaluations, Sousounis et al. (2004) performed NWP model intercomparisons among MM5, WRF, RUC, and ETA models to simulate heavy rainfall events in 2003 and concluded that WRF and MM5 provided the greatest number of configurations and were more applicable than other models. Furthermore, they indicated that the WRF model generated finer-scale structures closer to realistic conditions than those in other models. In the comparison between WRF and MM5 performances for cyclones in 2006 over the Indian Ocean, the WRF model makes better prediction in terms of their track and intensity (Pattanayak & Mohanty, 2008).

There are two substantial physical parameterization schemes of the WRF model that deal with atmospheric heat and moisture flux tendencies thus have direct impacts on QPF: cumulus parameterization and microphysics parameterization. Generally, cumulus parameterization is not necessary for a grid size (grid scale) less than 3 or 4 km because mesoscale processes and motion can be approximately resolved by the grid size (Gilliland & Rowe, 2007). However, in order to avoid the energy accumulation at grid points, cumulus parameterization is commonly activated simultaneously with microphysics parameterization for rainfall prediction for simulations with grid size of 4 km or even smaller, especially when the grid size falls in the so-called “no-man’s land” or “gray zone” (1 – 10 km, based on Gerard, 2007).. On the other hand, Clark et al. (2007) demonstrated that the diurnal precipitation cycle was better simulated using convection resolving microphysics schemes than non-convection-resolving cumulus parameterization scheme. Thus, in this study, we will test both approaches for finer-scale grid intervals, namely activating cumulus and microphysics parameterizations or using microphysics parameterization alone. The cumulus parameterization scheme will be chosen from Betts-Miller-Janjic (BMJ) scheme (Betts and Miller, 1993; Janjic, 1994), Grell 3D ensemble scheme (Grell & Devenyi, 2002), or Kain-Fritsch (new Eta) scheme (Kain & Fritsch, 1990; Kain, 2004). The BMJ scheme is a column moisture adjustment scheme with relaxation to a well-mixed profile in an operational Eta structure. The Grell 3D ensemble scheme includes subsidence in neighboring column thus is more appropriate for higher resolution simulations. The Kain-Frisch scheme is a sub-grid scheme with deep and shallow convection, a maximum flux approach in applications of downdrafts, and the Convective Available Potential Energy (CAPE) removal time scale (Lin, 2007).

Regarding microphysical parameterizations, we applied either Purdue Lin scheme (Lin et al., 1983 – Lin-Farley-Orville scheme; Chen and Sun, 2002), Thompson scheme (Thompson et al., 2004), or the Single-Moment 6-class microphysics scheme (WSM-6, Hong & Lim, 2006). All of the selected schemes include ice phase, i.e. ice, snow, and graupel/hail hydrometers in the microphysical processes thus are appropriate for simulating mid latitude deep convective clouds and smaller grid simulations. Microphysics parameterization schemes dictate properties and structures of cloud within meso- and cloud-scale models and thus dominate the evolution (e.g. generation, growth, decay, and fall) of precipitation using different categories (cloud ice, graupel/hail, and snow) of the ice phase.

The National Center for Environmental Prediction (NCEP) FNL (Final) Operational Global Analysis Data prepared every six hours with 1.0 by 1.0 degree grids was used to initialize and update the boundary conditions of the WRF model. These data were obtained from the Global Data Assimilation System (GDAS) using data from diverse sources such as the Global Telecommunication System (GTS). These FNL data consist of surface pressure, sea level pressure, sea surface temperature, geopotential height, temperature, soil moisture, ice cover, relative humidity, and u - and v -winds, at 26 mandatory stretching levels between 10mb and 1000mb.

3. Experimental Design

3.1 Regions of Study

To assess the capability of WRF applications for hydrological aspects, four specific locations, i.e. Sangkeug, Dongchun, Imsil and Bunchun, were selected (Figure 1). These four selected locations have the following geographical characteristics: plain area located in middle of Korean Peninsula (Sangkeug), surrounded by mountains (Dongchun), plain area (Imsil), and high mountains area near the east coast (Bunchun). These diverse characteristics may require different combinations of physical parameterization schemes including ensemble approaches in the WRF model for QPF targeted for hydrological applications. Table 1 summarizes the characteristics of the four selected rainfall sites. In fact, these four locations can be categorized in two regions, namely the plain region for Sangkeug and Imsil, and the mountainous region for Dongchun and Bunchun.

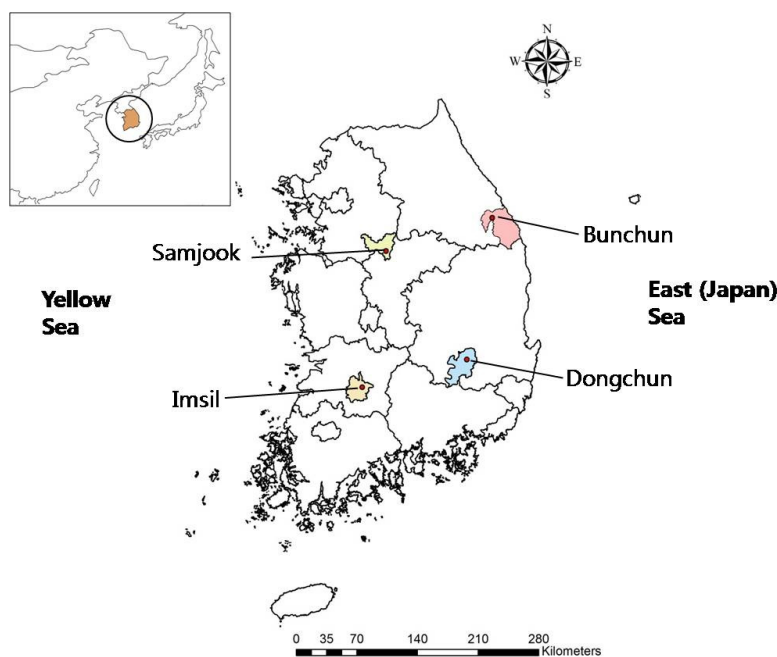


Figure 1. Four locations in two regions (plain region for Sangkeug and Imsil; mountainous region for Dongchun and Bunchun) in Korean Peninsula were selected for the evaluation of hydrological applications using WRF to make QPF for two heavy rainfall events 2006 and 2008

Table 1. Characteristics of four selected observatories

Observatory	Associated River Basin	Characteristic
Sangkeug	Chongmi River Basin (~600 km ²)	Plain Area located in the middle of Korean Peninsula
Dongchun	Kumho River Basin (~1000 km ²)	Surrounded by mountains
Imsil	Ohsoo River Basin (~370 km ²)	Plain Area
Bunchun	Colji River Basin (~560 km ²)	High mountain Area located near east side of Korean peninsula

For simulations using the WRF v3.1 model, three nested domains with two-way interactions (Figure 2) were selected to predict precipitation with relatively finer resolution. The grid sizes were 36 km, 12 km, and 4 km for the outer (D1), middle (D2), and inner (D3) domains, respectively. Domain D1 has 71x67 grid points in the south-north (SN) and west-east (WE) directions and is centered at (127.169°E, 37.561°N). Domain 2, which was embedded in D1, has 109 (SN) by 94 (WE) grid points. Domain 3, which was used for rainfall estimation as input data of hydrological models, has 97 (SN) by 157 (WE) grid points. Note that D3 covered the whole South Korea (Figure 2), including four selected locations and had a 4 km grid resolution (Figure 1). The map projections for these domains were Mercator.

3.2 Simulations

In order to predict precipitation for 2006 and 2008 storm events, 9 different combinations of physics parameterizations were examined to identify the better conditions for rainfall in a specific area because the accuracy of rainfall prediction is strongly influenced by regional and climate characteristics (Giorgi and Mearns, 1999). In addition, the planetary boundary layer (PBL) parameterization, domain and buffer zone, and initialization scheme are substantial components of regional climate models. PBL schemes calculate vertical fluxes of heat, moisture and momentum in the planetary boundary layer. In this study, the Yonsei University (YSU) PBL scheme (Hong et al., 2006), a non-local K-theory (eddy coefficient) scheme including explicit entrainment layer and parabolic K profile in the mixed layer, was selected for all tests. Table 2 shows different combinations of physics parameterizations in the WRF model chosen for testing in this study.

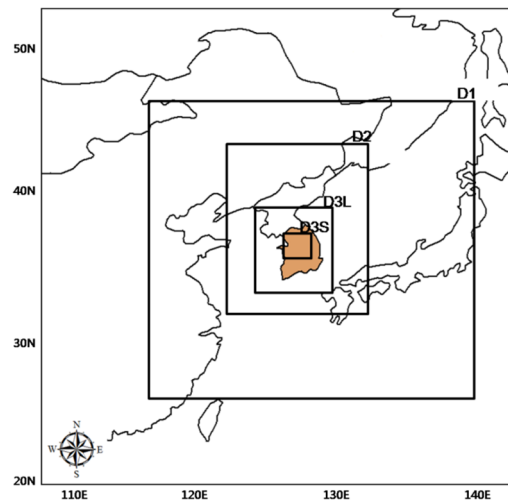


Figure 2. Three nested domains in Korean Peninsula designed for WRF simulations (D3L: Larger Domain 3, D3S: Smaller Domain 3)

Table 2. Combinations of microphysics and cumulus parameterizations for the regional scale weather model simulations for precipitation prediction

Acronym	Microphysics	Cumulus
LB	Purdue Lin scheme	Betts-Miller-Janjic scheme
LG	Purdue Lin scheme	Grell 3D ensemble scheme
LK	Purdue Lin scheme	Kain-Frisch scheme
TB	Thompson scheme	Betts-Miller-Janjic scheme
TG	Thompson scheme	Grell 3D ensemble scheme
TK	Thompson scheme	Kain-Frisch scheme
WB	WSM-6 scheme	Betts-Miller-Janjic scheme
WG	WSM-6 scheme	Grell 3D ensemble scheme
WK	WSM-6 scheme	Kain-Frisch scheme

Note. The YSU PBL scheme is used for all experiments listed above.

3.3 Storm Events

During the summer season from June to August in South Korea, most of heavy rainfall events are attributed to cloud clusters and local convection associated with summer monsoons. In this study, we considered two heavy rainfall events with the following simulation time periods, 00 UTC July 9 – 00 UTC July 22, 2006 (14 days) and 00 UTC July 10 – 00 UTC July 28, 2008 (19 days), including 3 days for spin-up time, to search for the optimal precipitation prediction at certain points using the WRF model with 6 hourly updates from NCEP FNL data. Although the selected 2006 and 2008 storm events were associated with typhoons, the heavy rainfall produced were not associated with typhoon rain bands directly (Lee et al., 1988). The predicted rainfall rates from the WRF model initialized by the FNL data required several conversion steps in the hydrologic models as one of the grid cell parameter files. The predicted rainfall rates have a format of network common data form (NetCDF). Observed rainfall rates are provided by the Water Management Information System (WAMIS) through Automated Weather Stations (AWS).

3.4 Hydrological Application

Once rainfall is predicted by the WRF model, its data was then used to start the simulations of the hydrologic model, i.e. the Hydrologic Engineering Center (HEC) – Hydrologic Modeling System (HMS) in this case. For applications of gridded rainfall data in the Modified Clark (also known as ModClark) unit hydrograph method, the distributed hydrologic model environment was provided by HEC-geoHMS prior to HMS operation for preprocessing of the data, and terrain and basin processing for HMS model setting. Terrain processing was based on the Digital Elevation Model (DEM) generated from numerical map by the National Geographic Information Institute in Korea. In addition, soil types and land cover information were obtained from the Water Management Information System (WAMIS, <http://wamis.go.kr/eng/main.aspx>) in the Ministry of Land and then converted to the United States Department of Agriculture Soil Conservation Service Curve Number System for rainfall-runoff. Before the hydrologic simulations, calibration processes of a hydrological model were required. For this process, observed rainfall data storage system (DSS) files were applied as gridded rainfall information. Using the optimization function such as univariate gradient procedure, time of concentration and the storage coefficient were obtained while minimizing the difference between observed and calculated discharge values. Based on the AMC-II of the Natural Resources Conservation Service (NRCS)'s standard antecedent moisture conditions, the initial abstraction rate and the potential abstraction scale factor were tweaked manually. AMC-II represents the average of antecedent moisture conditions. Finalized parameter values were adopted to make a calibrated model. For the four previously selected sites, the Chongmi River Basin was chosen for potential hydrological predictions. Figure 3 shows the watershed map file of the Chongmi River Basin. The predicted discharge values are then compared with the observed discharge values obtained from WAMIS.

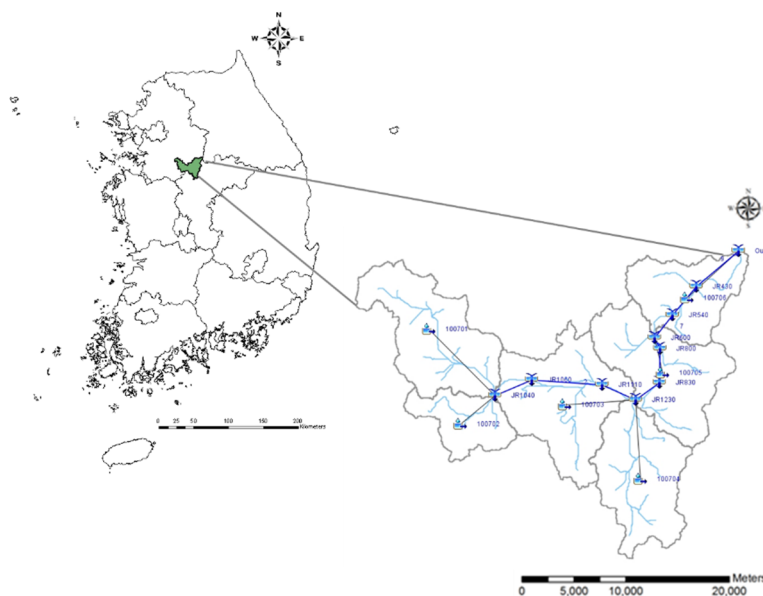


Figure 3. The watershed map of the Chongmi River Basin for hydrological applications

3.5 Error Metrics

For comparison, three numerical indicators were used; Root Mean Square Error (RMSE), Index of Agreement (IOA), and Mean Bias Deviation (MBD). RMSE and IOA represent the degree of agreement of the calculated and observed rainfall data, while MBD characterizes the bias of WRF simulations. Minimum RMSE values in terms of precipitation indicate better simulations in WRF applications. The IOA value is between 0 and 1, with a value closer to 1 indicating that the simulation is better matched to observations. A negative (positive) MBD value indicates that the simulations are under-predicted (over-predicted). In this study, the WRF predicted rainfall data were verified by the observational data (i.e. daily rainfall) from four selected sites. Since the grid points of rainfall prediction from the WRF model did not match exactly the locations of rainfall observation, they are averaged over the nine surrounding grid points for comparisons. There were a total of 44 (11 days/location \times 4 locations) comparisons and 64 (16 days/location \times 4 locations) rainfall data sets for 2006 and 2008, respectively. Note that to improve the accuracy, a test on nearest neighborhood or bilinear interpolation may be used. This will be considered in a follow-up study.

These numerical indicators are defined as follows:

$$IOA = 1 - \frac{\sum_{i=1}^N (Model_i - Obs_i)^2}{\sum_{i=1}^N (|Model_i - AVG(Obs)| + |Obs_i - AVG(Obs)|)^2} \quad (1)$$

$$MBD = \frac{\frac{1}{N} \sum_{i=1}^N (Model_i - Obs_i)}{\frac{1}{N} \sum_{i=1}^N Obs_i} \quad (2)$$

where

$Model_i$: WRF model predicted rainfall rate (mm/d) at location i

Obs_i : Observed rainfall rate (mm/d) at location i

AVG : Averaged value

N : Total number of observations or predictions

4. Results and Discussions

The rainfall rates predicted by WRF simulations using 9 combinations of microphysics and cumulus parameterization schemes were compared with observations (Figure 4). Note that the observed rainfall rates at Sangkeug, which is on a plain area near central Korean Peninsula, had two minor peaks of approximately 100 and 130 mm/d, respectively, on 14 and 16 July 2006. Note that none of the simulated results followed this observed trend. In particular, WB (WSM-6 - BMJ schemes; see Table 2 for acronyms hereafter) schemes showed an unusually high rainfall rate of approximately 470 mm/d on July 15. On the other hand, most of the other simulations provided better rainfall rate on July 15 comparable to the observed rainfall rate. The heavy rainfall rate on 16 July 2006 was attributed to the local orographic uplifting associated with the mountain range to the west of South Korea and the anti-cyclonic circulation associated with Gaema Heights in North Korea (Hong & Lee, 2009). However, precipitation in 2008 was not as intense as in 2006, in terms of the maximum daily rainfall. Maximum daily rainfalls were 66 mm/d on 19 July 2008 and 115 mm/d on 16 July 2006. In general, LB schemes followed this observed rainfall trend better than other scheme combinations, although the two peak rainfall rates did not match the observed rates. The first peak value was under-predicted, while the second peak was over-predicted by a rate of about 20 mm/d. In addition, the model-simulated time for these two rainfall peaks were delayed by one to two days.

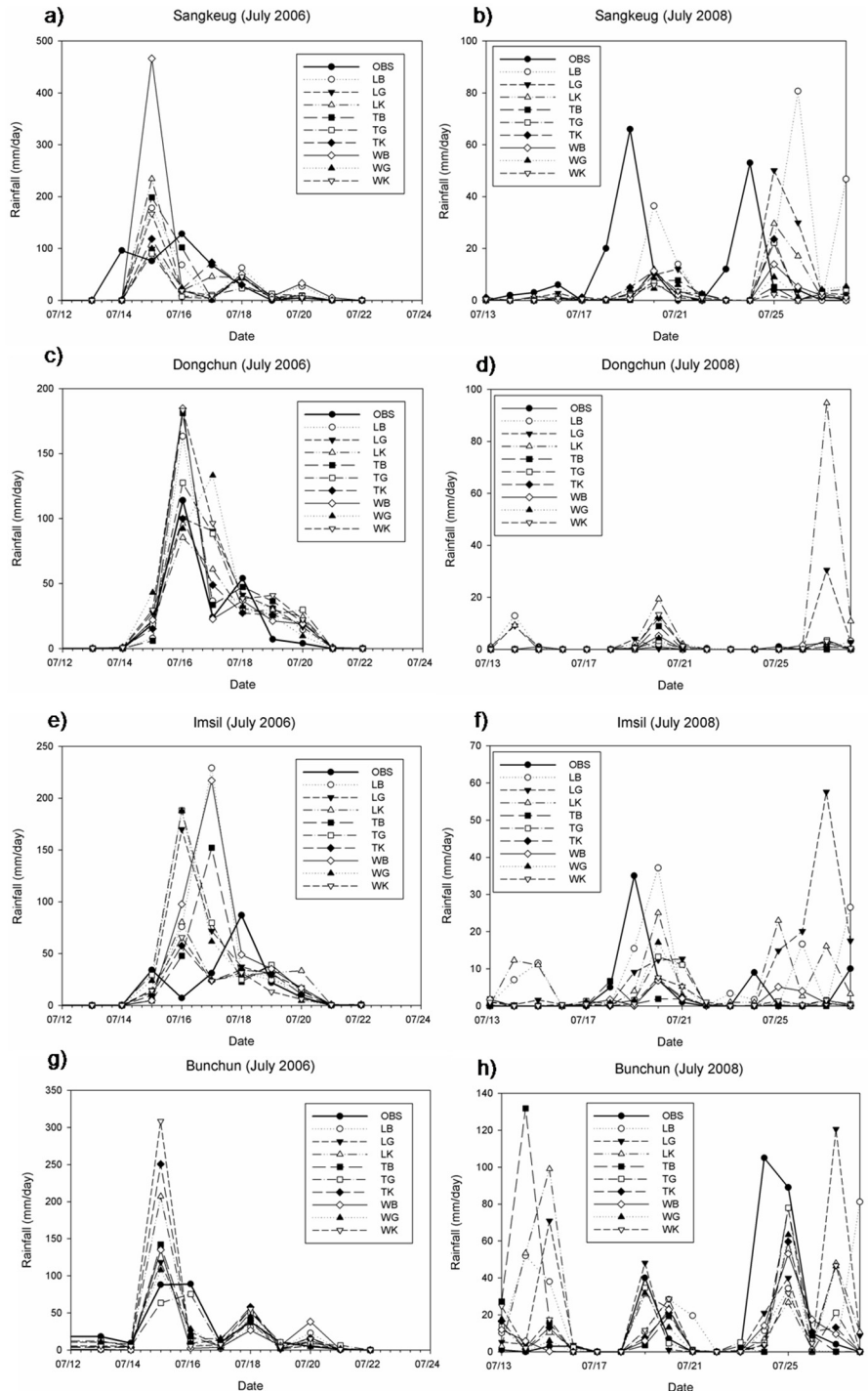


Figure 4. Comparison of observed daily rainfall rate with those predicted by WRF with various combinations of microphysics and cumulus parameterization schemes (See Table 2 for acronyms.)

For the second rainfall peak, LG simulated a mostly comparable daily rainfall rate with some delay. At Dongchun, which is surrounded by mountains, the 2006 prediction matched the observations closely, with two peaks occurring on July 16 and 18. Schemes TG appears to have best matched observations making it the better combination of physics parameterizations. Schemes WB followed the observation trend well with one higher and one lower rainfall peaks on July 18. In 2008, there was no substantial rate of rainfall observed at Dongchun; however, WRF predicted three different rainfall peaks on July 14, 20, and 27. In particular, on July 27, LK simulated a much higher precipitation (95 mm/d) than the observation (1 mm/d). Most of the 2006 predictions for Imsil, which is

located in the plain area, significantly over-predicted the rainfall, especially on July 17. Schemes LB and schemes WB predicted a peak rainfall greater than 200 mm/d for July 17, which may cause false flood warning in reality. Schemes LG, TG, and WG simulated unreasonable peak rainfall (approximately 190 mm/d) for July 16. For the 2008 event, there were three rainfall peaks observed on July 19, 24, and 28. From observations, the maximum daily rainfall rate was 35 mm/d on July 19. Schemes LB simulated a peak rainfall rate very close to the observation, though with some date discrepancy (1 day delay). The date discrepancy might be due to the spin-up of the precipitating system by the model, but could also be caused by other factors, such as imperfections in initial and boundary conditions, and model numeric, and chaotic behavior of the atmosphere etc. On July 27, a maximum daily rainfall peak was predicted, but no rainfall was observed in reality. Optimal predictions following the trend of observations were obtained for Bunchun, located in Kangwon Province on the east side of Korean Peninsula, for both 2006 and 2008. In 2006, two equal rates of approximately 89 mm/d were obtained on July 15 and 16. Another daily rainfall peak was observed two days later on July 18. In this event, schemes TG matched the observed trend very closely except for July 20. However, the rainfall difference was insignificant. Schemes WK, TK, and LK predicted excessive rates of daily rainfall for 15 July 2008, which were two to three times higher than observations. In particular, the daily rainfall rate predicted by schemes WK may mislead decision makers to send false warning for flood evacuations because this high rainfall rate (over 300 mm/d) could be able to generate severe flooding. For 2008, the rainfall predicted by schemes TG matched closely the trend of rainfall observations. However, this prediction strongly underestimated the daily rainfall on July 24 because the difference in the rainfall rates between schemes TG and observations was greater than 100 mm/d.

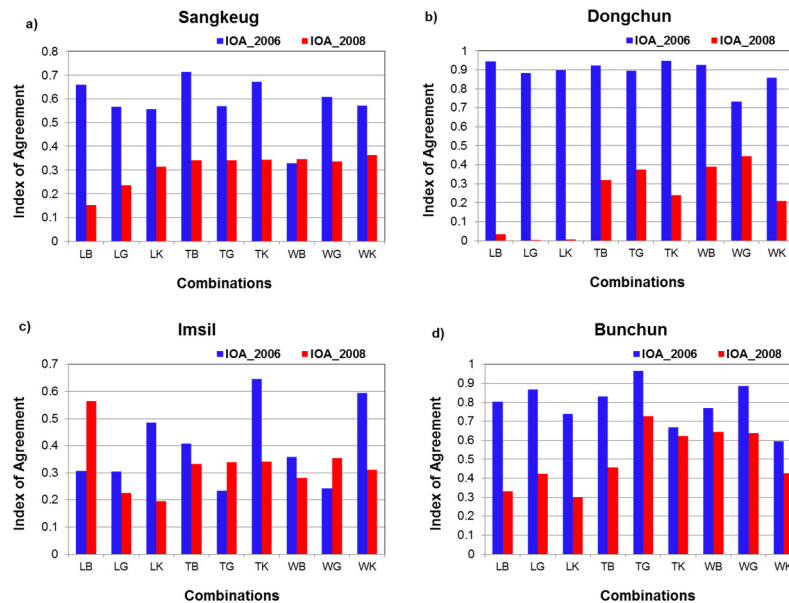


Figure 5. Index of Agreement (IOA) between observed and simulated rainfall rates

For more objective validations, index of agreement (IOA) were adopted for the comparisons (Figure 5). The selection of the better combinations of microphysics and cumulus parameterizations at each location was required to simultaneously determine data for both years 2006 and 2008. For Sangkeug, schemes TB and TK were selected as a better combination of schemes. Schemes LB was not selected because it had higher IOA in 2006 (~0.68), but a very low IOA in 2008 (~0.15). Schemes WB showed potential to be a better combination with the lowest IOA. Dongchun, a station surrounded by mountains, had both schemes TG and WB as a better combination for both years. In 2006, schemes LB, TK, and WB simulated an IOA greater than 0.9 at Dongchun, but LB and TK did not perform consistently in 2008. For Imsil, Kain-Frisch cumulus parameterization scheme had significant impacts on QPF. Schemes TK and WK combinations for 2006 showed the highest IOA (over 0.6). For Sangkeug, LB worked well in 2006 but not in 2008. For Bunchun, a station located on the east side of Korean Peninsula with high mountains, the Grell 3D ensemble cumulus parameterization scheme was a key physical option because it generated a precipitation rate closest to the observations for both years. In particular, TG showed a maximum IOA near 1 with a minimum RMSE for both 2006 and 2008. Combinations of WG and WB generated good IOA greater than 0.8 for 2006 and about 0.6 for 2008. Generally, the Purdue Lin scheme (Lin et al., 1983; Chen & Sun 2002)

with diverse cumulus parameterization options did not make a precipitation prediction close to observations for any of the four locations in either year.

Figure 6 shows the mean bias deviations of WRF simulated rainfall rates using different combinations of microphysics and cumulus parameterization schemes. The mean bias deviation (MBD) values were produced by average of 2006 and 2008 MBDs at each category of locations (mountainous and plain areas). For mountainous area, all of combined schemes over predicted the rainfall, compared to the observed rainfall data. Especially, the combination of Kain-Miller-Janjic cumulus parameterization scheme and Lin et al. microphysics scheme predicted over 11 times larger difference to the observations. The minimum biased combinations in mountainous area were TG and WG (0.34). In plain area, rainfall values were estimated negatively at some combinations (LK, TB, TG, TK, WG, WK). Lin et al. microphysics and Kain-Miller-Janjic cumulus parameterization schemes especially generated the minimum biased estimation. The maximum biased rainfall values were found at WK combination with -0.52 MBD. In terms of the magnitude of mean bias, mountainous area presented some difficulties for rainfall prediction. Based on RMSE, IOA, and MBD, for mountainous regions (Dongchun and Bunchun), the Grell 3D ensemble cumulus parameterization and Thompson microphysics schemes performed best compared to other combined schemes; while for plain areas (Sangkeug, Imsil), the Kain-Frisch cumulus parameterization and Thompson microphysics schemes performed best compared to other combined schemes.

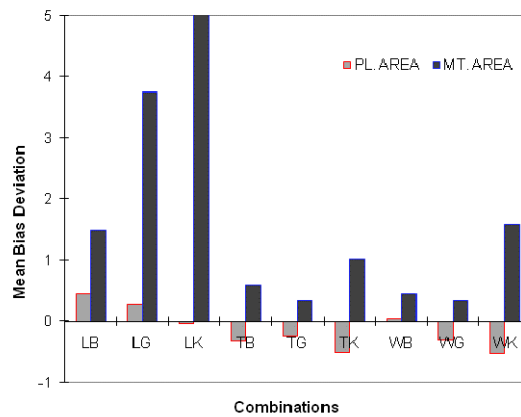


Figure 6. Mean bias deviation (MBD) for model simulated rainfall rates using nine combined microphysics-cumulus parameterization schemes

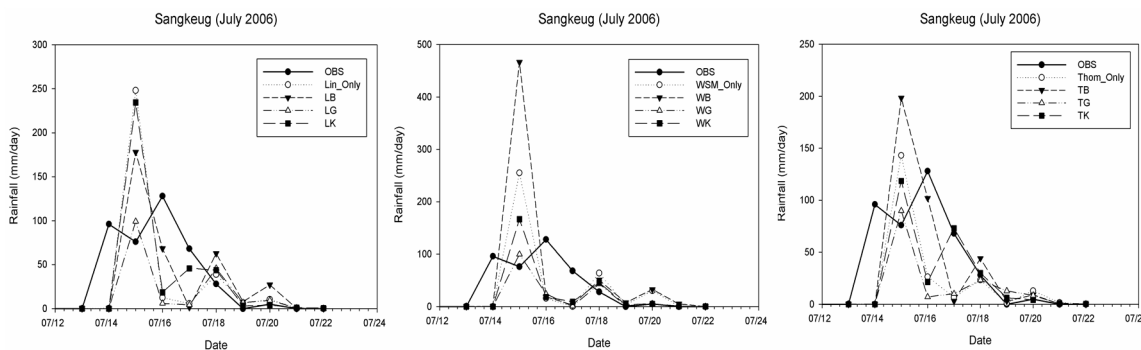


Figure 7. Sensitivity tests for cumulus parameterization functions at Sangkeug for the July 2006 storm event. (Lin_Only, Thom_Only, and WSM_Only indicate that results predicted by only include microphysics, but no cumulus, parameterization scheme.)

In simulations with finer resolutions (4 km), cumulus parameterizations played important roles in QPF, which are contrasted with comments, i.e. cumulus parameterization is not necessary for simulation with grid sizes finer than 4-5 km, made by some researchers (e.g. Gilliland & Rowe 2007). Figure 7 shows the sensitivity test for the cumulus parameterization scheme at Sangkeug for the July 2006 event. Based on these results, it appears that the cumulus parameterization schemes play considerable roles in the prediction of maximum rainfall rates. In particular, the

Betts-Miller-Janjic cumulus parameterization scheme coupled with the WSM microphysics scheme in the third panel produced two orders of magnitude difference in the maximum rainfall estimation on day 15. Furthermore, a cumulus parameterization scheme coupled with a PBL scheme is highly sensitive compared to the coupling with a microphysics scheme for warm season precipitation predictions (Lowrey & Yang 2008).

Hong and Lee (2009) proposed the possibility of highly localized rainfall events when 2006 storms were analyzed for Korean Peninsula. Based on their finding, a minimal domain size (45 by 45 with 4 km resolution, Figure 2) for the third nest near Sangkeug Station was applied to QPF. Figure 8 shows the results using a smaller inner domain compared with former simulations for Sangkeug Station for July 2006 and 2008. The smaller inner domain substantially improved the QPF. For the 2006 event, a smaller inner domain predicted precipitation rate over 0.8 IOA, which is approximately 0.2 units greater than that using the previous domain size. An appreciable improvement can be found in the 2008 results by using a smaller inner domain size. The IOA of 2008 simulated rainfall rates with a larger domain was between 0.3 and 0.4; however, an IOA greater than 0.9 was generated by TK_S using a smaller inner domain. The above results imply that a smaller inner domain can improve the ability of a regional-scale numerical weather model to predict precipitation rate for flood prediction. In the study of Lowery and Yang (2008), the relative domain size and locations are emphasized because these are the substantial factors in the localized rainfall estimation.

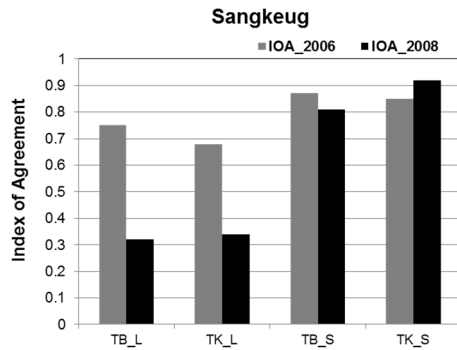


Figure 8. IOA comparisons between rainfall rates predicted by a larger domain and a smaller inner domain (TB_L, TK_L: combinations with large domain; TB_S, TK_S: combinations with localized smaller domain)

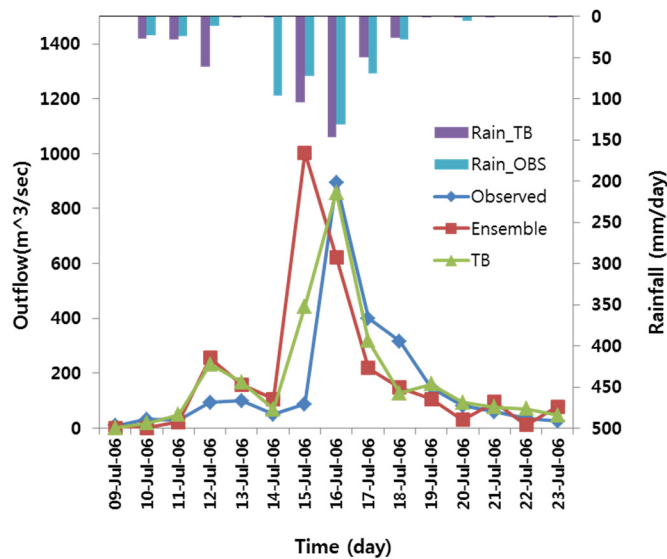


Figure 9. Comparison of discharge values for a 2006 rainfall event from the smaller domain at the Chongmi River Basin

The 2006 rainfall rates predicted by the smaller domain size in the combined Thompson-Betts-Miller-Janjic parameterization schemes were adopted to predict the rainfall-runoff response (Figure 9). Based on the optimized hydrological conditions, rainfall rates predicted by TB produced closely matched peak outflow at discharge point in the Chongmi River Basin on July 16. However, the discharge predicted from TB on July 15 was four times higher than the observed discharge. In addition, TB generated a larger discharge increase between July 11 and 12. Ensemble rainfall data (averaged rainfall amount) produced a greater than $100 \text{ m}^3 / \text{sec}$ higher peak discharge with one day earlier than the observed peak discharge. The predicted discharge values matched closely with the trend of observed discharge in both cases, which indicate the possibility of rainfall prediction by the WRF model and the discharge trend for flood event could be obtained prior to the extreme flood event. For more precise flood event alert, hourly time interval might be required especially mountainous regions.

4. Conclusions and Recommendations

In the assessment of a regional-scale weather prediction (WRF) model for hydrological applications in South Korea, diverse model configurations have been tested. Nine combinations of microphysics and cumulus parameterization schemes were evaluated for four selected locations, Sangkeug, Dongchun, Imsil, and Buchun using two storm events occurred in 2006 and 2008. Both Index of Agreement (IOA) and Root Mean Square Error (RMSE) are adopted to make objective analysis of the accuracy of quantitative precipitation forecast (QPF).

It was found that the better cumulus-microphysics parameterization (cumulus parameterization-microphysics) schemes are sensitive to the locations. In the mountainous regions (Dongchun, Bunchun), Thompson microphysics and Grell 3D Ensemble cumulus parameterization schemes performed better than other scheme combination, while the Thompson microphysics and Kain-Frisch cumulus parameterization schemes were selected for plain regions (Sangkeug, Imsil) for given flood events (summer of 2006 and 2008). Most of the 2006 predicted rainfall rates closely matched the observations as measured by IOA. The model simulated maximum IOA of rainfall rates in 2006 and 2008 at Bunchun was generated using the Thompson microphysics and Grell 3D ensemble cumulus parameterization schemes. Both physics parameterizations were more relevant to rainfall prediction. Based on the results predicted by these combinations, a smaller inner domain size (third nested domain) at Sangkeug was used for sensitivity tests to determine the effects of domain size on precipitation prediction. A smaller inner domain was found to substantially improve precipitation prediction, especially for 2008 events. In terms of IOA, the rainfall rate prediction was improved by more than 50 percent using a smaller inner domain. These results demonstrated that a regional-scale numerical weather prediction model with the specific combination of physical parameterizations and a smaller inner domain may significantly improve QPF, even with a finer grid size (4 km). In using a regional-scale numerical weather model, a smaller inner domain appears to be necessary for more accurate precipitation prediction. In addition, localized rainfall estimation with a smaller domain size produced discharge values that were reasonably well matched with observed data in the rainfall-runoff simulation. For further investigation, diverse domain size and flood forecasting could be pursued in detail in these regions and hourly rainfall simulation might be required for more precise flood event alert.

Note that some physics parameterization schemes might be region and/or region dependent due to their original design and the synoptic forcing. Thus, the conclusions drawn from our simulations might be only limited to the Korean Peninsula. In order to make a more general conclusion, a more thorough and fundamental study is needed, which might be due to the designs of individual schemes. For example, our results with Grell cumulus parameterization scheme are consistent with those studied in Dodla et al. (2013), i.e. better QPF over the mountainous region. On the other hand, the Kain-Fritsch scheme predicted rainfall patterns over the mountainous areas of the south Asian region, and Grell scheme realistically captured the rainfall patterns over the southern plain area of the region (Sarder et al., 2012). Thus, Sarder et al.'s finding is completely opposite to ours. Some other studies (e.g., Ardie et al., 2012; Yang and Tung 2003) have even pointed toward the possibility of case dependent due to synoptic forcing. Due to their original design, Kain-Fritsch cumulus scheme is heavily dependent on the CAPE, while the Grell cumulus scheme uses horizontal and vertical advection to compute the rate of destabilization, which could be sensitive to the updraft calculated at the top of the mixed layer (Cohen, 2012).

Acknowledgments

This research was supported partially by the National Oceanic and Atmospheric Administration Educational Partnership Program under Cooperative Agreement No: NA06OAR4810187 (2006-2012) and by the National Science Foundation Award AGS-1265783.

References

- Anderson, M. L., Chen, Z.-Q., Kavvas, M. L., & Feldman, A. (2002). Coupling HEC-HMS with atmospheric models for prediction of watershed runoff. *J of Hydrologic Engineering*, 7(4), 312-318. [http://dx.doi.org/10.1061/\(ASCE\)1084-0699\(2002\)7:4\(312\)](http://dx.doi.org/10.1061/(ASCE)1084-0699(2002)7:4(312))
- Ardie, W. A., Sow, K. S., Tangang, D. T., Hussin, A.G., Mahmud, M., & Juneng, L. (2012). The performance of different cumulus parameterization schemes in simulating the 2006/2007 southern peninsular Malaysia heavy rainfall episodes. *J Earth System Science*, 121, 317-327. <http://dx.doi.org/10.1007/s12040-012-0167-9>
- Bedient, P. B., Holder, A., Benavides, J. A., & Vieux, B. E. (2003). Radar-based flood warning system applied to tropical storm Allison. *J of Hydrologic Engineering*, 8(6), 308-318. [http://dx.doi.org/10.1061/\(ASCE\)1084-0699\(2003\)8:6\(308\)](http://dx.doi.org/10.1061/(ASCE)1084-0699(2003)8:6(308))
- Betts, A. K., & Miller, M. J. (1993). The Betts-Miller scheme. In “The Representation of Cumulus Convection in Numerical Models of the Atmosphere” (Eds. K. A. Emanuel and D. J. Raymond). *American Meteorology Society, Meteor. Mono*, 24(46), 107-121.
- Chen, S.-H., & Sun, W.-Y. (2002). A one-dimensional time dependent cloud model. *J. Meteor. Soc. Japan*, 80, 99-118. <http://dx.doi.org/10.2151/jmsj.80.99>
- Clark, A. J., Gallus, W. A., & Chen, T.-C. (2007). Comparison of the diurnal precipitation cyclone in convection-resolving and non-convection-resolving mesoscale models. *Mon Wea Rev*, 135, 3456-3473. <http://dx.doi.org/10.1175/MWR3467.1>
- Cohen, C. (2002). A comparison of cumulus parameterizations in idealized sea-breeze simulations. *Mon Wea Rev*, 130, 2554-2571. [http://dx.doi.org/10.1175/1520-0493\(2002\)130%3C2554:ACOCPI%3E2.0.CO;2](http://dx.doi.org/10.1175/1520-0493(2002)130%3C2554:ACOCPI%3E2.0.CO;2)
- Dodla, V. B. R., Ratna, S. B., & Desamsetti, S. (2013). An assessment of cumulus parameterization schemes in the short range prediction of rainfall during the onset phase of the Indian southwest monsoon using MM5 model. *Atmospheric Research*, 120-121, 249-267. <http://dx.doi.org/10.1016/j.atmosres.2012.09.002>
- Dolcine, L., Andrieu, H., Sempere-Torres, D., & Creutin, D. (2001). Flash flood forecasting with coupled precipitation model in mountainous Mediterranean basin. *J of Hydrologic Engineering*, 6(1), 1-10. [http://dx.doi.org/10.1061/\(ASCE\)1084-0699\(2001\)6:1\(1\)](http://dx.doi.org/10.1061/(ASCE)1084-0699(2001)6:1(1))
- EM-DAT (2014). The OFDA/CRED International Disaster Database – Retrieved from <http://www.emdat.be>, Université Catholique de Louvain, Brussels (Belgium)
- Evans, J. P., Ekstrom, M., & Ji, F. (2012). Evaluating the performance of a WRF physics ensemble over South-East Australia. *Clim Dyn*, 39, 1241-1258. <http://dx.doi.org/10.1007/s00382-011-1244-5>
- Gallus Jr., W. A., & Segal, M. (2001). Impact of improved initialization of Mesoscale features on convective system rainfall in 10-km Eta simulation. *Weather and Forecasting*, 16, 680-696. [http://dx.doi.org/10.1175/1520-0434\(2001\)016<0680:IOIOM>2.0.CO;2](http://dx.doi.org/10.1175/1520-0434(2001)016<0680:IOIOM>2.0.CO;2)
- Gerard, L. (2007). An integrated package for subgrid convection, clouds and precipitation compatible with meso-gamma scales. *Quart J Royal Meteor Soc.*, 133, 711-730. DOI: 10.1002/qj.58
- Gilliland, E. K., & Rowe, C. M. (2007). A comparison of cumulus parameterization scheme in the WRF model. *Proc. 87th AMS Annual Meeting & Conf. on Hydrology*, San Antonio, TX, USA, p216.
- Giorgi, F., & Mearns, L. O. (1999). Introduction to special section: regional climate modeling revisited. *J of Geophysics Research*, 104, 6335-6375. <http://dx.doi.org/10.1029/98JD02072>
- Grell, G. A., & Devenyi, D. (2002). A generalized approach to parameterizing convection combining ensemble and data assimilation techniques. *Geophysical Research Letters*, 29, 1693-1696. <http://dx.doi.org/10.1029/2002GL015311>
- Grell, G. A., Dudhia, J., & Stauffer, D. R. (1995). A description of the Fifth-Generation Penn State/NCAR Mesoscale Model (MM5). NCAR Tech. Note TN-398, 122pp.
- Hong, S.-Y., & Lee, J.-W. (2009). Assessment of the WRF model in reproducing a flash-flood heavy rainfall event over Korea. *Atmospheric Research*, 93, 818-831. <http://dx.doi.org/10.1016/j.atmosres.2009.03.015>
- Hong, S.-Y., & Lim, J.-O. (2006) The WRF single-moment 6 class microphysics scheme (WSM6). *J of the Korean Meteorological Society*, 42(2), 129-151.
- Hong, S.-Y., Noh, Y., & Dudhia, J. (2006) A new vertical diffusion package with an explicit treatment of entrainment processes. *Mon Wea Rev*, 134, 2318-2341. <http://dx.doi.org/10.1175/MWR3199.1>

- Hudson, P. F., & Colditz, R. R. (2003). Flood delineation in a large and complex alluvial valley, lower Panuco basin, Mexico. *J of Hydrology*, 268(1-4), 87-99. [http://dx.doi.org/10.1016/S0022-1694\(03\)00227-0](http://dx.doi.org/10.1016/S0022-1694(03)00227-0)
- Janjic, Z. I. (1994). The step-mountain eta coordinate model: Further development of the convection, viscous sub layer, and turbulence closure schemes. *Mon. Wea. Rev.*, 122, 927-945. [http://dx.doi.org/10.1175/1520-0493\(1994\)122%3C0927:TSMECM%3E2.0.CO;2](http://dx.doi.org/10.1175/1520-0493(1994)122%3C0927:TSMECM%3E2.0.CO;2)
- Ji, F., Ekstrom, M., Evans, J. P., & Teng, J. (2013). Evaluating rainfall patterns using physics scheme ensembles from a regional atmospheric model, *Theor. Appl. Climatol.* <http://dx.doi.org/10.1007/s00704-013-0904-2>
- Kain, J. S. (1990). The Kain-Fritsch convective parameterization: An update. *J of Applied Meteorology*, 43, 17-181. [http://dx.doi.org/10.1175/1520-0450\(2004\)043%3C0170:TKCPAU%3E2.0.CO;2](http://dx.doi.org/10.1175/1520-0450(2004)043%3C0170:TKCPAU%3E2.0.CO;2)
- Kain, J. S., & Fritsch, J. M. (1990). A one-dimensional entraining/detraining plume model and its application in convective parameterization. *J of Atmospheric Sciences*, 47, 2784-2802. [http://dx.doi.org/10.1175/1520-0469\(1990\)047%3C2784:AODEPM%3E2.0.CO;2](http://dx.doi.org/10.1175/1520-0469(1990)047%3C2784:AODEPM%3E2.0.CO;2)
- Knebl, M. R., Yang, Z.-L., Hutchison, K., & Maidment, D. R. (2005). Regional scale flood modeling using NEXRAD rainfall, GIS, and HEC-HMS/RAS: a case study for the San Antonio River Basin Summer 2002 storm event. *J of Environmental Management*, 75, 325-336. <http://dx.doi.org/10.1016/j.jenvman.2004.11.024>
- Lee, D. K., Kim, H. R., & Hong, S.-Y. (1998). Heavy rainfall over Korea during 1980-1990. *Korean Journal of Atmospheric Sciences*, 1, 32-50.
- Lin, Y.-L. (2007). *Mesoscale Dynamics*. Cambridge University Press, 630pp.
- Lin, Y.-L., Farley, R. D., & Orville, H. D. (1983). Bulk Parameterization of the snow field in a cloud model. *J Applied Meteorology and Climatology*, 22, 1065-1092. [http://dx.doi.org/10.1175/1520-0450\(1983\)022%3C1065:BPOTSF%3E2.0.CO;2](http://dx.doi.org/10.1175/1520-0450(1983)022%3C1065:BPOTSF%3E2.0.CO;2)
- Lowrey, M. R., & Yang, Z.-L. (2008) Assessing the capability of a regional-scale weather model to simulate extreme precipitation patterns and flooding in central Texas. *Weather and Forecasting*, 23, 1102-1126. <http://dx.doi.org/10.1175/2008WAF2006082.1>
- Pattanayak, S., & Mohanty, U. C. (2008) A comparative study on performance of MM5 and WRF models in simulation of tropical cyclones over Indian seas. *Current Science*, 95(7), 923-936.
- Sardar, S., Raza, S. S., & Irfan, N. (2012). Simulation of south Asian physical environment using various cumulus parameterization schemes of MM5. *Met. Apps.*, 19, 140-141. <http://dx.doi.org/10.1002/met.266>
- Skamarock, W. C., Klemp, J. B., Dudhia, J., Gill, D. O., Barker, D. M., Duda, M.G., ... Powers, J. G. (2008). A description of the advanced research WRF version 3. NCAR technical note, 113 pp. Retrieved from http://www.mmm.ucar.edu/wrf/users/docs/arw_v3.pdf
- Smedsmo, J. L., Foufoula-Georgiou, E., Vuruputur, V., Kong, F., & Droegemeier, K. (2005). On the vertical structure of modeled and observed deep convective storms: Insights for precipitation retrieval and microphysical parameterization. *J of Applied Meteorology*, 44, 1866-1884. <http://dx.doi.org/10.1175/JAM2306.1>
- Sousounis, P. J., Hutchinson, T. A., & Marshall, S. F. (2004). A comparison of MM5, WRF, RUC, ETA performance for great plains heavy precipitation events during the spring of 2003. *Preprints 20th Conf. on Weather Analysis and Forecasting*, Seattle, American Meteorological Society, J246.
- Thompson, G., Rasmussen, R. M., & Manning, K. (2004). Explicit forecasts of winter precipitation using an improved bulk microphysics scheme. Part I: Description and sensitivity analysis. *Mon Wea Rev*, 132, 519-542. [http://dx.doi.org/10.1175/1520-0493\(2004\)132%3C0519:EFOWPU%3E2.0.CO;2](http://dx.doi.org/10.1175/1520-0493(2004)132%3C0519:EFOWPU%3E2.0.CO;2)
- Westrick, K. J., Storck, P., & Mass, C. F. (2002) Description and evaluation of a hydrometeorological forecast system for mountainous watershed. *Wea. Forec.*, 17, 250-262. [http://dx.doi.org/10.1175/1520-0434\(2002\)017%3C0250:DAEOAH%3E2.0.CO;2](http://dx.doi.org/10.1175/1520-0434(2002)017%3C0250:DAEOAH%3E2.0.CO;2)
- Yang, M.-J., & Tung, Q.-C. (2003). Evaluation of rainfall forecasts over Taiwan by four cumulus parameterization schemes. *J Meteor Soc Japan*, 81, 1163-1183. <http://dx.doi.org/10.2151/jmsj.81.1163>
- Yoshitani, J., Chen, Z. Q., Kavvas, M. L., & Fukami, K. (2009). Atmospheric model-based streamflow forecasting at small mountainous watersheds by a distributed hydrologic model: Application to a watershed in Japan. *J of Hydrologic Engineering*, 14(10), 1107-1118. [http://dx.doi.org/10.1061/\(ASCE\)HE.1943-5584.0000111](http://dx.doi.org/10.1061/(ASCE)HE.1943-5584.0000111)

- Yu, Z., Lakhtakia, M. N., Yarnal, B., White, R. A., Miller, D. A., Frakes, B., Barron, E. J., Duffy, C., & Schwartz, F. W. (1999). Simulating the river-basin response to atmospheric forcing by linking a Mesoscale meteorological model and hydrologic model system. *J of Hydrology*, *218*, 72-91. [http://dx.doi.org/10.1016/S0022-1694\(99\)00022-0](http://dx.doi.org/10.1016/S0022-1694(99)00022-0)
- Yuan, X., Liang, X.-Z., & Wood, E. F. (2012). WRF ensemble downscaling seasonal forecasts of China winter precipitation during 1982-2008. *Clim. Dyn.*, *39*, 2041-2058. <http://dx.doi.org/10.1007/s00382-011-1241-8>

Copyrights

Copyright for this article is retained by the author(s), with first publication rights granted to the journal.

This is an open-access article distributed under the terms and conditions of the Creative Commons Attribution license (<http://creativecommons.org/licenses/by/3.0/>).

A Historical Perspective of the Maasai - African Wild Dog Conflict in the Serengeti Ecosystem

Richard D Lyamuya^{1,2}, Emmanuel H Masenga^{1,2}, Robert D Fyumagwa², Machoke N Mwita², Craig R Jackson³ & Eivin Røskaft¹

¹Department of Biology, Norwegian University of Science and Technology (NTNU), Norway

²Tanzania Wildlife Research Institute, P.O. Box 661, Arusha, Tanzania

³Norwegian Institute of Nature Research, Trondheim, Norway

Correspondence: Eivin Røskaft, Department of Biology, Norwegian University of Science and Technology (NTNU), Norway. E-mail: eivin.roskaft@ntnu.no

Received: March 2, 2016 Accepted: March 16, 2016 Online Published: March 23, 2016

doi:10.5539/enrr.v6n2p42 URL: <http://dx.doi.org/10.5539/enrr.v6n2p42>

Abstract

This study discusses the conflict between Maasai pastoralists and African wild dogs (*Lycaon pictus*) over livestock before and after the Maasai were evicted from the Serengeti National Park (SNP) in 1959. We surveyed 181 randomly selected households from six villages in the eastern Serengeti ecosystem. A semi-structured questionnaire was used to acquire the required information from the respondents. We found that males had a greater awareness of local wild dog presence and livestock-derived conflict than females, and reported more frequently to have chased and killed wild dogs that attacked their livestock. Moreover, the conflict existed before 1959, decreased during the 1990s, but increased from 2000 onwards. This increase is attributed to the growth in human, livestock and wild dog populations in the area. This study recommends that to foster their coexistence, the continued escalation in livestock numbers needs to cease while simultaneously protecting the region's wild prey populations.

Keywords: African wild dogs, predation, livestock, gender, conflict

1. Introduction

Human-carnivore conflict over livestock presents one of the most complex challenges facing wildlife management and conservation. This global problem (Ciucci & Boitani, 1998; Rodney & Rinchin, 2004; Røskaft, Bjerke, Kaltenborn, Linnell, & Andersen, 2003; Røskaft, Händel, Bjerke, & Kaltenborn, 2007; Treves & Karanth, 2003; Woodroffe, Lindsey, Romanach, Stein, & ole Ranah, 2005) is also a significant problem in the Serengeti ecosystem in northern Tanzania (Ikanda & Packer, 2008; Jackson, Ahlborn, Gurung, & Ale, 1996; Kaczensky, 1999; Larson, 2008). The most important driving factors include increasing human populations, loss of natural habitats and, in some regions, growing wildlife populations resulting from successful conservation programs (Wang & Macdonald, 2006). The endangered African wild dog (*Lycaon pictus*) has disappeared from much of its former range, due mostly to conflict with humans (Ogada, Woodroffe, Ouge, & Frank, 2003; Rasmussen, 1999; Treves & Karanth, 2003) which has led to their population decline (Swarnar, 2004; Woodroffe et al., 2005). This endangered species has been reported to prey on livestock wherever it comes into contact with domestic animals (Lyamuya, Masenga, Fyumagwa, & Røskaft, 2014; Rasmussen, 1999; Swarnar, 2004; Woodroffe et al., 2005). The Maasai pastoralists in the eastern Serengeti ecosystem are among those suffering livestock losses to wild dogs (Lyamuya et al., 2014; Masenga, 2011). The Maasai pastoralists have inhabited the Serengeti and Ngorongoro areas until the end of the eighteenth century, arriving from the north and displacing other tribes in the Serengeti area (e.g., Sukuma, Ikoma and Ndorobo) (Neumann, 1995). They became the dominant ethnic group in the Serengeti by the late 1800s (Homewood & Rodgers, 1991). Since then, the Maasai pastoralists in the Serengeti area have lived alongside wild animals, including the African wild dogs, up to 1959 when they were evicted from the Serengeti National Park and displaced to the Loliondo Game Controlled Area (LGCA) and Ngorongoro Conservation Area (NCA) (Neumann, 1995). Before that, the African wild dog population was most likely high, yet the wild dogs were declared locally extinct in the Serengeti National Park (SNP) in 1991 (Carbone et al., 2005; Gascoyne, Laurenson, Lelo, & Borner, 1993; Stearns & Stearns, 1999). A recent genetic study, however, has indicated that while the packs inside the national park disappeared, the population never went extinct and most probably survived in adjoining areas (Marsden, Wayne, & Mable, 2012).

Wild dogs currently inhabiting LGCA and NCA are genetically similar to those previously inhabiting the Serengeti plains, ruling out the possibility that this population has recolonized the area from elsewhere (Marsden et al., 2012). The LGCA and NCA support the only wild dog population in the area since the population has failed to naturally recolonize the Serengeti National Park (Masenga, 2011).

Therefore, there is little information on the historical distribution of wild dogs in the ecosystem, especially as to where the population successfully survived the supposed local extinction. There is also a lack of information as to whether the Maasai pastoralists had any conflict with the wild dogs over their livestock during their stay in the SNP before 1959, and whether this has escalated in recent years. Information on the status of the conflict will thus provide a much needed overview of the historical distribution of wild dogs and temporal trends in the conflict in the area. Insights into the conflict will aid conservation management of the threatened carnivore.

We tested three hypotheses in this study. The first hypothesis was that the wild dogs have continuously inhabited the LGCA, even directly after the reported extinction. The second hypothesis is that male Maasai pastoralists have a greater awareness of local wild dog presence and the livestock-derived conflict in their area. The third hypothesis is that the conflict between the Maasai pastoralists and wild dogs has increased in recent years due to human and livestock population growth and an increase in the wild dog population in the area.

2. Materials and Methods

The study was conducted in six villages in the LGCA in the eastern Serengeti ecosystem (Figure 1). LGCA borders the Maasai Mara National Reserve along the Kenyan border and the SNP in Tanzania between 2°5'00''–2°2'60''S and 35°61'67''–35°37'00''E (Masenga, 2011). The region is one of the most wildlife-rich areas in the world (Maddox, 2003). Hundreds of thousands of wildebeest (*Connochaetes taurinus*), zebra (*Equus burchelli*) and other ungulates pass through the communities during their annual migration from the Maasai Mara to the Serengeti Plains (Holdo et al., 2010). Large predators remain remarkably widespread throughout the LGCA compared with nominally unprotected areas in other parts of Tanzania and neighbouring countries. Maddox (2003) described a significant cheetah (*Acinonyx jubatus*) population in the LGCA and noted the large numbers of lions (*Panthera leo*), spotted hyenas (*Crocuta crocuta*), and jackals (*Canis mesomelas*) in the area. The Maasai pastoralists mostly inhabit the area closest to the SNP boundary, covering approximately 4500 km² (Lyamuya, Masenga, Fyumagwa, & Røskaft, 2014). The dominant form of land use and livelihood in the area is trans-human pastoralism (Homewood & Rodgers, 1991), which utilizes wet and dry season livestock grazing pastures according to traditional patterns of movement. Rangelands are managed communally but are not considered to be open access lands.

The data for this study were collected in January 2013 and encompassed 181 households chosen randomly from the six Maasai villages living in the eastern Serengeti ecosystem (Figure 1). The method used for data collection and sample size determination followed the same methods previously employed in other studies (Fa, Peres, & Meeuwig, 2002; Sancheti & Kapoor, 2003). No prior notice was given to the interviewees, although the village chairman was first consulted about the study and asked for permission to carry out interviews in his/her area. A purposive sampling strategy was used, with respondents chosen according to availability based on their age and gender. A semi-structured interview was administered through a questionnaire translated into "Swahili" language with the help of Maasai translators to acquire information related to their perspectives on the history of human-wild dog conflict in the area. The information collected included basic information such as the respondent's age, GPS location, tribe (only Maasai), educational level (e.g., had been to school, had not been to school) and occupation (e.g., livestock keeper, housewife, employee). Respondents were then asked if they were born before or after the Maasai eviction from the SNP. After that, respondents were asked the following questions regarding their coexistence with wild dogs: (1) "Have you ever seen wild dogs?" (2) "How often do you see wild dogs in your area?" (3) "How is the general population trend of wild dogs in your area?" (4) "Have you ever seen wild dogs preying on your livestock?" (5) "How often do you see wild dogs preying on your livestock?" (6) "How did you react when you observed wild dogs attacking your livestock?" (7) "If you compare the present situation on livestock attacks by wild dogs to those days when you were young, is it increasing, decreasing or does it remain stable?"

During the survey, we collected village centre GPS locations which assisted us in drawing our study area map in Arc View 9.0 (Environmental Systems Research Institute, Redlands, CA, USA). Statistical Package for Social Science (SPSS) Statistics 21.0 for Windows (<http://www.spss.com>) was used to perform all statistical analyses (Kirkpatrick & Feeney, 2010). We used both logistic and linear regression analyses to test different independent variables that could explain the variations existing among dependent variables in our data. Because most of our data were nominal, we primarily used non-parametric Chi-square tests (Fowler, Cohen, & Jarvis, 2009) to determine frequency differences among different variables; hence, in all tests, $P \leq 0.05$ was considered statistically significant.

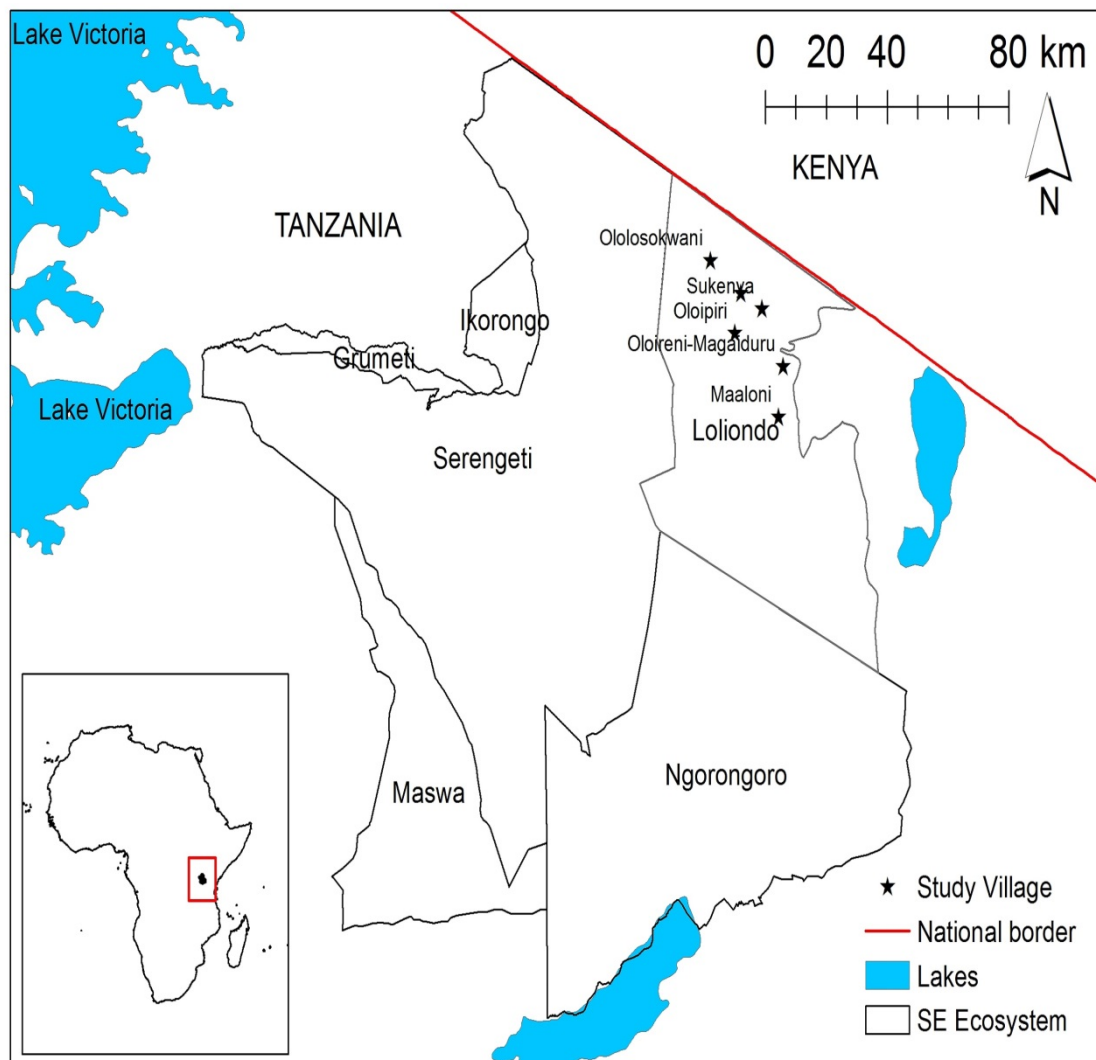


Figure 1. A map of the Serengeti ecosystem showing the study area with the surveyed villages marked with stars

3. Results

Male Maasai pastoralists (98 %, $n = 123$) reported more frequently to have seen wild dogs in their area than did females (66 %, $n = 58$; $\chi^2_1 = 36.5$, $P = 0.001$). Those who had been to school had more frequently (95 %, $n = 74$) seen wild dogs in the area than those who had never been to school (82 %, $n = 107$; $\chi^2_1 = 6.02$, $P = 0.014$). However, no difference in this respect was found between those born before or after the eviction from SNP (1959) ($\chi^2_1 = 0.479$, $P = 0.359$).

A logistic regression analysis with response to the question “Have you ever seen wild dogs? (yes/no)” as a dependent variable, and gender, education level and born before or after eviction from the SNP (1959) as independent variables indicated that gender ($B = 2.7$, $Wald = 15.8$, $P \leq 0.001$) was the only factor explaining whether wild dogs had been seen in their area ($Wald \chi^2_3 = 32.7$, $P \leq 0.001$, Nagelkerke $r^2 = 0.328$). The other factors such as born before or after the Maasai eviction from the SNP and education level were not found to be significant in explaining the variation in the observations (yes/no) of wild dogs in the area.

Males more frequently reported seeing wild dogs on a daily or weekly basis compared to females ($\chi^2_1 = 39.2$, $P \leq 0.001$, Table 1). Furthermore, the frequency on how often Maasai pastoralist had observed wild dogs varied with education level ($\chi^2_1 = 17.1$, $P = 0.002$, Table 1) and whether they were born before or after the eviction from SNP ($\chi^2_1 = 33.6$, $P \leq 0.001$, Table 1). Those who not had been to school observed wild dogs more frequent than those who had been to school, while those born before eviction from the SNP (1959) also observed wild dogs more common than those born after eviction.

Table 1. Responses to the question “How often do you see African wild dogs in your area?” in relation to gender, education level or whether born before or after the eviction from Serengeti National Park (1959)

Frequency		Daily	Weekly	Monthly	Rarely	Never	<i>n</i>
		%	%	%	%	%	
Gender	Males	24	27	12	35	2	123
	Females	14	10	9	33	35	58
Education	No school	27	18	8	30	18	107
	Been to school	11	27	16	41	5	74
Born	Before	35	28	11	15	10	79
	After	9	17	11	49	15	102

Furthermore, a linear regression analysis with how often Maasai pastoralist have observed wild dogs in their area as a dependent variable and with gender, education level and born before/after eviction as independent variables was significant ($F_{3,177} = 23.3$, $r^2 = 0.283$, $P < 0.001$). Here both born before/after eviction ($B = 1.11$, $t_1 = 6.07$, $P \leq 0.001$) and gender ($B = 1.09$, $t_1 = 5.64$, $P \leq 0.001$) explained the variation significantly, while education level did not.

Most males (55 %, $n = 123$) reported that the wild dog population was decreasing in the area while most females (45 %, $n = 58$), indicated that the population was increasing ($\chi^2_1 = 32.7$, $P \leq 0.001$). The assessment of the wild dog population trend also differed between the two groups with different education levels ($\chi^2_1 = 15.3$, $P = 0.002$). Most of those who had been to school (46 %) thought the population was increasing while a majority of those who had never been to school (23 %) had no opinion. No difference in this assessment of the current population trend was found between those born before or after eviction from the SNP ($\chi^2_1 = 5.37$, $P = 0.15$). A linear regression analysis with assessment of the population trend as a dependent variable and with gender, education level and born before or after the eviction from SNP as independent variables was significant ($F_{3,177} = 2.84$, Nagelkerker² = 0.046, $P = 0.039$), however, only gender ($B = 0.297$, $t_1 = 1.74$, $P = 0.083$) explained some of this variation, while education level and born before or after the eviction from SNP did not.

Males (81 %, $n = 123$) reported more frequently than females (50 %, $n = 58$) having seen wild dogs preying on their livestock ($\chi^2_1 = 18.9$, $P \leq 0.001$). Furthermore, those who had been to school more frequently (81 %, $n = 74$) reported to have seen wild dogs preying on their livestock than those who had never been to school (65 %, $n = 107$; $\chi^2_1 = 5.9$, $P = 0.015$). However, no difference in this respect was found between those born before or after eviction ($\chi^2_1 = 0.58$, $P = 0.445$). Logistic regression with wild dogs preying on livestock as a dependent variable and with gender, education level and born before or after eviction as independent variables were significant (Wald $\chi^2_3 = 30.6$, $P \leq 0.001$, Nagelkerke $r^2 = 0.156$). Gender ($B = 1.38$, Wald $\chi^2_1 = 13.7$, $P \leq 0.001$) was, however, the only factor explaining whether wild dogs had been seen preying on their livestock in their area while education level and born before or after the eviction from SNP was non-significant.

Although most respondents had seen wild dogs preying on their livestock rarely in their area the frequencies differed between the two gender ($\chi^2_1 = 23.9$, $P \leq 0.001$), the two education groups ($\chi^2_1 = 10.7$, $P = 0.015$), but not in relation to whether they were born before or after the eviction from SNP ($\chi^2_1 = 3.52$, $P = 0.32$). A linear regression analysis how often do you see wild dogs preying on your livestock as a dependent variable and with gender, education level and born before or after the eviction from SNP as independent variables was significant ($F_{3,177} = 6.81$, $P = 0.039$), however, only gender ($B = 0.406$, $t_1 = 3.61$, $P = 0.001$) explained some of the variation, while education level and born before or after the eviction from SNP did not.

Males reported more frequently chasing or killing wild dogs when they saw them attacking their livestock than did females ($\chi^2_1 = 10.8$, $P = 0.005$, Table 2). However, no differences in this reaction patterns were found concerning education level ($P = 0.32$) or between those born before or after the eviction from SNP ($P = 0.23$).

More males (71 %) than females (50 %) claimed that the present situation recording wild dog attacks is increasing compared to previous days ($\chi^2_3 = 12.7$, $P = 0.005$, Table 3), similarly 75 % among those born before the eviction from SNP claimed the wild dog attacks on livestock is increasing while only 56 % of those born after the eviction claimed so ($\chi^2_3 = 13.6$, $P = 0.004$, Table 3). No difference in this respect was found between those with or without education ($P = 0.85$).

A linear regression analysis with “If you compare the present situation on livestock attacks by wild dogs to those days when you were young, is it increasing, decreasing or does it remain stable?” as a dependent variable and with gender, education level and born before or after the eviction from SNP as independent variables was significant ($F_{3, 177} = 8.89, P \leq 0.001$). Born before or after the eviction from SNP ($B = 0.656, t_1 = 3.82, P \leq 0.001$) and gender ($B = 0.621, t_1 = 3.31, P \leq 0.001$) significantly explained this variation, while education level did not.

Table 2: Responses to the question “How did you react when you observed African wild dogs attacking your livestock?” in relation to gender

Gender	I chase them away or kill them	I try to find help or do nothing	Wild dogs flee when they see people	<i>n</i>
	%	%	%	
Males	57	19	24	112
Females	32	18	50	44

Table 3. Responses to the question “If you compare the present situation on livestock attacks by wild dogs to those days when you were young, is it increasing, decreasing or remains stable?” in relation to gender (only those born before 1959)

		Elder males	Elder females	<i>n</i>
Increasing	%	74	26	42
Stable	%	25	75	4
Decreasing	%	83	17	6
No opinion	%	50	50	2
TOTAL	%	70	30	54

4. Discussion

Our results reveal that male Maasai pastoralists more frequently reported having seen wild dogs in their area than did females. This finding supports our hypothesis that male Maasai pastoralists have a greater awareness of local wild dog presence in their area. This is because male Maasai normally follow the livestock out into the bush (Mmassy & Røskaft, 2013) and therefore, acquire more information. Also, this finding indicates that wild dogs were present in the LGCA long before and even after the Maasai were evicted from the SNP in 1959. Therefore, our results support our hypothesis that the wild dogs have continuously inhabited the LGCA, even directly after the reported extinction as from the results of the genetic study conducted by Marsden et al. (2012), indicated that the Serengeti population of African wild dogs did not go extinct in the region as previously reported (Stearns & Stearns, 1999). While Marsden et al. (2012) did postulate that the population may have survived unrecorded in the Loliondo region, our results confirm this and that the population has persisted there subsequently.

Furthermore, our results show that wild dogs were sighted more often by Male pastoralists on a daily or weekly basis compared to females, which supports our hypothesis that male Maasai pastoralists have a greater awareness of local wild dog presence in their area. Moreover, those born before eviction from the SNP (1959) also observed wild dogs more frequent than those born after eviction, because before 1959, the population of the African wild dogs in the area was most likely high (Carbone et al., 2005; Frame, Malcolm, Frame, & Vanlawick, 1979) and thus, those born before eviction from SNP were able to see more often than those born after eviction. Also, those born after eviction experienced more of the reported decline of African wild dogs in the SNP during the 1990s (Carbone et al., 2005; Stearns & Stearns, 1999) which reduced their chances to see wild dogs more frequently in the area. However, since 2000 onwards, the African wild dogs have been reported to be sighted more frequently in the LGCA and has increased to some extent their chances of being sighted in the area (H. E. Masenga & Mentzel, 2005).

In explaining the general population trend of wild dogs in the area, it was found that most males reported that wild dog population was decreasing while most females reported it was increasing. The reported decrease in wild dog population by males was probably because its population observed before 1990 was most likely high, but despite

their initially high numbers, African wild dogs were declared locally extinct in the Serengeti National Park (SNP) in 1991 (Carbone et al., 2005; Gascoyne et al., 1993; Stearns & Stearns, 1999). Due to the division of labour within the Maasai pastoralist society (FAO, 2013; Mmassy & Røskaft, 2013), males were expected to observe and be more aware of changes in the wild dog population.

Our results also supported the hypothesis that male Maasai pastoralists were more conscious of the conflict over livestock with wild dogs in their area since male Maasai pastoralists reported more frequently than females to have seen wild dogs, especially those preying on livestock. This finding may be attributed to the existing division of labour within the Maasai pastoralist society which favours males doing outdoor activities such as daily livestock herding (FAO, 2013; Mmassy & Røskaft, 2013), whereas females mostly do domestic work such as caring for children, cooking, milking livestock, fetching water and firewood collection (Mwebi, 2007). Our findings further indicate that the Maasai conflict with African wild dogs existed before their eviction from the SNP in 1959, but conflict occurred at a low level.

Males reported more frequently than females that they had seen wild dogs preying on their livestock, albeit rarely, which is in support of our hypothesis that male Maasai pastoralists are more aware of the conflict over livestock with wild dogs in their area than female Maasai. The rarity of sighting livestock depredation incidences by males Maasai is attributed to the abundant wild prey species reported to be found in the area (Grzimek & Grzimek, 1960; Thirgood et al., 2004) and also because previous studies have found no difference in terms of species diversity and density of both ungulates and carnivores between the SNP and its surrounding areas (Campbell & Borner, 1995; Maddox, 2003). Wild dogs have been found to prefer to prey on wild prey species rather than livestock wherever wild prey species are more abundant (Hayward, O'Brien, Hofmeyr, & Kerley, 2006; Rasmussen, 1999).

According to our results, males more frequently reported that they chased and killed wild dogs when they saw them preying on livestock. Therefore, our findings support previous studies showing that most livestock keepers do retaliate by killing problem animals following livestock losses (Bangs & Shivik, 2001; Gese, 2003; Ikanda & Packer, 2008; Kissui, 2008; Maddox, 2003; E. H. Masenga et al., 2013), which have brought some carnivore species close to local extinction (Rasmussen, 1999; Woodroffe et al., 2005), the African wild dog being one such species (Swarnar, 2004; Woodroffe et al., 2005).

Our findings concur with the previous studies as more males and those born before the eviction from SNP claimed that the present situation on livestock attacks by wild dogs is increasing, supporting our hypothesis that this conflict has risen in recent years due to human population growth and an increase in the wild dog population in the area. The human population at the time of eviction was small, comprising around 1000 Maasai pastoralists (Neumann, 1998), whereas recent settlements in the Ngorongoro district number more than 180,000 Maasai pastoralists (Homewood & Rodgers, 1991). This increase in number of livestock in the area has probably increased the rate of wild dogs encounters (Lyamuya et al., 2014; E. H. Masenga et al., 2013; H. E. Masenga & Mentzel, 2005). Our findings support what previous studies indicating that the endangered African wild dog population posed no significant problem to the Maasai pastoralists in the Serengeti Ecosystem (Ikanda & Packer, 2008; Maddox, 2003). This was perhaps because of the reported extinction of the African wild dogs in 1991 (Carbone et al., 2005; Creel, Creel, & Monfort, 1997; Gascoyne et al., 1993; Stearns & Stearns, 1999) that reflected a reduction in their numbers to a such extent that wild dogs were not easily detected (Marsden et al., 2012). Therefore, this conflict was considered to decrease during that period (Ikanda & Packer, 2008; Maddox, 2003) and then increased again from 2000 onwards (H. E. Masenga & Mentzel, 2005). Given wild dogs' wide-ranging behaviour, attacks on livestock would most likely have been low when the human and livestock population was small. The increase in the wild dog, human and livestock populations thus intensifies the probability of encounter and attacks.

5. Conclusion

This study confirms that male Maasai pastoralists have a greater awareness of local wild dog presence and the livestock-derived conflict in their area. Moreover, the conflict between the Maasai pastoralists and African wild dogs over livestock existed before 1959 and has continued to present days. Furthermore, wild dogs did not go completely extinct from the Serengeti ecosystem in 1991 and managed to survive in other areas including the LGCA (Burrows, Hofer, & East Marion, 1994; Marsden et al., 2012). Conflict decreased in 1990s and has increased in recent years. This study suggests that for the Maasai pastoralists to coexist better with African wild dogs, the continuing rise in livestock density needs to cease while wild prey population should be protected.

References

- Bangs, E., & Shivik, J. (2001). Managing wolf conflict with livestock in the Northwestern United States. *Carnivore Damage Prevention News*, 2-5.

- Burrows, R., Hofer, H., & East Marion, L. (1994). Demography, extinction and intervention in a small population: The case of the Serengeti wild dogs. *Proceedings of the Royal Society of London - Series B: Biological Sciences*, 256(1347), 281-292.
- Campbell, K., & Borner, M. (1995). Population trends and distribution of Serengeti herbivores: implications and management. In A. R. E. Sinclair & P. Arcese (Eds.), *Serengeti II: Dynamics, management and conservation of an ecosystem* (pp. 117-145). Chicago, Ill: University of Chicago Press.
- Carbone, C., Frame, L., Frame, G., Malcolm, J., Fanshawe, J., FitzGibbon, C., & du Toit, J. T. (2005). Feeding success of African wild dogs (*Lycaon pictus*) in the Serengeti: the effects of group size and kleptoparasitism. *Journal of Zoology, London*, 266, 153-161.
- Ciucci, P., & Boitani, L. (1998). Wolf and dog depredation on livestock in central Italy. *Wildlife Society Bulletin*, 26(3), 504-514. Retrieved from <Go to ISI>://BIOABS:BACD199900096141
- Creel, S., Creel, M. N., & Monfort, S. L. (1997). Radio collaring and stress hormones in African wild dogs. *Conservation Biology*, 11(2), 544-548.
- Fa, J. E., Peres, C. A., & Meeuwig, J. (2002). Bushmeat exploitation in tropical forests: an intercontinental comparison. *Conservation Biology*, 16(1), 232-237. Retrieved from <http://www.blackwell-synergy.com/links/doi/10.1046/j.1523-1739.2002.00275.x/abs>
- FAO. (2013). *Children's work in the livestock sector: Herding and beyond* (ISBN 978-92-5-107387-2).
- Fowler, J., Cohen, L., & Jarvis, P. (2009). *Practical statistics for field biology* (2nd ed.). London, UK: Wiley.
- Frame, L. H., Malcolm, J. R., Frame, G. W., & Vanlawick, H. (1979). Social organization of African wild dogs (*Lycaon pictus*) on the Serengeti-Plains, Tanzania 1967-1978. *ZeitschriftFürTierpsychologie*, 50(3), 225-249. Retrieved from <Go to ISI>://A1979HS91700001
- Gascoyne, S. C., Laurenson, M. K., Lelo, S., & Borner, M. (1993). Rabies in African wild dogs (*Lycaon pictus*) in the Serengeti region, Tanzania. *Journal of Wildlife Diseases*, 29(3), 396-402. Retrieved from <Go to ISI>://A1993LM64200004
- Gese, E. M. (2003). *Management of carnivore predation as a means to reduce livestock losses: the study of coyotes (Canislatrans) in North America* Paper presented at the 1st Work shop sobre Pesquisa e Conservação de Carnívoros Neotropicals, Atibaia, Sao Paulo, Brasil.
- Grzimek, M., & Grzimek, B. (1960). Census of plains animals in the Serengeti. *Journal of Wildlife Management*, 24, 27-61.
- Hayward, M. W., O'Brien, J., Hofmeyr, M., & Kerley, G. I. H. (2006). Prey preferences of the African wild dog *Lycaon pictus* (Canidae: Carnivora): Ecological requirements for conservation. *Journal of Mammalogy*, 87(6), 1122-1131.
- Holdo, R. M., Galvin, K. A., Knapp, E., Polasky, S., Hilborn, R., & Holt, R. D. (2010). Responses to alternative rainfall regimes and antipoaching in a migratory system. *Ecological Applications*, 20(2), 381-397. Retrieved from <Go to ISI>://000276635600006
- Homewood, K. M., & Rodgers, W. A. (1991). *Maasailand ecology: Pastoralist development and wildlife conservation in Ngorongoro, Tanzania* (Vol. Cambridge University Press). Cambridge, UK.
- Ikanda, D., & Packer, C. (2008). Ritual versus retaliatory killings of African lions in the Ngorongoro Conservation Area, Tanzania. *Endangered Species Research*, 6, 67-74.
- Jackson, R. M., Ahlborn, G. G., Gurung, M., & Ale, S. (1996). *Reducing livestock depredation losses in the Nepalese Himalaya*. Paper presented at the 17th Vertebrate Pest Conference.
- Kaczensky, P. (1999). Large carnivore depredation on livestock in Europe. *Ursus*, 11, 59-72.
- Kirkpatrick, L. A., & Feeney, B. C. (2010). *A simple guide to SPSS, Version 17.0*. Belmont, CA: Wadsworth.
- Kissui, B. M. (2008). Livestock predation by lions, leopards, spotted hyenas, and their vulnerability to retaliatory killing in the Massai Steppe, Tanzania. *Animal Conservation*, 11, 422-432. <http://dx.doi.org/10.1111/j.1469-1795.2008.00199.x>
- Larson, C. L. (2008). *Separating people and wildlife: Zoning as a conservation strategy for large carnivores*. (Degree of Bachelor of Arts with honors in Environmental Studies), Colby College, Waterville, Maine. Retrieved from <http://digitalcommons.colby.edu/honorsthesis/245>

- Lyamuya, R., Masenga, E., Fyumagwa, R., & Røskaft, E. (2014). Human-carnivore conflict over livestock in the eastern part of the Serengeti ecosystem, with a particular focus on the African wild dog *Lycaon pictus*. *Oryx*, 48(3), 378-384. <http://dx.doi.org/10.1017/S0030605312001706>
- Maddox, T. M. (2003). *The ecology of cheetahs and other carnivores in pastoralist-dominated buffer zone*. (PhD), Zoological Society of London, London.
- Marsden, C. D., Wayne, R. K., & Mable, B. K. (2012). Inferring the ancestry of African wild dogs that returned to the Serengeti-Mara. *Conservation Genetics*, 13(2), 525-533. doi:DOI 10.1007/s10592-011-0304-z
- Masenga, E. H., Lyamuya, R. D., Nyaki, A., Kuya, S., Jaco, A., Kohi, E., & Røskaft, E. (2013). Strychnine poisoning in African wild dogs (*Lycaon pictus*) in the Loliondo game controlled area, Tanzania. *International Journal of Biodiversity and Conservation*, 5(6), 367-370. <http://dx.doi.org/10.5897/IJBC12.100>
- Masenga, H. E. (2011). *Abundance, distribution and conservation threats of African wild dogs (Lycaon pictus) in the Loliondo Game Controlled Area, Tanzania*. (MSc), Sokoine University of Agriculture, Morogoro, Tanzania.
- Masenga, H. E., & Mentzel, C. (2005). *The African wild dogs (Lycaon pictus); Preliminary results from a newly established population in Serengeti-Ngorongoro ecosystem, northern Tanzania*. Paper presented at the Proceedings of fifth annual TAWIRI scientific conference Arusha, Arusha, Tanzania.
- Mmassy, E. C., & Røskaft, E. (2013). Knowledge on birds of conservation interest among the people living close to protected areas in Serengeti, Northern Tanzania. *International Journal of Biodiversity Science, Ecosystem Services & Management*, 9(2), 114-122. <http://dx.doi.org/10.1080/21513732.2013.788566>
- Msuha, M. J. (2009). *Human impacts on carnivore biodiversity inside and outside protected areas in Tanzania* (PhD), University College London and Institute of Zoology, Zoological Society of London London, UK.
- Mwebi, O. (2007). *Herding efficiency as a factor in the human-carnivore conflict in Kenya: A comparative study of the Laikipia and Mbirikani group ranches*. Retrieved from London South Bank University, Nairobi-Kenya:
- Neumann, R. P. (1995). Local challenges to global agendas: Conservation, economic liberalization and the pastoralists's rights movement in Tanzania. *Antipode*, 27, 363.
- Neumann, R. P. (1998). *Imposing wilderness: struggle over livelihood and nature preservation in Africa*. Berkely, NJ, USA: University of California Press.
- Ogada, M. O., Woodroffe, R., Oguge, N. O., & Frank, L. G. (2003). Limiting depredation by African carnivores: the role of livestock husbandry. *Conservation Biology*, 17(6), 1521-1530. <http://dx.doi.org/10.1111/j.1523-1739.2003.00061.x>
- Rasmussen, G. S. A. (1999). Livestock predation by the painted hunting dog *Lycaon pictus* in a cattle ranching region of Zimbabwe: a case study. *Biological Conservation*, 88(1), 133-139. Retrieved from <Go to ISI>://000078180000013
- Rodney, M. J., & Rinchen, W. (2004). A community-based approach to mitigating livestock depredation by snow leopards. *Human Dimensions of Wildlife*, 9, 307-315.
- Røskaft, E., Bjerke, T., Kaltenborn, B. P., Linnell, J. D. C., & Andersen, R. (2003). Patterns of self-reported fear towards large carnivores among the Norwegian public. *Evolution and Human Behavior*, 24(3), 184-198. doi: [http://dx.doi.org/10.1016/S1090-5138\(03\)00011-4](http://dx.doi.org/10.1016/S1090-5138(03)00011-4)
- Røskaft, E., Händel, B., Bjerke, T., & Kaltenborn, B. P. (2007). Human attitudes towards large carnivores in Norway. *Wildlife Biology*, 13(2), 172-185. [http://dx.doi.org/10.2981/0909-6396\(2007\)13\[172:HATLCI\]2.0.CO;2](http://dx.doi.org/10.2981/0909-6396(2007)13[172:HATLCI]2.0.CO;2)
- Sancheti, D. C., & Kapoor, V. K. (2003). *Statistics theory, methods and application*. Dublin: Sultan Chand and Sons.
- Stearns, P. B., & Stearns, S. C. (1999). Watching from the edge of extinction. In P. B. Stearns & S. C. Stearns (Eds.), *Watching from the edge of extinction*. New Haven & London: Yale University Press.
- Swarner, M. (2004). Human-carnivore conflict and perspectives on carnivore management world wide. *Conservation Biology*, 17, 1491-1499.
- Thirgood, S., Mosser, A., Tham, S., Hopcraft, G., Mwangomo, E., Mlengeya, T., & Borner, M. (2004). Can parks protect migratory ungulates? The case of the Serengeti wildebeest. *Animal Conservation*, 7, 113-120. Retrieved from <Go to ISI>://000221970100001

- Treves, A., & Karanth, K. U. (2003). Human-carnivore conflict and perspectives on Carnivore management worldwide. *Conservation Biology*, 17(6), 1491-1499. Retrieved from <http://www.blackwell-synergy.com/links/doi/10.1111/j.1523-1739.2003.00059.x/abs>
- Wang, S. W., & Macdonald, D. W. (2006). Livestock predation by carnivores in Jigme Singye Wangchuck National Park, Bhutan. *Biological Conservation*, 129, 558-565.
- Woodroffe, R., Lindsey, P., Romanach, S., Stein, A., & ole Ranah, S. M. K. (2005). Livestock predation by endangered African wild dogs (*Lycaon pictus*) in northern Kenya. *Biological Conservation*, 124(2), 225-234. <http://dx.doi.org/10.1016/j.biocon.2005.01.028>

Copyrights

Copyright for this article is retained by the author(s), with first publication rights granted to the journal.

This is an open-access article distributed under the terms and conditions of the Creative Commons Attribution license (<http://creativecommons.org/licenses/by/3.0/>).

Study on Changes of Textural and Biochemical Properties of Tuna during Ultra-Low Temperature Storage

Yu-ying PAN¹, Xiao-hua QIU² & Jin-sheng YANG¹

¹ Zhejiang Ocean University, Zhoushan 316022, Zhejiang, China

² Zhou Shan Tourism and Health College, Zhoushan 316000, Zhejiang, China

Correspondence: Jin-sheng YANG, Zhejiang Ocean University, Zhoushan 316022, Zhejiang, China. E-mail: yanhjinsheng@163.com

Received: February 15, 2016 Accepted: February 26, 2016 Online Published: April 25, 2016

doi:10.5539/enrr.v6n2p51

URL: <http://dx.doi.org/10.5539/enrr.v6n2p51>

Abstract

The effect of TPA and biochemical properties of Yellow Tuna during frozen storage at different temperatures (-18°C, -25°C, -35°C, -45°C, -55°C, -65°C) were studied by measuring the textural characteristics (the hardness, Springiness) salt-solubility of myofibrillar proteins, Ca²⁺ATPase activities. The results indicated that the hardness, springiness, actomyosin salt-solubility, Ca²⁺ATPase activities decreased during the process of frozen storage. Meanwhile, the frozen stored temperature showed great effect on the freezing denaturation of protein ($P < 0.05$). For the same longer of the storage time, the lower frozen temperature, the less extent of freeze denaturation; Stored in -18°C for three months, the content of Salt soluble protein reduced to zero; Stored in -25°C for 120 days, the content of salt soluble protein also reduced to zero; But stored in -55°C and -65°C, the change is very little. Ca²⁺ATPase activities also reduced to zero after stored in -18°C and -25°C for three months. But stored in -55°C and -65°C, there is no obvious change. Moreover, there is a Positive relationship between the change of texture profile and the content of Salt soluble protein, the lower the storage temperature, the less of the change of texture profile. Therefore, when it is stored in -55°C, the quality of Yellow Tuna can be maintained to the maximum extent within six months.

Keywords: tuna, ultra-lowtemperature, texture profile analysis (TPA), biochemical properties

1. Introduction

Yellowfin tuna (*Thunnus albacares*) are pelagic fish, usually living in tropical and temperate waters. Its main habitat is usually in the depth of 50–250 m, and the depth depends on the season and the different areas of sea level. Tuna meat is tender, tasty, high protein. Thus it has high nutritional value. However, the tuna meat preservation conditions are harsh. In the process of refrigeration, the good quality of tuna meat will lose. In order to make the tuna the same color and texture, tuna meat is frozen in the low temperature of -80°C. But meanwhile it consumes too much energy.

The texture, salt-soluble protein content, Ca²⁺ATP activity, WHC values of yellowfin tuna back muscles were studied at different frozen storage temperatures and finding the best frozen temperature was -55°C, which can guarantee the quality and save more energy. In this study, it is provided some theoretical basis for controlling tuna meat quality and transport.

2. Materials and Methods

2.1 Materials

Tuna was donated by a local tuna factory (Yuanyang, Ningbo); Ca²⁺ATPase kit was bought by Reagent Company (Jiancheng, Nanjing); All other chemicals were analytical grade products.

2.2 Fish Sample and Storage Condition

Take four Yellowfin tunas of the same size and divide each of them into four parts, then divide the back muscles of the each part into the shape of trapezoid. Take 500 g of the back muscles of the tuna, and then pack it in sealing. Then frozen it for 6 months in different temperatures (-18°C, -25°C, -35°C, -45°C, -55°C). It was measured every 15d before test it was thawed at 4°C in order to eliminate the influence of low temperature.

2.3 Determination of Texture

Take the TMS-Pro material analyzer under the measuring mode of Texture Profile Analysis (TPA) the size of whose probe is P/20. The speed of the probe before the test when testing are both 1 mm/s. The ratio of the compression is 60%, trigger type is automatic 1N. The reciprocating motion is done by two times, test three times of each sample by the quality and structure analyzer. The sample is the muscles of the back of the tuna, of which the size is 3 cm× 3 cm× 3 cm. the hardness, Springiness, Cohesiveness as the studied object.

2.4 The Extraction of the Actomyosin Salt-Solubility

Get 5 g fish, adding 10 times of the amount of Tris-HCl buffer (pH7.05), meanwhile homogenize three times at speed of 20000rpm, each time within 30s, then centrifuge 15min with 10000r/min under low temperature (4°C). After that discard the supernatant and precipitate with cold 0.1MKCl 50mM Tris-HCl (pH = 7.05) and dissolve in buffer solution. After fully homogenized at 4°C to extract salt-soluble protein 1h, centrifuge at 9000r/min under 10min, and supernatant is the experimental actomyosin salt-solubility protein solution. actomyosin salt-solubility quantification: Coomassie brilliant blue method.

2.5 Ca²⁺ATPase Values

Using Nanjing Jiancheng ATP kit

Operating procedures:

- 1) Enzymatic reactions: the instructions 100l added to the sample and reagent mixing, 37°C accurate for 10 minutes;
- 2) Plumed R7,3500 rev / min, centrifuged for 10 minutes and got the supernatant
- 3) Phosphorus compounds was added into the supernatant at room temperature for 2 minutes and plumed terminator
- 4) At 636 nm wavelength, 1 cm light path, colorimetric

2.6 Statistical Analysis

Data are expressed as mean values (n =3) accompanied by the standard errors of means. Data from the different composition and quality parameters were subjected to one-way ANOVA (p<0.05) by employing an SPSS software (version 17.0). Comparison of means after the ANOVA test was performed using the Duncan's multiple range test (p<0.05).

3. Results and Discussion

3.1 Texture Profile Analysis

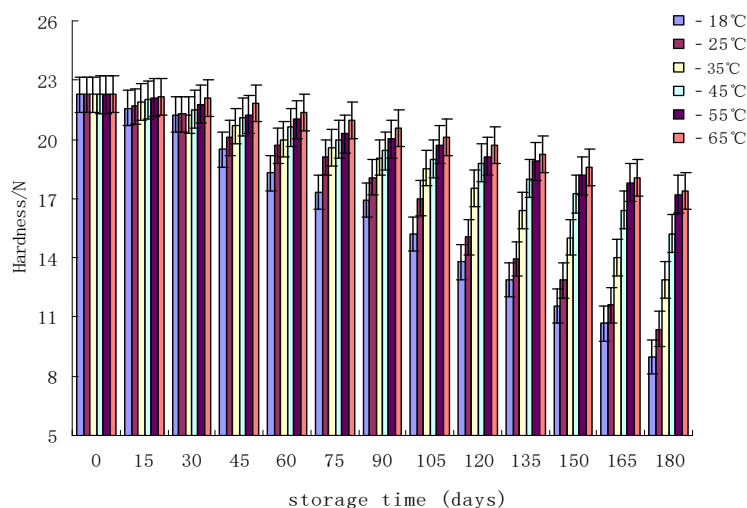


Figure 1. Effect of different storage temperatures on the Hardness of Tuna

Texture and appearance of food, flavor, nutrition together constitute the four quality factors of the food (Kristiansen et al., 2007). Hardness showed the tactile sense of human body soft or hard, the power can make food to a certain deformation. we can draw the conclusion from the figure, in the frozen process, the longer the frozen storage time, the smaller the hardness gradually became, but at different temperatures, the hardness changes ($p < 0.05$) significantly. When frozen at -18°C , the hardness of tuna changed maximum and frozen for six months, the hardness decreased from the beginning of 22.7 N to 8.98 N and dropped 61%; -25°C frozen, the hardness dropped 46.5%; -35°C frozen, the hardness dropped 26.9%; -45°C the hardness dropped 23.1%; -55°C the hardness dropped 17.1%. -65°C the hardness dropped 16.5%. The change of hardness related to the decrease of salt-soluble protein content and enzyme activity. On the one hand, during the frozen because ATP activity decreased fast, leading to serious action protein denaturation. On the other hand, due to the process of frozen, free water in tuna meat frozen into ice crystals, formed mechanical damage to the muscle cells, changed the protein three-dimensional structure, resulted in the decrease of muscle hardness (Katsunori et al., 2009; CHOW et al., 1985).

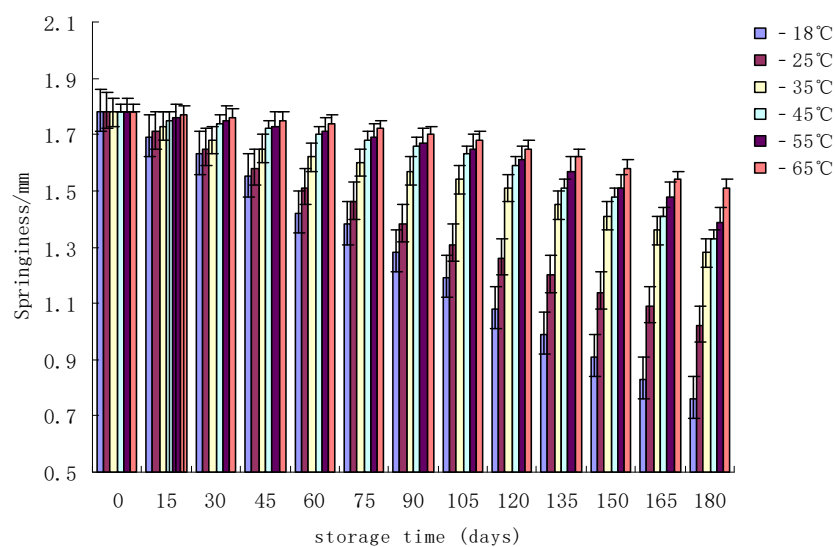


Figure 2. Effect of different storage temperatures on the Springiness of Tuna

Springiness reflected the recovery degree of deformation after eliminating force in external force. From the chart above, in the frozen process, when frozen at -18°C , the Springiness change of tuna was maximum and frozen for six months, the Springiness decreased 57.8%; -25°C the Springiness decreased 46.5%; -35°C frozen, the Springiness decreased 26.9%; -45°C the Springiness decreased 23.1%; -55°C the Springiness decreased 17.1%; -65°C the Springiness decreased 16.8%. The change of Springiness related to the degree of protein denaturation (WOOJ et al., 2007; Sato et al., 1986; Luis, 1999).

3.2 Actomyosin Salt-Solubility Analysis

We can draw the conclusion from the Figure 3 that refrigerating at different temperatures, with frozen time increasing, the salt-soluble protein content showed a downward trend. The lower frozen storage temperature, the more slowly salt-soluble protein content decreased. Under the temperature of -18°C , the change in former 45 d is great. It decreased from 47.5 mg/g to 15.2 mg/g . After 90 days, it decreased to 0; under the temperature of -25°C , the salt-soluble myofibril protein content changed rapidly from 30 d to 75 d, in the 120th days, it closes to 0; under the temperature -35°C , it changed rapidly from 120 d; under the temperature -45°C , it changed rapidly from 135 d; under the temperature -55°C and -65°C , it changed small after 6 months.

Features function of protein is determined by act myosin salt-soluble protein. After protein denatured, the act myosin salt-soluble protein decreased and the content of salt-soluble protein also decreased. Therefore, the content of salt-soluble protein, in a certain extent, reflected the penetration of proteins (Somjit et al., 2005).

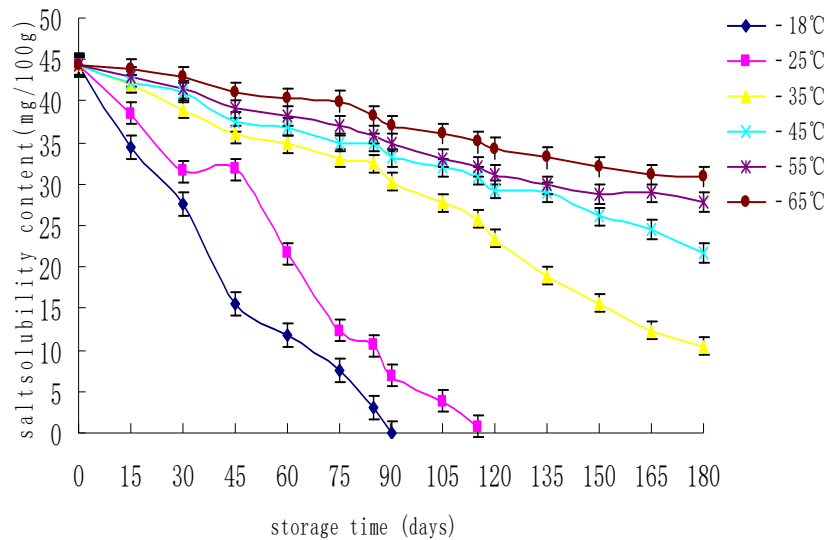


Figure 3. Effect of different storage temperatures on the salt-solubility of Tuna

3.3 Activity of Ca^{2+} ATPase Analysis

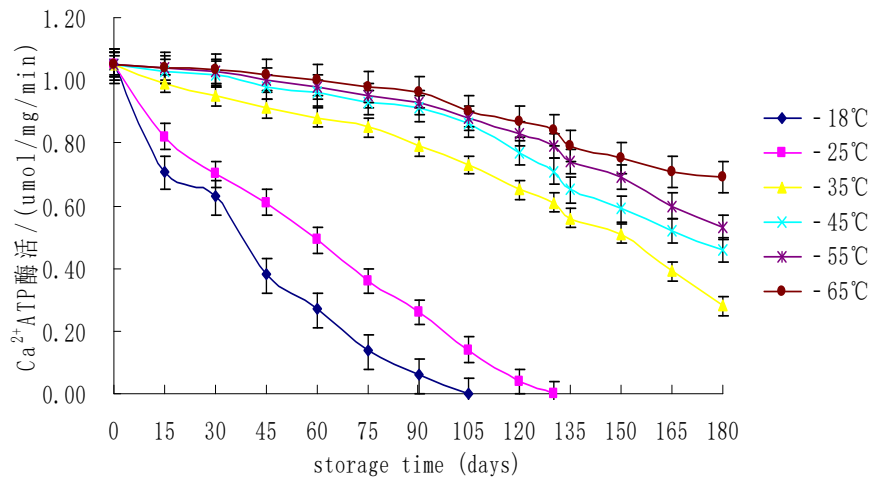


Figure 4. Effect of different storage temperatures on the activity of Ca^{2+} ATPase

We can draw the conclusion from the Figure 4 that under the temperature of -18°C , -25°C , -35°C , -45°C , it changed obvious, however, -55°C and -65°C it changed small. Ca^{2+} ATP activity declined with frozen storage time. The lower temperature, the better ATP activity maintained the higher. Activity of Ca^{2+} -ATPase Was directly related to the degree of actomyosin denaturation, thus, determined the Ca^{2+} -ATP activity had the significance in study the Protein Traits as well as judged the degree of act myosin denaturation (Hatful et al., 2012). On the one hand, Some people thought the reason of decrease the Ca^{2+} -ATPase's activity was caused by the configuration change in the myosin's globular head. On the other hand, interactions rearrangement in protein was also been thought to cause the Ca^{2+} ATP activity decreased (Li et al., 2009).

3.4 Water-Holding Capacity Analysis

Water is one of the most important ingredients in meat and meat products. The water of muscles is about 75% and it has relation with the structure, tenderness, flavor, color, processing characteristics of meat products. Water holding capacity will directly affect the meat's quality and economic benefits.

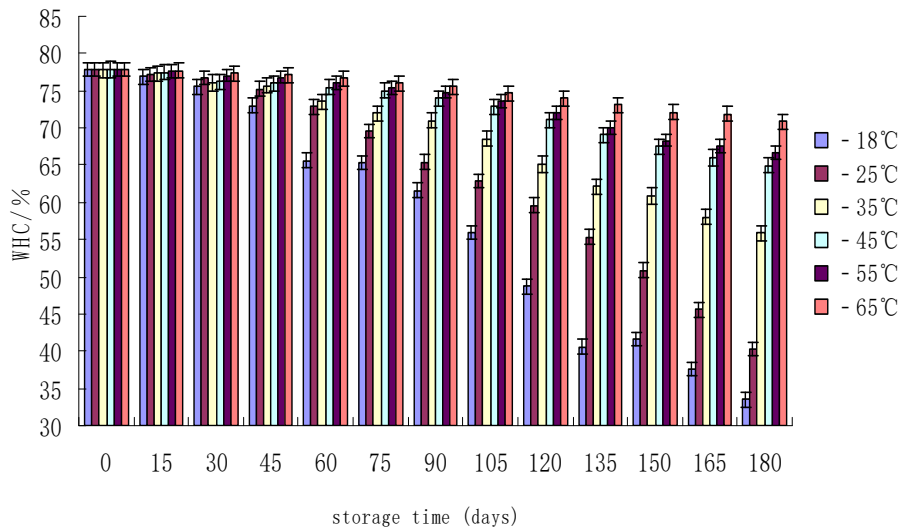


Figure 5. Effect of different storage temperature on the WHC of Tuna

We can draw the conclusion from the figure4 that under the temperature of -18°C . WHC decreased to 35%, -25°C it decreased to 43%, -35°C it decreased to 27%, -45°C it decreased to 23%, -55°C it decreased to 17%, -65°C it decreased to 16%. WHC decreased because the hydrophobic bonding of protein was damaged. Molecule of water of affinity protein became into free water, Meanwhile the combination chance of Amino acid was increased and the degeneration of protein condensed during frozen storage (Bengkulu et al., 2003).

4. Summary

Different frozen temperatures significantly impacted on the texture and biochemical characteristics of tuna back muscle. With frozen time increasing, hardness, springiness of tuna muscle decreased, the higher frozen storage temperature, the worse texture. With frozen time increasing, the content of actomyosin salt-soluble protein, and Ca^{2+} ATP activity showed a downward trend. The higher frozen temperature is, and the higher degree of protein penetration.

Change of texture related to protein denaturation, but the function features of protein is determined by actomyosin salt-soluble protein, thus change of texture related to the content decreasing of actomyosin salt-soluble protein. Under the temperatures of -55°C , the change of the content of actomyosin salt-soluble was not obvious and the change of texture was also small. Thus refrigerating in -55°C could keep the best quality of tuna during these six months.

References

- Badii, F., & Howell, N. K. (2002a). A comparison of biochemical changes in cod (*Gadus morhua*) and haddock (*Melanogrammus aeglefinus*) fillets during frozen storage. *J. Sci. Food Agric.*, *82*, 87–97. <http://dx.doi.org/10.1002/jsfa.998>
- Badii, F., & Howell, N. K. (2002b). Changes in the texture and structure of cod and haddock fillets during frozen storage. *Food Hydrocolloids*, *16*, 313–319. [http://dx.doi.org/10.1016/S0268-005X\(01\)00104-7](http://dx.doi.org/10.1016/S0268-005X(01)00104-7)
- Godiksen, H., & Jessen, F. (2001). Sarcoplasmic reticulum Ca^{2+} -ATPase activity in cod (*Gadus morhua*) muscle measured in crude homogenates. *J. Food Biochem*, *25*, 343–358.
- Godiksen, H., Hyldig, G., & Jessen, F. (2003). Sarcoplasmic reticulum Ca^{2+} -ATPase and cytochrome oxidase as indicators of frozen storage in cod (*Gadus morhua*). *J. Food Sci.*, *68*, 2579–2585. <http://dx.doi.org/10.1111/j.1365-2621.2003.tb07064.x>
- Kristinsson, H. G., Ludlow, N., Balaban, M. O., Otwell, W. S., & Welt, B. A. (2011). Muscle Quality of Yellowfin Tuna (*Thunnus albacares*) Steaks After treatment with Carbon Monoxide Gases and Filtered Wood Smoke. *J Aquat Food Prod T*, *15*, 49-67.
- Leelapongwattana, K., Benjakul, S., Visessanguan, W., & Howell, N. K. (2005). Physicochemical and biochemical changes during frozen storage of minced flesh of lizardfish (*Saurida micropectoralis*). *Food Chemistry*, *90*(1), 141-150.

- Nielsen, J., & Jessen, F. (2007). Quality of frozen fish in Handbook of Meat, Poultry and Seafood Quality. In L. M. L. Nollet (Ed.) *Blackwell Publishing: Iowa* (pp. 577–586). <http://dx.doi.org/10.1002/9780470277829.ch44>
- Ruiz-Capillas, C., & Moral, A. (2001a). Correlation between biochemical and sensory quality indices in hake stored in ice. *Food Res Int.*, *34*, 441–447. [http://dx.doi.org/10.1016/S0963-9969\(00\)00189-7](http://dx.doi.org/10.1016/S0963-9969(00)00189-7)
- Saguy, I., & Karel, M. (1980). Modeling of quality deterioration during food processing and storage. *Food Technol.*, *34*, 78–85.
- Sikorski, Z. E. (1978). Protein changes in muscle foods due to freezing and frozen storage. *Int. J. Refrig.*, *1*, 173–180. [http://dx.doi.org/10.1016/0140-7007\(78\)90094-4](http://dx.doi.org/10.1016/0140-7007(78)90094-4)
- Steen, C., & Lambelet, P. (1997). Texture changes in frozen cod mince measured by low-field nuclear magnetic resonance spectroscopy. *J. Sci. Food Agric.*, *75*, 268–272. [http://dx.doi.org/10.1002/\(SICI\)1097-0010\(199710\)75:2%3C268::AID-JSFA881%3E3.3.CO;2-F](http://dx.doi.org/10.1002/(SICI)1097-0010(199710)75:2%3C268::AID-JSFA881%3E3.3.CO;2-F)
- Tironi, V. A., & Toma's, M. C. (2007). Lipid and protein deterioration during the chilled storage of sea salmon (*Pseudoperca semifasciata*). *J Sci Food Agr*, *87*(12), 2239–2246. <http://dx.doi.org/10.1002/jsfa.2949>
- Ueki, N., & Ochiai, Y. (2004). Primary structure and thermostability of bigeye tuna myoglobin in relation of those of other scombridae fish. *Fisheries Sci.*, *70*, 875–884. <http://dx.doi.org/10.1111/j.1444-2906.2004.00882.x>
- Uresti, R., Téllez-Luis, S., Ramírez, J., & Vázquez, M. (2004). Use of diary proteins and microbial transglutaminase to obtain low-salt fish products from filleting waste from silver carp (*Hypophthalmichthys molitrix*). *Food Chem.*, *86*, 257-262.
- Visessanguan, W., Chutima, T., & Munchiko, T. (2005). Effect of frozen storage on chemical and gel-forming properties of fish commonly used for surimi production in Thailand. *Food Hydrocol.*, *19*, 197-207.
- Watanabe, H., Yamanaka, H., & Yamanakawa, H. (1992). Post mortem biochemical changes in the muscle of disk abalone during storage. *Nippon Suisan Gak.*, *58*, 2081–2088. <http://dx.doi.org/10.2331/suisan.58.2081>
- Zhu, S., Ramamwamy, H. S., & Simpson, B. K. (2004). Effect of high-pressure versus conventional thawing on color, drip loss and texture of Atlantic salmon frozen by different methods. *Food Sci. Technol-Leb.*, *37*, 291-299.

Copyrights

Copyright for this article is retained by the author(s), with first publication rights granted to the journal.

This is an open-access article distributed under the terms and conditions of the Creative Commons Attribution license (<http://creativecommons.org/licenses/by/3.0/>).

COD Removal of Edible Oil Content in Wastewater by Advanced Oxidation Process

Aola Hussein Flamarz Tahir¹, Nagham Obeid Kareim¹ & Shatha Abduljabbar Ibrahim¹

¹ Faculty of Engineering, Al Mustansiriayah University, Baghdad, Iraq

Correspondence: Aola Hussein Flamarz Tahir, Faculty of Engineering, Al Mustansiriayah University, Baghdad, Iraq. E-mail: aola90@gmail.com

Received: March 2, 2016 Accepted: March 17, 2016 Online Published: April 30, 2016

doi:10.5539/enrr.v6n2p57

URL: <http://dx.doi.org/10.5539/enrr.v6n2p57>

Abstract

Different Advanced Oxidation Processes (Photo Fenton process, Fenton process and H₂O₂/UV) were studied in order to reduce COD from oily compounds aqueous solution using batch system. To get the optimum condition, different variables were studied for each of these processes; such as pH, time, concentration of H₂O₂, concentration of oil, concentration of FeSO₄·7H₂O and temperature as parameters. It was found that the optimal pH value for the three processes was 3 and the optimal temperature was 30°C for Photo-Fenton and UV/H₂O₂ system and 20°C for Fenton process. Photo-Fenton process gave a maximum COD reduction of 80.59 % (COD from 2684 to 521 mg/l), Fenton gave 53.22 % (COD from 2587-1130) and the combination of UV/H₂O₂ gave a COD reduction of 22.69 % (COD from 2450 to 1894). The percentage of removal found was after the total reaction time (180 min.). The optimum chemical reagents for Photo-Fenton, Fenton and UV/H₂O₂ were as the following H₂O₂ = 800 mg/l, 1500 mg/l and 2000 mg/l, Fe₂SO₄·7H₂O = 60 mg/l, 100 mg/l.

Keywords: advanced oxidation process, edible oil, sunflower oil, photo-fenton, fenton, hydrogen peroxide

1. Introduction

Edible refined oil processing industry is a major issue of environmental concern due to the increase in production and demand in developing countries in the past three decades. The waste streams effluents creates serious environmental problem such as great threat to aquatic life due to its high organic content. Hence its treatment is essential prior to its disposal. The choice of effluent treatment methods depends on the organic content present in the effluent and its discharge conditions (Sharma et al., 2014). The oil seeds are usually processed to obtain the oil contents which are subsequently processed for human consumption and industrial applications. Thus the vegetable oil industries are, equally, associated with oil extraction, refining, transportation, uses and reuses. However, these industries have been linked with environmental pollutions resulting from oil spill, oily effluent discharge into water bodies and oily sludge discharge into the environment indiscriminately, untreated or in conditions below the standard discharge limits (Alade et al., 2011).

Crude vegetable oils are mainly triacylglycerols (around 95%) along with some free acids, monoacylglycerols, and diacylglycerols. They also contain variable amounts of other components such as phospholipids, free and esterified sterols, triterpene alcohols, tocopherols and tocotrienols, carotenes, chlorophylls and other coloring matters, and hydrocarbons as well as traces of metals, oxidation products and some undesirable flavors (Gunstone, 2005). Vegetable oil wastewater (VOWW) has been treated in different ways. Its characteristics depend largely on the type of oil processed and on the process implemented that are high in COD, oil and grease, sulphate and phosphate content, resulting in both high inorganic as well as organic loading of the relevant wastewater treatment works. The wastewater varies both in quantity and characteristics from one oil industry to another. The composition of wastewater from the same industry also varies widely from day to day (Chin & Wong, 1981). Also the oil type processed may be a reason for these fluctuations.

Wastewaters containing oil can be treated either in chemical or biological units. The efficiency of treatment depends on the ratio of free oil to emulsified oil. The free oil can be easily removed from wastewater by physical processes but in order to remove emulsified oil from wastewater, de-emulsification should be done. The conventional treatment of vegetable oil industry wastewater consists of mechanical dewatering of sludge produced with physical, chemical and biological processes. In general, biological treatments that are applied in the industry to treat the VOWW. It will start with oil removal and dissolved air flotation (DAF) with alum as

coagulant before entering into biological treatments. Variation in wastewater flow and composition has led to the inefficiency of bioprocess resulting the treated effluent could not meet the discharge limits (Ng, 2006).

Advanced oxidation processes (AOPs) belong to the chemical treatment category and are used to oxidise organic compounds found in wastewater which are difficult to handle biologically into simpler end products. Advanced oxidation processes (AOPS) are technologies based on the generation of hydroxyl radicals, especially the hydroxyl radical (OH), which is highly reactive substance used to degrade toxic organic compound in a medium. The main reason why AOPs was chosen in this study is due to its reputation in treating highly recalcitrant pollutant and removal wide range of (Wols & Hofman-Cal, 2012).

Depending upon the nature of the organic species, four types of initial attack are possible: Radical addition Equation (2.1), hydrogen abstraction Equation (2.2), electron transfer Equation (2.3) and radical combination Equation (2.4). In the following equations, R is used to describe the reacting organic compound (Heponiemi & Lassi, 2012):

Radical addition: Reaction of the hydroxyl radical and unsaturated or aliphatic organic compound produces organic radical which can further oxidize by oxygen or ferrous iron to form stable oxidized end products.



Hydrogen abstraction: Generated hydroxyl radical can be used to remove hydrogen from an organic compound forming an organic radical and initiating a chain reaction where the organic radical reacts with oxygen. This produces a peroxy radical, which can react with another organic compound, and so on.



Electron transfer: Electron transfer results in the formation of ions with a higher valence. Oxidation of a monoatomic negative ion will result in the formation of an atom or a free radical.



A radical combination: Two radicals form a stable product.



Generally, the reaction of hydroxyl radicals and organic compounds will produce water, carbon dioxide and salts (SES, 1994).

Three processes are investigated in this study:

Fenton process (H₂O₂/UV): The conventional 'dark' Fenton process was reported first by Fenton (1894) over a century ago for the oxidation of maleic acid. The process involves the reaction between dissolved Fe²⁺ and hydrogen peroxide in acidic aqueous solution, leading to the formation of hydroxyl radicals.

Photo-Fenton process (H₂O₂/Fe²⁺/UV): This process involves the hydroxyl radical (·OH) formation in the reaction mixture through photolysis of hydrogen peroxide (H₂O₂/UV) and Fenton reaction (H₂O₂/Fe²⁺).

Hydrogen peroxide/UV light process: This process includes H₂O₂ injection and mixing followed by a reactor that is equipped with UV light (200 to 280 nm). During this process, ultraviolet radiation is used to cleave the O-O bond in hydrogen peroxide and generate the hydroxyl radical.

2. Method

Commercial sunflower oil was been used as the model pollutant and to prepare an artificial sample. The commercial sunflower oil used was from Bil Bak, double refined sunflower oil and imported for Iraqi ministry of trade/ state company for foodstuff trading, for the purpose of ration card. It was analyzed at the Iraqi vegetable oil company laboratories (Table 1). Artificial sunflower oil-water emulsion was prepared as it is the critical level of oil wastewater. The emulsion was prepared by using 2.5 ml of 100 ppm sodium dodecyl sulphate (Biltrec, Spain) for every 100 ml of oil in 1 liter distilled water (Ebrahim et al., 2013).

All experiments are conducted in a 2 Liter thermostatic batch glass reactor mounted at magnetic stirrer with hot plate (LMS-1003, DAIHAN LAB TECH, KOREA). UV radiation (254 nm) is produced from UV lamps (UVM 9311 G, 6 watt 4P-SE, SO SAFE WATER TECHNOLOGIES, UAE), which is set vertically at the top of the reactor. The lamp is totally immersed in the cylindrical reactor. UV lamp is covered in a quartz sleeve for protection and has the characteristics shown in Table (3.5). The distance between the lamp and the reactor wall is fixed to be 5 cm to ensure maximum light irradiation as shown in Figure (2.1).

Table 1. Physical properties of sunflower oil sample

Test	Result	Standard
Relative Density	0.920	0.918- 0923
Refractive index (40 °C)	1.468	1.467 – 1.469
Cloud point	2	+ 6°C
Peroxide value	1.6	Max. 2
F.F.A	0.05	0.18 – 0.20
Fe	5	Max. 15 ppm
Colour	0.9R 4.8Y	3R 30Y
Odor	Acceptable	Acceptable

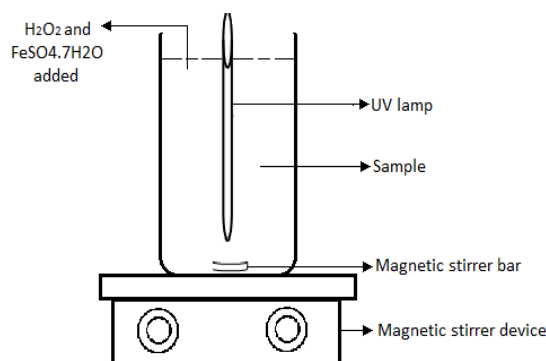


Figure 1. Laboratory unit – scale batch reactor

2.1 Reagents

All the reagents used in the experiments was research grade reagents without further purification whereby H₂O₂ (50%, w/w) from Solvochem, FeSO₄·7H₂O from Hopkin and Williams (England) and Na₂S₂O₃, NaOH and H₂SO₄ from Central Drug House (India).

2.2 Analytical Method

Chemical oxygen demand of samples was analyzed by using Lovibond Checkitdirect COD Photometer (Germany). The COD ranges used were from 0-15000 mg/l and 0-1500 mg/l.

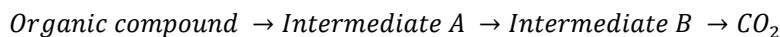
3. Results and Discussion

Different important factor were studied in this study to discuss its different effects on the AOP's. The performance of single Fenton's reagent, Photo-Fenton and combination of UV radiation with hydrogen peroxide for COD removal from oily compounds aqueous solution using batch system were investigated. The following topics were also studied: wastewater characterization, pH value, temperature, effect of H₂O₂ concentration, effect of Fe₂SO₄·7H₂O concentration and irradiation time.

3.1 The Effect of Irradiation Time

The effect of time required for the Photo-Fenton process and UV/H₂O₂ in order to get best removal efficiency was studied. For both processes fixed initial amount of H₂O₂, Fe₂SO₄·7H₂O pH, and temperature was set. Initial oil concentration (1000) mg/l (COD = 2500 ± 500) was used in the experiments. The results for Photo-Fenton and UV/H₂O₂ process plotted in Figure (1).

The optimum time that gave best removal efficiency was found after 180 min. for both processes. It gave a total 67.07 % and 16.34 % COD reduction for Photo-Fenton and UV/H₂O₂ process respectively. It also found that the oil degradation rate did not increase after 180 min. process time. The removal efficiency was decrease slightly or no change. The total degradation of organic compounds undergoes this reaction sequence (Nasr et al., 2004):



Some intermediates are non volatiles compounds, causing the lowness of COD reduction increase. Such intermediates (quinines, acetic acid etc.) require sufficient time to push reaction beyond CO₂ (Nasr et al., 2004).

3.2 The Effect of H₂O₂ Concentration

The effect of initial concentration of H₂O₂ on Photo-Fenton, Fenton and UV/H₂O₂ process was tested to optimize the amount of H₂O₂ required to reduce the COD. The H₂O₂ concentration range for Photo-Fenton was (200, 400, 600, 800 and 1000) mg/l, whereas for Fenton and UV/H₂O₂ the range was (500, 1000, 1500, 2000 and 2500 mg/l). Fixed initial oil concentration, Fe₂SO₄·7H₂O concentration, pH and temperature was used in all experiments. The results were plotted in Figure (2).

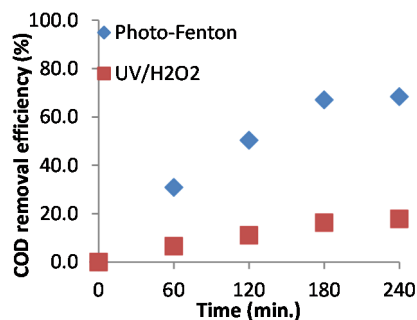


Figure 2. Effect of irradiation time on the COD removal by Photo-Fenton and UV/H₂O₂ system at H₂O₂ = 1000 mg/l, pH = 7, oil conc. = 1000 mg/l, temp. = 20°C and Fe₂SO₄·7H₂O = 100 mg/l (for Photo-Fenton process only)

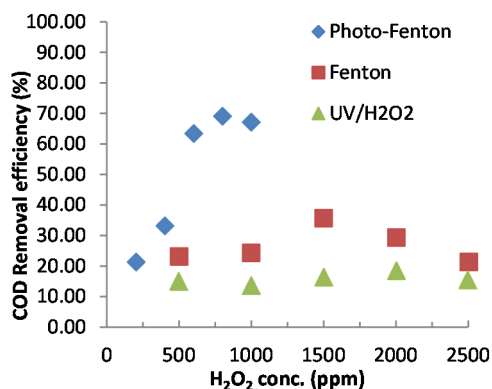


Figure 3. Effect of initial H₂O₂ concentration on the COD removal by Photo-Fenton, Fenton and UV/H₂O₂ system at pH = 7, oil conc. = 1000 mg/l and temp. = 20°C and Fe₂SO₄·7H₂O = 100 mg/l (for Photo-Fenton and Fenton process only)

From this figure it can be noticed that the COD removal increased as the concentration of H₂O₂ increased with the increasing of its dosage, reaching a maximum removal efficiency of 69.02 %, 35.68 % and 18.44 % for Photo-Fenton, Fenton and UV/H₂O₂, respectively. At higher H₂O₂ dosage than the optimum found there was an increase or no change in COD removal efficiency, the following point is a brief explanation about the H₂O₂ effect:

Hydrogen peroxide was the main responsible species of the degradation process by the generating of hydroxyl radicals from the direct photolysis. It can be observed that the degradation rate increased considerably when H₂O₂ was used (Esplugas et al., 2002).

After optimum H₂O₂ conc. it was found that further increase of H₂O₂ concentration retarded effluents COD. This inhibition of mineralization is probably due to both auto decomposition of H₂O₂ into oxygen and water and the scavenging of hydroxyl radicals by the excess of H₂O₂ according to the following reactions (Chatzisyseon et al., 2008):



Hydroxyl radical may recombine and participate in radical-radical reactions to form H₂O₂



At higher H_2O_2 concentrations lower light intensity available for oil degradation, since H_2O_2 also absorb lights in the system (Ebrahim et al., 2013).

3.3 The Effect of $Fe_2SO_4 \cdot 7H_2O$ Concentration

The effects of initial $Fe_2SO_4 \cdot 7H_2O$ on Photo-Fenton and Fenton process were tested by carrying out experiments with different concentration of $Fe_2SO_4 \cdot 7H_2O$ (20, 40, 60, 80 and 100 mg/l) for Photo-Fenton process and (50, 100, 150, 200 and 250 mg/l) for Fenton process. Fixed initial oil concentration, pH and temperature was used in all experiments. The results were plotted in Figure (3). By these figures it can be noticed that the degradation rate of oil increased with the increasing amounts of iron salt. It reached its maximum value (72.35 %) at 60 mg/l for Photo-Fenton process and (35.68 %) at 100 mg/l for Fenton process after about 180 min. of irradiation time. The addition of the iron salt above these values this did not affect the degradation; it decreased and or remained unchanged.

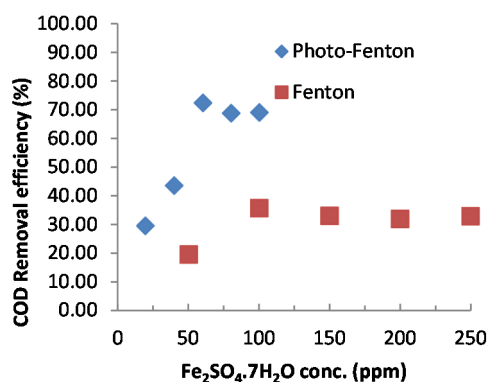


Figure 4. Effect of initial $Fe_2SO_4 \cdot 7H_2O$ concentration on the COD removal by Photo-Fenton, and Fenton system at pH = 7, oil conc. = 1000 mg/l and temp. = 20°C, H_2O_2 = 800 mg/l and 1500 mg/l for Photo-Fenton and Fenton process, respectively

The decrease and increase in the removal efficiency can be explained by the following points:

Addition of ferrous ions increases wastewater brown turbidity during the photo-treatment, which hinders the absorption of the UV light, required for the Photo-Fenton process (Dincer et al., 2008). Also excessive formation of Fe^{+2} which can compete with the organic carbon for OH radical may be a reason for the decrease. High Fe ions disposal will require another process to remove the iron residual so for an economical point of view, in this condition, it is not necessary to have high concentration of Fe ion (Galvão et al., 2006). Fixed H_2O_2 concentration can be the limiting factor (Rodriguez et al., 2002).

3.4 The Effect of pH Value

The pH plays an important role in the AOP's and has a considerable effect on the reactions, because of the big influence to the oxidation potential of OH radical according to the reciprocal relation of the oxidation potential to the pH value ($E_0=2.8$ V and $E_{14}=1.95$ V) (Alalm & Tawfik, 2013). Different values of pH were examined in this study (3, 7 and 11) keeping the other parameters and dosage constant. The results are plotted in Figure (4).

Optimum pH was found equal to 3 for Photo-Fenton, Fenton and UV/ H_2O_2 system which gave a removal efficiency of (79.4 %, 40.3 % and 21.31 %).

The optimum pH found (3) can be explained by:

The operational pH must be low (pH <4) to nullify the effect of sequestering radical species, specifically ionic species such as carbonate and bicarbonate ions, leading to a better degradation rate (Mota et al., 2008). At lower pH (< 2.5), the formation of $[Fe(H_2O)_6]^{2+}$ complex occurs. These reacts more slowly with H_2O_2 than does $[Fe(OH)(H_2O)_5]^+$ complex therefore produces less amount of reactive hydroxyl radicals thereby reducing the COD removal efficiency as mentioned by (De Laat and Gallard, 1999). At high pH, iron reacts with the hydroxide ions (HO^-), precipitating the iron hydroxide ($Fe(OH)_2$ or $Fe(OH)_3$), which does not react with H_2O_2 , which will decrease the degradation rate (Mota et al., 2008).. The removal efficiency of COD was improved at

the acidic conditions, raising the pH from 3 to 7 decreased the COD removal efficiency. Similar findings was reported by (Li et al., 2009) who found that the decomposition rate of H_2O_2 is low at pH exceeding 4 resulting a drop in the hydroxyl radicals production. In high pH condition, the reaction between Fe^{3+} and OH^- will lead to the formation of $Fe(OH)_3$. This species will start to precipitate after pH 4.8 based on the calculation from its solubility constant value; K_{sp} ($Fe(OH)_3$) is 2.79×10^{-9} . This precipitate will then act as coagulant. Therefore, it is expected that no dominance oxidation and OH radicals generation will occur at this stage (Fadzil et al., 2013).

An adjustment in pH may be required in the wastewater to be treated before adding the Fenton reagents.

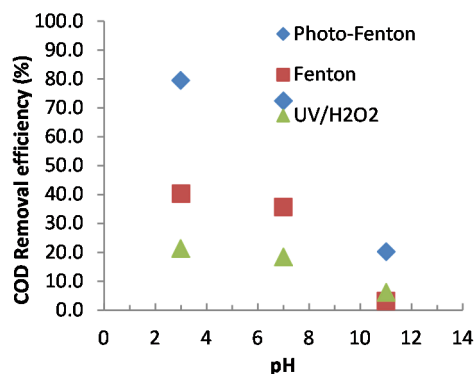


Figure 5. Effect of pH value initial concentration on the COD removal by Photo-Fenton, Fenton and UV/ H_2O_2 system at oil conc. = 1000 mg/l and temp. = 20°C, H_2O_2 = 800 mg/l, 1500 mg/l, H_2O_2 = 2000 and $Fe_2SO_4 \cdot 7H_2O$ = 60 mg/l, 100 mg/l for Photo-Fenton, Fenton process and UV/ H_2O_2 system, respectively

3.5 The Effect of Oil Concentration

Different concentrations of vegetable oil (1000, 2000 and 3000) mg/l were used at fixed pH, temperature, H_2O_2 and $Fe_2SO_4 \cdot 7H_2O$ dosage for all experiments. The results were plotted in Figure(5).

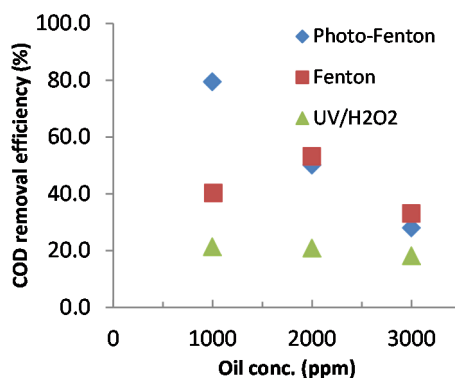


Figure 6. Effect of oil concentration on the COD removal at pH = 3, temp. = 20°C, H_2O_2 = 800 mg/l, 1500 mg/l, 2000 and $Fe_2SO_4 \cdot 7H_2O$ = 60 mg/l, 100 mg/l for Photo-Fenton, Fenton and UV/ H_2O_2 system, respectively

By these figures it can be observed that the removal efficiency decreases linearly in Photo-Fenton from 79.4 % to 28.05 % as the concentration of oil increases from 1000 to 3000 mg/l respectively. Similarly, in UV/ H_2O_2 process the maximum removal efficiency at 1000 mg/l was 21.31 % and decrease down to (18.17) % at 3000 mg/l. In Fenton process the removal efficiency increased at the oil concentration increased up to 2000 mg/l, from (53.22 %) to (24.62 %).

This can be attributed to the increase in COD which leads to high turbidity of the solution. In Photo-Fenton the COD for 3000 mg/L oil solution was measured to be 5861, whereas for 1000 mg/L oil solution the COD was 2587 only. As turbidity in the solutions during the photo treatment hinders the absorption of the UV light for the

photo Fenton process (Rodriguez et al., 2002). (Dincer et al., 2008) diluted wastewater with 21000 ppm COD (80%) in order to treat it with Photo-Fenton. On the other, more COD was removed at higher oil conc. (COD strength) than lower COD in Fenton process and this may due to the absence of UV irradiation and turbidity effect, also because it enhances the attack on the organic matter due to its high content.

3.6 The Effect of Temperature

Reaction temperature is another important process parameter that affects the degradation process. Different temperatures (20, 30 and 40)°C were used. The dosage of the reagents and other parameters were remained constant as obtained from previous sections.

The results were plotted in Figure (6). These figures shows that the COD removal efficiency increases at 30°C and then decreased at 40°C for Photo-Fenton process. For Photo-Fenton and UV/H₂O₂ system the maximum removal efficiency were 80.59 and 22.69%, respectively. For Fenton process the removal efficiency is 53.22 % at 20°C

The increase in temperature accelerated the decomposition of H₂O₂ thus increasing the generation of OH radicals which enhances the degradation process slightly. There is no significant COD removal different with different temperatures; the range of the COD removal on predetermined time for these three different temperatures is less than 10%. This finding is in agreement with the previous observation of (Leong & Bashah, 2012). The optimal temperature is in the range of 20-40°C and this result is similar to other researches findings (Leong & Bashah, 2012; Lucas & Peres, 2009; Nieto et al., 2011).

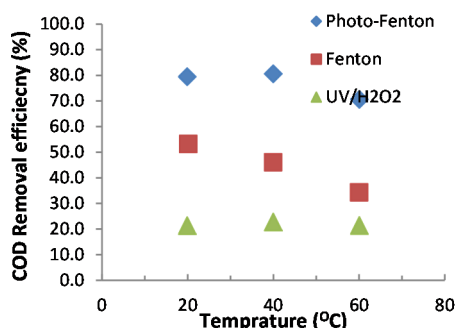


Figure 7. Effect of temperature on the COD removal at pH = 3, oil concentration = 1000 mg/l, 2000 mg/l, 1000 mg/l, H₂O₂ = 800 mg/l, 1500 mg/l, 2000 and Fe₂SO₄.7H₂O = 60 mg/l, 100 mg/l for Photo-Fenton, Fenton and UV/H₂O₂ system, respectively

5. Conclusions

The COD removal from synthetic vegetable oil wastewater was investigated by the Photo-Fenton, Fenton and UV/H₂O₂ processes. The COD removal efficiency was strongly affected by many factors such as the concentration of H₂O₂, Fe₂SO₄.7H₂O, pH, temperature and the oily content amount.

It was found that the Photo-Fenton, Fenton and combination of UV and H₂O₂ processes have the potential to partially reduce the COD of oily wastewater in different removal percentage. The overall results of this study indicate that the application of Photo-Fenton process is a feasible method to treat vegetable oily content wastewaters achieving a significant decrease of COD. Optimum initial pH was found 3 for all three processes studied, temperature of 30°C was found optimum for Photo-Fenton and UV/H₂O₂ system and 20°C for Fenton system. Optimum chemical reagents dosage for Photo-Fenton at H₂O₂ = 800 mg/l and Fe₂SO₄.7H₂O = 60 mg/l, leads to a COD reduction of 80.59 %. Fenton's reagent at H₂O₂ = 1000 mg/l and Fe₂SO₄.7H₂O = 1500 mg/l, leads to a COD reduction of 53.22 %. UV/H₂O₂ combination process a low COD removal efficiency 22.69 % was found.

References

- Alade A. O., Jameel A. T., Muyubi A. S., Abdul Karim M. I., & Alam, M. D. Z. (2011). Removal of oil and grease as emerging pollutants of concern (EPC) in wastewater stream. *Iranian Journal of Oil & Gas Science and Technology*, 2(4), 01-11
- Alalm M. G., & Tawfik, A. (2013). Fenton and solar Photo-Fenton oxidation of industrial wastewater containing pesticides. *Seventeenth International Water Technology Conference, IWTC17*.

- Chatzisymeon E., Stypas, E., Boosios, S., Xekoukoulotakis, N. P., & Mantzavinos, D. (2008). Photocatalytic treatment of black table olive processing wastewater. *J. Haz. Mater.*, *154*, 1090-1097.
- Chin, K. K., & Wong, K. K. (1981). Palm oil refinery wastes treatment. *Water Res.*, *15*, 1087.
- De Laat, J., & Gallard, H. (1999). Catalytic decomposition of hydrogen peroxide by Fe(III) in homogeneous aqueous solution: Mechanism and kinetic modeling. *Environmental Science and Technology*, *33*, 2726–2732.
- Dincer, A. R., Karakaya, N., Gunes, E., & Gunes, Y. (2008). Removal of COD from Oil Recovery Industry wastewater by the Advanced Oxidation Processes (AOP) based on H₂O₂. *Global NEST Journal*, *10*(1), 31-38.
- Ebrahim, M., Mustafa, Y. A., & Alwarded, A. I. (2013). Removal of oil wastewater by advanced oxidation process/homogenous process. *Journal of Engineering*, *6*(19).
- Esplugas, S., Gimenez, J., Contreras, S., Pascual, E., & Rodriguez, M. (2002). Comparison of different advanced oxidation processes for phenol degradation. *Water Res.*, *36*(4), 1034-42.
- Fadzil, N. A. M., Zainal, Z., & Abdullah, A. H. (2013). COD Removal for Palm Oil Mill Secondary Effluent by Using UV/Ferrioxalate/TiO₂/O₃ system. *International Journal of Emerging Technology and Advanced Engineering*, *3*(7), 237-243.
- Galvão S. A. O., Mota, A. L. N., Silva, D. N., Moraes, J. E. F., Nascimento, C. A. O., & Chiavone-Filho, O. (2006). Application of the photo-Fenton process to the treatment of wastewaters contaminated with diesel. *Science of The Total Environment*, *367*, *1*(15), 42–49.
- Gunstone, F. (2005). Bailey's Industrial Oil and Fat Products (6th Ed.). *Vegetable oils*, *1*, 213 – 269. Wiley Interscience, Memorial University of Newfoundland, Canada.
- Leong, S. K., & Bashah, N. A. A. (2012). Kinetic study on COD removal of palm oil refinery effluent by UV-Fenton. *APCBEE Procedia*, *3*, 6-10.
- Li, R., Yang, C., Chen, H., Zeng, G., Yu, G., & Guo, J. (2009). Removal of triazophos pesticide from wastewater with Fenton reagent. *Journal of hazardous materials*, *167*(1), 1028-1032.
- Lucas, M. S., & Peres, J. A. (2009). Removal of COD from olive mill wastewater by Fenton's reagent: Kinetic study. *J Hazard Mater*, *168*(2-3), 1253-1259.
- Mota, A. L. N., Albuquerque, L. F., Beltrame, L. T. C., Chiavone-Filho, O., Machulek, Jr. A., & Nascimento, C. A. O. (2008). Advanced oxidation processes and their application in the petroleum industry a review. *Brazilian Journal of Petroleum and Gas*, *2*(3), 122-142.
- Nasr, B., Ahmed, B., & Abdellatif, G. (2004). Fenton treatment of olive oil mill wastewater–applicability of the method and parameters effects on the degradation process. *Journal of Environmental Sciences*, *16*(6), 942-944.
- Ng, W. J. (2006). *Industrial Wastewater Treatment*. London: Imperial College Press.
- Nieto, L. M., Hodaifa, G., Rodraguez, S., Gimacnez, J. A., & Ochando, J. (2011). Degradation of organic matter in olive-oil mill wastewater through homogeneous Fenton-like reaction. *Chem Eng J*, *173*(2), 503-510.
- Rodriguez, M., Sarria, V., Esplugas, S., & Pulgarin, C. (2002). Photo-Fenton treatment of a biorecalcitrant wastewater generated in textile activities: biodegradability of the phototreated solution. *J Photoch Photobio A*, *151*, 129-135.
- Sharma, S., Ashok, K. Sharma, Sanjay, V., Himmat, S. D. (2014). Edible oil refinery waste water treatment by using effluent treatment plant. *International Journal of Chemical Studies*, *2*(3), 36-42.
- Wols, B. A., & Hofman-Cari, C. H. M. (2012). Review of photochemical reaction constants of organic micropollutants required for UV advanced oxidation processes in water. *Water Research*, *46*(9), 2815–2827.

Copyrights

Copyright for this article is retained by the author(s), with first publication rights granted to the journal.

This is an open-access article distributed under the terms and conditions of the Creative Commons Attribution license (<http://creativecommons.org/licenses/by/3.0/>).

A Simultaneous Model for Simulating the Propagation of Hydraulic Head in Aquifers with Leakage Pathways

Seong Jun Lee¹

¹ Department of Civil and Environmental Engineering, University of Utah, Salt Lake City, United States

Correspondence: Seong Jun Lee, Department of Civil and Environmental Engineering, University of Utah, Salt Lake City, UT, United States. Tel: 1-801-585-4484. E-mail: sjlee@egi.utah.edu

Received: March 17, 2016 Accepted: April 14, 2016 Online Published: May 4, 2016

doi:10.5539/enrr.v6n2p65 URL: <http://dx.doi.org/10.5539/enrr.v6n2p65>

Abstract

A three-dimensional simultaneous solution model was developed for analysis of variable transient flows, specifically leakage associated with arbitrary groundwater aquifers. The model simultaneously calculates leakage rates using the hydraulic gradients between coupled leakage points at two leaky aquifers and evaluates the propagation of hydraulic heads in multiple aquifers resulting from that leakage. Important considerations for leakage simulation are variant leakage rates with time and leakage starting time. Two types of leakage pathways are specified in terms of the generated time, including (1) pre-existing leakage pathways and (2) abruptly-induced leakage pathways at specific times. The governing equation with a leakage term is composed of three finite difference equations, and its form depends on whether leakage pathways pre-exist or are induced at specified times according to known or assumed aquifer histories. The developed numerical code was validated by comparison with the results of the TOUGH2/EOS1 program for a three-dimensional conceptual domain.

Keywords: leaky aquifers, simultaneous solution model, pre-existing leakage pathways, abruptly-induced leakage pathways

1. Introduction

We developed a simultaneous solution model for the three-dimensional analysis of transient flow in arbitrary multilayered groundwater aquifers with leakage. The developed model uses the Finite Difference Method (FDM) and is designed to understand the propagation of groundwater through several possible leakage zones in porous media, such as fractures and abandoned wells. We view this research as an applied single-phase flow analysis in a research program focused on storage of CO₂ in geological formations and associated potential leakage. In the geologic carbon storage (GCS) project, CO₂ injected into deep storage reservoirs saturated with brine may induce pressure buildup and migration of brine. The existence of fractures and faults or abandoned pre-existing wells in the storage system can cause the leakage of pressurized brine into adjacent formations. Before CO₂ leakage occurs, the adjacent aquifers saturated with brine act as single-phase reservoirs; therefore, the single-phase code can be an effective tool in evaluating the brine leakage features in multiphase flow systems (Lee et al., in press). In addition, Cihan et al. (2013) demonstrated that the analytical solution model for single-phase fluids is efficient in evaluating the regional pressure buildup in a two-phase flow system. This study was thus conducted as part of fundamental research to realize pressure anomalies induced by CO₂ leakage in the GCS.

Researchers have recently developed the methodologies to quantify leakage behaviors and pressure anomalies induced by leakage in multilayered aquifer systems: Nordbotten et al. (2004) developed an analytical methodology to simulate the leakage in multiple aquifers. Zhou et al. (2009) applied both one-dimensional radial flow equations and vertical flow equations for the semi-analytical leakage modeling. Cihan et al. (2011) studied semi-analytical solutions for pressure anomalies induced by leakage in a multilayered aquifer system. This method was later applied to simulating pressure perturbations resulting from leakage pathways of various sizes and permeability values by Cihan et al. (2013). Veling and Maas (2009) also studied the method of solution for both horizontal and vertical flow induced by leakage in multilayered aquifers. The commercial MLU (Multi-Layer Unsteady State) code was developed for leakage diffuse due to pumping and injection in multiple aquifers (Hemker & Post, 2013). Those existing studies focused on the methodology to model leakage resulting from pre-existing leakage pathways but not abruptly-induced leakage pathways which can be induced by an external effect such as a micro-seismic event caused by overpressure from water (or CO₂). Therefore, in this

study, we describe abruptly induced leakage pathways at specific times as well as pre-existing leakage pathways for more realistic predictions of leakage behavior and pressure perturbation in nature leaky multiple aquifers. This study provides an improvement in methods discussed above to solve the flows in porous media.

The developed code simulates the transient release of leakage into adjacent aquifers along abandoned wells and fractures penetrating confining layers from the confined aquifers with higher hydraulic heads (or pressures) by water injection and anomalies of hydraulic heads in the aquifers caused by the transient release of leakage. The leakage simulations can be performed using a three-dimensional flow equation with a leakage term intended to represent leakage. Leakage rates expressed as Darcy's flow equation depend on the hydraulic conductivity of the leakage pathway, the cross-sectional area of the leakage pathway, and the hydraulic gradient between the leakage aquifers overlying and underlying the confining bed. The hydraulic gradient between the leakage aquifers is calculated from two leakage points on the leakage pathway. Thus, the inflow and outflow rates along the leakage pathway through the confining bed are calculated based on the hydraulic conductivity and the cross-sectional area of the leakage pathway, and the hydraulic heads of the confined leakage aquifers caused by leakages can be modeled simultaneously. Section 2 introduces the basic theory and the methodology of the leakage modeling. In Section 3, a synthetic model domain and parameters are described. In addition, Section 3 illustrates the simulation results from different leakage applications to both the pre-existing and the abruptly-induced leakage pathways in the model domain, and the developed model is verified by comparison with the results of a commercial numerical code for pre-existing leakage scenarios.

2. Methodology

As suggested previously, this study is associated with potential CO₂ leakage in the storage of CO₂ in geological formations. Cihan et al. (2013) suggested that the methodology of solving for the groundwater (or single-phase fluid) governing equation can be applied to simulations of mobile brine/CO₂ entering or exiting the confined aquifers through leakage pathways if equivalent volumes of water are used to mimic the CO₂ injection in the CO₂ storage reservoirs. Lee et al. (in press) also determined that the inverse simulator for a single-phase fluid is applicable for leakage pathway estimation in the multilayered system of two-phase fluids (brine and CO₂). However, those studies were applied to the analysis of pressure induced by a pre-existing leakage pathway. Increased pressure from water (or CO₂) injection can cause fractures or cracks in confining beds with vulnerable areas (for example, incompletely plugged abandoned wells). In addition, leakage pathways can be abruptly induced. In this study, the important consideration is the abruptly-induced leakage at specific times. However, this study does not consider specific mechanisms for how leakage pathways are generated in the confining beds by increased pressure. Rather, these analyses focus only on the migration of leakage along leakage pathways under the assumption that the leakage pathways are generated in the confining beds. Two types of leakage pathways are specified in terms of the generated time: (1) pre-existing leakage pathways and (2) induced leakage pathways at specific times. First, the pre-existing leakage pathway corresponds to a leakage pathway that is completely generated and saturated before water injection. The instantaneous inflow rate into the leakage pathway is assumed to be equivalent to the outflow rate from the leakage pathway, corresponding to the fundamental continuity equation. Second, the induced leakage pathway corresponds to a leakage pathway that is generated at an arbitrary time through injection-induced increased pressure or other mechanisms. The model releases leakage from the pathway into an adjacent confined aquifer at the time when the pathway is generated. By assumption (see the next section), the inflow rate into the leakage pathway and the outflow rate from the leakage pathway are simultaneous and equivalent.

2.1 Governing Equation and Methodology of Leakage Simulation

The governing equation is the mass conservation equation for the three-dimensional movement of groundwater of constant density through porous media. The governing equation may be described by a partial differential equation as follows:

$$\frac{\partial}{\partial x} \left(Kx \frac{\partial h}{\partial x} \right) + \frac{\partial}{\partial y} \left(Ky \frac{\partial h}{\partial y} \right) + \frac{\partial}{\partial z} \left(Kz \frac{\partial h}{\partial z} \right) + W - L = Ss \frac{\partial h}{\partial t}, \quad (1)$$

where Kx , Ky , and Kz are values of hydraulic conductivity (L/T) along each direction; h is the hydraulic head (L); W is sources and/or sinks of water (a volumetric flux per unit volume) (T⁻¹); L is the leakage term, the leakage rate per unit volume (T⁻¹); Ss is the specific storage coefficient of the porous media (L⁻¹); and t is time (T).

Equation (1) describes groundwater flow with a leakage term for a heterogeneous and anisotropic medium. The leakage induces changes of hydraulic heads in the aquifers, which is referred to as "leakage effects" in this study.

The leakage term has been added in the governing equation to consider the leakage effects, and the Finite Difference Method (FDM) is used to solve for the governing equation. In this study, hydraulic heads are calculated at discrete points in space, which are nodes in the centers of meshes; therefore, assigning hydraulic conductivities and specific storage coefficients for the cells is straightforward. In addition, multiple aquifers should be considered to simulate a confined system with possible leakage pathways (Cihan et al., 2011). Figure 1 shows a schematic of the leakage confined system, with a confining bed (or caprock) and two confined aquifers overlying and underlying the confining bed. In this study, the underlying aquifer in which water is injected is referred to as the “storage formation” and the aquifer above the caprock is referred to as the “overlying formation.”

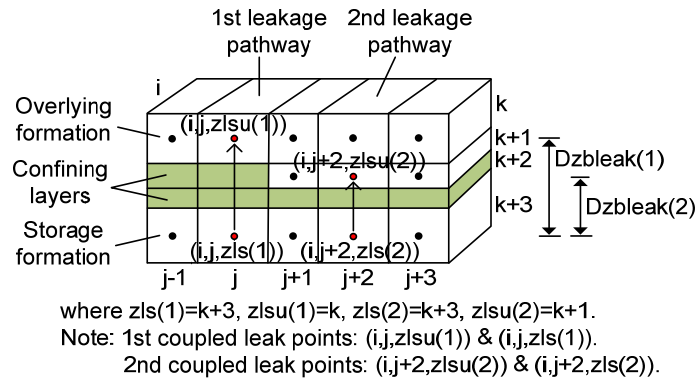


Figure 1. Schematic showing leakage pathways and relation parameters

Darcy’s Law is used to model the leakage term (Anderson & Woessner, 1992):

$$Q_{leak_{i,j,k}} = Kzbleak_{i,j,k} \frac{A_{leak_{i,j,k}}}{Dzbleak(I)} (h_{i,j,zls(I)} - h_{i,j,zlsu(I)}), \quad (2)$$

where the leakage rate (L) in Equation (1) is expressed to $Q_{leak_{i,j,k}}$ per unit volume. I is the leakage pathway number, $A_{leak_{i,j,k}}$ is the cross-sectional leakage pathway area, $Dzbleak(I)$ is the length of I -th leakage pathway, $Kzbleak_{i,j,k}$ is the z -directional hydraulic conductivity of the leakage pathway, $zls(I)$ is the z -coordinate at a storage formation of I -th leakage, and $zlsu(I)$ is the z -coordinate at an overlying formation of I -th leakage (Figure 1 depicts how the leakage pathways and parameters are related). It is assumed that there are no lateral flows at the interface between the leakage pathway and the confining bed, i.e., leakage migrates vertically in confining beds along specific leakage pathways. In addition, the leakage pathway is not deformable and the continuity equation is satisfied in the leakage pathway; therefore, the leakage rates in all cross-sections of a leakage pathway are instantaneously identical.

Consistent with Darcy’s Law, the leakage rates can change with time because the leakage affects the hydraulic heads in the overlying and storage formations. Thus, the leakage rates should be simultaneously modeled using the hydraulic heads between the overlying and storage aquifers; the transient flow in these two aquifers caused by the leakage must also be calculated. The leakage simulations are performed by solving the hydraulic heads at the “coupled leakage points” within each leakage pathway (see Figure 1). The methodology uses three finite difference equations for leakage simulations: two finite difference equations for coupled leakage points and one finite difference equation for no leakage points (these finite difference equations are discussed in the subsequent section). The hydraulic head at one leakage point is determined using hydraulic heads at seven discrete nodes, which consist of six discrete adjacent FDM nodes and one corresponding leakage point. The hydraulic head at the corresponding leakage point is also determined in the same manner. We can simultaneously calculate hydraulic heads at coupled leakage points and leakage rates, which are based on the difference of hydraulic heads between the coupled leakage points. In general, the leakage simulations using the conventional method are conducted by calculating hydraulic heads (or pressures) at the inner nodes of an explicitly meshed leakage pathway in the confining layers. However, this methodology does not require the geometry of the leakage pathways to be specified by meshes because the leakage term implies the geometry of the leakage pathways, thereby providing an advantage by reducing the leakage simulation computations.

2.2 Discretization of the Governing Equation

Figure 2 illustrates x-directional cross-sections through three cells and the numerical approximation of derivatives of hydraulic head under anisotropic and heterogeneous conditions (Bennett, 1976). In terms of node (i, j, k), the notation f indicates the region in which water flows into node (i, j, k) from the upstream node, and the notation b indicates the region in which water flows out from node (i, j, k) to the downstream node.

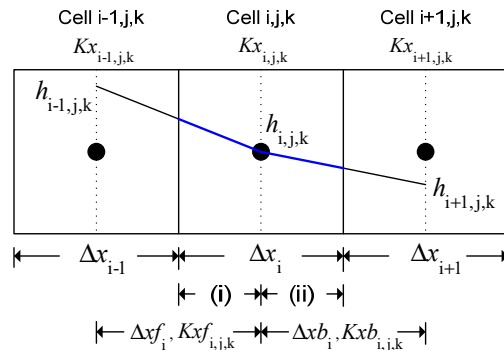


Figure 2. Schematic showing x-directional cross-section

The effective hydraulic conductivity is calculated as a weighted harmonic mean, as described by Collins (1961). For example,

$$Kxf_{i,j,k} = \frac{(\Delta x_{i-1} + \Delta x_i)}{\left(\frac{\Delta x_{i-1}}{kx_{i-1,j,k}} + \frac{\Delta x_i}{kx_{i,j,k}}\right)} \text{ and } Kxb_{i,j,k} = \frac{(\Delta x_i + \Delta x_{i+1})}{\left(\frac{\Delta x_i}{kx_{i,j,k}} + \frac{\Delta x_{i+1}}{kx_{i+1,j,k}}\right)} \quad (3)$$

The time derivative of the heads can be approximated with the backward difference method (Burden & Faires, 2005):

$$\left(\frac{\partial h}{\partial t}\right)_{t^n} \approx \left[\frac{h_{i,j,k}^n - h_{i,j,k}^{n-1}}{t^n - t^{n-1}}\right], \quad (4)$$

where n is the time step index. This finite difference formula has a local truncation of order $O(\Delta t)$.

The x-directional 1st order partial derivative at node (i, j, k) can be approximated by the arithmetic mean of the fluxes of sections (i) and (ii):

$$\left(Kx \frac{\partial h}{\partial x}\right)_{i,j,k} \approx \frac{1}{2} \left[Kxf_{i,j,k} \frac{(h_{i-1,j,k} - h_{i,j,k})}{\Delta x_{fi}} + Kxb_{i,j,k} \frac{(h_{i,j,k} - h_{i+1,j,k})}{\Delta x_{bi}} \right]. \quad (5)$$

The 2nd order approximation for the x-directional second order partial derivative of head at node (i, j, k) can be expressed as:

$$\begin{aligned} \left(\frac{\partial}{\partial x} \left(Kx \frac{\partial h}{\partial x}\right)\right)_{i,j,k} &\approx \frac{\left(Kx \frac{\Delta h}{\Delta x}\right)_{(i)} - \left(Kx \frac{\Delta h}{\Delta x}\right)_{(ii)}}{\Delta x_i} \\ &\approx \frac{1}{\Delta x_i} \left[Kxf_{i,j,k} \frac{(h_{i-1,j,k} - h_{i,j,k})}{\Delta x_{fi}} + Kxb_{i,j,k} \frac{(h_{i+1,j,k} - h_{i,j,k})}{\Delta x_{bi}} \right]. \end{aligned} \quad (6)$$

These finite difference formulas for 2nd order partial derivatives have the local truncation error of order $O(\Delta x^2)$.

The finite difference equations of $\left(\frac{\partial}{\partial y} \left(Ky \frac{\partial h}{\partial y}\right)\right)_{i,j,k}$ and $\left(\frac{\partial}{\partial z} \left(Kz \frac{\partial h}{\partial z}\right)\right)_{i,j,k}$ can be determined in the same

manner.

The three finite difference equations have been specifically derived from the governing equation with the leakage term. One of three finite difference equations is applied to the nodes in a model depending on whether the nodes exhibit the leakage pathways at the specific time. The first finite difference equation is

$$h_{i,j,k}^n = \frac{1}{\mu 2_{i,j,k}^n} [(Cxf_{i,j,k} h_{i-1,j,k}^n + Cxb_{i,j,k} h_{i+1,j,k}^n) + (Cyf_{i,j,k} h_{i,j-1,k}^n + Cyb_{i,j,k} h_{i,j+1,k}^n) + (Czf_{i,j,k} h_{i,j,k-1}^n + Czb_{i,j,k} h_{i,j,k+1}^n) + W_{i,j,k}^n + \frac{Ss_{i,j,k} h_{i,j,k}^{n-1}}{t^n - t^{n-1}} + Czbleak_{i,j,k} h_{i,j,zlsu(I)}^n], \quad (7)$$

Where $\mu 2_{i,j,k}^n = Cxf_{i,j,k} + Cxb_{i,j,k} + Cyf_{i,j,k} + Cyb_{i,j,k} + Czf_{i,j,k} + Czb_{i,j,k} + Czbleak_{i,j,k} + \frac{Ss_{i,j,k}}{t^n - t^{n-1}}$,

$$Czbleak_{i,j,k} = Kzbleak_{i,j,k} \frac{Aleak_{i,j,k}}{Dzbleak(I) \cdot (\Delta x_i \cdot \Delta y_j \cdot \Delta z_k)},$$

$$Cxf_{i,j,k} = Kxf_{i,j,k} \frac{1}{\Delta x_i \Delta x_f_i}, \quad Cxb_{i,j,k} = Kxb_{i,j,k} \frac{1}{\Delta x_i \Delta x_b_i}, \quad Cyf_{i,j,k} = Kyf_{i,j,k} \frac{1}{\Delta y_j \Delta y_f_j},$$

$$Cyb_{i,j,k} = Kyb_{i,j,k} \frac{1}{\Delta y_j \Delta y_b_j}, \quad Czf_{i,j,k} = Kzf_{i,j,k} \frac{1}{\Delta z_k \Delta z_f_k}, \quad Czb_{i,j,k} = Kzb_{i,j,k} \frac{1}{\Delta z_k \Delta z_b_k}.$$

Equation (7) is applied for a leakage node (i, j, k) of the I-th leakage pathway in the storage aquifer. If the leakage node (i, j, k) has an induced leakage pathway, the above equation is applied to node (i, j, k) after the time at which the leakage is induced at node (i, j, k).

The second finite difference equation is

$$h_{i,j,k}^n = \frac{1}{\mu 2_{i,j,k}^n} [(Cxf_{i,j,k} h_{i-1,j,k}^n + Cxb_{i,j,k} h_{i+1,j,k}^n) + (Cyf_{i,j,k} h_{i,j-1,k}^n + Cyb_{i,j,k} h_{i,j+1,k}^n) + (Czf_{i,j,k} h_{i,j,k-1}^n + Czb_{i,j,k} h_{i,j,k+1}^n) + W_{i,j,k}^n + \frac{Ss_{i,j,k} h_{i,j,k}^{n-1}}{t^n - t^{n-1}} + Czbleak_{i,j,k} h_{i,j,zls(I)}^n]. \quad (8)$$

If the node (i, j, k) is a leakage point in the overlying aquifer of the I-th leakage pathway, Equation (8) is applied to the leakage node (i, j, k). If the node (i, j, k) becomes a point on the induced leakage pathway, this equation is applied to node (i, j, k) after the time at which the leakage is induced.

The following finite difference equation is applied to a normal node (i, j, k) without leakage at the aquifers, or to a leakage node before leakage is induced at the specific time:

$$h_{i,j,k}^n = \frac{1}{\mu 1_{i,j,k}^n} [(Cxf_{i,j,k} h_{i-1,j,k}^n + Cxb_{i,j,k} h_{i+1,j,k}^n) + (Cyf_{i,j,k} h_{i,j-1,k}^n + Cyb_{i,j,k} h_{i,j+1,k}^n) + (Czf_{i,j,k} h_{i,j,k-1}^n + Czb_{i,j,k} h_{i,j,k+1}^n) + W_{i,j,k}^n + \frac{Ss_{i,j,k} h_{i,j,k}^{n-1}}{t^n - t^{n-1}}], \quad (9)$$

where $\mu 1_{i,j,k}^n = Cxf_{i,j,k} + Cxb_{i,j,k} + Cyf_{i,j,k} + Cyb_{i,j,k} + Czf_{i,j,k} + Czb_{i,j,k} + \frac{Ss_{i,j,k}}{t^n - t^{n-1}}$.

3. Results and Discussion

This section demonstrates how abrupt leakage has an effect on the hydraulic head anomalies in the aquifers of a synthetic model domain. In addition, the newly developed model is validated by comparison with the results of the TOUGH2 model of a general equation of state (EOS1) in the case of a three-dimensional example under isothermal conditions. The TOUGH2/EOS1 program developed by the Lawrence Berkeley National Laboratory is a code to provide the simulation of pure water in its liquid and/or vapor state (i.e., single-phase or two-phase states) under non-isothermal and isothermal conditions (Pruess et al., 1999).

3.1 Model and Parameters

Figure 3 illustrates a conceptual domain of multiple aquifers designated to simulate the hydraulic head anomalies caused by water release through leakage pathways. Figure 3 (a) presents a schematic of three formations with an injection well (IW), a pre-existing leakage pathway (LP1) and two abruptly induced leakage pathways (LP2 and LP3). Figure 3 (b) shows a schematic of the leakage pathway with higher permeability than that of confining layers. In Figure 3 (b), the z-directional 4th to 8th layers between both aquifers are confining layers (caprock), and the vertical leakage pathways penetrate through the confining layers. Water injection into the storage formation produces the transient leaks through the leakage pathway. The TOUGH2/EOS1 model should specify the leakage pathways by meshes (i.e., the white zone in Figure 3 (b)). However, as discussed previously, the new

code conducts the leakage simulations using the coupled leakage points without the meshed leakage pathway. The hydrogeological properties are assigned in the synthetic domain depending on information about the deep CO₂ storage reservoirs from Metz et al. (2005). The initial hydraulic head is assigned as 10 m for all of the cells. The left and right boundaries of the XZ-planes are specified by constant head boundary conditions, but the other boundaries are assigned as no-flow boundary conditions.

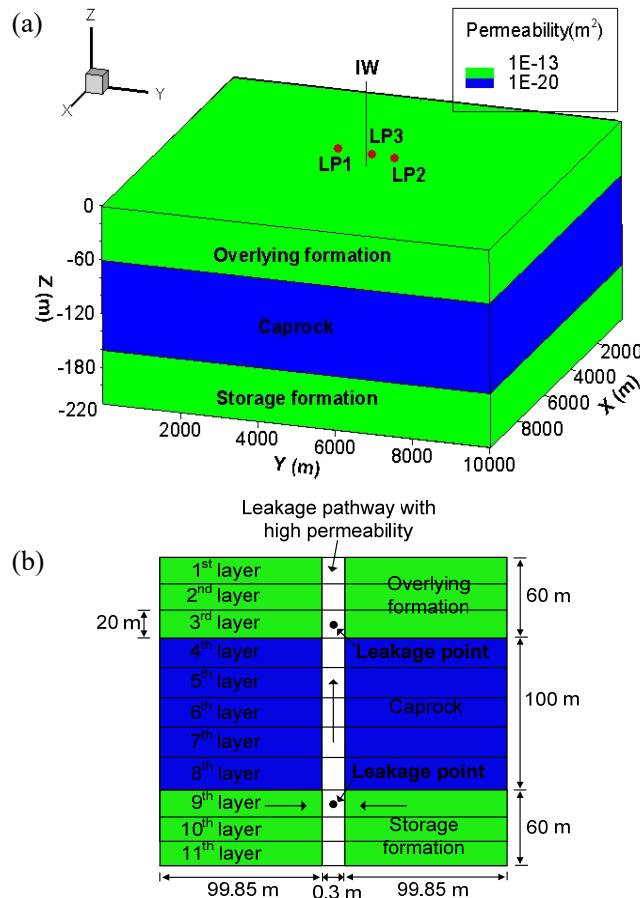


Figure 3. Conceptual model domain: (a) a schematic of multiple formations with an injection well (IW), a pre-existing leakage pathway (LP1), and two abruptly induced leakage pathways (LP2 and LP3); and (b) a schematic of the leakage pathway, layers, and leakage points

The TOUGH2 model and the developed codes use mass injection rates and volumetric injection rates, respectively. Based on an industrial-scale CO₂ injection rate of approximately one million tons per year, a constant rate of 31.71 kg/s is assigned to TOUGH2, and an equal volume rate of 0.03179 m³/s, which is converted from water density (997.3 kg/m³) at the injection point (calculated from TOUGH2), is assigned to the new model. Water is injected at the assigned rates into an injection well point located at (x, y, z) = (5100 m, 5100 m, -190 m) from the origin during the simulation period of 10 years. The x-, y-, and z-directional permeability values of the overlying and storage formations are designated as 10⁻¹³ m², and those of the caprock are specified as 10⁻²⁰ m². The porosity in the overlying and storage formations is designated as 0.2, but in the caprock porosity is set at 0.02. In addition, the new code uses a constant hydraulic conductivity ($K = k\rho g/\mu$, where K is the hydraulic conductivity, k is the permeability, ρ is the water density, g is the gravitational acceleration and μ is the water dynamic viscosity), but TOUGH2 employs a constant permeability (k) for each cell in the model domain. Both initial density and dynamic viscosity values (before water injection begins) at each cell calculated from TOUGH2 are assigned to the new code; therefore, the hydraulic conductivity value at each cell is equivalent to the permeability. Specific storage of the aquifers is calculated using $S_s = \phi\rho g(\beta_w + \beta_p)$, where ϕ is the porosity, ρ is the water density, g is the gravitational acceleration, β_w is the water compressibility, and β_p is the aquifer pore compressibility. Table 1 denotes the specific dimensions and parameter values of the conceptual model.

Table 1. Specification of the conceptual model

Domain size (m)	10,000 × 10,000 × 220	Porosity	Both formations	0.2
Normal cell size (m)	200 × 200 × 20		Caprock	0.02
Number of cells	52 × 52 × 11 (29,744 total)	Permeability (m²)	Both formations	1 × 10 ⁻¹³
Simulation time (yr)	0 ~ 10	(kx = ky = kz)	Caprock	1 × 10 ⁻²⁰
Time step size (sec)	100		Overlying formation	1.494 × 10 ⁻⁶
Tolerance	1e-7	Hydraulic		
Density (kg/m³)	996.57 ~ 997.41	conductivity (m/s)	Caprock	1.495 × 10 ⁻¹³
Viscosity (kg/m·s)	6.538 × 10 ⁻⁴ ~ 6.541 × 10 ⁻⁴	(Kx = Ky = Kz)	Storage formation	1.496 × 10 ⁻⁶
Water compressibility (Pa⁻¹)	4.5 × 10 ⁻¹⁰	Specific storage (m⁻¹)	Both formations	1.96 × 10 ⁻⁶
Pore compressibility (Pa⁻¹)	5.5 × 10 ⁻¹⁰		Caprock	1.96 × 10 ⁻⁷
Leakage pathways				
	1st pathway (LP1)	2nd pathway (LP2)	3rd pathway (LP3)	
Coordinate (x, y)	(5300 m, 4100 m)	(5300 m, 5700 m)	(5300 m, 5100 m)	
Leakage starting time (yr)	0	3.171 (1 × 10 ⁸ sec)	4.76 (1.5 × 10 ⁸ sec)	
Cross-sectional size (m)	0.3 × 0.3	0.3 × 0.3	0.5 × 0.5	
Vertical permeability (m²)	1 × 10 ⁻¹³	1 × 10 ⁻¹⁰	1 × 10 ⁻¹¹	
Hydraulic conductivity (m/s)	1.495 × 10 ⁻⁶	1.495 × 10 ⁻³	1.495 × 10 ⁻⁴	

In the modeling scenario, the leakage occurs at three pathways with different properties (see Table 1). The first pathway (LP1), located at node (x, y) = (5300 m, 4100 m), has leakage at time zero (this is a pre-existing pathway). The second pathway (LP2) at node (5300 m, 5700 m) and third pathway (LP3) at node (5300 m, 5100 m) are induced at time 3.171 years and 4.76 years after the simulation begins, respectively. The three pathways are arranged in a straight line at coordinate (x) = (5300 m). It is assumed that LP2 and LP3 (abruptly-induced leakage pathways) will arise at the confining beds by an external forces such as increased pressure from water injection. Therefore, the simulation using the new model was performed using three leakage conditions with time intervals.

3.2 Validation of the Developed Code and Simulation Results

Figure 4 illustrates the simulated pressure distributions at each leak point of the three leakage pathways in the 3rd and 9th layers from both the newly developed code (dashed lines) and TOUGH2 code (solid lines). Pressure is a dependent variable of TOUGH2 to describe variable density groundwater flow, and hydraulic head is a dependent variable of the new code to describe constant density groundwater flow; therefore, the results of the new code were converted from the hydraulic head (m) to pressure (Pa) using $P = \rho g(H - z)$, where P is the pressure, H is the hydraulic head and z is the elevation.

From results of the new code in Figure 4 (a), the leak point of LP1 in the overlying formation reflects gradual changes of hydraulic heads as soon as water is injected into the storage formation caused by the increased gradient of hydraulic heads between coupled leak points of LP1. After the LP2 pathway is generated at 3.171 years, the leak point of LP2 in the 3rd layer immediately shows a rapid rise of hydraulic heads, and it causes the propagation of hydraulic head anomalies throughout the overlying formation; therefore, the leak points of LP1 and LP3 also exhibit the sudden rise of hydraulic heads. The effect of leakage induced by LP3 at 4.76 years is similar to that of LP2, but the largest increase of hydraulic head occurs from LP3 because of the larger size (0.5 m × 0.5 m) of the LP3 and the substantial hydraulic head gradient between coupled leak points of LP3, which is the closest leakage pathway to the injection well. In Figures 4 (a) and (b), TOUGH2 is simulated from time 0 to 3.170 years (0.99 × 10⁸ sec) before LP2 is induced because the TOUGH2 model could not directly simulate pressure anomalies through the abruptly induced leakage pathways. The results from the newly developed code and TOUGH2 for the pre-existing leakage condition (by LP1) through 3.170 years are thus compared to validate the new code. The simulated pressure distributions through 3.170 years from the new code are generally analogous to those from TOUGH2, as shown in Figures 4 (a) and (b).

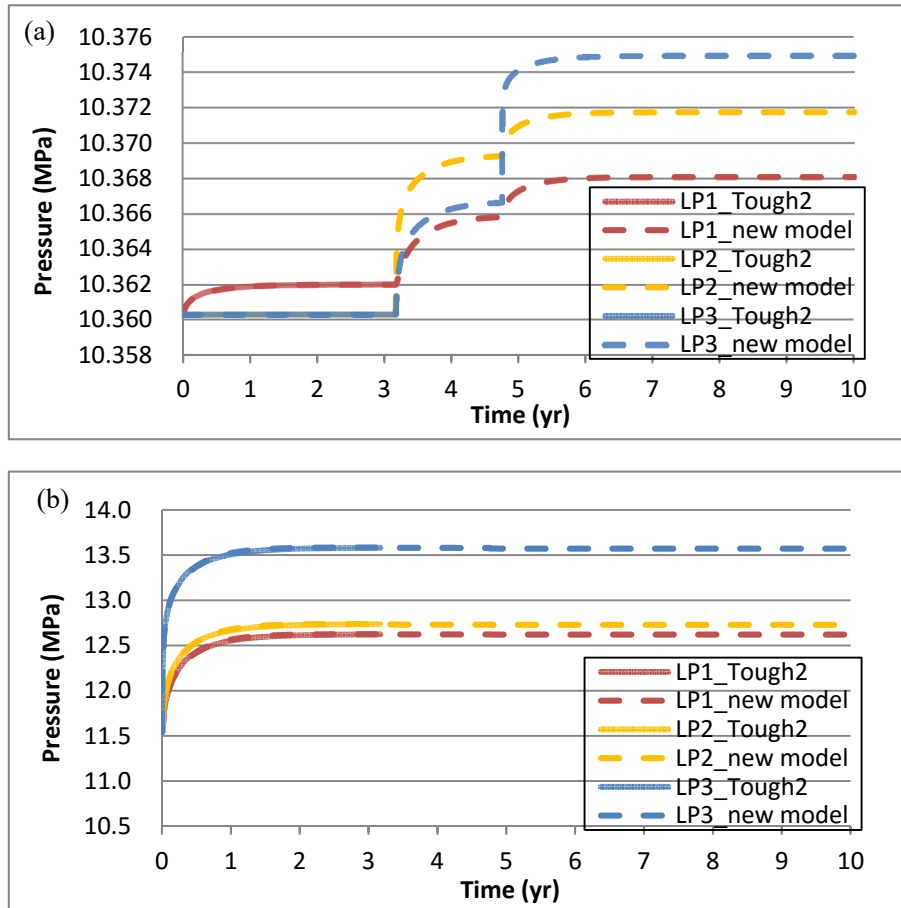


Figure 4. Pressure distributions at each leak point in the (a) 3rd layer and (b) 9th layer of three leakage pathways from both models

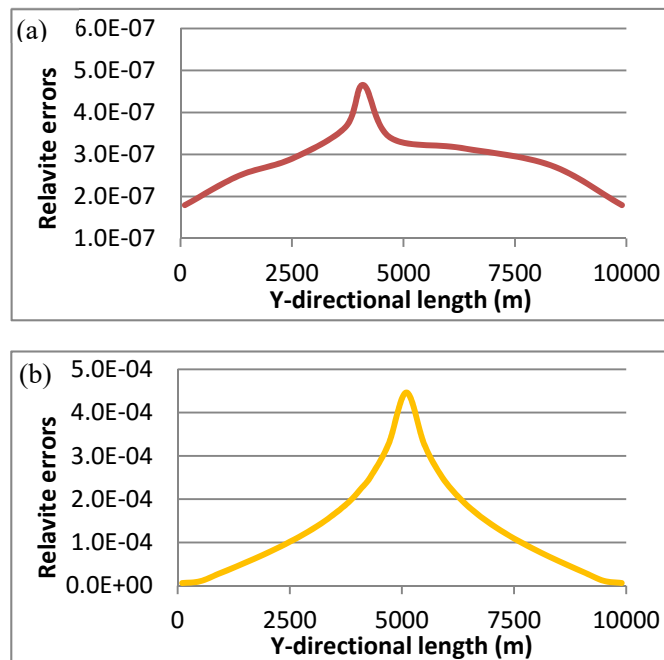


Figure 5. Relative errors in the (a) 3rd layer and (b) 9th layer in the YZ-plane of the first leakage pathway (LP1) at 3.170 years before the abruptly-induced leakage pathway occurs

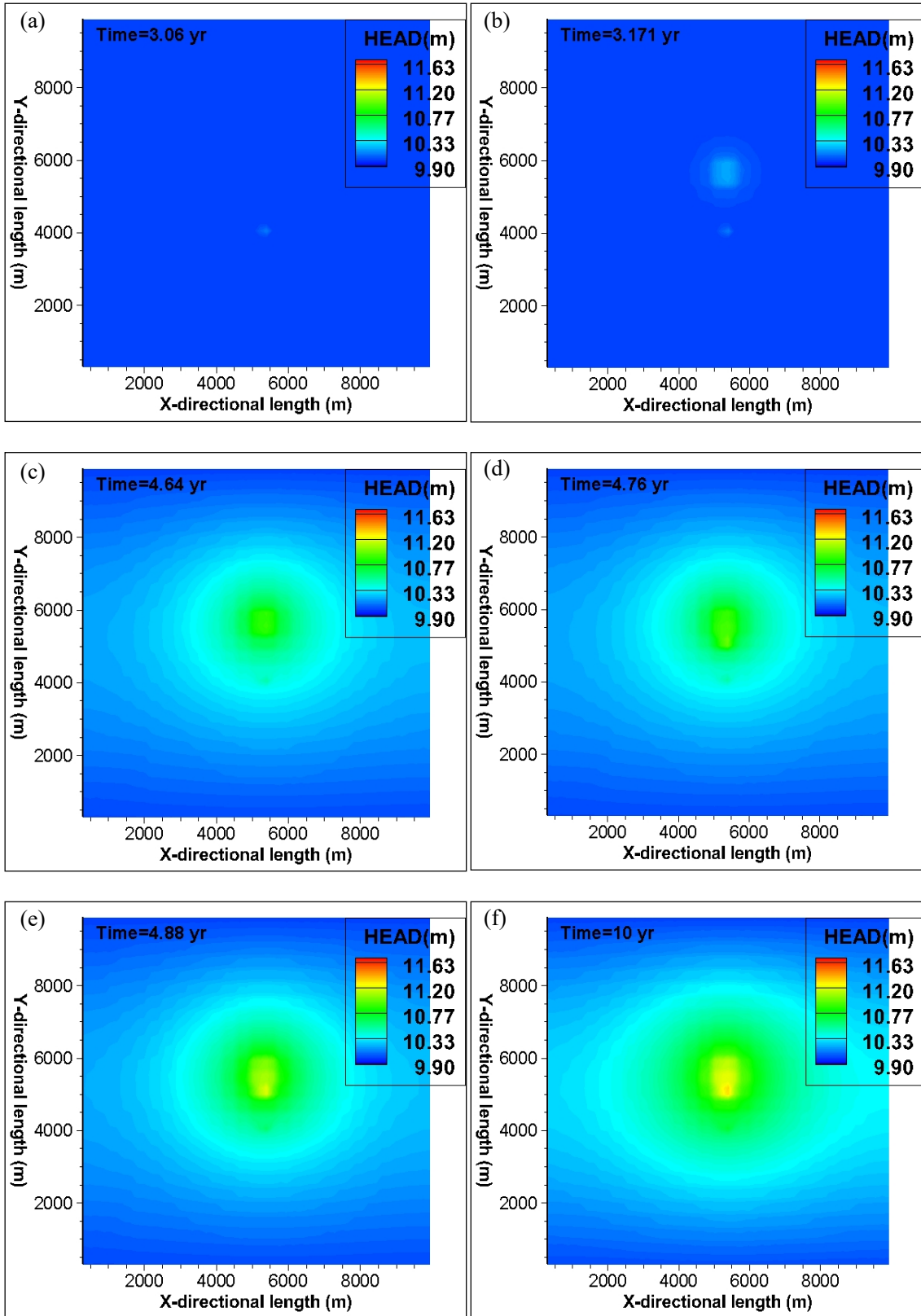


Figure 6. Simulated hydraulic head distributions in the XY-plane of the third layer: (a) after 3.06 years, (b) after 3.171 years, (c) after 4.64 years, (d) after 4.76 years, (e) after 4.88 years and (f) after 10 years

Figure 5 illustrates the relative errors between both models at $(x) = (5300 \text{ m})$ in the 3rd and 9th layers of the YZ-plane, in which LP1 is located at 3.170 years before the abruptly-induced leakage occurs. The maximum relative errors in the 3rd layer and in the 9th layer are approximately $4.65\text{E-}7$ (0.0000465%) at $(y) = (4100 \text{ m})$ (i.e., the leak point of LP1) (Figure 5 (a)) and $4.46\text{E-}4$ (0.0446%) at $(y) = (5100 \text{ m})$ (closest to the injection well) (Figure 5 (b)), respectively. The increased errors in the 9th layer might be caused by the effects of variable water density on changes in pressure. As discussed previously, TOUGH2 calculates pressures based on variable density, while the new code employs hydraulic heads in terms of the constant density; therefore, the change of density caused by an increased pressure buildup in the storage formation can lead to a slight increase in relative errors between both models.

Figure 6 illustrates the hydraulic head propagation in the XY-plane of the third layer over a period of 10 years. Figure 6 (a) represents the hydraulic head distribution at time 3.06 years before LP2 is induced, which slowly evolves at LP1, located at $(x, y) = (5300 \text{ m}, 4100 \text{ m})$. The hydraulic head begins to rapidly increase at LP2 at the coordinate $(x, y) = (5300 \text{ m}, 5700 \text{ m})$ after time 3.171 years when LP2 is generated (Figure 6 (b)). The hydraulic head in the overlying formation is consistently and substantially increased by LP2 (Figure 6 (c)). The occurrence of LP3 causes the sudden increase of hydraulic head in the vicinity of node $(5300 \text{ m}, 5100 \text{ m})$ (Figs. 6 (d) and (e)), and the hydraulic head anomalies are continuously propagated in the 3rd layer (Figure 6 (f)). As discussed previously, the increasing amount of hydraulic head from LP3 is more substantial because of the larger cross-sectional size of LP3 and the greater hydraulic gradient between the coupled leak points of LP3 than those of other pathways.

The results for the time period prior to 3.170 years demonstrate that the methodology of the newly developed model using the coupled leak points originating from a leakage term in the governing equation can be applied for the transient flow simulations caused by the pre-existing leakage pathway. In addition, the methodology can efficiently recognize hydraulic head anomalies caused by the abruptly induced leakage pathways because it does not require the use of meshes to specify leakage pathway geometries and hydrogeological properties, which is different from the conventional models such as TOUGH2 (i.e., the methodology can readily parameterize/generate the leakage pathway features at a specific time without the meshes). This methodology also provides an advantage in terms of the number of computations because the number of cells decreases in the leakage simulations. Finally, the new model can be used as a tool to evaluate the flow patterns caused by potential leakage in porous media.

4. Conclusions

This study focused on the analysis of transient flows caused by leakage in porous media. A developed model provides the three-dimensional analysis of transient flows caused by leakage in the arbitrary groundwater aquifers. The leakage effects are considered when the leakage term is added in the governing equation using Darcy's Law. In the model, the leakage rates are simultaneously simulated by using parameterized hydrogeological properties of leakage pathways and hydraulic gradients between multiple aquifers, and the transient flow in two aquifers caused by the leakage migration is calculated. The hydraulic gradient is determined using coupled leakage points and parameterizing the geometries and the hydrogeological properties of leakage pathways. The hydraulic head at one of the coupled leakage points is calculated from aggregate hydraulic heads at six discrete adjacent nodes of the leakage point and one corresponding leakage point. The hydraulic head at the corresponding leakage point is also calculated in the same manner. Thus, the transient/dynamic flow caused by leakage can be effectively simulated without the use of a meshed leakage pathway in the confining layers, so the methodology provides an advantage by reducing the number of computations for the leakage simulations. In particular, unlike the existing studies, the method enables the simulation of the effect of the leakage migration through induced leakage pathways at specific times as well as pre-existing leakage pathways. The new model was validated through application of the TOUGH2/EOS1 model for a three-dimensional conceptual domain. The maximum relative errors in the 3rd and 9th layers in the domain between both models were $4.65\text{E-}7$ and $4.46\text{E-}4$, respectively.

By the given assumptions, our method does not allow the lateral flow from the leakage pathways into the caprock, so cannot simulate the leakage diffuse through the caprock from the leakage pathway. In the future, our study will solve this problem for a more realistic modeling of the transient flow caused by the leakage in multiple aquifer systems. In addition, this study will be applied to develop a leakage detection system using the inverse analysis. The future study will proceed to be helpful in evaluating/reducing the risk of CO₂ leaks so that it can be applied to the CO₂ storage project in deep subsurface formations with leakage issues.

Acknowledgments

This study was supported by the Department of Energy (DOE), the United States government agency, under contract number DE-FC26-05NT42591.

References

- Anderson, M. P., & Woessner, W. W. (1992). *Applied groundwater modeling: simulation of flow and advective transport*. Elsevier Science, Oxford, UK.
- Bennett, G. D. (1976). *Introduction to groundwater hydraulics*. U.S. Geological Survey, Denver, CO.
- Burden, R. L., & Faires, J. D. (2005). *Numerical analysis*. Brooks/Cole, USA.
- Cihan, A., Birkholzer, J. T., & Zhou, Q. (2013). Pressure buildup and brine migration during CO₂ storage in multilayered aquifers. *Groundwater*, 51(2), 252-267. <http://dx.doi.org/10.1111/j.1745-6584.2012.00972.x>
- Cihan, A., Zhou, Q., & Birkholzer, J. T. (2011). Analytical solutions for pressure perturbation and fluid leakage through aquitards and wells in multilayered-aquifer systems. *Water Resources Research*, 47(10), W10504. <http://dx.doi.org/10.1029/2011WR010721>
- Collins, R. E. (1961). *Flow of fluids through porous materials*. Reinhold Publishing Corp., New York, NY.
- Hemker, K., & Post, V. (2013). *MLU for Windows, Well flow modeling in multilayer aquifer systems*. Amsterdam, Netherlands.
- Lee, S. J., McPherson, B. J., Vasquez, F. G., & Lee, S.-Y. (in press). Application of the developed inverse model of single-phase flow analysis for early leakage pathway detection in a multiphase system for geologic CO₂ storage. *Environmental Earth Sciences*.
- Metz, B., Davidson, O., de Coninck, H., Loos, M., & Meyer, L. (2005). *IPCC special report on carbon dioxide capture and storage*. Cambridge University Press, New York, NY.
- Nordbotten, J. M., Celia, M. A., & Bachu, S. (2004). Analytical solutions for leakage rates through abandoned wells. *Water Resources Research*, 40(4), W04204. <http://dx.doi.org/10.1029/2003WR002997>.
- Pruess, K., Moridis, G., & Oldenburg, C. (1999). TOUGH2 user's guide, version 2.0. *Report LBNL-43134*. Lawrence Berkeley National Laboratory, Berkeley, CA.
- Velting, E., & Maas, C. (2009). Strategy for solving semi-analytically three-dimensional transient flow in a coupled N-layer aquifer system. *Journal of Engineering Mathematics*, 64(2), 145-161. <http://dx.doi.org/10.1007/s10665-008-9256-9>.
- Zhou, Q., Birkholzer, J. T., & Tsang, C.-F. (2009). A semi-analytical solution for large-scale injection-induced pressure perturbation and leakage in a laterally bounded aquifer-aquitard system. *Transport in Porous Media*, 78(1), 127-148. <http://dx.doi.org/10.1007/s11242-008-9290-0>

Copyrights

Copyright for this article is retained by the author(s), with first publication rights granted to the journal.

This is an open-access article distributed under the terms and conditions of the Creative Commons Attribution license (<http://creativecommons.org/licenses/by/3.0/>).

Orographic Effects on Supercell: Development and Structure, Intensity and Tracking

Galen M Smith¹, Yuh-Lang Lin^{1,2} & Yevgenii Rastigejev^{1,3}

¹ Department of Energy & Environmental Systems, North Carolina A&T State University, USA

² Department of Physics, North Carolina A&T State University, USA

³ Department of Mathematics, North Carolina A&T State University, USA

Correspondence: Yuh-Lang Lin, Department of Energy & Environmental Systems, North Carolina A&T State University, E. Market St., Greensboro, NC 27411, USA. Tel: 336-285-2127, E-mail: ylin@ncat.edu

Received: March 2, 2016 Accepted: March 17, 2016 Online Published: May 5, 2016

doi:10.5539/enrr.v6n2p76

URL: <http://dx.doi.org/10.5539/enrr.v6n2p76>

Abstract

Orographic effects on tornadic supercell development, propagation, and structure are investigated using Cloud Model 1 (CM1) with idealized bell-shaped mountains of various heights and a homogeneous fluid flow with a single sounding. It is found that blocking effects are dominant compared to the terrain-induced environmental heterogeneity downwind of the mountain. The orographic effect shifts the storm track towards the left of storm motion, particularly on the lee side of the mountain, when compared to the storm track in the control simulation with no mountain. The terrain blocking effect also enhances the supercells inflow, which was increased more than one hour before the storm approached the terrain peak. The enhanced inflow allows the central region of the storm to exhibit clouds with a greater density of hydrometeors than the control. Moreover, the enhanced inflow increases the areal extent of the supercells precipitation, which, in turn enhances the cold pool outflow serving to enhance the storm's updraft until becoming strong enough to undercut and weaken the storm considerably. Another aspect of the orographic effects is that downslope winds produce or enhance low-level vertical vorticity directly under the updraft when the storm approaches the mountain peak.

Keywords: tornadic supercell, CM1, orographic effect, storm track, cold pool outflow

1. Introduction

Despite decades of observations and numerical simulations of supercell thunderstorms and tornados, our understanding of how orography affects tornadic supercell thunderstorms (SCs) has been limited mainly to case studies of tornadic supercells that occurred over various terrain (e.g. Bluestein 2000, Homar 2003, LaPenta et al. 2005, Bosart et al. 2006, Schneider 2009). In general, the aforementioned case studies have found that; 1) mountains can modify winds so that there is locally enhanced storm-relative helicity, 2) upslope winds may intensify storm updrafts strengthening the mesocyclone, 3) the mesocyclone may be enhanced as the storm descends a mountain, and 4) orographic blocking/channeling can lead to environments that are more favorable to tornadogenesis. In addition to the aforementioned environmental modifications enhancing tornadogenesis potential a few researchers have directly attributed the formation of a tornado to orographic effects (Bosart et al., 2006).

Homar et al. (2003) investigated tornadoes that occurred over complex terrain in eastern Spain on 28 AUG 1999. They used the 5th generation of the Pennsylvania State University - National Center for Atmospheric Research Mesoscale Model (MM5.v3, Dudhia, 1993; Grell et al. 1995) to perform a triple nested simulation varying the resolution of the reference terrain and they found that during this tornadic event terrain was essential in modifying the environment to produce super cellular convection. They specifically attempted to reproduce the mesoscale environment rather than any one of the supercells or tornadoes themselves. Specifically, they found that large scale terrain at the 20-50 km scale enhanced super cellular convective potential, and they attributed small scale terrain features at 2-5 km scales can enhance tornadogenesis potential.

Ćurić et al. (2007) investigated the effects that the terrain of the Western Morava basin, a mainly east-northeast to west-southwest oriented river valley in Serbia, had on the development of individual cumulonimbus formation in an environment with strong directional wind shear in the lowest kilometer. They investigated vertical vorticity characteristics of individual cumulonimbus clouds using the Advanced Regional Prediction System (ARPS, Xue

et al. 2001), with a single domain with 600 m resolution. They concluded that vertical vorticities were enhanced at the lowest levels of the simulated clouds when terrain was included in the simulation. Additionally, they found that terrain had intensified the splitting of the simulated cloud. Čurić and Janc (2012) also investigated the effect of differential heating associated with complex terrain on the evolution of hailstorm vortex pairs. This investigation incorporated both observational analysis and a numerical cloud model (Čurić et al., 2003a, 2008). They determined that differential heating modified environmental wind shear to favor the right mover in split hail storms. This is due to stronger convection over the sunward side of terrain generating vertical vorticity that weakens the anticyclonic storm (left mover) more than the cyclonic storm (right mover). Furthermore, they find that hail point maximums occur more frequently over complex terrain.

Even though the above studies found terrain to enhance low-level rotation they were of actual tornadic supercells and the models were initialized with observations and used real terrain (although smoothed). Even though researchers do not discount that terrain influences the strength and development of supercells, the primary difficulty with observational studies is that observations are incomplete (uncertainties and/or limitations in the observation resolution lead to missing data) and that necessitates speculative attribution about the impact of terrain on the observed structure and evolution of supercells and tornados. Thus, in order to thoroughly understand the influence of terrain on supercells, an idealized model investigation is necessary.

Frame and Markowski (2006) and Reeves and Lin (2007) previously have studied the effects of mountain ridges on mesoscale convective systems (MCSs). It was found that the forward speed and depth of the outflow are affected by its passage over a terrain barrier, with the outflow slowing and thinning as the mountain crest is approached, and then accelerating and deepening rapidly in the lee of the barrier, often forming a hydraulic jump. Because the evolution of an MCS is critically tied to the behavior of the cold pool - the MCS is maintained by the continuous triggering of new cells by the cold pool - terrain-induced modifications of cold pool evolution and structure unavoidably affect the evolution and structure of the MCS. Frame and Markowski (2006) found that many MCSs weaken as they approach a mountain crest and then re-intensify in the lee of the mountain where a hydraulic jump develops in the outflow (i.e., where the outflow depth rapidly deepens). Markowski and Dotzek (2011) have investigated the effects of idealized terrain on supercells. In their research they considered two types of idealized terrain in three-dimensional simulations. The first is a bell-shaped mountain 500 m tall and the second a gap incised into a flat topped hill 500 m tall both have a half-width of 10 km. In both situations they aimed the supercell at the location of the maximum positive vertical vorticity anomaly, as identified by an environmental simulation in which a storm was not initiated.

Specifically, germane to the bell-shaped mountain simulation, their results showed that the most notable change in the supercells evolution is a gradual strengthening of the mid-level and low-level updraft by upslope winds; then followed by a weakening of the updrafts but a rapid spin-up of low-level vorticity when the storm propagates over the vertical vorticity anomaly. Although Markowski and Dotzek (2011) advanced our understanding of how supercells are affected by terrain induced environmental modifications, there are several factors that were not considered in their study such as mountain height variation and its impact supercell track, intensity, structure and development. Although these areas are not independent of one another they can be separated into a few main areas: the supercells structure and development, intensity, and track. Knowing how the terrain affects the storm helps forecasters to issue severe storm watches and warnings. Secondly, this knowledge allows forecasters to know if the storm will become more severe, change its direction of propagation, or more likely to experience tornadogenesis.

In this paper, we intend to numerically investigate the effects of an idealized bell-shaped mountain on supercells. In particular, we are very interested in the scientific problems mentioned above, such as orographic effects on supercell track, intensity, and internal structures and development. Our study, on the influence of terrain on supercells, uses bell-shaped mountains of varying height that possess the same half-width. In the next section, we discuss the methodology and model selection. In section 3, we present the results of our control simulation with flat terrain; this section will describe the evolution of the environment in simulations with mountain. Section 4 describes the orographic effects on simulated supercells, which is broken down into three subsections: first the orographic effects on the supercells track; secondly the intensity of the storm is investigated; and thirdly the structure and development of the supercell is studied. Section 5 contains our summary and closing remarks.

2. Methodology

2.1 Model Selection and Description

Our simulations utilize the Bryan Cloud Model Version 1, Release 16 (CM1) (Bryan and Fritsch 2002). CM1 is a non-hydrostatic idealized numerical model designed to utilize high resolutions, particularly for severe local storms

which contain deep moist convection. The governing equations that CM1 utilizes conserve mass and total energy, but they are not fully conserved in the model due to limitations in numerical integration. The CM1 introduced new equations for calculating gradients that better conserve mass and energy in simulations containing terrain and that employ stretched vertical coordinate. CM1 uses the Gal-Chen and Somerville (1975) terrain-following coordinates to map the model levels to the terrain while the model top is at constant height, and the governing equations are adapted from those described by Wicker and Skamarock (2002). The advection terms are discretized using fifth-order spatial finite difference and artificial diffusion may be applied both horizontally and vertically using separate coefficients. The subgrid turbulence parameterization is similar to the parameterization of Deardorff (1980). CM1 has several options in microphysics parameterization schemes and the default scheme is the Morrison double-moment scheme (Morrison, 2005).

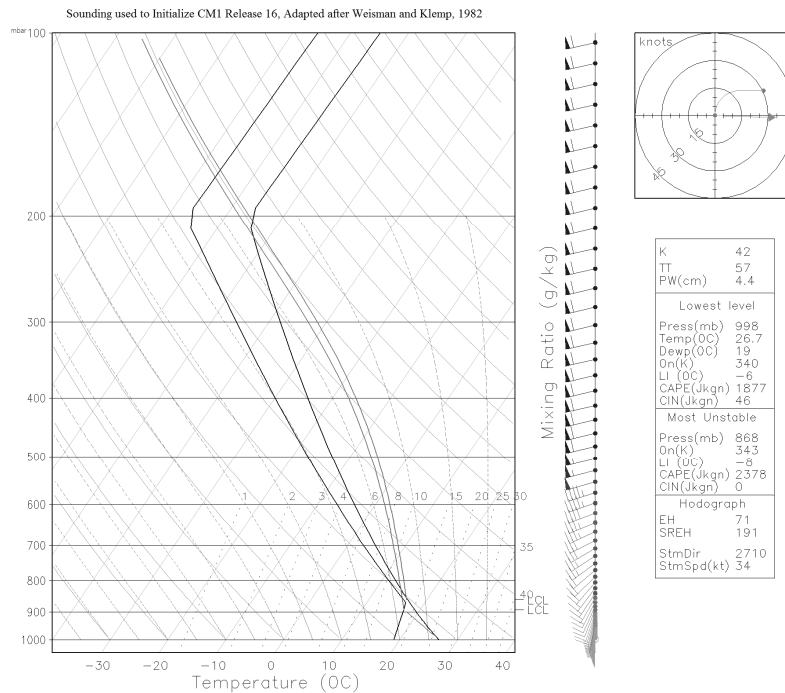


Figure 1. The sounding and wind profile used to initialize simulations in this study (Adapted after Weisman and Klemp 1982). The hodograph can be seen in the upper right corner and several indices are indicated to the right of the wind profile. The black lines represent the dew point temperature and the temperature, left and right respectively. The grey lines represent the surface parcel ascent for the lowest level and the most unstable level, left and right respectively

2.2 Model Configuration and Experimental Design

The domain is $300 \times 100 \times 18$ km in the x , y , and z directions, respectively. The horizontal grid spacing is 500 m; the vertical grid spacing varies from 25 m in the lowest 500 m, to constant 500 m from 11 km to 18 km (74 vertical levels total). The environments are horizontally homogeneous at the start of the simulations except in cases where storms were initialized with a warm bubble, 2 K warmer than the environment, centered 46 km north and 35 km east of the southern and western domain boundary, respectively. The warm bubble was centered at 1.4 km above the lower boundary, was 1.4 km thick and had a horizontal radius of 10 km. Simulations were run for a period of 4 h. Simulations with storms were initialized in a way that the supercell arrived near the terrain's central point at approximately the 180 min of simulation time (i.e. the supercell would be quasi-steady when it interacted with the terrain). In addition, the location was chosen such that the supercell propagated as close to the peak of the terrain as possible. The terrain used in this research is centered at 200 km from the eastern boundary and 50 km from the northern and southern boundaries and is a bell-shaped mountain. The bell-shaped mountain is defined by the following:

$$h(x, y) = \frac{h_m}{\left[1 + \left(\frac{x-x_0}{a}\right)^2 + \left(\frac{y-y_0}{b}\right)^2\right]^{\frac{3}{2}}} \quad (1)$$

where h_m is the mountain height, a and b are the mountain half-widths, and (x_0, y_0) is the center of the mountain. The half-width is a constant 10 km in both the x and y directions and the height is varied from flat terrain to 500 m, 1000 m, and 1500 m bell-shaped mountain. Keeping the halfwidth the same effectively increases the terrain blocking and lifting effect.

The lower boundary is free-slip and the upper boundary utilizes a Rayleigh damping layer (Durran & Klemp, 1983) in the uppermost 3 km of the model domain so that gravity waves generated by the terrain and convection are not reflected back into the domain. Lateral boundaries are open and radiative (Durran & Klemp, 1983). Surface heat fluxes, atmospheric radiative heating, and the Coriolis force are set to zero for our simulations. The simulation uses the NASA-Goddard version of the Lin-Farley-Orville (LFO) microphysics parameterization scheme (Lin et al., 1983). The environments of the simulated storms are initialized with a sounding very similar to the analytic sounding of Weisman and Klemp (1982, 1984 denoted as WK82 hereafter) (Figure 1) and a warm bubble as described above. Although it has been found that models initialized with the WK82 (standard) sounding resulted in a moist absolutely unstable layer when ascending over a relatively small hill (Bryan and Fritsch 2000, Markowski and Dotzek 2011); we believe that this was due to issues with the way previous models handled momentum and energy, as our model output did not indicate a moist absolutely unstable layer generated by the terrain. The sounding has a mixed layer convective available potential energy (MLCAPE) value of 1955 J kg^{-1} and a mixed layer convective inhibition (MLCIN) of 33 J kg^{-1} . The environmental wind profile is defined by the analytical quarter-circle hodograph described by WK82 (Figure 1). The WK82 wind profile has a bulk shear (0–6 km shear vector magnitude) of 32 m s^{-1} and storm-relative helicity (SRH) of $191 \text{ m}^2\text{s}^{-2}$. The *supercell composite parameter* (Thompson, et al. 2005 and 2007) of this wind profile is approximately 15. This is not surprising since the vertical moisture and wind profile for the WK82 was developed to simulate supercellular convection, although many of the included soundings in their analysis were tornadic. Moreover, the *significant tornado parameter* (STP) is greater than 2. Note that values of the STP greater than 1 are associated with the majority of tornadoes stronger than F2 while non-tornadic supercells are associated with STP values less than 1 (Thompson et al., 2005, 2007).

3. Terrain Induced Environmental Modifications

3.1 Environmental Simulation (Mountain Only – MTNO)

To investigate how the environment evolved with a mountain without the presence of a storm, simulations were performed with bell-shaped mountains of 500, 1000, and 1500 m heights. One method to measure the terrain blocking effect is the moist Froude number (F_w) and is defined as $F_w = U/N_w h$ (e.g., see Lin, 2007; Chen & Lin, 2005, and Emanuel, 1994), where U is the basic wind, N_w is the moist Brunt–Väisälä frequency, and h is the mountain height. Both the basic wind and the Brunt–Väisälä frequency are averaged over the depth of the mountain. Changing the terrain heights effectively varied the F_w : 1.78, 0.89, and 0.59; for the above terrain heights respectively.

The model output for these MTNO simulations showed a general region of reduced MLCIN over and around the underlying terrain. The MLCIN mostly associated with a reduction in the distance from the surface to the Lifting Condensation Level (LCL), however, as the simulation progresses, the greatest MLCIN reduction occurred just north-east of the mountain peak. Evidence of gravity waves modifying MLCAPE were present starting 90 min into the simulation as regions of alternating reductions in MLCAPE were seen radiating away from the terrain toward the east-northeast (Figure 2). Moreover, the control simulation output showed a general region of increased MLCAPE over and around the underlying terrain, with the greatest MLCAPE increase occurring near the peak of the 500 m terrain. However, as the terrain height is increased above the LCL there is an associated reduction in the MLCAPE that evolves throughout the simulation to produce lower MLCAPE over the terrain peak (Figure 2). As with the MLCAPE field, evidence of gravity waves modifying MLCIN is present with alternating regions of increased/decreased MLCIN radiating away from the terrain toward the east-north-east.

In simulations with higher mountains the modifications to MLCAPE/MLCIN were stronger, and in fact, supercellular convection was initiated by terrain induced environmental modifications (gravity waves) at approximately the 60 and 120 min for the 1500 and 1000 m simulations respectively. The location of the terrain induced supercell was approximately 40 km north-east of the terrain peak. It appears that this does not hinder our results as the cold pool did not significantly propagate over or around the mountain. Furthermore, the cold pool

did not interact with that of the initialized storms until after our analysis is complete. Further analysis of the low-level vorticity and wind field showed that the 1500 m terrain simulation is the only one that generated a closed pair of counter-rotating vortices (Figure 3). Although the maximum vertical vorticity generated by the 1500 m mountain was 0.013 s^{-1} at the 60 min of the simulation this weakened as the simulation progressed. The vertical vorticity extrema, cyclonic and anticyclonic, is $\pm 0.001 \text{ s}^{-1}$ for the 500 m and $\pm 0.0025 \text{ s}^{-1}$ for the 1000 m mountain simulations.

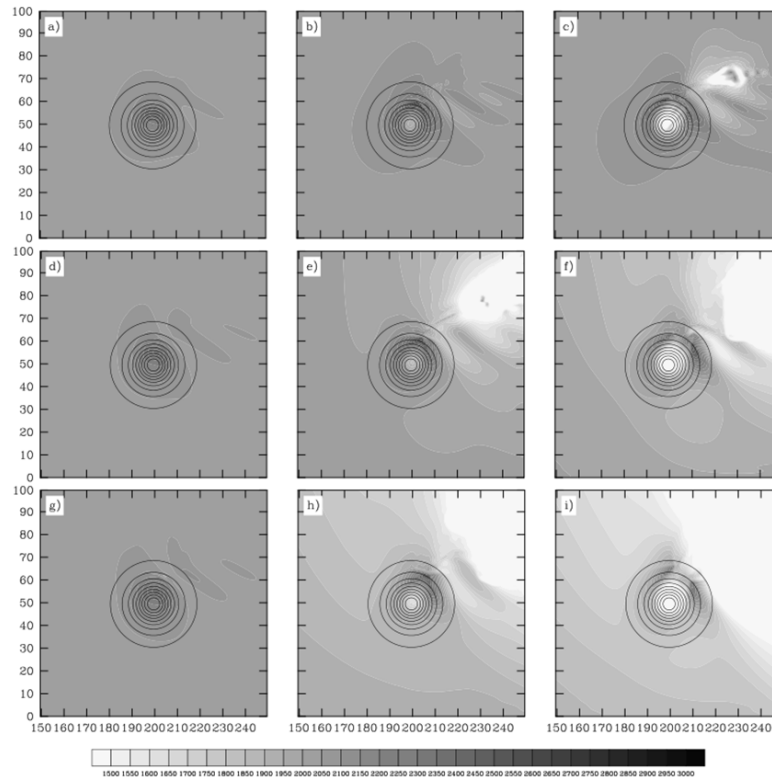


Figure 2. MLCAPE for simulations with the columns panels represent $h_m = 500 \text{ m}$, 1000 m , and 1500 m (left to right); and the row panels represent different times at mins 60, 120, and 180. Note the region of depleted MLCAPE in c, e, f, h, and i are associated with storms triggered by terrain induced gravity waves. The contours represent the percent reduction in height; each contour from the peak represents a 10% reduction

3.2 No Mountain Control Simulation (NMTN)

To establish a baseline of how CM1 simulates a supercell thunderstorm we performed a simulation without terrain. This simulation was initiated by the same warm bubble as those for the MTN (mountain) cases. This will also allow us to better isolate the effects of terrain.

The control simulation produced well-defined right-moving supercell thunderstorms with sustained midlevel, 5 km Above Ground Level (AGL), updrafts (downdrafts) exceeding 30 m s^{-1} (15 m s^{-1}) and low-level, 500 m AGL, updrafts (downdrafts) exceeding 5 m s^{-1} (10 m s^{-1}). Organization of midlevel rotation (vertical vorticity 0.003 s^{-1}) was incipient within 30 min of simulation time and was well organized by 45 min (with vertical vorticity 0.02 s^{-1}), see Figure 4. Midlevel cyclones were sustained throughout the end of the simulations and cyclic intensity is seen as indicated by the 1 km AGL updraft strength, see Figure 4; consistent with observations (Burgess et al., 1982; Beck et al., 2006) and previous numerical simulations (Klemp & Rotunno, 1983; Wicker & Wilhelmson, 1995).

Simulated radar reflectivity gives a clear indication of the classic supercell structure at the 105 min (Figure 5). Figure 5 also shows that the midlevel rotation is aligned with the updraft, indicated by rotating winds aligned with the bounded weak echo region (BWER), which makes the storm more conducive to tornadogenesis. The control simulation vertical vorticities ranged from $0.02\text{-}0.05 \text{ s}^{-1}$ 50 m AGL, from the end of the 60 min and to the 180 min. This storm propagates eastward at approximately 15 m s^{-1} , with small north to south variation in the location of the storm staying within approximately $\pm 5 \text{ km}$ north-south from the location of the warm bubble used to initiate convection. The NMTN also had an anticyclonic left-moving storm that propagated out of the domain by the 120 min.

4. Mountain Simulations (MTN)

In the following we focus on the investigation of orographic effects on supercell thunderstorm; structure and development, intensity, and track.

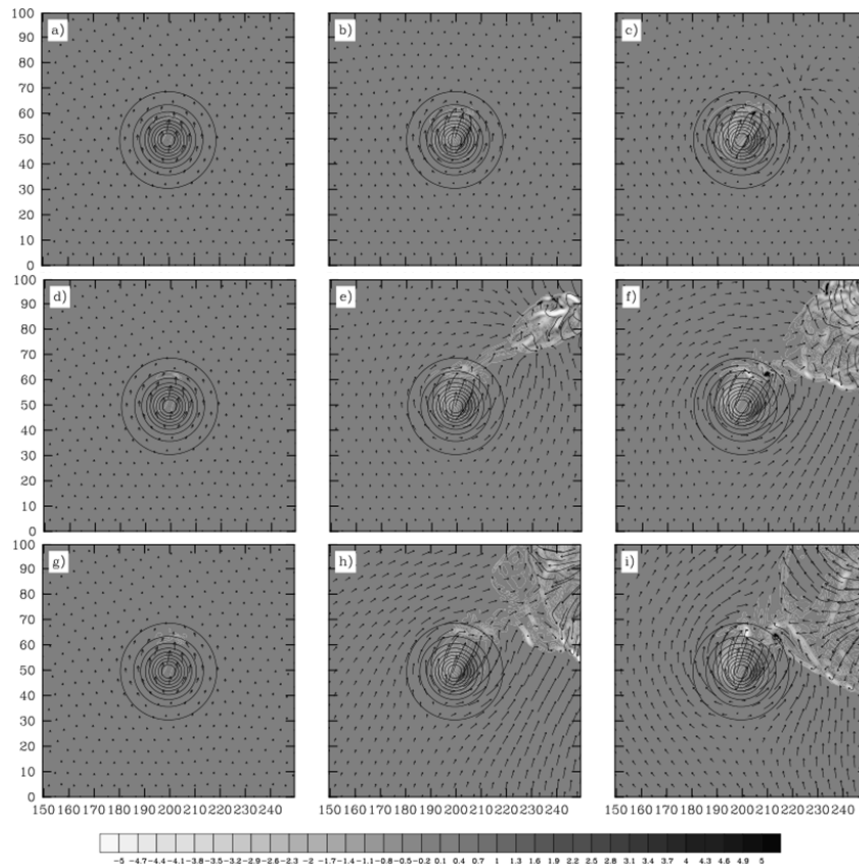


Figure 3. Low-level vorticity and horizontal wind vectors for simulations with column panels represent $h_m = 500, 1000,$ and 1500 m (left to right); and the row panels represent different times mins 60, 120, and 180. Note the region of convergence associated with the outflow from the storms initiated to the north-east of the terrain. The 1500 m mountain was the only one that generated a closed pair of counter rotating vortices with vertical vorticities of 0.008 and -0.006 s^{-1} , respectively at the 180^{th} min

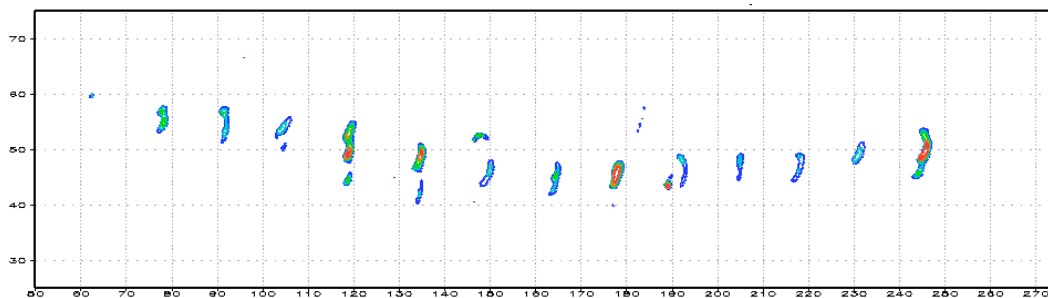


Figure 4. The cyclic nature of the simulated supercell thunderstorm can be seen in the strengthening and weakening of the 1km AGL updraft. The contours show the strength of the updraft and are blue, light blue, green, orange, and red; 10, 12.5, 15, 17.5, and 20 $m s^{-1}$, respectively

4.1 Orographic Effects on Supercell Structure and Development

Overall the initial development of these supercells are quite similar for the NMTN and MTN simulations, the storms undergo more or less identical storm development during the first 60 min of the simulation, and begin to

exhibit the structure of the classical High Precipitation Supercell conceptual model (Lemon & Doswell, 1979). They remain structurally quite similar throughout the maturing phase, ~90 min, although there are increased rainfall areas in the 1000 and 1500 m MTN cases, (M1000 and M1500 respectively). The structure of these storms diverged significantly by the 150 min.

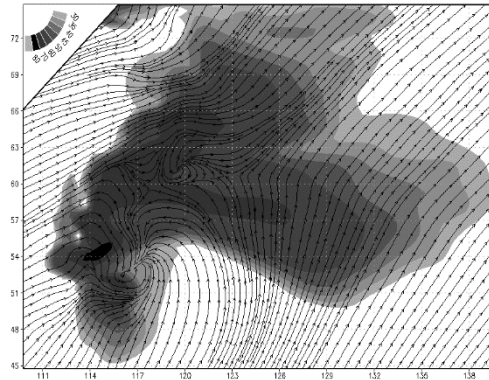


Figure 5. Reflectivity and wind stream-lines for the no-terrain control simulation (NMTN) at the 105 min. Note that the mid-level rotation is aligned with the BWER

A remarkable difference between the MTN cases and the NMTN case at the 150 min is the distribution of hydrometeors within the cloud. NMTN case has a distribution of cloud water and ice water that is approximately twice as large in horizontal extent as compared to the MTN simulations (Figure 6). The cloud size is partially attributable to the midlevel winds advecting the cloud and ice hydrometeors towards the east as the eastward winds are stronger in the NMTN case than in the MTN simulations, see Figure 6 and Figure 7. Furthermore, the cloud hydrometeor differences are also noticeable, which are related to the increased rainfall in MTN simulations reducing the overall amount of water available. The cloud that is indicated by reflectivity in the MTN simulations is accounted for as a mixture of snow and graupel hydrometeors. The decreased cloud region at the lower levels is also attributable to the updraft core being larger, stronger, and better organized in the MTN cases than that of the NMTN case. The stronger updraft produced a larger overshooting top and allowed the anvil cloud to become deeper on the upwind side of the storm.

The hydrometeor densities in and around the main updraft region of MTN cases is higher than that of the NMTN case (not shown). The distribution of hydrometeors is primarily affected by the redirection of additional air into the storm modifying the storms structure; consistent with the findings of Curic and Janc (2012) in which they found that differential heating associated with terrain could favor an enhanced right moving storm and intern alter the hydrometeor distribution.

The augmented air-flow into the supercell produced rain over a greater areal extent and a more continuous rainfall in the MTN cases. The rainfall area is also shifted towards the north in relation to the NMTN case. This is consistent with our findings that the track was shifted towards the north in MTN cases. The increased areal extent of rain allowed the cold pool to strengthen and intensify the storm until the gust front undercut the updraft which weakened the storms midlevel updraft considerably (Figure 6d and Figure 7d). The M1500 storm reorganized once it propagated away from the area where the gust front undercut the supercell.

The NMTN simulated storm developed a low pressure in the 6 to 10 km layer immediately east of the main updraft (Figure 6a), indicated by divergent winds associated with precipitation loading. As this low pressure strengthened (Figure 7a) winds from the main updraft were turned toward the east, until the main updraft was effectively split horizontally at approximately 8 km (Figure 8a). This shifted the cloud base to the east of the main updraft and reduced the rain rate as indicated by the reduction of reflectivity (Figure 6a-9a). Interestingly, the upper-level updraft intensified while the mid-level updraft weakened (Figure 8a and 10a).

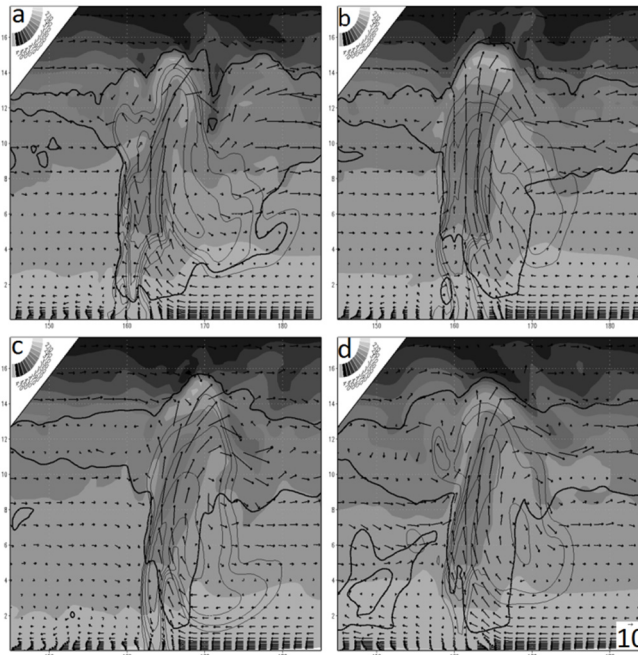


Figure 6. Zonal cross section of potential temperature, reflectivity, cloud outline, and wind vectors, at the 150 min in cases NMTN, M500, M1000, and M1500 simulations a, b, c, and d respectively. Theta is shaded. Reflectivity values start at 50 dBZ and are contoured every 5 dBZ (thin contours). The cloud boundary is indicated by the 0.5 g kg^{-1} cloud water/ice mixing ratio. The reference vector is in the lower right corner of panel d and is the same for all panels. Cross section is along the direction of propagation (east-west) and is at the point of maximum UHW

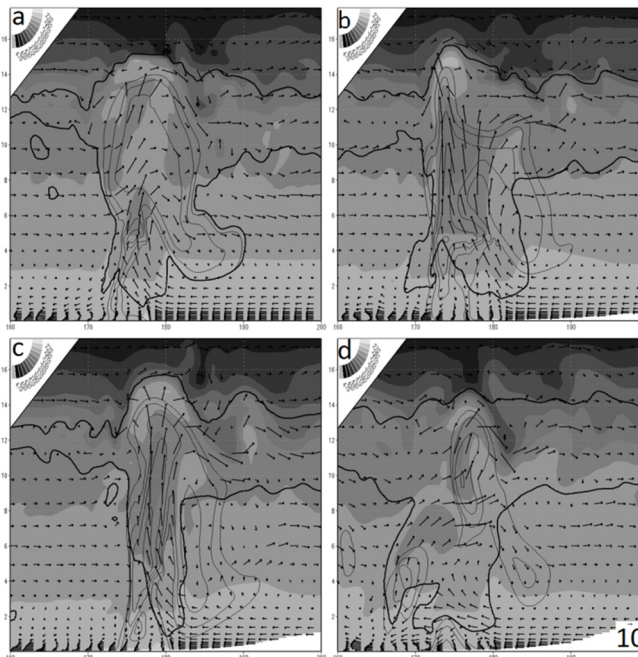


Figure 7. Zonal cross section of potential temperature, reflectivity, cloud outline, and wind vectors, at the 165 min in cases NMTN, M500, M1000, and M1500 simulations a, b, c, and d respectively. Theta is shaded. Reflectivity values start at 50 dBZ and are contoured every 5 dBZ (thin contours). The cloud boundary is indicated by the 0.5 g kg^{-1} cloud water/ice mixing ratio. The reference vector is in the lower right corner of panel d and is the same for all panels. Cross section is along the direction of propagation (east-west) and is at the point of maximum UHW

The M500 simulated storm maintained its updraft size and strength more than those of the other simulations (Figure 6-9). The updraft became larger and stronger as the storm approached the mountain peak and the gust front converged with the winds which were diverted by the mountain. However, the larger updraft started to ingest air from its cold pool (Figure 6b and 10b) essentially offsetting the enhancement of the upslope winds coupled with the main updraft. This effectively produced a storm that varied less structurally throughout the time the storm was interacting with the terrain.

The M1000 simulated updraft intensified slightly and became more upright and the upwind part of the anvil cloud shallowed as it approached the mountain (Figure 6c and 8c). However, as the storm propagated up the mountain the blocking effects on both the storm inflow and the cold pool weakened its updraft considerably (compare the low-level in-flow in Figure 7c and 9c). The blocking effect also reduced the storm's propagation speed which allowed the rear flank downdraft to interact with the storm's updraft, further weakening the storm's main updraft (Figure 8c). Once the storm propagated to the lee side of the mountain, downslope winds coupled with the storm's cold pool to enhance lifting of the lee side convergence region and the storm's updraft became much larger (Figure 9c). The mid-level structure of the storm at the 195 min resembled that of the M500 simulation (Figure 9b and 9c). Once on the lee side of the mountain, the storm started to ingest cool dense air, which was associated with storms triggered further to the west of the mountain, and dissipated quickly after this time (not shown).

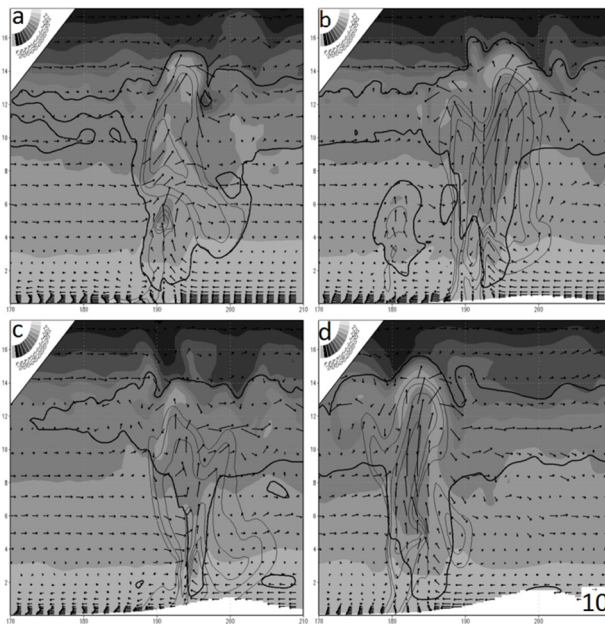


Figure 8. Zonal cross section of potential temperature, reflectivity, cloud outline, and wind vectors, at the 180 min in cases NMTN, M500, M1000, and M1500 simulations a, b, c, and d respectively. Theta is shaded. Reflectivity values start at 50 dBZ and are contoured every 5 dBZ (thin contours). The cloud boundary is indicated by the 0.5 g kg^{-1} cloud water/ice mixing ratio. The reference vector is in the lower right corner of panel d and is the same for all panels. Cross section is along the direction of propagation (east-west) and is at the point of maximum UHW

The propagation of the M1500 simulated storm was slowed down when it started to interact with the terrain and thus it did not propagate past the mountain during the same time interval as that of the storms simulated in the NMTN or other mountain cases. The storm of M1500 was also slowed down due to the reduction in the strength of the updraft associated with its ingestion of air from its cold pool and weakened considerably (Figure 6d and 9d). The ingesting of the cooler air from the cold pool also reduced the amount of precipitation, weakened the cold pool and allowed the storm to propagate out ahead of the gust front and re-intensified quite rapidly (Figure 8d). Once the supercell propagates further behind the mountain the inflow is blocked at low levels and the inflow jet is essentially cut off from the storm (Figure 9d). Similar to the M1000 simulation, the mid-level updraft widens considerably at 195 min. Once the storm propagates over the lee side convergence zone, the inflow becomes unblocked and the storm starts to re-intensify up until the point where it starts to ingest cold air from the terrain initiated storms, as mentioned in section 3.1 (not shown).

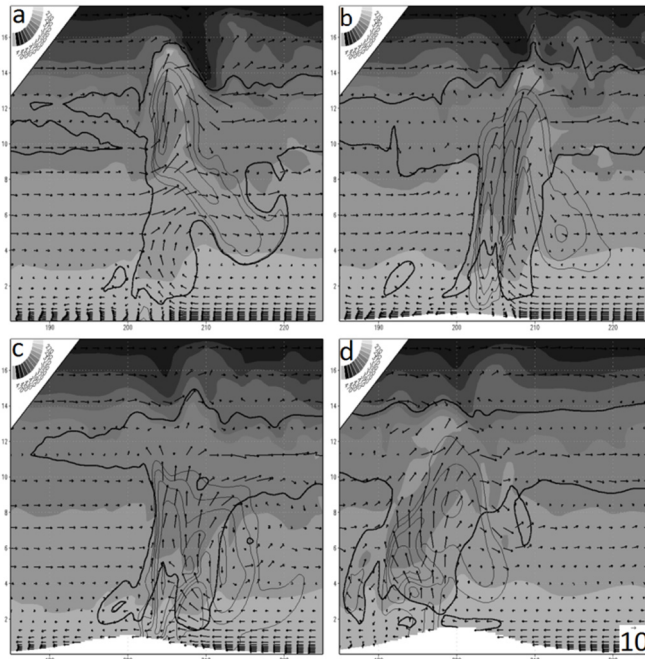


Figure 9. Zonal cross section of potential temperature, reflectivity, cloud outline, and wind vectors, at the 195 min in cases NMTN, M500, M1000, and M1500 simulations a, b, c, and d respectively. Theta is shaded. Reflectivity values start at 50 dBZ and are contoured every 5 dBZ (thin contours). The cloud boundary is indicated by the 0.5 g kg^{-1} cloud water/ ice mixing ratio. The reference vector is in the lower right corner of panel d and is the same for all panels. Cross section is along the direction of propagation (east-west) and is at the point of maximum UHW

4.2 Orographic Effects on Supercell Intensity

Our intensity investigation will primarily focus on the strength of the updraft (downdraft) and the vorticity in the mesocyclone at mid-levels (5 km AGL) and low levels (500 m AGL); The impacts on tangential wind speed, how well the vortex is formed, and the strength of the gust front will also be discussed.

The supercell in all simulations exhibits cyclic intensification and decay, consistent with observations (Burgess et al., 1982, Beck et al., 2006) and previous numerical simulations (Klemp & Rotunno, 1983, Wicker & Wilhelmson, 1995). Although all simulations exhibit cyclic intensity the timing of the peak intensities is altered by the terrain such that it is shortened from approximately 75 min in the control case (NMTN) to 60 min in case with terrain (MTN). In both cases, there are three intensity peaks produced throughout the simulation. The change in the intensity cycle appears due to an increase in the storms inflow rather than the storms updraft coupling with the upslope winds of the terrain, as the second cycle peak is simulated before the upslope wind could become significant. After the second intensity peak of the NMTN and M500 simulations surface vorticity weaken whereas the M1000 and M1500 simulations intensify as the storms couple with upslope winds. On the lee side of the mountain the storms low-level updraft of MTN simulations weakens most notably in the M1500 simulation, while the M1000 and M1500 weaken considerably after the 210 min as they encounter the area of reduced CAPE associated with the outflow of storms triggered on the lee side of the terrain. Although the first two intensity peaks in the MTN storms are stronger than that of NMTN storm the MTN storms are weaker at the third intensity peak.

Although a complete account of all minor variances of the terrain simulations from the NMTN simulation would be exhaustive and tedious, as they start after the 60 min of simulation, very early from when the terrain effects become significant (nearly 100 km from the peak of the mountain). We look at the differences in the near surface vertical vorticities, the low and mid-level updraft, and the speed of the gust front (a measure of the cold pool intensity) for the time interval from the 165 to the 210 min.

At the 165 min, the 1 km AGL updraft of the NMTN simulation was 15 m s^{-1} while the M500, M1000, and M1500 simulations were 9, 12, and 15 m s^{-1} , respectively (Table 1). The decrease in updraft velocity in the M500 and M1000 is most likely attributable to the hydrometeor density being higher in the main updraft resulting in precipitation loading. The downdraft for the M500 and M1000 simulations is stronger than the NMTN or M1500 simulations, 15 vs. 9 m s^{-1} respectively, the weaker updrafts and stronger downdrafts are due to the precipitation

loading effect. At 5 km AGL the strongest updraft of the control simulation was 35 m s^{-1} , and is 30 m s^{-1} for all three terrain simulations. The downdrafts at this altitude are 15, 10, 15, and 5 m s^{-1} for the NMTN, M500, M1000, and M1500 cases, respectively. The speed of the gust front in the NMTN and M1000 simulations is 33 m s^{-1} , while the M500 and M1500 storms are 35 and 45 m s^{-1} , respectively.

Table 1. Selected Variables for intensity comparison from 165 - 210 min

Simulated Time	Case	w1km (m s^{-1})	w5km (m s^{-1})	Gust Front (m s^{-1})	Max θ' (K)	Surface Vertical Vorticity (s^{-1})
165 min	NMTN	15/-9	35/-15	33	-8	0.038
	M500	9/-15	35/-15	40	-7	0.031
	M1000	12/-15	30/-15	33	-8	0.025
	M1500	15/-9	30/-5	45	-8	0.038
180 min	NMTN	12/-15	35/-10	33	-11	0.034
	M500	12/-12	30/-20	30	-9	0.042
	M1000	12/-12	40/-10	33	-8	0.027
	M1500	18/-9	35/-15	40	-8	0.053
195 min	NMTN	9/-12	30/-15	30	-8	0.023
	M500	9/-15	30/-10	33	-8	0.023
	M1000	10/-10	30/-15	27	-8	0.031
	M1500	12/-10	30/-10	35	-8	0.035
210 min	NMTN	10/-10	30/-15	27	-8	0.027
	M500	10/-12	30/-10	33	-10	0.018
	M1000	10/-14	35/-15	24	-7	0.02
	M1500	8/-8	30/-10	30	-8	0.036

At the 180 min, the M500 and NMTN simulations surface vorticity weakens by 0.011 and 0.004 s^{-1} , respectively. There is a little change in the M1000 simulation vorticity and the M1500 simulation surface vorticity strengthens to 0.053 s^{-1} (Table 1). This increase in vorticity for the M1500 simulation is not due to the supercell coupling with the terrain induced vortex generated on the lee side of the mountain, as the storm's location is still relatively far from the location of the lee side vortex, $\sim 30 \text{ km}$. The vorticity enhancement is due to stretching and terrain blocking effects physically redirecting air flow. The enhancement due to vorticity stretching is evident as the 1 km AGL updraft strength increases from 15 to 18 m s^{-1} during this time. Interestingly, the updraft of the M500 simulation increases in strength from 9 to 12 m s^{-1} , however, in this simulation the surface vorticity decreases (Table 1), due to weaker coupling of the storm's updraft with the upslope winds and reduced blocking effect not channeling the winds such that the vertical vorticity would be enhanced. At upper levels the updraft has strengthened for the M1000 and M1500 simulations by 10 and 5 m s^{-1} respectively and actually decreases for the M500 simulation. There is no change in the speed of the gust front for the NMTN or M1000 simulations; the gust fronts simulated in M500 and M1500 simulations are weakened by approximately 10 and 5 m s^{-1} , respectively.

The increase or decrease in the updraft is attributable to two effects, the first and strongest contributor is the terrain blocking effect, as it channels air into the storm, and couples the updraft with the upslope winds. The turning of the winds increases the inflow wind speed from $\sim 10 \text{ m s}^{-1}$ for the NMNT storm to 16, 14, 17 m s^{-1} for the M500, M1000, and M1500 storms respectively, just as the storm is encountering the terrain. These together increase the precipitation rate (the rain coverage is increased in the M1000 and M1500 m simulations compared to that of NMTN and M500 simulations) (not shown) and strengthen the cold pool and intern the strength of the gust front. As expected higher terrain heights allowed the storms to generate consistently more rain.

The low level vorticity is the strongest and the most organized in the M500 and M1500 simulations at the 180 min; the updraft is also aligned with the vertical vorticity (Figure 10). In addition to the vertical vorticity aligning with the updraft the down slope winds enhance the vertical vorticity by accelerating the horizontal winds on the northern

section of the storm's updraft. It is possible that the M1000 simulation also experienced this enhancement of vertical vorticity by the downslope winds on the northern section of the storm's updraft, however, the storm's Rear Flank Downdraft proximity weakens the low level updraft considerably (Figure 10).

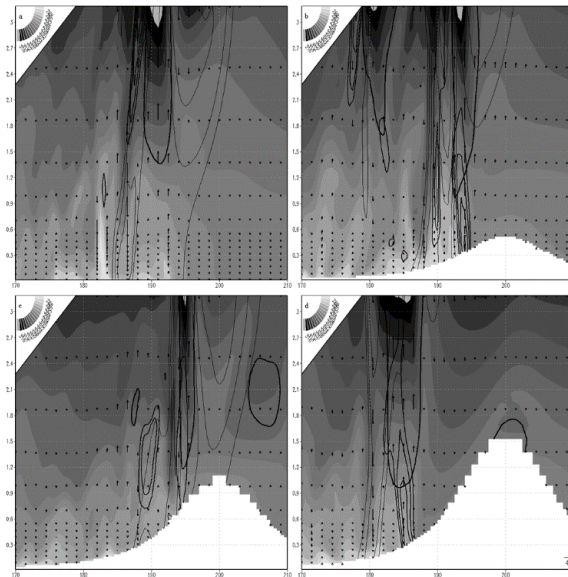


Figure 10. Vertical cross section along the east-west mountain ridge at the 180 min of simulation time. Potential temperature (shaded), reflectivity (starting at 50 dBZ, thin contours every 5 dBZ), cloud outline (thick contour), and vertical vorticity (medium contour, levels are 0.01, 0.015, 0.02, 0.025 s^{-1})

4.3 Investigation of Methods for Tracking Supercell Thunderstorms and Orographic Effects

A selection of parameters for determining the accurate location of a supercell thunderstorm is necessary for determining the track. First, assuming a supercell is present, we try to identify the location of the maximum updraft velocity which would yield a good track representative of the supercell's location. Although this provides a good starting point, the track is rather rough during the early part of the simulations when one would expect the simulations to be nearly identical (Figure 11a). Next, we identify the track using the classic identifier of a supercell the rotating updraft; this parameter is the updraft velocity, at 500 and 1000 m AGL, multiplied by the vertical vorticity at that level. This provides a smoother track than that identified by the maximum updraft alone. Using the classic supercell identifier, we can conclude that the track is shifted towards the north in simulations with increasing mountain height.

We continue our investigation along these lines, and use the location of maximum updraft helicity (UH) to determine the supercells location, UH is a parameter that has recently been used to identify the areas where convective storms are more likely to occur (Kain et al., 2008). UH has proved useful in its ability to detect areas more likely to exhibit convection in model output (Sobash et al., 2008). Although the UH does indicate that a storm was in the approximate vicinity of the supercell, the identified track is rather sporadic and produced quite an erratic track, this rules out the usage UH alone as a supercell tracking method. The storm track is initially smooth during the storm's development phase, however, the track becomes erratic throughout the rest of the simulation (not shown).

The next parameter used to identify the supercell's track was the maximum UH multiplied by the updraft velocity (UHW), which makes the track smoother than that identified by UH. The storm location is identified by tracing the maximum UHW. Again, we use the updraft velocities at 500 and 1000 m AGL. UHW noticeably improves the track and we can say that as the Froude Number decreases the supercell track is shifted towards the north, particularly at lower levels. The combination of the updraft with the updraft helicity produces a smooth track that is free of significant jumps and is more consistent at the two heights used to identify the supercells track.

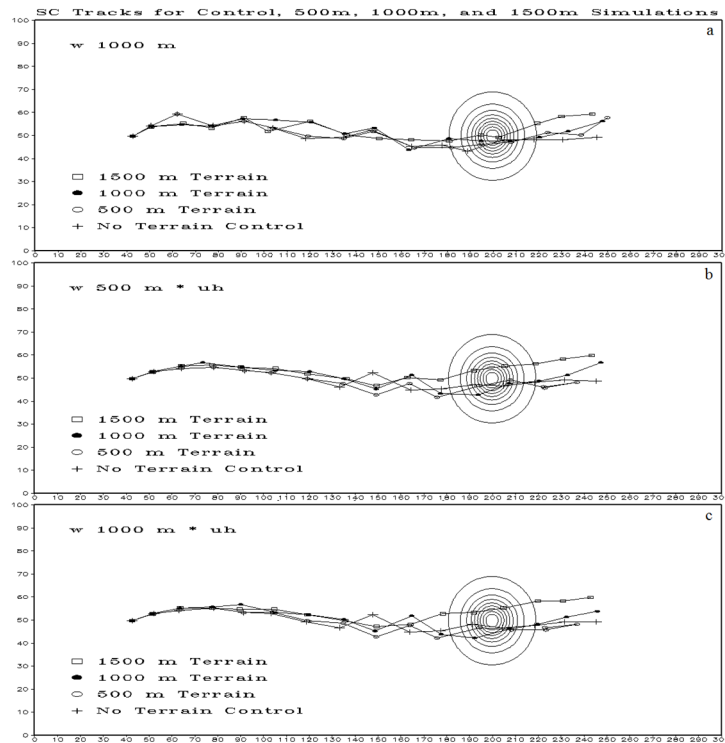


Figure 11. Tracks of supercell thunderstorms as identified by (a) 1000 m AGU Updraft strength (b) Updraft Helicity (UH) multiplied by vertical velocity at 500 m AGU (c) Updraft Helicity multiplied by vertical velocity (UHW) 1000 m AGU. The contours represent the normalized terrain height

Of the parameters used to identify the track of a supercell our UHW parameter yields the best track; both based on smoothness and consistency (between different levels). Following closely after the UHW, the updraft strength produces the smoothest track as long as supercells are known to exist. The classic definition of a rotating updraft produced good results in track identification, although it produced jumps that are uncharacteristic of storm propagation. Interestingly the updraft helicity parameter yields the poorest track identification with erratic track identification just after the initial strengthening phase.

5. Concluding Remarks

The effects of idealized, bell-shaped mountains on supercell thunderstorms are investigated in this study. The mountain produces gravity waves that modified the downwind environment by producing alternating reductions and increases in the amounts of moisture, MLCAPE, and MLCIN. The simulations with higher mountains, such as mountain heights of 1000 m (M1000) and 1500 m (M1500), produce gravity waves that had enough vertical motion to initiate convection near the 120 and 60 min, respectively. Cold outflow from these storms reaches the lee side at approximately the 225 and 180 min for the M1000 and M1500 simulations, respectively. Although these storms produce large environmental modifications our analysis is focused before these effects could influence the investigated supercells.

Several combinations of variables are used to create parameters for the identification of a supercell's location. Although the updraft helicity (UH) indicates the general vicinity of the supercell the identified track that is rather erratic, in that is produced a track that was not consistent with observed supercell propagation. Other parameters that are used based on the characteristics of supercells yields smoother tracks, however, the maximum UHW (UH multiplied by the updraft velocity) produces the smoothest tracks and tracks that are the most similar far from the mountain where the terrain effects are minimal. Using the maximum UHW to identify the storm track we determine that increasing the mountain height shifts the track of a supercell towards the north, to the left of storm motion.

The intensity of supercells is cyclic in all simulations, however, the period between intensity peaks is reduced in mountain (MTN) cases, as compared to the no mountain (NMTN) case. The intensity, structure and development of the storms are mainly a result of the mountain directing an increased amount of environmental air into the storms inflow. This creates differences in the distributions of hydrometeors and increases the rainfall areal extent. This allows the cold pool to be stronger in the MTN simulations, most notably when the cold pool undercut the M1500 storm.

Airflow is also modified such that vorticity is generated and/or intensifies when approaching the mountain peak. The near surface rotation of the M500 storm intensifies as it approaches the mountain peak. The M1000 storm propagation speed is reduced as it crosses the terrain, which allows the storm's rear flank downdraft to run into the storm's low-level updraft and reduces the near surface vorticity greatly. The M1500 storm experiences a greater reduction storm motion, however, its rear flank downdraft is farther away from its updraft and its intensity is not affected in the same manner as M1000. The M1500 storm propagates around to the north of the mountain peak and its cold pool works in conjunction with the terrain to block the storm's inflow and causing the storm to weaken considerably until it propagates into the lee side convergence region.

Although these simulations do not produce tornadic supercells as the grid spacing is too coarse to reproduce such systems, model output shows several instances throughout the MTN simulations where vertical vorticity is greater than 0.1 s^{-1} at the lowest model level (12.5 m). It appears that tornadogenesis could occur if the simulations are run at higher resolutions.

We have shown that blocking effects may direct additional air into the storm's inflow and enhance low-level vorticity along the gust front and that these blocking effects are far more important than the terrain induced environmental modifications, especially since we observe these differences before the storm even interacts with the environmental modifications on the lee side of the mountain. The direction of additional moist air into the storm is particularly of interest to now/forecasting because this increases the precipitation amount and is observed far from the mountain and could increase the likelihood of flash flooding. The M1000 and M1500 simulations initiates supercellular convection that reduced the MLCAPE and increases the MLCIN far more than the gravity waves excited by the mountain and indeed when the simulated storms propagate into this region they quickly dissipate.

This investigation is conducted using an idealized simulation and terrain. Initialized homogeneously with and idealized sounding at a relatively high-resolution. Our use of idealized the simulations allows investigation with as little variations in the initialization as possible. Additionally, using a sounding developed from the storm environments that we are investigating allows us to produce a reliable repeatable storm. However, this is far removed from the real world where storm environments and terrain are often much more complex.

Future studies should include variation of the arrival time of the storm to investigate the terrain effects on developing or mature storms. Additionally, the track and/or terrain configuration could be modified to test the robustness of our conclusion that the terrain blocking effects are more important than the environmental modifications.

List of Symbols and Abbreviations

AGL - Above Ground Level

BWER - Bounded Weak Echo Region

CM1 - Bryan Cloud Model Version 1, Release 16

F_w - Moist Froude number

h - Height of terrain

LCL - Lifting Condensation Level

LFO - Lin-Farley-Orvill (1983) microphysics parameterization

M500, M1000, M1500 - Simulations with mountains of the indicated height in meters

MCS - mesoscale convective system

MLCAPE - Mixed Layer Convective Available Potential Energy

MLCIN - Mixed Layer Convective Inhibition

MTN - Simulations with a mountain

NMTN - Simulations without a mountain

N_w - Unsaturated moist Brunt-Väisälä frequency

SC - Supercell Thunderstorm

SRH - Storm-Relative Helicity

STP - Significant Tornado Parameter

U - Basic wind

UH - Updraft Helicity

UHW - Updraft Helicity * w

w - Vertical wind speed

WK82 - Weisman and Klemp (1982) analytic sounding

θ - Potential temperature

θ' - Potential temperature perturbation

Acknowledgments

We would like to thank the National Oceanic and Atmospheric Administration (NOAA) Educational Partnership Program and the NOAA Earth System Research Laboratory for the use of their ZEUS supercomputer to conduct these simulations. Dr. George Bryan and NCAR are appreciated for allowing us to use CM1 and NCL, respectively. We thank IGES for the use of their Grid Analysis and Display System (GrADS) plotting software. This research was partially supported by the NOAA Cooperative Agreement No. NA06OAR4810187, and National Science Foundation Awards AGS-1265783 and HRD-1036563.

References

- Beck, J. R., Schroeder, J. L., & Wurman, J. M. (2006). High-resolution dual-Doppler analyses of the 29 May 2001 Kress, Texas, cyclic supercell. *Monthly weather review*, *134*(11), 3125-3148.
- Bluestein, H. B. (2000). A tornadic supercell over elevated, complex terrain: The Divide, Colorado, storm of 12 July 1996. *Monthly weather review*, *128*(3), 795-809.
- Bosart, L. F., Seimon, A., LaPenta, K. D., & Dickinson, M. J. (2006). Supercell tornadogenesis over complex terrain: The Great Barrington, Massachusetts, tornado on 29 May 1995. *Weather and forecasting*, *21*(6), 897-922.
- Bryan, G. H., & Fritsch, J. M. (2002). A benchmark simulation for moist nonhydrostatic numerical models. *Monthly Weather Review*, *130*(12), 2917-2928.
- Burgess, D. W., Wood, V. T., & Brown, R. A. (1982, January). Mesocyclone evolution statistics. In *Preprints, 12th Conf. on Severe Local Storms, San Antonio, TX, Amer. Meteor. Soc* (pp. 422-424).
- Chen, S.-H., & Lin, Y.-L. (2005). Effects of the basic wind speed and CAPE on flow regimes associated with a conditionally unstable flow over a mesoscale mountain. *J. Atmos. Sci.*, *62*, 331-350.
- Ćurić, M., & Janc, D. (2012). Differential heating influence on hailstorm vortex pair evolution. *Quarterly Journal of the Royal Meteorological Society*, *138*(662), 72-80. <http://dx.doi.org/10.1002/qj.918>
- Ćurić, M., Janc, D., & Vučković, V. (2007). Numerical simulation of a Cb cloud vorticity. *Atmos. Res.*, *83*, 427-434.
- Ćurić, M., Janc, D., & Vučković, V. (2008). Precipitation change from a cumulonimbus cloud downwind of a seeded target area. *Journal of Geophysical Research: Atmospheres*, *113*(D11). <http://dx.doi.org/10.1029/2007JD009483>
- Ćurić, M., Janc, D., Vujović, D., & Vučković, V. (2003). The effects of a river valley on an isolated cumulonimbus cloud development. *Atmospheric research*, *66*(1), 123-139.
- Deardorff, J. W. (1980). Stratocumulus-capped mixed layers derived from a three-dimensional model. *Boundary-Layer Meteorology*, *18*(4), 495-527.
- Dudhia, J. (1993). A nonhydrostatic version of the Penn State-NCAR mesoscale model: Validation tests and simulation of an Atlantic cyclone and cold front. *Monthly Weather Review*, *121*(5), 1493-1513.
- Durrant, D. R., & Klemp, J. B. (1983). A compressible model for the simulation of moist mountain waves. *Monthly Weather Review*, *111*(12), 2341-2361.
- Emanuel, K. A. (1994). *Atmospheric convection*. Oxford University Press on Demand.
- Frame, J., & Markowski, P. (2006). The interaction of simulated squall lines with idealized mountain ridges. *Monthly weather review*, *134*(7), 1919-1941.
- Gal-Chen, T., & Somerville, R. C. (1975). On the use of a coordinate transformation for the solution of the Navier-Stokes equations. *Journal of Computational Physics*, *17*(2), 209-228. [http://dx.doi.org/10.1016/0021-9991\(75\)90037-6](http://dx.doi.org/10.1016/0021-9991(75)90037-6)
- Grell, G. A., Dudhia, J., & Stauffer, D. R. (1994). A description of the fifth-generation Penn State/NCAR mesoscale model (MM5).
- Homar, V. (2003). Tornadoes over complex terrain: an analysis of the 28th August 1999 tornadic event in eastern Spain. *Atmos. Res.*, *67-68*, 301-317.
- Kain, J. S., Weiss, S. J., Bright, D. R., Baldwin, M. E., Levit, J. J., Carbin, G. W., ... & Thomas, K. W. (2008). Some practical considerations regarding horizontal resolution in the first generation of operational convection-allowing NWP. *Weather and Forecasting*, *23*(5), 931-952.

- Klemp, J. B., & Rotunno, R. (1983). A study of the tornadic region within a supercell thunderstorm. *Journal of the Atmospheric Sciences*, 40(2), 359-377.
- LaPenta, K. D., Bosart, L. F., Galarneau Jr, T. J., & Dickinson, M. J. (2005). A multiscale examination of the 31 May 1998 Mechanicville, New York, tornado. *Weather and forecasting*, 20(4), 494-516.
- Lemon, L. R., & Doswell III, C. A. (1979). Severe thunderstorm evolution and mesocyclone structure as related to tornadogenesis. *Monthly Weather Review*, 107(9), 1184-1197.
- Lin, Y. L., Farley, R. D., & Orville, H. D. (1983). Bulk parameterization of the snow field in a cloud model. *Journal of Climate and Applied Meteorology*, 22(6), 1065-1092.
- Lin, Y.-L. (2007). *Mesoscale Dynamics*. Cambridge University Press.
- Markowski, P. M., Dotzek, N. (2011). A numerical study of the effects of orography on supercells. *Atmospheric Research*, 100, 457-478.
- Morrison, H., Curry, J. A., & Khvorostyanov, V. I. (2005). A new double-moment microphysics parameterization for application in cloud and climate models. Part I: Description. *Journal of the Atmospheric Sciences*, 62(6), 1665-1677.
- Reeves, H. D., & Lin, Y. L. (2007). The effects of a mountain on the propagation of a preexisting convective system for blocked and unblocked flow regimes. *Journal of the atmospheric sciences*, 64(7), 2401-2421.
- Schneider, D. G. (2009). The impact of terrain on three cases of tornadogenesis in the Great Tennessee Valley. *Electronic Journal of Operational Meteorology, EJ11*.
- Sobash, R., Bright, D. R., Dean, A. R., Kain, J. S., Coniglio, M., Weiss, S. J., & Levit, J. J. (2008, October). Severe storm forecast guidance based on explicit identification of convective phenomena in WRF-model forecasts. In *Preprints, 24th Conf. on Severe Local Storms, Savannah, GA, Amer. Meteor. Soc* (Vol. 11).
- Thompson, R. L., Edwards, R., & Mead, C. M. (2004, October). An update to the supercell composite and significant tornado parameters. In *Preprints, 22nd Conf. on Severe Local Storms, Hyannis, MA, Amer. Meteor. Soc. P* (Vol. 8).
- Thompson, R. L., Mead, C. M., & Edwards, R. (2007). Effective storm-relative helicity and bulk shear in supercell thunderstorm environments. *Weather and forecasting*, 22(1), 102-115.
- Wicker, L. J., & Skamarock, W. C. (2002). Time-splitting methods for elastic models using forward time schemes. *Monthly Weather Review*, 130(8), 2088-2097.
- Wicker, L. J., & Wilhelmson, R. B. (1995). Simulation and analysis of tornado development and decay within a three-dimensional supercell thunderstorm. *Journal of the atmospheric sciences*, 52(15), 2675-2703.
- Xue, M., Droegemeier, K. K., Wong, V., Shapiro, A., Brewster, K., Carr, F., ... & Wang, D. (2001). The Advanced Regional Prediction System (ARPS)—A multi-scale nonhydrostatic atmospheric simulation and prediction tool. Part II: Model physics and applications. *Meteorology and atmospheric physics*, 76(3-4), 143-165.

Copyrights

Copyright for this article is retained by the author(s), with first publication rights granted to the journal.

This is an open-access article distributed under the terms and conditions of the Creative Commons Attribution license (<http://creativecommons.org/licenses/by/3.0/>).

Preparation and Antimicrobial Evaluation of Neem Oil Alkyd Resin and Its Application as Binder in Oil-Based Paint

Haruna Musa¹ & Sharif N. Usman²

¹ Department of Pure and Industrial Chemistry, Bayero University, Kano, Nigeria

² Department of Chemical Sciences, Federal University Kashere, Gombe, Nigeria

Correspondence: Haruna Musa, Department of Pure and Industrial Chemistry, Bayero University, Kano, Nigeria.
E-mail: hmusa.chm@buk.edu.ng

Received: February 22, 2016 Accepted: March 17, 2016 Online Published: May 7, 2016

doi:10.5539/enrr.v6n2p92

URL: <http://dx.doi.org/10.5539/enrr.v6n2p92>

Abstract

Neem oil Alkyd resin (NOAR) was synthesized by alcoholysis and polycondensation using glycerol and phthalic anhydride respectively at 230-250°C. The alkyd resin was characterized by FT-IR spectroscopy, viscometry, solubility in various solvents and antimicrobial activity against some selected bacterial species. FT-IR analyses indicated the successful synthesis of alkyd resin as also evident from titrimetric determination of acid number of the mixture which decreases as the reaction progresses. Microbiological analyses of the resin show that it is active against some selected bacterial specie particularly at concentrations of 100 and 50mg/ml in DMSO. The synthesized resin was used as binder in the formulation of oil-based paints using varying resin concentration i.e. 0, 10, and 20% w/v. The prepared paints were found to have excellent fastness properties to light, water, alkali but poor to xylene. The results obtained suggested that NOAR can serve as binder with potential applications in the production of antimicrobial paints.

Keywords: binder, Neem oil (NO), Neem oil alkyd resin (NOAR), paint

1. Introduction

In recent years there have been increasing demands for the application of natural products to address problems in the environment, in waste disposal, and in the depletion of non-renewable resources. Renewable resources can provide an interesting sustainable platform to substitute partially, and to some extent totally, petroleum-based polymers through the design of bio based polymers that can compete or even surpass the existing petroleum based materials on a cost-performance basis with a positive environmental impact (Lligadas, Ronda, Galia, & Cadiz, 2013). Generally, there have been research interest aimed at harnessing various seeds oil for used in the chemical industries. The need is as result of ever increasing world demand for oil and challenges to expand the existing supplies of oils for human consumption and industrial utilization (Odetoye, Ogunniyi, & Olatuji, 2008). Before, the cheaply supply of crude oil, vegetable oil have been used for painting and coating industries. But, trend has been spurred by depleted supply of fossil fuels, environmental issues and waste disposal problems (Derksen, Derksen, Pestrus, & Peter, 1995). The current utilization of renewable raw material resources by chemical industries is 10-20% and it is expected to reach up to 25% by 2020 (Lucas, 2010). Polymer industries compel from its dependence on non-renewable sources and accept industrially applicable renewable sources (Meier & Lucas, 2010). Undoubtedly, there is domination of crude oil by products but it does not limits the use of vegetable oils in the production of paints, inks, pharmaceuticals, cosmetics and chemical intermediates (Aigbodion & Pillai 2000). Condensation polymerization reaction by which polyhydric alcohols and polybasic acid form polymers with resinous characteristics has long been known. In Nigeria, the demand of alkyd resin has increased over the years even though technical information on local production is scanty and large quantities of oils are always needed for the production of alkyd resin (Onukwli & Igbokwe, 2008). Alkyd resins are widely used in the paint and coating industries and are formed by condensation reaction between polyalcohol and carboxylic acids (Blaise, Ogunniyi, Ongoka, Moussounga, & Ouamba, 2012). Organic coatings are compatible to almost all materials, applied purposely to enhance appearance and protect the surface by the help of skeleton of resins (Johnsson & Katarina, 2006). However, due to alkyd compatibility with many polymers made them suitable for the production of a very broad range of coating materials (Shaker, Alian, & Elsayy, 2012). Paints could be described as colloidal mixture of chemical substances which when spread over a surface in a thin layer, form a solid, cohesive and adherent film.

They are used in our daily life for decorative purposes as well as for protecting surface against various environmental effects like UV-radiation, chemical invasion, and mechanical stresses. A conventional paint consists of binder, pigment, solvent and additives. The polymer-binding material (alkyd resin) with a large extent of variation is responsible for the formation of continuous film that adheres to the substrate and holds the other substance together (Oladipo, Eromosele, & Folarin, 2013).

2. Material and Methods

The Neem oil sample was obtained from National Research Institute for Chemical Technology (NARICT), Zaria, Nigeria. Glycerol, phthalic anhydride, white spirit, xylene, ethanol, methanol, Iron (III) oxide, calcium carbonate, calcium acetate were all obtained from Sigma Aldrich.

The apparatus and equipment used include: three-neck flask equipped with Dean and Stark apparatus, Reflux condenser, Brookfield Viscometer, Oswald Viscometer, suction filtration apparatus, pH meter Jenway model 3320, FTIR Spectrophotometre Agilent Technologies, and nitrogen source.

2.1 Preparation of Alkyd Resin

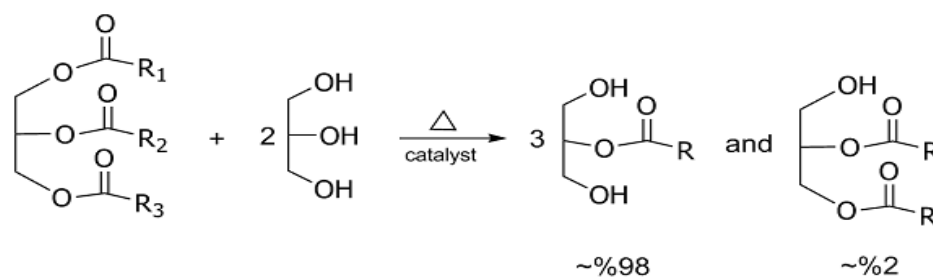
Monoglyceride was first prepared by heating a mixture of oil:glycerol (1:2 molar ratio) and 0.3g CaCO₃ (catalyst) in a 500ml three necked round-bottom flask fitted with condenser, Dean and Stark apparatus. The mixture was heated to 240°C and maintained at this temperature for 2 hours. An aliquot was taken at interval to check for solubility in methanol which indicates the formation of the monoglyceride.

At the onset of the second phase, the temperature was lowered to about 180 °C and measured quantity of phthalic anhydride (3:2 molar ratio of phthalic anhydride:glycerol) was added, followed by addition of xylene (10% of total weight charged) into the reaction mixture. The water of esterification evolved forms an azeotrope with xylene and removed at intervals. The temperature was increased to 230-250 °C while the reaction lasted. Aliquots were withdrawn from the reaction mixture at intervals of 60 minutes to determine the drop in acid value. The reaction was stopped when the acid value attained about 15 mg KOH/g and the alkyd resin was allowed to cool (Onukwli & Igbokwe, 2008).

The physicochemical parameters of NOAR such as colour, acid value and viscosity, were determined. The FTIR of the resin was acquired using FTIR (Agilent Technologies) while the antimicrobial properties were determined using well diffusion method.

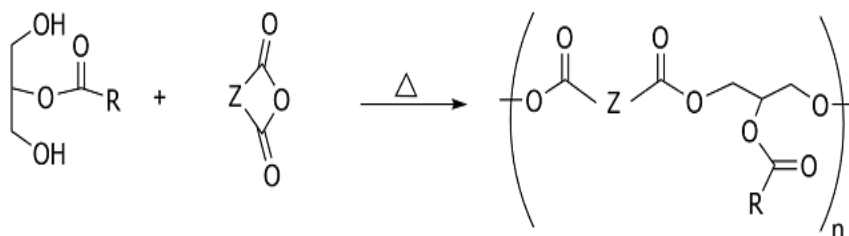
2.2 Reaction Scheme

Alcoholysis stage:



scheme 1

Polyesterification stage:



scheme 2

3. Results and Discussion

The physical properties of the Neem oil sample were evaluated using standard methods of analyses and the results are presented in Table 1.

Table 1. Physico-Chemical Properties of Neem Oil

Physico-Chemical Properties	Neem Oil
Colour	Golden yellow
Refractive index	1.5301
pH	5.53
Nature at room temperature	Liquid
Moisture content (%)	0.05%
Specific gravity at 25°C (g/cm ³)	0.9382
Acid value (mg/g)	1.980
Iodine value (mg/g)	69.780
Saponification value (mg/g)	176.30
%FFA	1.0
Ester Value	174.32

The FT-IR spectra of the prepared NOAR exhibits a characteristic aromatic ring C=O ester band at 1723 cm⁻¹. The disappearance of O-H band in the range 3300-3500 cm⁻¹ was observed in the NOAR. The peaks observed at 1601 and 1581 cm⁻¹ indicates the presence of benzene ring in the resin arising from the reaction of monoglyceride and phthalic anhydride to form the alkyd resin.

The acid value was found to decrease progressively as in figure 1, which can be attributed to desperate reactivity of primary hydroxyl group (react at about 160°C) and secondary hydroxyl group (react above 230°C) with carboxylic group of phthalic anhydride. Also, the drop of acid value with time was linked to characteristics of step-growth polymerization process in which all the reactants were incorporated into the polymer chain. Similar observation was reported by (Onukwli & Igbokwe, 2008). There was high evolution of water as in figure 2, followed by reduced rate at longer reaction period which was attributed to high initial esterification reaction resulted in condensation reaction. Similar result was reported by (Oladipo et al., 2013). It was also observed that the viscosity of the reaction mixture decreases as the reaction progresses.

Table 2. FTIR absorption frequencies of some key functional groups of Glycerol, NO and NOAR

Functional Group	O-H	-C=O	C-O
Glycerol	3291.44 cm ⁻¹	–	1110, 1032 cm ⁻¹
NO	–	1745.49 cm ⁻¹	1099.77 cm ⁻¹
NOAR	–	1723.29 cm ⁻¹	1071.37, 1121.36 cm ⁻¹

Table 3. Physical Properties of Neem Oil Alkyd Resin (NOAR)

Properties	Specific value
Colour	Black
Viscosity (Cp)	1.34
Solubility in; Xylene	Completely soluble
Turpentine	Completely soluble
Ethanol	Partially soluble
Methanol	Partially soluble

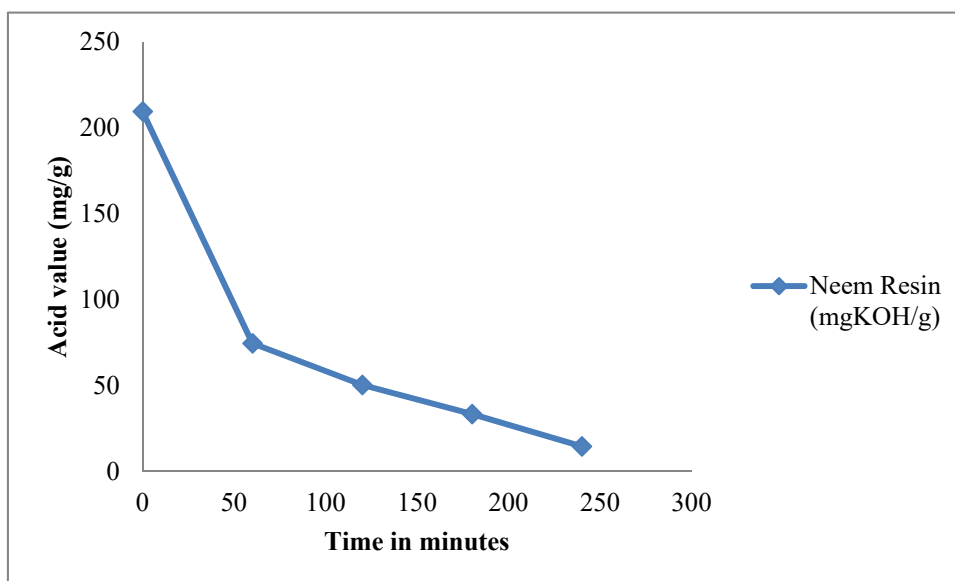


Figure 1. The drop of acid value with polycondensation time

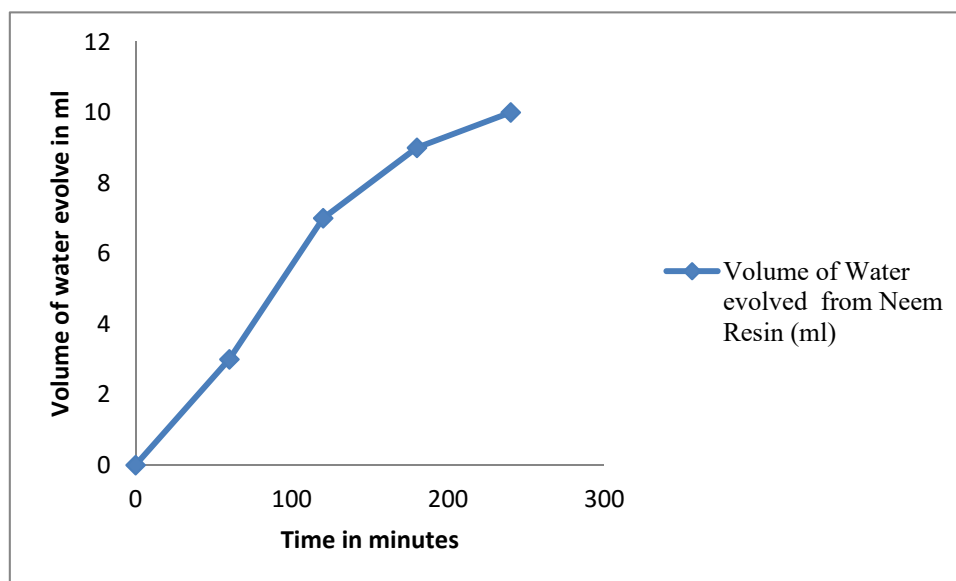


Figure 2. Volume of water evolved during synthesis of NOAR with reaction time

The Antimicrobial activity of NOAR was evaluated using well diffusion method of diameter 6mm and the results obtained is presented in Table 4.

Table 4. Antimicrobial Activity of Neem Oil Alkyd Resin

Isolates/Resin concentration	100mg/ml	50mg/ml	25mmg/ml	2mg/ml control
<i>Esterichia coli</i>	9	8	7	35
<i>Salmonella typhi</i>	12	10	7	32
<i>Staphylococcus aureus</i>	12	11	6	31

* Control = Ciprofloxacin

The NOAR show varying inhibition zone when tested against *Escherichia coli*, *Salmonella typhi* and *Staphylococcus aureus* bacterial species at various resin concentration. Also, the activity of NOAR was found to increase with increasing concentration.

In *E.coli* species, the inhibition zones are 9, 8 and 7mm when resin concentrations of 100mg/ml, 50mg/ml and 25mg/ml respectively. Also, in *Salmonella* species the inhibition zones were 12, 10, and 7mm at resin concentration of 100, 50 and 25mg/ml respectively. The resin was found to be active against *Staphylococcus* only at concentrations of 100 and 50mg/ml and shows no activity (no observed change in well diameter) at 25mg/ml resin concentration as presented in Table 4.

3.1 Paint Formulation

An oil-based paint was formulated according to standard method reported by (Udeo, Umedum, Okoye & Kelle, 2013). At first, 100ml of white spirit was measured, followed by dissolving measured quantity of resin (0% w/v, 10% w/v, and 20% w/v) and then mixed with stirring. Pigment (15g) and 5 gram extender (CaCO₃) i.e. a ratio of 1:3 w/w were added, followed by 0.3 gram of drying agent (calcium acetate). The mixture was then stirred for a period of one hour. The paint was then transferred and stored in an air tight container.

Table 5. Properties of Neem Oil Resin based Paint

Mechanical/Physical Test	0% w/v NOAR	10% w/v NOAR	20% w/v NOAR
Bending at 180°(Flexibility test)	Crack Observed	No cracked observed	No cracked observed
Light Fastness Properties (At 94 hours)	5 (Good)	8 (Outstanding)	8 (Outstanding)
Chemical Resistance;			
-Water	Good	Excellent	Excellent
-Salt (NaCl)	Fair	Very Good	Very Good
-Acid (H ₂ SO ₄)	Fair	Good	Good
-Alkali (NaOH)	Fair	Fair	Fair
-Xylene	Poor	Poor	Poor
Viscosity (cp)		5.61	10.36

The paints formulated were subjected to bending/flexibility test at 180° in which the crack evidence was only observed at 0% w/v resin content paint. Also, the fastness to intense artificial UV-light source was found to be outstanding for 10% and 20%w/v resin paints but good for 0%w/v resin paint. The resistivity test of paints in different media shows an excellent resistance to water and very good resistance to brine but moderately to acid, alkali and very poor to xylene as seen in Table 5.

4. Conclusion

Alkyds resin (NOAR) was successfully prepared using renewable, non-edible Neem Oil as raw material. Antimicrobial evaluation of the resin shows that it is active against *Escherichia coli*, *Staphylococcus aureus* and *Salmonella typhi*. The resin at various concentrations was employed as binder in the formulation of oil-based paints. The formulated paint containing NOAR as binder was found to have satisfactory properties in terms of flexibility, light fastness and resistance to water, acid and brine. The results obtained suggests the potentiality of Neem Oil bioresource in the preparation of NOAR that could have promising applications in the manufacture of antimicrobial surface coatings for use in schools, laboratories, hospitals and other public places.

Acknowledgement

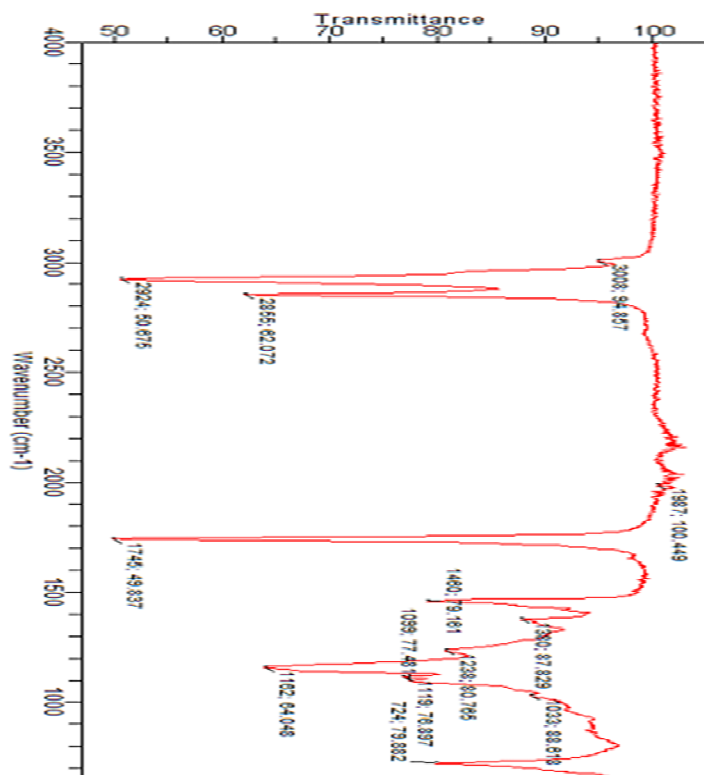
The Authors would like to acknowledge Federal University Kashere, Gombe-Nigeria for granting study fellowship to Sharif N Usman to study MSc Polymer Chemistry at Bayero University Kano-Nigeria.

Reference

- Aigbodion A. I., & Pillai, C. S. K. (2000). Preparation, analysis and application of rubber seed oil and its derivatives in surface coatings. *Progress in Organic Coatings*, 38, 187-192.
- Blaise V. I., Ogunniyi, D. S., Ongoka, P. R., Moussounga, J. E., & Ouamba, J. M. (2012). Physicochemical properties of alkyds resin and palm oil blends. *Malaysian Polymer Journal*, 7(2), 42-45.

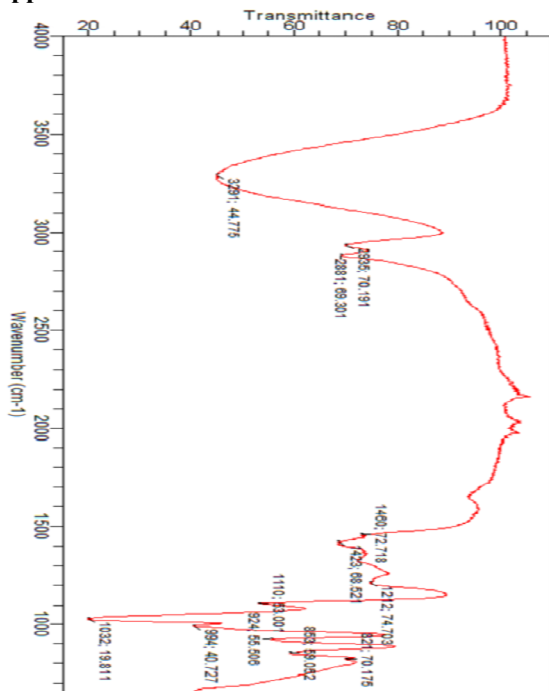
- Derksen, T. P. J., Pestrus, F. C., & Peter, K. (1995). Renewable resources in coatings technology: a review. *Progress in Organic Coatings*, 27, 45-53.
- Johansson M., & Katarina, J. (2006). A model study on fatty acid methyl esters as reactive diluents in thermally cured coil coating systems. *Progress in Organic Coatings*, 55, 382-387.
- Lligadas, G., Ronda, C. J., Galia, M., & Cadiz, V. (2013). Renewable Polymeric Materials from Vegetable Oils; a perspective. *Materials Today*, 16(9), 337-343. <http://dx.doi.org/10.1016/j.matto.2013.08.016>
- Lucas, E. M. (2010). *Plant Oil as Renewable Precursors of Thermosetting and Flame Retardant Polymers* (Unpublished doctoral dissertation). University Of Rovira I Virgili, Spain.
- Meier A. R. M., & Lucas, M. E. (2010). Plants oil: The Perfect Renewable Resource for Polymer Science, *European Polymer Journal*, 47, 837-852. <http://dx.doi.org/10:1016/j.eurpolymj.2010.11.020>
- Nagehan, K. (2011). *Synthesis and characterization of solvent free alkyd resin with hyperbranched melamine Core* (Unpublished Masters thesis). Graduate School of Natural Sciences of Middle East Technical University.
- Odetoye T. E., Ogunniyi, D., & Olatuji, S. (2008). Vegetable oil as industrial raw material. *Proceeding of the 1st Kwara Conference of Chemical Society of Nigeria, 2008 Ilorin-Nigeria*.
- Oladipo, G. O., Eromosele, I. C., & Folarin, O. M. (2013). Formation and Characterization of Paint Based on Alkyd Resin Derivative of Ximenia americana (wild olive) Seed Oil. *Environmental and Natural Resources Research*, 4(3), 52-62. <http://dx.doi.org/10.5539/enrr.v3n3p52>
- Onukwli, O.D., & Igbokwe, P. K. (2008). Production and Characterization of Castor Oil Modified Alkyd Resin. *Journal of Engineering and Applied Sciences*, 3(2), 160-165.
- Shaker, N. O., Alian, N. A., & Elsayy, M. M. (2012). Preparation and Characterization and Evaluation of Jojoba seed oil modified alkyd resins. *Pelagia Research Library*, 3(5), 1157-1162.
- Udeo, I. P., Umedum, N. L., Okoye, N. H., & Kelle, I. H. (2013). Formulation of Glossy Emulsion Paint. *Experimental Journal*, 13(1), 822-828.

Appendix A



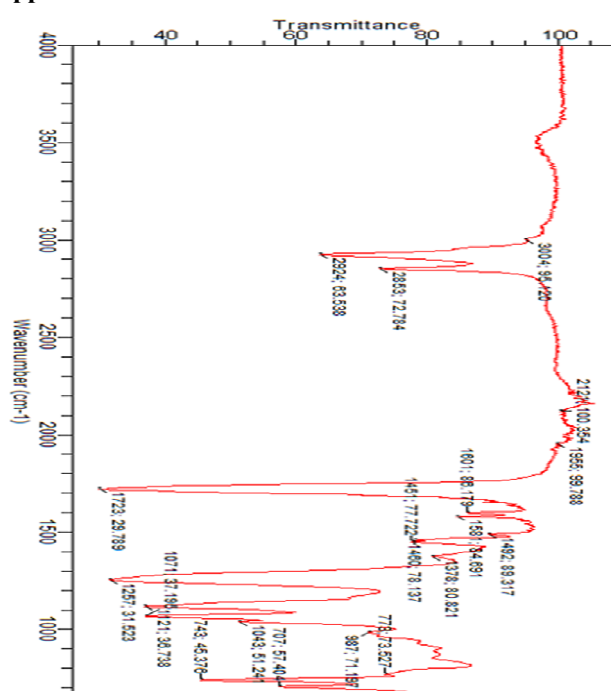
Neem Oil FT-IR Spectra

Appendix B



Glycerol FT-IR Spectrum

Appendix C



Neem Oil Alkyd Resin FT-IR Spectrum

Copyrights

Copyright for this article is retained by the author(s), with first publication rights granted to the journal.

This is an open-access article distributed under the terms and conditions of the Creative Commons Attribution license (<http://creativecommons.org/licenses/by/3.0/>).

Water Quality Assessment of *Aflaj* in the Mountains of Oman

Mohammed Saif Al-Kalbani¹, Martin F. Price¹, Mushtaque Ahmed², Asma Abahussain³ & Timothy O'Higgins⁴

¹ Centre for Mountain Studies, Perth College, University of the Highlands and Islands, Perth, UK

² Department of Soils, Water & Agricultural Engineering, College of Agricultural and Marine Sciences, Sultan Qaboos University, Sultanate of Oman

³ Department of Natural Resources and Environment, College of Graduate Studies, Arabian Gulf University, Manama, Kingdom of Bahrain

⁴ Scottish Association for Marine Sciences, University of the Highlands and Islands, Scottish Marine Institute, Argyll, UK

Correspondence: Mohammed Saif Al-Kalbani, Centre for Mountain Studies, Perth College, University of the Highlands and Islands, Crieff Road, Perth PH1 2NX, UK. E-mail: Kmohd2020@yahoo.com

Received: December 21, 2015 Accepted: December 28, 2015 Online Published: May 16, 2016

doi:10.5539/enrr.v6n2p99

URL: <http://dx.doi.org/10.5539/enrr.v6n2p99>

Abstract

The research was conducted to assess the *aflaj* water quality in Al Jabal Al Akhdar, Oman. 9 *aflaj* were sampled during summer and winter seasons in 2012-2013 to evaluate for the physico-chemical characteristics of major quality parameters; and assess the suitability of *aflaj* for irrigation purposes. Samples collection, handling and processing followed the standard methods recommended by the *American Public Health Association* and analysed in quality assured laboratories using appropriate analytical methods and instrumental techniques. The quality parameters of the selected *aflaj* water indicated their suitability for irrigation as most of the quality parameters were within the permissible limits set by Omani regulations of wastewater reuse for irrigation. These selected water resources are excellent or good in quality for irrigation purposes based on the evaluation of different hazards parameters including the salinity-alkalinity hazards which indicate good to admissible water based on electrical conductivity and sodium adsorption classification; and water quality indices which reveal high or moderate classes, indicating the suitability of *aflaj* for irrigation of the majority of crops and soils. This study is a first comprehensive assessment towards providing indicators and classification indices on irrigation water quality of this fragile mountain ecosystem, which will be the basis for future planning decisions on agricultural demand management measures to protect these principal resources for agricultural production in Al Jabal Al Akhdar.

Keywords: *Aflaj*, Al Jabal Al Akhdar, hazards, irrigation water, mountains, Oman, water quality index

1. Introduction

Like other countries located in arid regions, the Sultanate of Oman suffers from rainfall scarcity and limited renewable water resources. Oman depends totally on groundwater and *aflaj* for domestic and irrigation purposes. *Aflaj* (singular *falaj*) are surface and/or underground channels fed by groundwater, springs, or streams, built to provide water to communities for domestic and/or agricultural use (Al-Marshudi, 2001; Zekri & Al-Marshudi, 2008). *Aflaj* have been constructed in Oman for thousands of years to tap concentrated lines of groundwater flow and guide them to the surface along a channel (often several kilometers long) at a lesser gradient than the water table (Al-Marshudi, 2007). On reaching ground level, the main channel splits into many smaller channels, which in turn divide to supply individual farms. *Aflaj* are managed by local people, with their own designated administrative structure, who are responsible for the overall organization of *falaj* affairs and water distribution for irrigation without government involvement in this organizational structure (Al-Marshudi, 2007; Zekri & Al-Marshudi, 2008). The *aflaj* system is mainly based on a time-share among water rights holders, but in some areas volume is used instead, especially during drought periods (Al-Ghafri et al., 2003; Zekri et al., 2014). Given the importance of *aflaj* as a unique Omani water resource, UNESCO has listed five of the *aflaj* in Oman on the World Heritage list (MRMWR, 2008a).

Most of the *aflaj* are located in the northern Oman Mountains; mountains cover 15% of the country total area. Al Jabal Al Akhdar (Green Mountain) is the largest structural domain, located in the central part of the northern Oman Mountains (Figure 1). It reaches heights between 1500 to 3000 m above sea level. Because of its altitude,

temperatures are some 10 to 12°C lower than in the coastal plains (DGMAN, 2014). In general, the temperatures drop during winter to below 0°C and rise in summer to around 22°C. Rainfall is highly variable and irregular and is the main source of fresh water in the mountain, where the mean annual rainfall is about 300 mm (DGMAN, 2014; Al-Kalbani et al., 2014; Al-Kalbani et al., 2015a). Agriculture has been the principal traditional economic sector with around 70 % of the local inhabitants practice agriculture and animal husbandry (Al-Riyami, 2006; Al-Kalbani et al., 2015b). The mountain terraces produce a variety of perennial fruits, especially pomegranates as well as roses for producing rose water, as a unique business in the area. Tourism is a growing sector in the area where the number of tourists and tourism infrastructure has increased over the last few years (Al-Balushi et al., 2011; Ministry of Tourism, 2014; Al-Kalbani et al., 2015b).

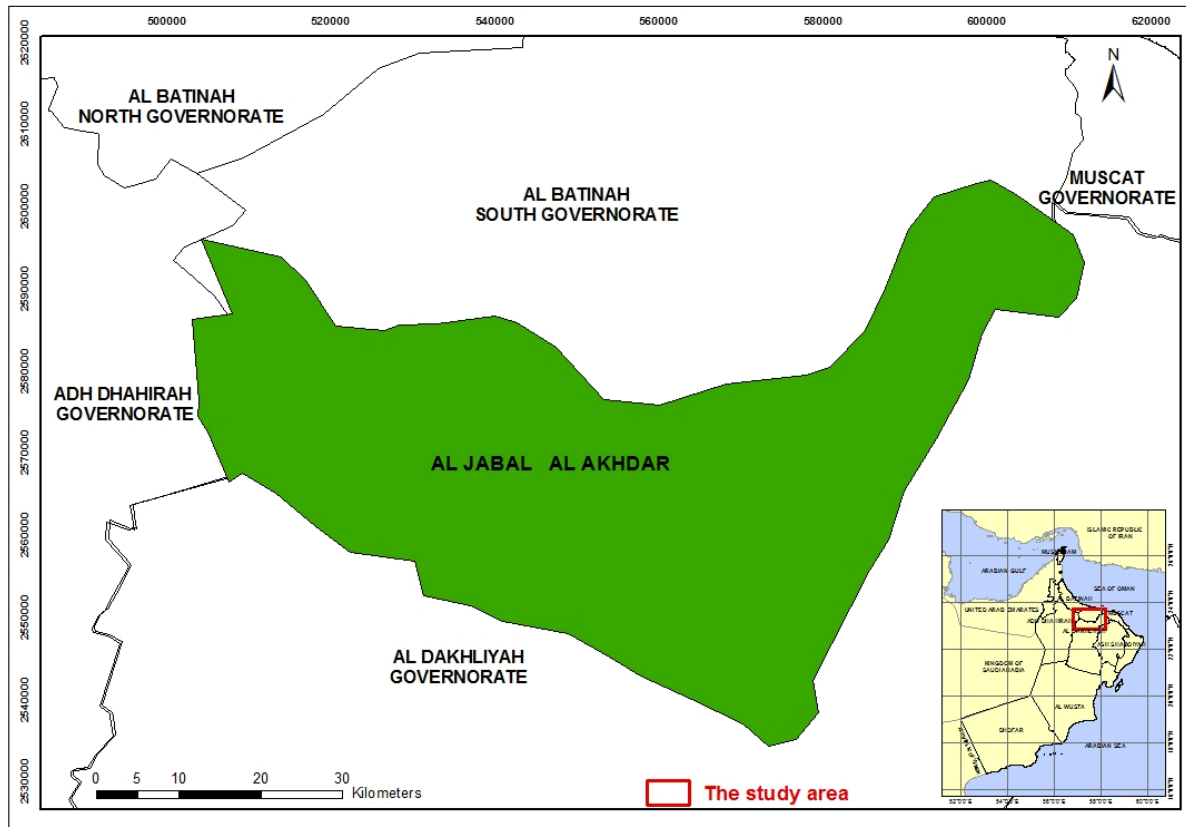


Figure 1. Location of the study area in the Sultanate of Oman map (Source: MECA, 2015)

Al Jabal Al Akhdar has experienced rapid socioeconomic development and urbanization in recent decades. These changes have influenced the water resources, which are the lifeline of its natural ecosystems and therefore human well-being. According to the National *Aflaj* Inventory conducted from March 1997 to June 1998, there were 72 *Aflaj* in Al Jabal Al Akhdar (MWR, 1999; MRMEWR, 2001). However, this number has decreased to 38 based on the recent study by Al-Kalbani et al. (2015b). Many studies have conducted on *aflaj* in Oman: their physical structure, method of construction and governance, irrigation scheduling, water right and market (e.g. Abdel Rahman & Omezzine, 1996; Norman et al., 1998; Al-Marshudi, 2007; Zekri et al., 2014). However, there is very little information assessing and classifying the water quality of *aflaj* and their suitability for irrigation and domestic purposes, especially in the mountains.

Irrigation water quality is an important tool in the assessment and sustainable management of water resources and agricultural production. The presence of excessive amounts of ions in irrigation water affects soil's physical and chemical properties, reduce soil productivity, create crop toxicity and eventually reduce yields (Kraiem et al., 2014; Nag, 2014; Varol & Davraz, 2015). Major water quality problems for irrigation are salinity, sodicity and alkalinity (Simsek & Gunduz, 2007; Sadashivaiah et al., 2008; Nazzal et al., 2014). An appropriate assessment of water for irrigation requires the determination of physical, chemical and biological parameters that are greatly influenced

by geological formations and anthropogenic activities (Sarath Prasanth et al., 2012; Al-Khashman & Jaradat, 2014; Al-Harbi et al., 2014) and directly related to the classifying of water quality (Saber et al., 2014; Aly, 2014; Aly et al., 2014). Several quality indices can be used to assess the suitability of water for irrigation; the most commonly used are salinity hazards, percent sodium (% Na), sodium adsorption ratio (SAR), residual sodium carbonate (RSC), soluble sodium percentage (SSP), residual sodium bicarbonate RSBC), permeability index (PI), potential salinity (PS), Kelley's index (KI) and magnesium hazard (MH) (Tatawat & Chandel, 2008; Sarath Prasanth et al., 2012; Al-Harbi et al., 2014; Nag, 2014). Water quality index (WQI) also provides a simple and concise method for assessing the water quality by integrating the water quality variables into one single number depending on several quality variables: salinity hazard, infiltration or permeability hazard, specific ion toxicity, trace element toxicity, and various miscellaneous effects to susceptible crops (Lou & Han, 2007; Simsek & Gunduz, 2007; Tatawat & Chandel, 2008; Mohammed Muthanna, 2011; Al-Bahrani et al., 2012; Adhikari et al., 2013; Aly et al., 2014).

This study interprets and classifies the hydro-chemical characteristics and WQI of *aflaj* water in Al Jabal Al Akhdar and evaluates their suitability for irrigation. Previous studies on water quality in this fragile mountainous region (e.g. Al-Haddabi, 2003; Ahmed et al., 2006; Al-Haddabi et al., 2009; Victor et al., 2009) focused only on the general physico-chemical characteristics of few *aflaj*. This paper presents a comprehensive assessment and classification of water quality of principal *aflaj* for agricultural activities in the area, using several quality parameters and classification indices.

2. Materials and Methods

2.1 Water Sampling and Analytical Methods

Nine *aflaj* were selected for water sampling (Figure 2; Table 1): these are the main *aflaj* that are most reliable for agriculture and active annually most of the time. The other *aflaj* were inactive or do not continuously flow during the whole year and are less reliable in terms of number of demand areas. At least two sampling points were identified along the channel of each *falaj*: the first at the source, and the second in a demand area (total area irrigated by the *falaj*. For longer *aflaj*, or those with many demand areas, a third sampling point was also used.

Table 1. Characteristics of the *aflaj* sampled in the study area (Data source: National *Aflaj* Inventory, March 1997-June 1998) (MWR, 1999)

Code	<i>Falaj</i> Name	Village	Type	Length (m)	<i>Falaj</i> mother well		Altitude (m)	No. of demand areas	Total demand area (m ²)	Total annual water demand (m ³ /year)
					Coordinates (UTM)					
					North	East				
F1	Masirat Al Jawamid	Masirat Al Jawamid	Ayni	153	2558682	554283	1420	1	21,147	41,583
F2	Masirat Ar Rawajih	Masirat Ar Rawajih	Ayni	1,979	2548880	570600	1212	4	39,208	76,802
F3	Al Azizi	Sayq	Ayni	428	2552062	564891	1942	3	118,690	234,740
F4	Qatam	Sayq	Ayni	331	2552199	564435	1914	4	2,984	5,889
F5	Al Awar	Al Ayn	Ayni	140	2551912	567800	1970	4	62,630	123,348
F6	Al Kabari	Ash Shirayjah	Ayni	1,077	2552208	568992	1941	1	272,564	539,879
F7	As Sawjrah	As Sawjrah	Ayni	22	2558641	568788	1863	2	12,541	24,723
F8	Wadi Bani Habib	Wadi Bani Habib	Ayni	833	2552346	562507	1935	9	6,512	12,839
F9	Al Khamirah Al Sufla	Sayq	Ghayli	128	2550653	565729	1864	4	9,457	18,611

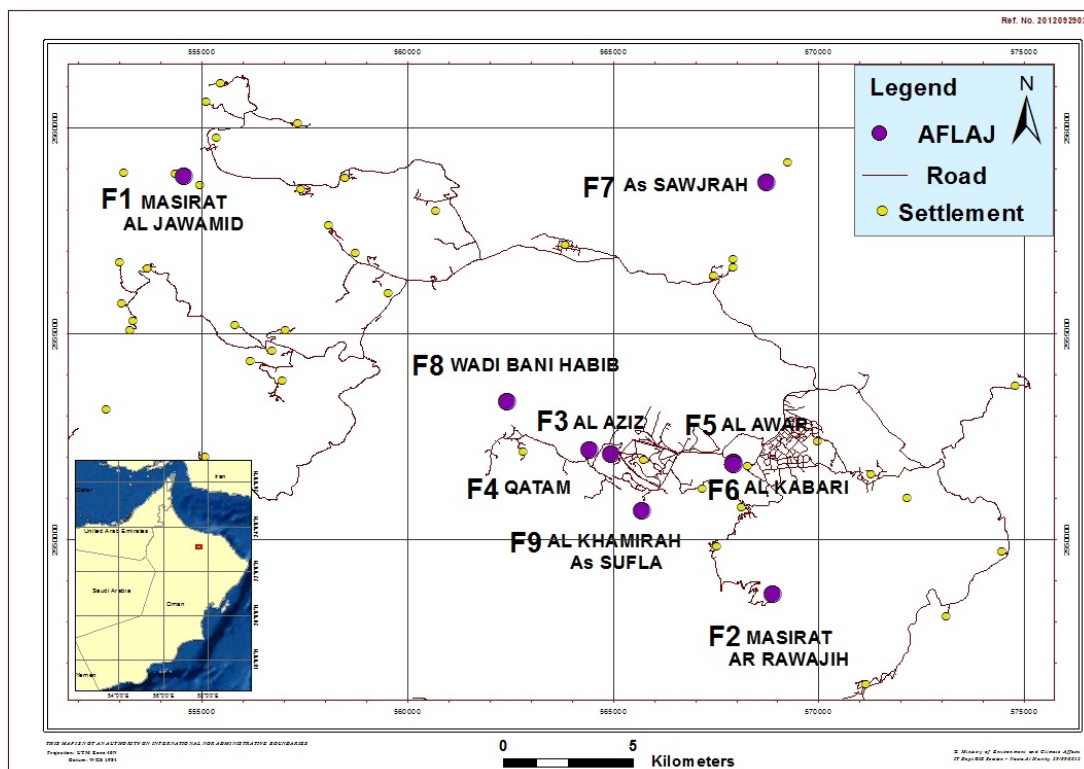


Figure 2. The location of sampled *aflaj* of the study area during summer and winter 2012-2013

Table 2. Determination of physiochemical parameters by different methods/instruments used

Parameters	Method/Instrument Used
Electrical Conductivity (EC)	Measured in the field using a battery-operated conductivity meter (SevenGo, Mettler-Toledo AG 8603 Schwerzenbach, Switzerland) and in the laboratory using the Orion Thermo 550A.
pH	Determined in the field using a pH meter (SevenGo, Mettler-Toledo GmbH, 8603 Schwerzenbach, Switzerland), and in the laboratory using a pH meter (Mettler Toledo)
Turbidity	Turbidity meter (Orion AQ 4500), Nephelometric Turbidity Units (NTU)
Total Dissolved Solids (TDS)	Gravimetric method
Alkalinity (CaCO ₃ , HCO ₃ and CO ₃)	Autotitration
Total Hardness (TH) (mg/l as CaCO ₃)	Complexometric titration method using Ethylene Diamine Tetra Acetic Acid (EDTA)
Dissolved Oxygen (DO)	Measured in the field using Multi Probe System/data logger, YSI Incorporated 556 Instrument, Bramum Lane and in the laboratory using Mettler Toledo Seven Go Pro
Biochemical Oxygen Demand (BOD ₅)	$BOD_5 = (D_2 - D_1) / P$ D1: DO of diluted sample immediately after preparation, mg/l D2: DO of diluted sample after 5 days incubation at 20 °C, mg/l P: Decimal volumetric fraction of sample used
Sodium, Calcium, Magnesium, Potassium	Inductively Coupled Plasma (ICP-OES) (Perkin-Elmer Optima 3300 DV)
Fluoride, Chloride, Nitrate, Sulphate, Phosphate	Metrohm Professional Compact Ion Chromatography System 881 with Metrohm 858 Professional Sample Processor
Heavy Metals	Inductively Coupled Plasma (ICP-OES) (Perkin-Elmer Optima 3300 DV)

The locations of sampled *aflaj*, mother well and points along their channels, were determined using GPS (etrex, Garmin). The sampling regime for all selected *aflaj* was 3 months in winter and 3 months in summer, taking into account that seasonal events such as rainfall and storms may influence sampling; and to obtain a reasonable range of data in each season. Sample collection, handling and processing followed the methods recommended by the *American Public Health Association* [APHA] (2005); water quality parameters were selected according to Chapman and Kimstach (1996). Major physico-chemical and microbiological parameters were analysed in quality assured laboratories in Oman using the analytical methods and instrumental techniques shown in Table 2. The accuracy of the chemical analysis was verified by the calculation of ion-balance errors of 5% for all the sampled water resources. The respective values for all these parameters are compared with standard limits recommended by Omani standards for Un-bottled Drinking Water 8/2006 (MD, 2007) and the World Health Organization [WHO], (2011) for drinking water, and Omani regulations of Wastewater reuse for irrigation (MD, 1993). Statistical analysis was performed using descriptive statistics for all physico-chemical and microbiological parameters as well as correlation analyses using Pearson's coefficient (r) among the levels of parameters in water samples.

2.2 Hydrochemical Water Quality

Water quality indicators, including salinity hazards, percent sodium, sodium adsorption ratio, residual sodium carbonate, soluble sodium percentage, residual sodium bicarbonate, permeability index, potential salinity, Kelley's index, and magnesium hazard, were calculated for the water sampled in summer and winter from the selected *aflaj* of the study area using the equations in Table 3.

Table 3. Chemical composition indicators used for classifying irrigation water quality of the selected *aflaj* of the study (All ionic concentrations are in milliequivalents/l; meq/l)

Chemical Composition Indicator	Equation	Reference
%Na	$(\text{Na}^+ + \text{K}^+) / (\text{Ca}^{2+} + \text{Mg}^{2+} + \text{Na}^+ + \text{K}^+) * 100$	Wilcox, 1955
RSC (meq/l)	$(\text{HCO}_3^- + \text{CO}_3^{2-}) - (\text{Ca}^{2+} + \text{Mg}^{2+})$	Richard, 1954
SSP (%)	$(\text{Soluble sodium concentration}/\text{total cations concentration}) * 100$	Todd, 2005
RSBC (meq/l)	$\text{HCO}_3^- - \text{Ca}^{2+}$	Richard, 1954
PI (%)	$\text{Na}^+ + (\text{HCO}_3^-)^{0.5} / (\text{Ca}^{2+} + \text{Mg}^{2+} + \text{Na}^+) * 100$	Doneen, 1964
PS (meq/l)	$\text{Cl}^- + 0.5 \text{SO}_4^{2-}$	Richard, 1954
KI (Ratio)	$\text{Na}^+ / \text{Ca}^{2+} + \text{Mg}^{2+}$	Kelley, 1951
MH (%)	$\text{Mg}^{2+} / (\text{Ca}^{2+} + \text{Mg}^{2+}) * 100$	Szabolcs & Darab, 1964
Sodium Adsorption Ratio (SAR)	$\frac{[\text{Na}^+]}{\sqrt{[\text{Ca}^{2+}] + [\text{Mg}^{2+}]}}/2$	Todd, 2005

2.3 Irrigation Water Quality Index

WQI was used in this study to assess the quality of *aflaj* water and provide an overall indication for their suitability for irrigation purposes. The methodology requires that all five hazards (Appendix I) are simultaneously included in the analysis and combined to form a single WQI value, which is then assessed to determine the suitability of the irrigation water. The five hazards were grouped into five weighing coefficients, given the numbers 5, 4, 3, 2, 1, respectively, such that the most and the least important groups in irrigation water quality are given the highest (5) and lowest (1) points. For each hazard, several parameters were determined with different ranges and rating suitability. Three categories - high, medium and low - were given to the three rating suitability (3, 2, 1), respectively (Appendices I, II, III). After the total value of the index was computed, a suitability analysis was done based on the three different categories of WQI: low (< 22), medium (22-37) and high (> 37) (Simsek & Gunduz, 2007). The detailed calculation of all five hazard categories and the WQI are summarized in Appendix IV.

3. Results and Discussion

3.1 Physico-Chemical and Microbiological Parameters of Water Quality

The physico-chemical parameters of the selected *aflaj* of the study area are presented in Table 4, as mean, median, standard deviation, minimum and maximum over the summer and winter seasons of 2012-2013, and compared to the quality standards and guidelines for Omani Wastewater Reuse for irrigation and Discharge (Ministerial Decision, MD 145/1993) as there are no specific guidelines set for *aflaj* water.

Table 4. Physiochemical and microbiological characteristics of *aflaj* water quality for 22 sampling points from the study area during the two periods in 2012-2013

Variables	Mean	Median	Std. Deviation	Minimum	Maximum	Omani Standard	WHO Standard	MD 145/1993
EC ($\mu\text{S}/\text{cm}$)	564	538	159	294	896	160-1600	2000	2000
pH	8.11	8.18	0.26	7.41	8.51	6.5-9.0	6.5-9.5	6-9
Turbidity (NTU)	0.79	0.56	1.00	0.06	4.48	1 - < 5	NG	NG
TDS (mg/l)	345	329	100	172	562	120-1000	1000	1500
CaCO ₃ (mg/l)	235	237	49	134	326	NG	NG	NG
HCO ₃ (mg/l)	240	237	50	137	336	NG	NG	NG
Total Hardness (mg/l as CaCO ₃)	272	265	58	158	376	$\leq 200 - 500$	500	NG
Sodium (mg/l)	19.68	16.11	11.50	7.48	48.88	$\leq 200 - 400$	200	200
Calcium (mg/l)	48.98	48.60	12.54	26.83	78.98	200	NG	NG
Magnesium (mg/l)	27.34	26.58	7.66	13.44	46.03	150	NG	150
Potassium (mg/l)	3.79	4.04	3.07	0.51	10.08	NG	NG	NG
Fluoride (mg/l)	0.12	0.12	0.04	0.04	0.18	1.5	1.5	1
Chloride (mg/l)	26.29	19.71	18.02	12.08	76.68	$\leq 250 - 600$	250	650
Nitrate (NO ₃) (mg/l)	6.54	2.98	9.30	0.34	35.03	50	50	50
Sulphate (SO ₄) (mg/l)	26.59	20.91	15.93	10.89	74.16	$\leq 250 - 400$	400	400
Phosphate (PO ₄) (mg/l)	0.27	0.08	0.81	0.03	3.80	NG	NG	NG
Dissolved Oxygen (mg/l)	5.85	5.96	0.82	4.29	7.30	NG	NG	NG
BOD5 (mg/l)	1.91	1.77	0.76	0.73	3.84	NG	NG	15
Coliforms (MPN/100 ml)	133.68	155.93	82.12	3.75	> 200.50	10	10	200
<i>E-Coli</i> (MPN/100 ml)	7.30	2.25	10.83	0.00	37.50	0	0	NG

Omani Standard: Un-bottled Drinking Water Standard (No. 8/2006), WHO Standard: World Health Organization Drinking Water Standard, MD: Ministerial Decision (145/1993): Regulation for wastewater discharge and reuse standards, NG: No guideline is recommended.

According to the Omani regulations of wastewater reuse for irrigation water, the Electrical Conductivity (EC) of irrigation water has a maximum limit of 2000 $\mu\text{S}/\text{cm}$. The results of EC measured in all sampled *aflaj* water ranged from 341 to 793 $\mu\text{S}/\text{cm}$ (mean 528.18 $\mu\text{S}/\text{cm}$) in summer, and from 246 to 999 $\mu\text{S}/\text{cm}$ (mean 599.91 $\mu\text{S}/\text{cm}$) in winter. None of the *aflaj* water samples exceed the maximum limit of 2000 $\mu\text{S}/\text{cm}$ specified in the Omani regulations of wastewater reuse for irrigation water. During summer, the pH values ranged from 7.37 to 8.41 and during winter they ranged from 7.44 to 8.61. These pH values are within the limits of the recommended Omani wastewater maximum quality regulations for irrigation water (pH 6-9). The measured turbidity (TR) in all selected *aflaj* during summer ranged from 0.060 to 6.67 NTU (mean 1 NTU) and from 0.050 to 2.29 NTU (mean 0.57 NTU) in winter.

Total dissolved solids (TDS) in the selected *aflaj* water ranged from 183.20 to 475.42 mg/l (mean 300.44 mg/l) in summer and 160.16 to 649.35 mg/l (mean 389.95 mg/l) in winter. These levels are well below the permissible level of TDS of 1500 mg/l in the Omani regulations of wastewater reuse for irrigation water. The total hardness (TH) measurements in the *aflaj* samples ranged from 157.43 to 348.19 mg/l; and from 159.49 to 402.84 mg/l with means of 256.86 mg/l; and 286.17 mg/l during summer and winter, respectively. Adopting Sawyer (2003) classification criteria, these water resources of the entire study area are hard to very hard as the total hardness (mg/l as CaCO_3) is in the range of 150-300 and more than 300 mg/l. The hardness of the water is due to the presence of alkaline earths such as calcium and magnesium, and anions such as carbonate, bicarbonate, chloride and sulphate.

According to Omani regulation of wastewater reuse, the results of cations and anions concentrations in the selected *aflaj* water studied showed no values exceeding the permissible limits and all quality values are within these standards. The mean concentration of cation (in mg/l) in the selected *aflaj* water sampled during summer and winter was in order $\text{Ca}^{2+} > \text{Mg}^{2+} > \text{Na}^+ > \text{K}^+$. The mean concentration of anions (in mg/l) in the *aflaj* water sampled during summer and winter was in order $\text{HCO}_3^- > \text{SO}_4^{2-} > \text{Cl}^- > \text{NO}_3^- > \text{CO}_3^{2-} > \text{PO}_4^{3-} > \text{F}^-$. None of the cation and anion concentrations in the samples exceeded the permissible limits according to the Omani regulation of wastewater reuse. Monitoring programs of phosphates particularly for cyanobacteria blooms are very important since some of the *aflaj* waters in the area are used for washing cloths by detergents containing phosphates which can be a source of pollution and contaminate these water resources and promote algal blooms growth.

Although the amount of dissolved oxygen (DO) often gives a good indication of water quality, the Omani regulations of wastewater reuse do not recommend guidelines regarding the acceptability of low levels. Generally, concentrations in unpolluted waters are usually close to, but less than 10 mg/l; concentrations below 5 mg/l may adversely affect the functioning and survival of biological communities (Chapman & Kimstach, 1996). All samples had DO concentrations less than 10 mg/l, but some samples were below 5 mg/l, taking into account changes in field water temperatures. Measurements of DO in the *aflaj* water samples during summer and winter had mean values of 7.93 and 3.77 mg/l; they ranged from 6.16 to 9.89 mg/l; and from 2.41 to 4.70 mg/l, respectively.

Omani regulations of wastewater reuse recommend 15 mg/l as a guideline values for biochemical oxygen demand (BOD_5). However, unpolluted waters typically have BOD_5 values of 2 mg/l or less whereas those receiving wastewater may have values up to 10 mg/l or more (Chapman & Kimstach, 1996). In the selected *aflaj* water samples, BOD_5 concentrations were generally very low with means of 1.71 and 2.12 mg/l during summer and winter. All recorded values were below the range of BOD_5 from 15 to 20 mg/l recommended in the Omani regulations of wastewater reuse for irrigation.

Most heavy metals in *aflaj* water sampled during summer and winter were below the detection levels of the ICP instrument. These include cadmium, chromium, cobalt, copper, vanadium, lithium, selenium, titanium and beryllium. In some *aflaj* water samples, concentrations of manganese, molybdenum and arsenic were just above the limit specified in the Omani standards of wastewater reuse for irrigation water. Other heavy metals were found in the *aflaj* water samples but within the safe limits for irrigation water. The chemical weathering and soil leaching are the primary natural sources that contribute in the presence of trace metals in water (Fetter, 2001; Şen, 2014).

Although all the physico-chemical parameters of *aflaj* water are within the permissible limits set by Omani standard for Un-bottled Drinking Water 8/2006 (MD, 2007) and the World Health Organization (WHO, 2011) for drinking water, most of the *aflaj* water resources studied were contaminated with coliform and *E. coli* bacteria. Of the 22 *aflaj* sampling points, 12 showed more than 200.5 total numbers of coliform bacteria in summer, and 9 in winter. Most of the *aflaj* water samples showed the presence of *E. coli* bacteria. These results indicate that *aflaj* waters are unacceptable and hazardous for drinking according to Omani standard for Un-bottled Drinking Water 8/2006 (MD, 2007) and the World Health Organization (WHO, 2011). The Omani and WHO standards allow the Most Probable Number (MPN) of 10/100 ml. In both guidelines, total *E. coli* should be 0 MPN/100 ml of a sample.

3.2 Hydro-Chemical Water Quality

Table 5 shows the mean, median, standard deviation, minimum and maximum of chemical composition indicators including percent sodium (%Na), residual sodium carbonate (RSC), soluble sodium percentage (SSP), residual sodium bicarbonate (RSBC), permeability index (PI), Kelley's index (KI), and magnesium hazard (MH) in the *aflaj* water samples in summer and winter. The selected *aflaj* of the study area have excellent or good quality; none of the water samples exceeded the limits and all were under the satisfactory category values, indicating their suitability for irrigation for the most crops and soils, based on % Na, SSP, RSC, RSBC, PI, PS and MH and their irrigation water classification criteria (Table 6).

Table 5. Descriptive statistics of chemical composition indicators for 22 sampling points of the selected *aflaj* water of the study area sampled during summer and winter 2012-2013

Chemical Composition Indicators		Mean	Median	Std. Deviation	Minimum	Maximum
%Na	Summer	11.43	10.48	4.15	6.29	23.71
	Winter	19.82	18.58	6.56	9.36	30.48
RSC (meq/l)	Summer	-1.21	-0.98	0.59	-2.72	-0.63
	Winter	-0.68	-0.62	0.73	-2.83	0.75
SSP (%)	Summer	10.60	9.53	3.76	5.85	21.63
	Winter	10.60	9.53	3.76	5.85	21.63
RSBC (meq/l)	Summer	0.90	0.94	0.54	-0.12	1.80
	Winter	1.74	1.87	0.69	0.39	3.22
PI (%)	Summer	45.77	46.81	4.02	36.30	54.39
	Winter	54.02	53.29	5.38	46.54	64.54
PS (meq/l)	Summer	0.90	0.74	0.50	0.43	2.36
	Winter	1.13	0.81	0.84	0.47	3.50
KI (Ratio)	Summer	0.12	0.11	0.05	0.06	0.28
	Winter	0.22	0.20	0.09	0.10	0.39
MH (%)	Summer	42.21	41.21	7.49	28.22	59.19
	Winter	54.00	54.47	6.42	40.49	63.74

Table 6. Classification of irrigation water based on different hazards

Parameter	Range	Water class	<i>Aflaj</i> Samples
%Na (After Wilcox, 1955)	< 20	Excellent	F1, F2, F3, F4, F5, F6, F7, F8
	20-40	Good	F9
	40-60	Permissible	
	60-80	Doubtful	
	> 80	Unsuitable	
RSC (meq/l) (After Richard, 1954)	< 1.25	Good	F1, F2, F3, F4, F5, F6, F7, F8, F9
	1.25-2.50	Doubtful	
	> 2.5	Unsuitable	
SSP (%) (After Todd, 2005)	0-20	Excellent	F1, F2, F3, F4, F5, F6, F7, F8
	20-40	Good	F9
	40-60	Permissible	
	60-80	Doubtful	
	80-100	Unsuitable	
KI (Ratio) (After Kelley, 1944)	<1	Suitable	F1, F2, F3, F4, F5, F6, F7, F8, F9
	>1	Unsuitable	
MH (%) (After Szabolcs & Darab, 1964)	<50	Suitable	F1, F2, F3, F4, F5, F6, F7
	>50	Unsuitable	F8, F9
PI (%) (After Doneen, 1964)	50-75	Suitable	F1, F2, F3, F4, F5, F6, F7, F8, F9
	25	Unsuitable	

The assessment of irrigation water quality based on the combination of salinity hazard using Electrical Conductivity (EC) and alkalinity hazard using Sodium Adsorption Ratio (SAR) is another classification for the suitability of water for irrigation. As presented in section 4.1, all the *aflaj* water have mean EC values below 700 $\mu\text{S}/\text{cm}$ indicating good water quality for irrigation (Tatawat & Chandel, 2008). SAR in *aflaj* water samples ranged from 0.61 to 4.70; and from 0.53 to 2.73 with average values of 1.21 and 1.35 during summer and winter, respectively. Using the combined results of EC measurements and the SAR values, the analytical data plot on the EC-SAR diagram illustrates that most of the summer and winter water samples from the *aflaj* (Figure 3) fall in the field of C2-S1 (good: medium salinity/low sodium hazards) suitability based on the EC and SAR classification of irrigation water (Appendix V). These categories of water quality can be used for irrigation of most crops and majority of soils (Richard, 1954; Simsek & Gunduz, 2007).

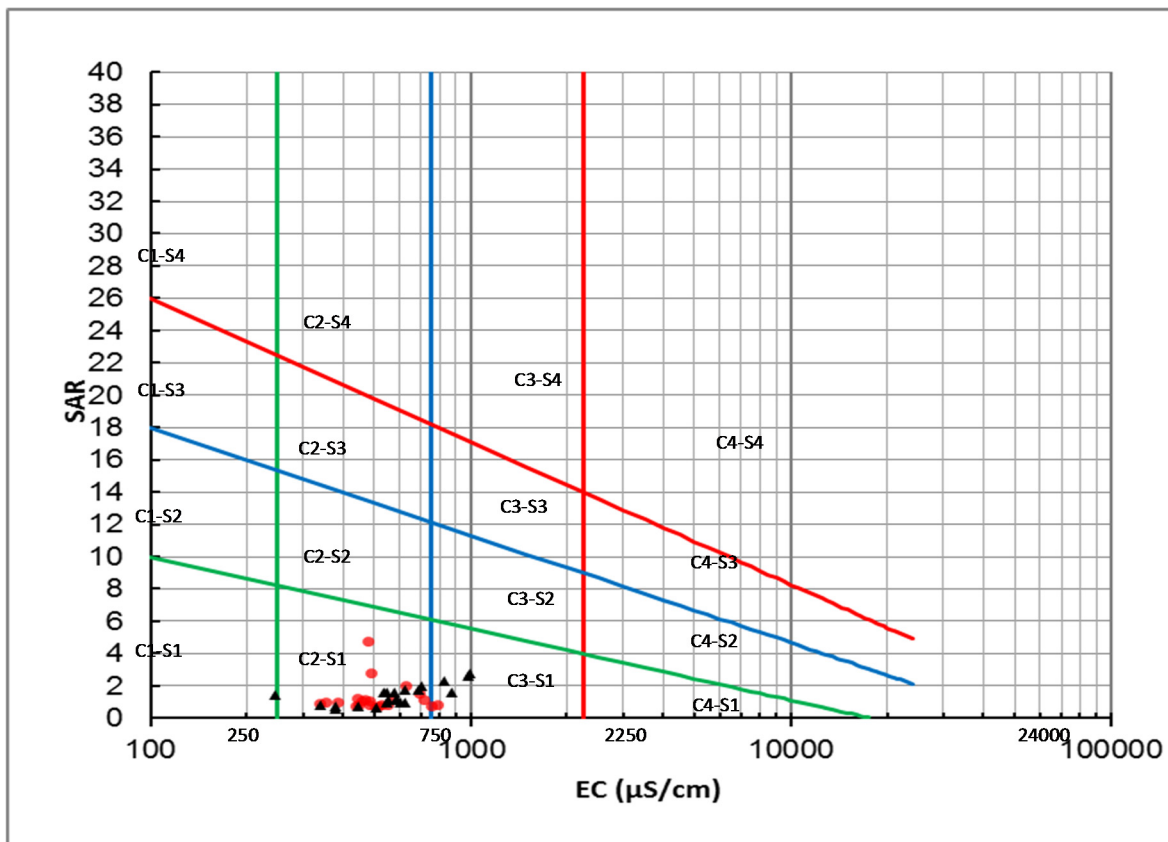


Figure 3. EC and SAR classification of *aflaj* water sampled during summer (in red circle) and winter (in black triangle) in 2012-2013

3.3 Correlation of Water Quality Parameters

Correlation analyses using Pearson's coefficient (r) among the levels of parameters in water samples indicates the existence of an association, and thus, a single parameter can act remarkably as a reliable indicator of the presence of a number of parameters (El Maghraby et al., 2013; Mohammed et al., 2014; Varol & Davraz, 2015). In the present study, statistical analysis has shown that some of the parameters correlate significantly with one another. The terms strongly, moderately and weakly correlations in this study refer to $r > 0.7$, $r = 0.5-0.7$, and $r < 0.5$, respectively.

The correlation matrix among water quality parameters of the selected *aflaj* sampling points (Table 7) showed the highest positive correlation between EC and TDS ($r = 0.978$), highly statistically significant at $p < 0.01$. Other positive strongly correlations, highly statistically significant at $p < 0.01$ include: between TDS with TH, Na^+ , Mg^{2+} , Cl^- , NO_3^- and SO_4^{2-} ; between EC with TH, Na^+ , Mg^{2+} , K^+ , Cl^- , HCO_3^- , NO_3^- and SO_4^{2-} ; between HCO_3^- with TH and Ca^{2+} ; between TH with Na^+ , Mg^{2+} and Cl^- ; between Na^+ with Mg^{2+} , Cl^- , NO_3^- and SO_4^{2-} ; and between Mg^{2+} with Cl^- , NO_3^- and SO_4^{2-} . Moderately positive correlations ($p < 0.01$) were found between TDS with K^+ and HCO_3^- ;

between pH with CO_3^{2-} ; between HCO_3^- with Mg^{2+} ; between TH with NO_3^- and SO_4^{2-} and between Na^+ with K^+ . Other positively weakly correlated and statistically significant ($p < 0.01$) relationships were found between EC with Ca^{2+} and K^+ ; between HCO_3^- with Na^+ , Cl^- and NO_3^- ; between TR with Ca^{2+} and K^+ ; between Ca^{2+} with NO_3^- ; and between Mg^{2+} with K^+ .

Table 7. Correlation matrix among quality parameters for *aflaj* water of the study area sampled during summer and winter 2012-2013

	TR	TDS	EC	pH	HCO_3^-	CO_3^{2-}	TH	Na	Ca	Mg	K	F	Cl	NO_3^-	SO_4^{2-}
TR															
TDS	-0.197														
EC	-0.187	0.978**													
pH	0.222	-0.351*	-0.376*												
HCO_3^-	-0.243	0.632**	0.727**	-0.667**											
CO_3^{2-}	0.139	-0.086	-0.096	0.681**	-0.341*										
TH	-0.263	0.897**	0.905**	-0.536**	0.826**	-0.228									
Na	-0.124	0.861**	0.827**	-0.093	0.398**	0.123	0.765**								
Ca	0.057	0.288	0.436**	-0.398**	0.702**	-0.247	0.431**	0.082							
Mg	-0.290	0.861**	0.871**	-0.177	0.639**	0.109	0.853**	0.813**	0.272						
K	-0.207	0.578**	0.493**	-0.196	0.251	-0.063	0.464**	0.601**	-0.307*	0.440**					
F	-0.133	0.083	0.092	0.132	0.175	0.058	0.167	0.059	0.179	0.211	-0.040				
Cl	-0.057	0.829**	0.836**	-0.008	0.390**	0.136	0.705**	0.909**	0.296	0.807**	0.335*	0.082			
NO_3^-	-0.110	0.725**	0.764**	-0.182	0.432**	0.038	0.656**	0.745**	0.431**	0.701**	0.189	0.037	0.835**		
SO_4^{2-}	-0.031	0.735**	0.756**	0.113	0.305*	0.201	0.603**	0.856**	0.296	0.744**	0.316*	0.107	0.951**	0.853**	

*significantly correlated at 0.05 level, **significantly correlated at 0.01 level.

These correlation relationships between parameters in *aflaj* water samples clearly identify the main elements that are normally found in the studied water resources. The strongest significant relationship ($r > 0.80$) between Mg^{2+} and Cl^- , and the moderately significant relationships between total hardness with Ca^{2+} ($r > 0.50$) and the strongest with Mg^{2+} ($r > 0.80$) in *aflaj* water samples, indicate that the hardness of the water was permanent in nature. The statistically significant and strong correlation ($r > 0.90$) between Cl^- and Na^+ confirms their common origin: the dissolution of the halite resulting from the action of water on salts. The concentrations of SO_4^{2-} are tightly correlated to the presence of Na^+ and Mg^{2+} , which is explained by the dissolution of evaporate minerals.

3.4 Irrigation Water Quality Index

Based on the assessment criteria of EC, infiltration hazard, sodium as SAR, chloride, boron, pH, the concentrations of bicarbonate, nitrate-nitrogen and trace elements, values of the WQI of the *aflaj* water samples in the study area were not significantly different between summer and winter ($F = 1.181$, $P = 0.283 > 0.05$). The WQI of the selected *aflaj* ranged from 35.20 to 40.31 (mean 39.57, median 39.86, standard deviation 1.05) during summer, and from 38.53 to 40.67 (mean 39.84, median 39.92, standard deviation 0.53) during winter.

These results show that the water of the selected *aflaj* was of high or medium suitability for irrigation, falling within the 3 or 2 rating categories of irrigation water classification criteria. In the selected 22 *aflaj* water sampling points during summer, 21 were classified as high in quality and only one as medium. The selected *aflaj* channel points sampled during the winter were all classified as highly suitable for irrigation based on WQI classification criteria (Figure 4).

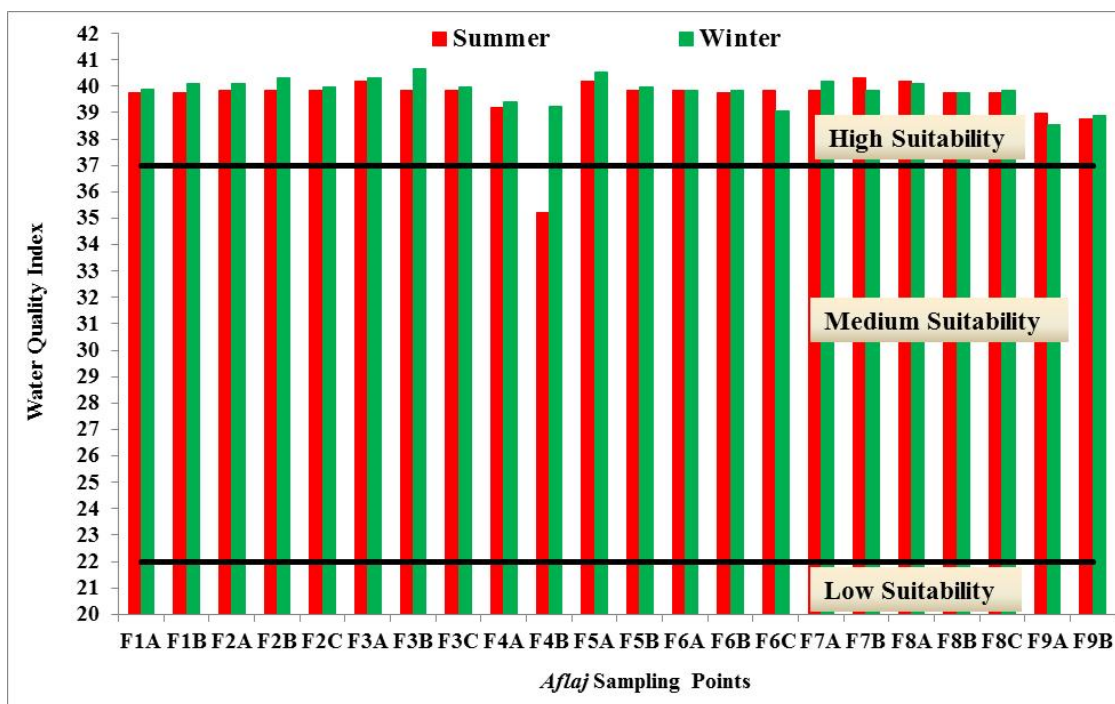


Figure 4. WQI of the selected *aflaj* water sampling points during summer and winter 2012-2013

4. Conclusions and Recommendations

Water quality assessment of the selected *aflaj* in Al Jabal Al Akhdar area indicated that quality parameters are within the permissible limits set by Omani regulations of wastewater reuse for irrigation. However, most of the *aflaj* are contaminated with *E. coli* bacteria; indicating unacceptable for drinking as per the guidelines of Omani and WHO standards. Overall, the selected *aflaj* are excellent or good in quality for irrigation purposes based on the evaluation of different hazards parameters including percent sodium, residual sodium carbonate, soluble sodium percentage, residual sodium bicarbonate, permeability index, Kelley's index, and magnesium hazard; indicating their suitability for irrigation for the majority of crops and soils. The salinity-alkalinity hazards assessment showed that the *aflaj* water are C2-S1 (Good) based on EC and SAR classification; such slightly high salinity and low sodium water can be used for irrigation on almost all types of soil with little danger of exchangeable sodium. All computed water quality indices showed that most of the *aflaj* have high suitability for irrigation and only one has moderate suitability, and no serious problems with respect to irrigation quality. To keep all *aflaj* of the study area under good water quality for domestic and irrigation purposes, the study recommends further corrective demand management measures, such as water conservation, reuse of treated wastewater effluents, reusing greywater, redesigning septic tanks and protecting *aflaj* mother well and their channels. Water quality monitoring programmes should be also carried out on a regular basis to ensure the suitability of water for domestic and agricultural uses.

Acknowledgments

The authors would gratefully acknowledge the Ministry of Regional Municipalities and Water Resources (MRMWR), and *aflaj* committee of the study area for their logistic support and permission to sample *aflaj* water. Our grateful thanks also go to Sultan Qaboos University and MRMWR, Muscat, Oman for their assistance and facilities provided to analyse the water samples in their laboratories. Finally, we would like to send our greatest appreciations to the Ministry of Environment and Climate Affairs, Muscat, Oman for funding this research.

References

- Abdel Rahman, H. A., & Omezzine, A. (1996). *Aflaj* water resources management: tradable water rights to improve irrigation productivity in Oman. *Water International*, 21(2), 70-75.
- Adhikari, K., Chakraborty, B., & Gangopadhyay, A. (2013). Assessment of irrigation potential of ground water using water quality index tool. *Asian Journal of Water, Environment and Pollution*, 10(3), 11-21.

- Ahmed, M., Victor, R., Al Haddabi, M., & Al-Handali, J. (2006). Water Quality Assessment in Al Jabal Al Akhdar Region of Oman for Sustainable Water Resources Management. Paper presented at the IAESTED International Conference on Environmentally Sound Technology in Water Resources Management, ESTW. Gabarone, Botswana, 11-13 September 2006.
- Al-Bahrani, H. S., Razzaq, K. A. A., & Saleh, S. A. H. (2012). Remote sensing of water quality index for irrigation usability of the Euphrates River. *WIT Transactions on Ecology and the Environment*, 164, 55-66.
- Al-Balushi, A. S., Al Mukhtar, B., Al-Hayis, A. J., Orfan, M., Hamza, J., Al-Busaidi, Y. S., & Al-Busaidi N. H. (2011). Socioeconomic Study of Tourism Development in Al Jabal Al Akhdar. Muscat, Oman: Sultan Qaboos University and Ministry of Tourism.
- Al-Ghafri, A. S., Inoue, T., & Nagasawa, T. (2003). Irrigation scheduling of *aflaj* of Oman: Methods and Modernization. In Z. Adeel (Ed.), *Sustainable Management of Marginal Drylands - Application of Indigenous Knowledge for Coastal Drylands* (pp. 147-166). United Nations University, Tokyo, Japan.
- Al-Haddabi, L. H. S. (2003). *Environmental Assessment of an Area Associated with a Diesel Contaminated Stream in Jebel AL-Akhdar, Sultanate of Oman* (Unpublished master's thesis). Department of Biology, College of Science, Sultan Qabios University, Muscat, Sultanate of Oman.
- Al-Haddabi, L. H. S., Victor, R., & Pillay, A. (2009). Assessment of Water Quality in a Mountain Aquatic Resource in Al-Jabal Al-Akhdar (Oman) after Ten Years of Diesel Contamination. In R. Victor & M. D. Robinson (Eds.), *Proceedings of the International Conference on Mountains of the World: Ecology, Conservation and Sustainable Development*, Held on 10-14 February 2008 (pp. 121-126). Center for Environmental Studies and Research, Sultan Qaboos University, Muscat, Oman.
- Al-Harbi, M., Al-Ruwaih, F. M., & Alsulaili, A. (2014). Statistical and analytical evaluation of groundwater quality in Al-Rawdhatain field. *Environmental Progress and Sustainable Energy*, 33(3), 895-904.
- Al-Kalbani, M. S., Price, M. F., Abahussain, A., Ahmed, M., & O'Higgins, T. (2014). Vulnerability assessment of environmental and climate change impacts on water resources in Al Jabal Al Akhdar, Sultanate of Oman. *Water (Switzerland)*, 6(10), 3118-3135.
- Al-Kalbani, M. S., John, C., Martin, F. P. (2015a). Recent Trends in Temperature and Precipitation in Al Jabal Al Akhdar, Sultanate of Oman, and the Implications for Future Climate Change. *J Earth Sci Clim Change*, 6, 295. <http://dx.doi.org/10.4172/2157-7617.1000295>.
- Al-Kalbani, M. S., Price, M. F., O'Higgins, T., Ahmed, M. & Abahussain, A. (2015b). Integrated environmental assessment to explore water resources management in Al Jabal Al Akhdar, Sultanate of Oman. *Regional Environmental Change*, First online: 11 September 2015.
- Al-Khashman, O. A., & Jaradat, A. Q. (2014). Assessment of groundwater quality and its suitability for drinking and agricultural uses in arid environment. *Stochastic Environmental Research and Risk Assessment*, 28(3), 743-753.
- Al-Marshudi, A. S. (2001). Traditional irrigated agriculture in Oman: Operation and management of the *aflaj* system. *Water International*, 26(2), 259-264.
- Al-Marshudi, A. S. (2007). The falaj irrigation system and water allocation markets in Northern Oman. *Agricultural Water Management*, 91(1-3), 71-77.
- Al-Marshudi, A. S. (2008). Economic instruments for water management in the Sultanate of Oman. *Water International*, 33(3), 361-368.
- Al-Riyami, Y. N. S. (2006). Investment opportunities in Agriculture Sector in Al Jabal Al Akhdar. In Oman chamber of commerce and industry (Ed.), Working paper presented in the Symposium on Economic Development of Al Jabal Al Akhdar, Nizwa, Oman, 11th September 2006. (In Arabic).
- Aly, A. A. (2014). Hydrochemical characteristics of Egypt western desert oases groundwater. *Arabian Journal of Geosciences*. <http://dx.doi.org/10.1007/s12517-014-1680-8>.
- Aly, A. A., Al-Omran, A. M., Alharby, M. M. (2014). The water quality index and hydrochemical characterization of groundwater resources in Hafar Albatin, Saudi Arabia. *Arabian Journal of Geosciences*.
- APHA (American Public Health Association). (2005). *Standard methods for the examination of water and wastewater* (21st ed.). American Public Health Association, American Water Works Association and Water Environment Federation Publication, Washington D.C., USA.

- Chapman, D., & Kimstach, V. (1996). The selection of water quality variables. In D. Chapman (Ed.), *Water Quality Assessments* (pp. 59-126). E & FN Spon, London, UK.
- DGMAN (Director General of Meteorology and Air Navigation). (2014). Climatic Data: Rainfall and Temperatures Data Series. [unpublished]. Public Authority of Civil Aviation, Muscat, Sultanate of Oman.
- Doneen, L. D. (1964). *Notes on water quality in agriculture*. Published as a Water Science and Engineering Paper 4001. Department of Water Science and Engineering, University of California, Davis, USA.
- El Maghraby, M. M. S., El Nasr, A. K. O. A., & Hamouda, M. S. A. (2013). Quality assessment of groundwater at south Al Madinah Al Munawarah area, Saudi Arabia. *Environmental Earth Sciences*, 70(4), 1525-1538.
- Fetter, C. W. (2001). *Applied hydrogeology* (4th ed.). Upper Saddle River, N.J.: Prentice Hall.
- Kelley, W. P. (1951). *Alkali, Soils, their Formation, Properties and Reclamation*. Reinhold Pub, New York, USA.
- Kelley, W. P. (1944). Permissible composition and concentration of irrigation water, *Proc Am Soc Civ Eng*, 66, 607-613.
- Kraiem, Z., Zouari, K., Chkir, N., & Agoune, A. (2014). Geochemical characteristics of arid shallow aquifers in Chott Djerid, south-western Tunisia. *Journal of Hydro-Environment Research*, 8(4), 460-473.
- Lou, J., & Han, J. (2007). Assessing water quality of drinking water distribution system in the South Taiwan. *Environmental monitoring and assessment*, 134(1-3), 343-354.
- MD (Ministerial Decision). (2007). *Omani Standard 8/2006 for Un-Bottled Drinking Water*. Issued by Ministerial Decision (MD 2/2007) dated on 15 January 2007, based on the International Guidelines for Drinking Water Quality vol. 1. Recommendations - World Health Organization, 2004. Published by Directorate General for Specifications and Measurements, Ministry of Commerce and Industry, Muscat, Sultanate of Oman.
- MD (Ministerial Decision). (1993). Regulations for Wastewater Re-use and Discharge. Ministry of Regional Municipalities and Environment, Muscat, Sultanate of Oman.: Issued by Ministerial Decision 145/93 dated on 13 June 1993.
- MECA (Ministry of Environment and Climate Affaires). (2015). Unpublished data and maps. Ministry of Environment and Climate Affaires, Muscat, Sultanate of Oman.
- Ministry of Tourism. (2014). Number of Tourists and Tourism Projects in Al Jabal Al Akhdar [Unpublished Data]. Retrieved April 14, 2014, from Department of Statistics and Information, Ministry of Tourism, Muscat, Oman.
- Mohammed, A. A. J., Rahman, I. A., & Lim, L. H. (2014). Groundwater quality assessment in the urban-west region of Zanzibar Island. *Environmental monitoring and assessment*, 186(10), 6287-6300.
- Mohammed, Muthanna, N. (2011). Quality assessment of Tigris River by using Water Quality Index for irrigation purpose. *European Journal of Scientific Research*, 57(1), 15-28.
- MRMEWR (Ministry of Regional Municipalities, Environment and Water Resources). (2001). National *Aflaj* Inventory, summary report. MRMEWR, Muscat, Sultanate of Oman.
- MRMWR (Ministry of Regional Municipalities and Water Resources). (2008). *Aflaj* Oman in the World Heritage List. MRMWR, Muscat, Sultanate of Oman.
- MWR (Ministry of Water Resources). (1999). *Aflaj* Inventory Project: *Aflaj* System Reports & Plots, Wilayah Nizwa. Ministry of Water Resources, Muscat, Sultanate of Oman.
- Nag, S. K. (2014). Evaluation of Hydrochemical Parameters and Quality Assessment of the Groundwater in Gangajalghati Block, Bankura District, West Bengal, India. *Arabian Journal for Science and Engineering*, 39(7), 5715-5727.
- Nazzal, Y., Ahmed, I., Al-Arifi, N. S. N., Ghrefat, H., Zaidi, F. K., El-Waheidi, M. M., Batayneh, A., Zumlot, T. (2014). A pragmatic approach to study the groundwater quality suitability for domestic and agricultural usage, Saq aquifer, northwest of Saudi Arabia. *Environmental monitoring and assessment*, 186(8), 4655-4667.
- Norman, W. R., Shayya, W. H, Al-Ghafri, A. S., McCann, I. R. (1998). *Aflaj* irrigation and on-farm water management in northern Oman. *Irrigation and Drainage Systems*, 12(1), 35-48.
- Richard, L. A. (1954). Diagnosis and Improvement of Saline Alkali Soils (pp. 98-99). IBH Publishing Co. Ltd., New Delhi, India.

- Saber, M., Abdelshafy, M., Faragallah, M. E. A., Abd-Alla, M. H. (2014). Hydrochemical and bacteriological analyses of groundwater and its suitability for drinking and agricultural uses at Manfalut District, Assuit, Egypt. *Arabian Journal of Geosciences*, 7, 4593-4613. <http://dx.doi.org/10.1007/s12517-013-1103-2>.
- Sadashivaiah, C., Ramakrishnaiah, C. R., & Ranganna, G. (2008). Hydrochemical analysis and evaluation of groundwater quality in Tumkur Taluk, Karnataka State, India. *International Journal of Environmental Research and Public Health*, 5(3), 158-164.
- Sarath Prasanth, S. V., Magesh, N. S., Jitheshlal, K. V., Chandrasekar, N., & Gangadhar, K. (2012). Evaluation of groundwater quality and its suitability for drinking and agricultural use in the coastal stretch of Alappuzha District, Kerala, India. *Applied Water Science*, 2(3), 165-175.
- Sawyer, C. N. (2003). *Chemistry for environmental engineering and science* (International ed.). McGraw-Hill, Boston; London.
- Şen, Z. (2014). *Practical and applied hydrogeology* (1st ed.). Elsevier, Amsterdam; New York.
- Simsek, C., & Gunduz, O. (2007). IWQ Index: A GIS-integrated technique to assess irrigation water quality. *Environmental monitoring and assessment*, 128(1-3), 277-300.
- Szabolcs, I., & Darab, C. (1964). The influence of irrigation water of high sodium carbonate content of soils. *Proc. Int. Congress Trans*, 2, 803-812.
- Tatawat, R. K., & Chandel, C. P. S. (2008). A hydrochemical profile for assessing the groundwater quality of Jaipur City. *Environmental monitoring and assessment*, 143(1-3), 337-343.
- Todd, D. K. (2005). *Groundwater hydrology*, 3rd edn. Wiley, Hoboken, New York; Great Britain, p 656.
- Varol, S., & Davraz A. (2015). Evaluation of the groundwater quality with WQI (Water Quality Index) and multivariate analysis: a case study of the Tefenni plain (Burdur/Turkey). *Environmental Earth Sciences*, 73(4), 1725-1744.
- Victor, R., Ahmed, M., Al Haddabi, M., & Jashoul, M. (2009). Water Quality Assessments and Some Aspects of Water Use Efficiency in Al Jabal AlAkhdar. In R. Victor & M. D. Robinson (Eds.), *Proceedings of the International Conference on Mountains of the World: Ecology, Conservation and Sustainable Development*, Held 10-14 February 2008 (pp. 165-170). Center for Environmental Studies and Research, Sultan Qaboos University, Muscat, Oman.
- WHO (World Health Organization). (2011). *Guidelines for drinking-water quality* (4th ed.). World Health Organization, Geneva, Switzerland.
- Wilcox, L. V. (1955). *Classification and Use of Irrigation Water*. US Department of Agriculture, Washington, D.C., 969,19.
- Zekri, S., & Al-Marshudi, A. S. (2008). A millenarian water rights system and water markets in Oman. *Water International*, 33(3), 350-360.
- Zekri, S., Powers, D., & Al-Ghafri, A. S. (2014). Century old water markets in Oman. In K. W. Easter & Q. Huang (Eds.), *Water Markets for the 21st Century - What Have We learned?* Global Issues in Water Policy 11, Chapter 8 (pp. 149-162). Springer Science Dordrecht Heidelberg, New York and London.

Appendices

Appendix I: Classification for irrigation WQI parameters (Simsek & Gunduz, 2007)

Hazard	Weight	Indicator	Rating		
			3	2	1
Salinity hazard	5	Electrical conductivity ($\mu\text{S}/\text{cm}$)	$\text{EC} < 700$	$700 \leq \text{EC} \leq 3,000$	$\text{EC} > 3,000$
Infiltration and permeability hazard	4	See Table 5			
Specific ion toxicity	3	Sodium adsorption ratio	$\text{SAR} < 3.0$	$3.0 \leq \text{SAR} \leq 9.0$	$\text{SAR} > 9.0$
		Boron (mg/l)	$\text{B} < 0.7$	$0.7 \leq \text{B} \leq 3.0$	$\text{B} > 3.0$
		Chloride (mg/l)	$\text{Cl} < 140$	$140 \leq \text{Cl} \leq 350$	$\text{Cl} > 350$
Trace element toxicity	2	See Table 6			
Miscellaneous effects to sensitive crops	1	Nitrate Nitrogen (mg/l)	$\text{NO}_3\text{-N} < 5.0$	$5.0 \leq \text{NO}_3\text{-N} \leq 30.0$	$\text{NO}_3\text{-N} > 30.0$
		Bicarbonate (mg/l)	$\text{HCO}_3 < 90$	$90 \leq \text{HCO}_3 \leq 500$	$\text{HCO}_3 > 500$
		pH	$7.0 \leq \text{pH} \leq 8.0$	$6.5 \leq \text{pH} < 7.0$ and $8.0 < \text{pH} \leq 8.5$	$\text{pH} < 6.5$ or $\text{pH} > 8.5$

Appendix II: Classification for infiltration and permeability hazard (Simsek & Gunduz, 2007)

	Sodium Adsorption Ratio (SAR)					Rating
	< 3	3-6	6-12	12-20	> 20	
Electrical	> 700	>1,200	>1,900	>2,900	>5,000	3
Conductivity	700-200	1,200-300	1,900-500	2,900-1,300	5,000-2,900	2
($\mu\text{S}/\text{cm}$)	<200	<300	<500	<1,300	<2,900	1

Appendix III: Classification for trace element toxicity (Simsek & Gunduz, 2007)

Parameter (mg/l)	Rating		
	3	2	1
Aluminum (Al)	Al < 5.0	5.0 ≤ Al ≤ 20.0	Al > 20.0
Arsenic (As)	As < 0.1	0.1 ≤ As ≤ 2.0	As > 2.0
Beryllium (Be)	Be < 0.1	0.1 ≤ Be ≤ 0.5	Be > 0.5
Cadmium (Cd)	Cd < 0.01	0.01 ≤ Cd ≤ 0.05	Cd > 0.05
Chromium (Cr)	Cr < 0.1	0.1 ≤ Cr ≤ 1.0	Cr > 1.0
Cobalt (Co)	Co < 0.05	0.05 ≤ Co ≤ 5.0	Co > 5.0
Copper (Cu)	Cu < 0.2	0.2 ≤ Cu ≤ 5.0	Cu > 5.0
Fluoride (F)	F < 1.0	1.0 ≤ F ≤ 15.0	F > 15.0
Iron (Fe)	Fe < 5.0	5.0 ≤ Fe ≤ 20.0	Fe > 20.0
Lead (Pb)	Pb < 5.0	5.0 ≤ Pb ≤ 10.0	Pb > 10.0
Lithium (Li)	Li < 2.5	2.5 ≤ Li ≤ 5.0	Li > 5.0
Manganese (Mn)	Mn < 0.2	0.2 ≤ Mn ≤ 10.0	Mn > 10.0
Molybdenum (Mo)	Mo < 0.01	0.01 ≤ Mo ≤ 0.05	Mo > 0.05
Nickel (Ni)	Ni < 0.2	0.2 ≤ Ni ≤ 2.0	Ni > 2.0
Selenium (Se)	Se < 0.01	0.01 ≤ Se ≤ 0.02	Se > 0.02
Vanadium (V)	V < 0.1	0.1 ≤ V ≤ 1.0	V > 1.0
Zinc (Zn)	Zn < 2.0	2.0 ≤ Zn ≤ 10.0	Zn > 10.0

Appendix IV: Summary of the five hazard categories, weighing coefficient and formula used for the calculation of each parameter group and irrigation WQI (Simsek & Gunduz, 2007)

Category	weighing coefficient (w)	Formula used	Description
Salinity (EC)	5	$G_1 = w_1 r_1$	w: weight value of this hazard r: rating value (Appendix I)
Infiltration & permeability hazard (EC-SAR)	4	$G_2 = w_2 r_2$	w: weight value of this hazard r: rating value (Appendix II)
Specific ion toxicity (SAR, Cl, B)	3	$G_3 = w_3/3 \sum (r_j)$	J: incremental index w: weight value (Appendix I) r: rating value of each parameter
Trace element toxicity (elements in Appendix III)	2	$G_4 = w_4/N \sum (r_k)$	k: incremental index N: total number of trace elements w: weight value of this group r: rating value of each parameter (Appendix III)
Miscellaneous effects to sensitive crops (NO ₃ -N, HCO ₃ , pH)	1	$G_5 = w_5/3 \sum (r_m)$	m: incremental index w: weight value of this group r: rating value of each parameter (Appendix I)
Irrigation Water Quality Index		$WQI = \sum (G_i)$	i: incremental index G: hazard category

Appendix V: Classification of irrigation water based on EC and SAR parameters (After Richard, 1954)

Water Class	Suitability	Water Class	Suitability
C1 – S1	Excellent	C3 – S1	Admissible
C1 – S2	Good	C3 – S2	Marginal
C1 – S3	Admissible	C3 – S3	Marginal
C1 – S4	Poor	C3 – S4	Poor
C2 – S1	Good	C4 – S1	Poor
C2 – S2	Good	C4 – S2	Poor
C2 – S3	Marginal	C4 – S3	Very Poor
C2 – S4	Poor	C4 – S4	Very Poor

Copyrights

Copyright for this article is retained by the author(s), with first publication rights granted to the journal.

This is an open-access article distributed under the terms and conditions of the Creative Commons Attribution license (<http://creativecommons.org/licenses/by/3.0/>).

Flood Risk Assessment of Residential Neighbourhoods in Calabar Metropolis, Cross River State, Nigeria

Benedict E. Ojikpong¹, Bassey E. Ekeng², Ukpali E. Obongha³ & Samuel I. Emri⁴

¹ Department of Urban and Regional Planning, Cross River University of Technology, Calabar, Nigeria

Correspondence: Benedict E. Ojikpong, Department of Urban and Regional Planning, Cross River University of Technology, Calabar, Nigeria. E-mail: benojik2008@gmail.com

Received: November 5, 2015 Accepted: November 21, 2015 Online Published: May 23, 2016

doi:10.5539/enrr.v6n2p115

URL: <http://dx.doi.org/10.5539/enrr.v6n2p115>

Abstract

The study is aimed at examining the vulnerability of some residential neighbourhoods in Calabar to the menace of flooding with a view to determining residential areas of high, medium and low flood risk. Two hypotheses were formulated such as: there is no significant relationship between the magnitude of flood, and the vulnerability of residential neighbourhoods and the elements-at-risk to flood in residential neighbourhoods in Calabar do not vary significantly according to the topography of the area. The major primary data were obtained from the metric measurement of the coverage of flood and the assessment of the numerical value of the residential buildings considered vulnerable to flood within the areas measured. Secondary data were also obtained from the collection of both published and unpublished materials and data on flooded buildings and displaced persons were also obtained from the State Emergency Management Agency (SEMA), Calabar. The data were analyzed using descriptive statistics and hypotheses tested using the regression coefficient of the least square method and scatter grams for prediction. The results of the hypotheses were found to be significant as the magnitude of flood determined the vulnerability of some residential neighbourhoods. Vulnerability was found to be higher in low lying residential neighbourhoods. The study, however, recommends among others, planned and autonomous adaptation responses, flood plain zoning to urban agriculture, landscaping and recreational uses. Proper channelization of Calabar urban drainage system, stringent flood control legislation, and development control measures should be enforced so as to discourage people from building on or near flood-prone areas of Calabar.

Keywords: flood risk, vulnerability, residential neighbourhoods

1. Introduction

Flood is among the most devastating natural hazards in the world claiming lives and property more than any other natural phenomena (Ologunorisa, 2006). In the past decade in Nigeria, thousands of lives and property worth millions of naira have been lost directly or indirectly from flooding every year. In most urban centers of Nigeria such as Lagos, Port Harcourt, and Calabar, human population increase is high thus resulting to exploding cities (Oyesiku, 2009). This results in congestion of people and buildings leading to increased risk of flooding. In Calabar for instance over 3000 buildings were affected by flood, displacing about 34000 people in the year 2011(SEMA, 2013).

Landscaping in paved areas, narrow drainage channels, streams and channel obstruction due to poor waste disposal habit and other human activities at flood plains are considered to be the major causes of flood.

Flooding in urban areas and River basins is intensifying due to rapid urbanization which is causing a major change in rainfall-runoff phenomenon and the drainage system as well. Flooding primarily occurs because of drainage congestion of inland flow and/or over bank flow of river during severe rainfall event. The overland flow pattern is becoming complex due to huge structural development, and therefore, the correct prediction of surface runoff is becoming a challenging issue (Ologunorisa, 2006). Flood is an excess of water on land that is normally dry and is a situation where the inundation is caused by high flow, or over flow of water in an established watercourse, such as a river, stream, drainage channel, or pond of water at or near the point where the rain falls.

According to Abua and Eze (2002), two types of floods are common in Nigeria namely flash and perennial floods. Floods have affected some residential neighbourhoods in the metropolitan areas of Nigeria. This has posed a lot of danger to lives and property and thereafter, renders some people vulnerable. In Calabar for instance, the effect of flood could be felt on the disruption of economic activities, traffic problems, destruction of infrastructure and buildings, prevention of human and vehicular movements, psychological impact on human beings, environmental effect and degradation (such as damage to surroundings, forests, bridges, wild life, urban community trees, water bodies, shrubs, grass, turfs, and vegetables). Flooding in Calabar is also known to affect the planned and unplanned environments. So far the assessment of the risk of residential neighbourhoods to floods has not been determined and this is the main thrust of this research.

1.1 Aim and Objectives

The aim of this study is to examine the vulnerability of some residential neighbourhoods in Calabar to the menace of flooding with a view to determining residential areas of low, medium and high flood risk zones.

The specific objectives of the study are:

- (1) To define the boundaries of residential neighbourhoods affected by flood in Calabar Metropolis.
- (2) To determine the impact of flood in relation to the topography of the affected residential neighbourhoods.
- (3) To evaluate the level of vulnerability of residential neighbourhoods to the magnitude of flood.
- (4) To proffer recommendations through predictive models on management of flood risk and flood incidence in the study area.

2. Study Area

Calabar, with a population of over 500,000, is the Capital City of Cross River State of Nigeria. It is located between latitudes $04^{\circ} 56''N$ and $05^{\circ} 4''N$ and longitudes $08^{\circ} 18''E$ and $08^{\circ} 24''E$. It is bounded at both sides by Great Kwa River and Calabar River (Figure 1). It can be accessed by sea, land and air. Its present settlement is on the Eastern flank of the Calabar River. To the South, its growth is limited by mangrove swamps. There are two Local government areas in the city. They include Calabar Municipality and Calabar South local government areas.

Calabar has a subequatorial type of climate. The annual temperature is moderately high about $31-35^{\circ}C$ and does not fluctuate greatly. The rainfall distribution shows that it is characterized by double rainfall maxima, which starts from the months of April to October, reaching its climax in the months of July and September. The annual average rainfall is about 2000-3000mm with a short dry period in August. The heavy rainfall tends to accelerate runoff volume and rate thereby resulting in flooding and environmental degradation in the city.

3. Conceptual Framework/ Literature Review

3.1 The Concept of Risk

Risk is an integral part of life. Its management according to Kates and Kasperson (1983) comprises three distinct steps:

- (1) An identification of hazard likely to result in disasters for example, what hazard event may occur?
- (2) An estimation of the risk of such event, for example, what is the possibility of such event appearing?
- (3) An evaluation of the social consequences of the derived risk, for example, what is the loss, created by each event?.

However, for sound risk management to occur, Ologunorisa (2004) asserts that, there should be a forth step, (iv) which addresses the need to take post audits of all risk assessment exercises. When risk analysis is undertaken, risk (R) is taken as some product of probability (P) and (L) the scale of occurrence. $R = P \times L$ - equation 1. Flood risk involves both the statistical probability of an event occurring and the scale of the potential consequences (Smith, 1996). Development of land within the flood plain of a water course is at some risk of flooding, however small. The degree of flood is calculated from historical data and expressed in terms of the expected frequency of 10 years, 50 years and 100 years of flood.

Flood risk is a function and product of hazard and vulnerability. That is Risk = Hazard x Vulnerability (Plate, 2002). A real flood risk level requires a certain level of hazard, and for the same location, a certain level of vulnerability. A situation of risk is due to the compatibility between hazard and vulnerability levels on the same land (The United Nations Commission for Human Settlement, UNCHS, 1981).

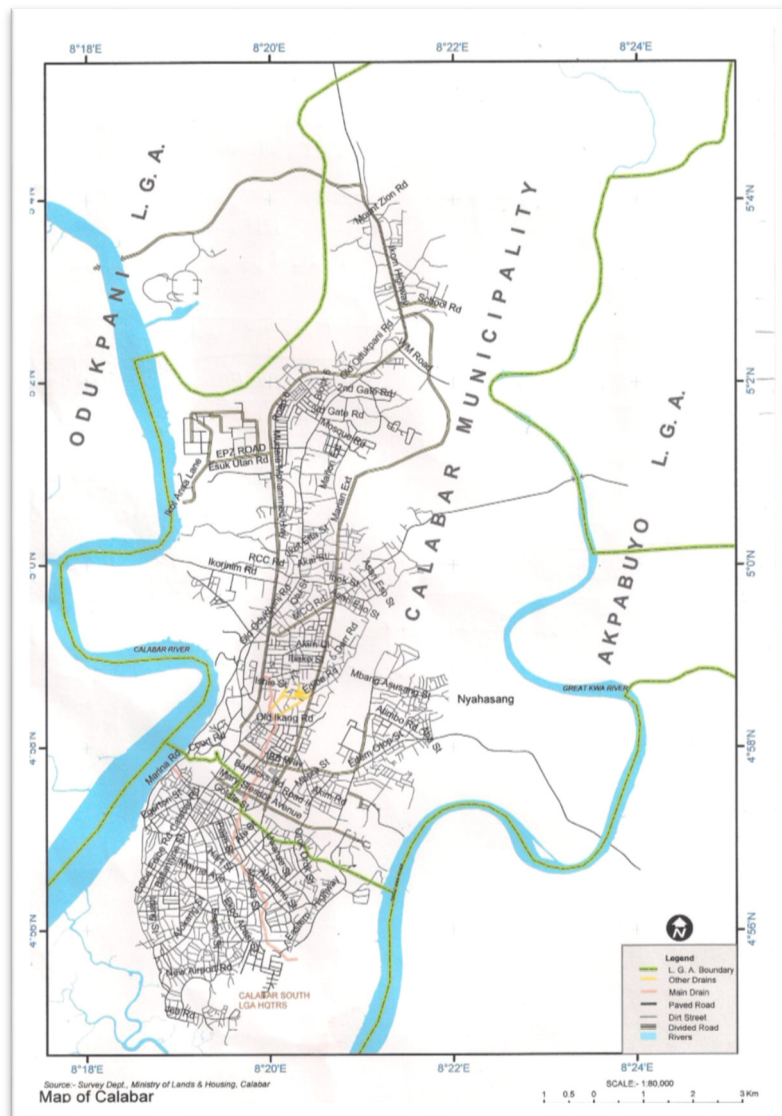


Figure 1. Map of Calabar showing the study area

3.2 The Concept of Vulnerability

The concept of vulnerability is central in discussion of environmental risk in the context of climate change and offers a vulnerable framework for this study. The Intergovernmental Panel on Climate Change (IPCC, 2008) defines vulnerability as the extent to which a natural or social system is susceptible to sustaining damage from climate change. Vulnerability is a function of the sensitivity of a system to changes in climate and ability to adapt the system to changes in climate. Cong et al. (2008) noted that the two factors that contribute to vulnerability are largely determined by the development context which has such a strong influence on households' income, education and access to information on people's exposure to environmental hazards in their homes and work places on the quality and extent of provision for infrastructure and services.

In urban areas, vulnerability is also influenced by the extent and quality of infrastructure and services, especially for vulnerable population (UNFCCC, 2008). Three perspectives of vulnerability from climate change and hazard research have been identified, which combined address the dynamic and integrated nature of social and environmental vulnerability. The first perspective characterizes vulnerability in terms of exposure to hazardous events and how these affect people and structures. The second perspective views vulnerability as basically a human relationship and not a physical one, this is, social vulnerability, while the third integrates both the physical events and the underlying causal characteristic of population that lead to risk exposure and limited

capacity of communities to respond. The integrated vulnerability approach is useful in cities where inherent susceptibilities and resiliencies of both biophysical and social environments interact to result in observed vulnerability (Few et al., 2006).

However, the concepts of risk and vulnerability are both adopted into this study. The study is out to assess the risk of flood on the residential neighbourhoods in Calabar Metropolis. The concept of risk addresses hazards and vulnerabilities as related to the study, while the concept of vulnerability takes assessment of the extent of damage to natural and social systems by flood. On this note, the two concepts are highly applicable and useful in this study.

3.3 Literature Review

Flood risk has been researched on by a number of authors in different parts of the globe. Hogue et al. (1997) for instance, undertook an assessment of the flood risk involved with cyclones and storm surges in Chitagong, Bangladesh through depth measurement. The study finds that the extent of storm surge flooding and the related risk in the Metropolitan area was significant. To identify the risk, the depth and extent of storm surge flooding for different probabilities of occurrence have been predicted and were expressed in a hazard index. The city area was divided into five categories of land use:- Industrial area, commercial area, planned housing area, unplanned housing area and mixed area. For each, population density and economic importance of the areas have been considered and were expressed as an important index. Using the hazard index, the risk for each area was calculated. In the analysis, the whole city was classified into four categories, the low risk area, the medium risk area, the high risk area and the severe flood risk area. Most Cities in developing countries especially in Africa have a large proportion of their population in informal settlements, which developed outside of the control of authorities charged with the regulation of land uses and building construction (Rakodi & Leduka, 2003). Officials formally charged with land delivery for housing have largely failed to meet the needs of the people. Thus the disadvantaged and the poor have little or no access to land for housing. In Lusaka, Zambia, attempts are made to allocate free land to people in or adjacent to the regularized informal settlements, but this requires good political or official connections which are beyond the reach of the poor (Mwange, 2006). It is hard therefore to stop people from building houses where they see vacant land. Since rain in Zambia is seasonal, many marshy areas are built on during dry periods only to be flooded when the rains come, displacing mostly the poor who build in such areas (Chooma, 2006).

In considering some specific effects of flood, it is observed that in the autumn of 2000 in the United Kingdom 16,000 residential properties were affected by flood, some more than once. In 2003, about 1,200 properties were flooded in Central and Southern England (Bada, 1997). In Nigeria, the flood disaster of 1980 in the city of Ibadan rendered 50,000 people homeless and property worth millions of naira were destroyed. In 1988 over 40,000 people were rendered homeless in Kano state and another 2,000 people displaced in Dekina, Kogi State. In Nassarawa state, 1,000 people were rendered homeless in floods that ravaged Pategi, Kpada and Gbogdondogi Local Government Areas in May 1997 (UNDP, 2005).

Ologunorisa (2004) undertook a flood-risk assessment of the Niger-Delta region of Nigeria using a combination of hydrological techniques considering some measurable physical characteristics of flooding and socio-economic techniques of vulnerability. Some of the physical characteristics of flooding selected and measured include depth of flooding (metres), duration of flood (hours/ weeks), perceived frequency of flood occurrence, and relief or elevation (metres) while the vulnerability factors selected and measured include proximity to hazard source, land use or dominant economic activity and adequacy of flood alleviation schemes and perceived extent of flood damage. He derived rating scale for the nine parameters selected, and 18 settlements randomly selected across the three ecological zones in the region were rated on the basis of the parameters. Three flood risk zones emerged from the analysis. These are the severe flood risk, moderate flood risk, and low flood risk zones. This methodology could be adopted in this study based on its validity and clarity.

Similarly, Oriola (2000) carried out flood studies in Abeokuta, Ogun state through a careful observation method. He observed that various socio-cultural activities have promoted flooding in many Nigerian urban environments. These activities are characterized by stream or river channel encroachment and abuse, increased paved surfaces and poor solid waste disposal techniques due to high level of illiteracy, a low degree of community awareness, poor environmental education, ineffective town planning laws, and poor environmental management. He argued that government, at various levels needs to address these issues.

Oriola (2000) concluded that flood risk in Abeokuta urban environment was a function of the following factors: land use pattern, refuse disposal habits, the nature of the surroundings, distance of buildings from the course of streams, the relief or terrain, slope, gradient, and rainfall amount and duration. The rainfall amount and duration

can also be carefully observed in Calabar. For instance, the State Emergency Management Agency reported that on July 23, 2011, rainfall lasting 5 hours resulted in serious flooding of some parts of Calabar city.

Durotoye (2009), through observation methods highlighted the increasing tendency of human occupation of potential hazards area in the Niger-Delta region. She observed that the physical condition and natural processes prevailing in the Niger-Delta environment that impinges on the people living there are numerous such as flooding, marine incursion, coastal recession, and subsistence. This research will rely on some of these techniques applied in other areas for the study of flood risk in Calabar.

4. Method of Study

The research adopted survey and regression approaches. The survey approach involved the metric measurement of the magnitude of flood by taking linear measurements across the areas covered by the hazard in the affected residential neighbourhoods. The vulnerability of residential neighbourhoods was determined through assessment of the numerical value of the affected residential buildings and other structures in November, 2013. Through the regression approach the relationship between the magnitude of flood and the vulnerability of residential neighbourhoods was measured. The variation of flood risk was also determined using the simple linear regression analysis.

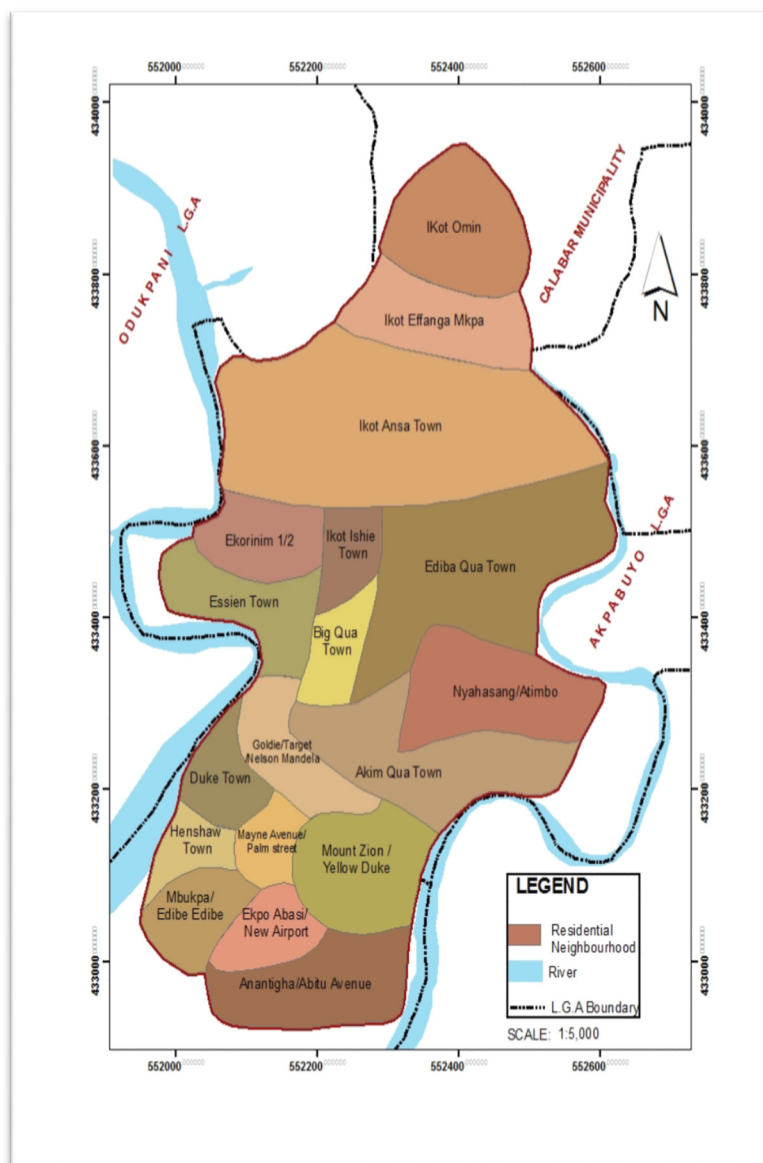


Figure 2. Map of Calabar showing the 18 residential neighbourhoods

Table 1. Some selected residential neighbourhoods in calabar metropolis

S/N	NEIGHBOURHOOD NAME	LOCATION
1.	IkotAnsa Town	Calabar Municipal
2.	IkotIshie Town	Calabar Municipal
3.	Ediba Qua Town	Calabar Municipal
4.	Big Qua Town	Calabar Municipal
5.	Nyahasang/Atimbo	Calabar Municipal
6.	Akim Qua Town	Calabar Municipal
7.	Mount Zion, Yellow Duke	Calabar South
8.	Goldie, Target/Nelson Mandela	Calabar South
9.	Mayne Avenue, Palm Street	Calabar South
10.	EkpoAbasi/New Airport Road	Calabar South
11.	Anantigha /Abitu Avenue	Calabar South

Source: Researchers Field Survey, (2013).

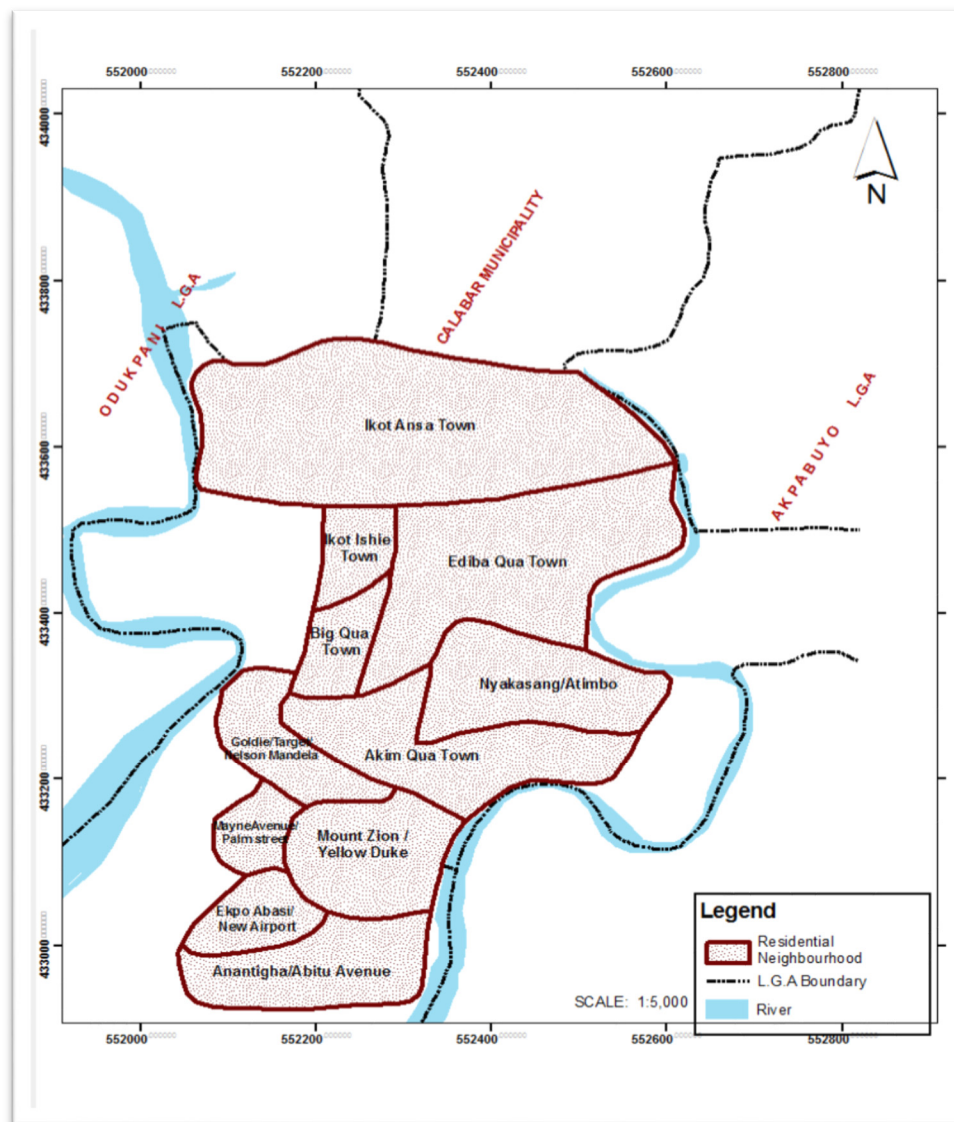


Figure 3. Map of Calabar showing 11 selected residential neighbourhoods under study

Furthermore, the survey in general was a cross sectional one in that it took place in 2013 and longitudinal survey which was very useful for comparison of flood risk assessment over a period of time spanning from 2009 to 2013. This research covered the residential neighbourhoods in Calabar Metropolis. These residential neighbourhoods were delineated based on shared drainage channels. They include, IkotOmin, IkotEfanga, IkotAnsa, IkotIshie, Ekorinim 1 and 2, EssienTown, Ediba qua town, Big qua town, Nyahasang/Atimbo, Akimqu town, all in Calabar Municipality. Others include, Mount Zion/Yellow Duke, Goldie, Target/Nelson Mandela, Mayne Avenue/Anantigha, Mbukpa/Edibedibe, Henshaw Town and Duke Tow in Calabar South Local Government area (see Figure 2).

Floods do not occur evenly in all the residential neighbourhoods listed above. Flood phenomena are found in sections of the Metropolitan area that are mentioned in Table 1 below. These residential neighbourhoods were carefully selected based on the fact the flood phenomenon is frequently experienced by residents of the areas. These selected residential neighbourhoods make up 61 percent of the total number of neighbourhoods mentioned above (see Figure 3).

4.1 Sampling Technique

The stratified sampling technique was adopted for the study. Each neighbourhood was taken as a stratum. In each residential neighbourhood, there are places of flood occurrences or vulnerable to flood. These places also have elements that are at risk to flood including buildings, human beings and physical features.

The magnitude of flood could also be observed in each residential neighbourhood that was selected in Table 1 above. Since there may be more than one point of flood in each area, the points or streets of flood were selected randomly in each neighbourhood.

5. Presentation of Data

The data from the field survey is hereunder presented in a tabular form. This information is therefore used for the analysis of data using descriptive statistics of percentages which was used in achieving the set objectives of this study.

Table 2. Magnitude of flood in residential neighbourhood streets

S/N	NEIGHBOURHOOD NAME	LINEAR MEASUREMENT ACROSS PRONE AREAS (METERS)	PERCENTAGE
1	IkotAnsa Town	578	5.57
2	IkotIshie Town	599	9.92
3	Ediba Qua Town	345	5.71
4	Big Qua Town	174	2.88
5	Nyahasang/Atimbo	397	6.58
6	Akim Qua Town	403	6.67
7	Mount Zion/Yellow Duke	772	12.79
8	Goldie, Target/Nelson Mandela	997	16.51
9	Mayne Avenue/Palm Street	368	6.09
10	EkpoAbasi/New Airport	835	13.83
11	Anantigha/Abitu Avenue	570	9.44
	TOTAL	6,038	100

Source: researchers field survey, 2013.

Goldie, Target/Nelson Mandela residential neighbourhood has the largest area affected by flood with 997 (16.51 percent) followed by Ekpo Abasi/New Airport residential neighbourhood with 835 (13.83 percent) while the least was found to be Big Qua Town residential neighbourhood with 174 (2.88percent) as illustrated in Table 2 above. However, the flood coverage was measured as a straight line along the residential streets prone to flood in meters. This measurement was drawn from the drainage channels of each neighbourhood street.

Table 3. Vulnerability of residential neighbourhood buildings

S/N	NEIGHBOURHOOD NAME	NUMBER OF BUILDINGS VULNERABLE TO FLOOD	PERCENTAGE
1	IkotAnsa Town	161	12.02
2	IkotIshie Town	99	7.39
3	Ediba Qua Town	26	1.94
4	Big Qua Town	24	1.79
5	Nyahasang/Atimbo	142	10.60
6	Akim Qua Town	60	4.48
7	Mount Zion/Yellow Duke	188	14.04
8	Goldie, Target/Nelson Mandela	250	18.67
9	Mayne Avenue/Palm Street	98	7.32
10	EkpoAbasi/New Airport	118	8.82
11	Anantigha/Abitu Avenue	173	12.92
	TOTAL	1,339	100

Source: researchers field survey, 2013.

As indicated in table 3 above, Goldie/Target/Nelson Mandela residential neighbourhood was found to have the highest number of buildings (250 or 18.67 percent) affected by flood surge, followed by Mount Zion/Yellow Duke with 188 (14.04 percent) buildings. The least was found to be Big Qua Town residential neighbourhood with 24 (1.79 percent) buildings. Vulnerability to flood was determined by counting the residential buildings possessing the marks of flood surge in each residential neighbourhood street as illustrated in the Table 3 above.

Table 4. Average height of residential neighbourhoods derived from contour crenulations

S/N	NEIGHBOURHOOD NAME	AVERAGE HEIGHT IN METERS	PERCENTAGE
1	IkotAnsa Town	8.0	12.68
2	IkotIshie Town	6.2	9.83
3	Ediba Qua Town	10.0	15.85
4	Big Qua Town	5.8	9.19
5	Nyahasang/Atimbo	5.6	8.87
6	Akim Qua Town	10.0	15.85
7	Mount Zion/Yellow Duke	3.1	4.91
8	Goldie, Target/Nelson Mandela	2.6	4.12
9	Mayne Avenue/Palm Street	4.9	7.77
10	EkpoAbasi/New Airport	3.9	6.18
11	Anantigha/Abitu Avenue	3.0	4.75
	TOTAL	63.1	100

Source: researchers field survey, 2013.

The Table 4 above shows the average height (in meters) above sea level of residential neighbourhoods under study. The average height was obtained by finding the averages of all the heights in each residential neighbourhood from contour crenulations. The highest average height was found in IkotAnsa Town and Akim Qua Town residential neighbourhoods with 10.0 metres (15.85percent) each and the least being Goldie/Target/Nelson Mandela residential neighbourhood with 2.6 (4.12percent)metres. Flooding is found to be common among these neighbourhoods with a low-lying terrain.

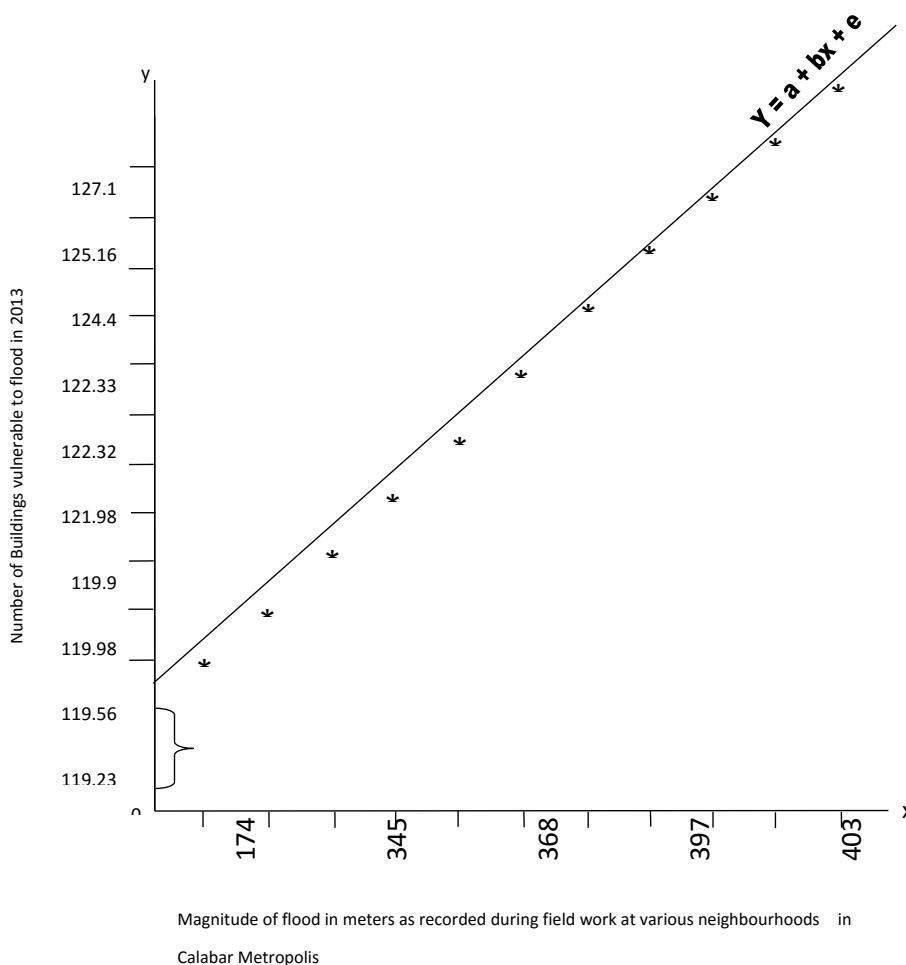


Figure 4. SCATTERGRAM OF RESIDENTIAL BUILDINGS VULNERABLE TO FLOOD IN CALABAR METROPOLIS

Calculated coefficient of regression = 115.14. t-value at 0.05 significance level and degree of freedom of 10 = 1.81
 SOURCE: RESEARCHERS FIELD SURVEY, 2013.

Table 5. Magnitude of flood and vulnerability of residential buildings

S/N	NEIGHBOURHOOD NAME	MAGNITUDE OF FLOOD (X)	VULNERABILITY OF RESIDENTIAL BUILDINGS (Y)
1	IkotAnsa Town	578	161
2	IkotIshie Town	599	99
3	Ediba Qua Town	345	26
4	Big Qua Town	174	24
5	Nyahasang/Atimbo	397	1142
6	Akim Qua Town	403	60
7	Mount Zion/Yellow Duke	772	188
8	Goldie, Target/Nelson Mandela	997	250
9	Mayne Avenue/Palm Street	368	98
10	EkpoAbasi/New Airport	835	118
11	Anantigha/Abitu Avenue	570	173
	TOTAL	6,038	1,339

Source: Researchers Field Survey, 2013.

The Table 5 above was used in testing the hypothesis, (there is a significant relationship between the magnitude of flood and the vulnerability of residential buildings). The magnitude of flood is represented by 'x' (the independent variable) used in predicting the vulnerability of residential buildings 'y' (dependent variable). Using the regression equation, the result showed that at 0.05% significance and degree of freedom of 10 the t. value was less than the regression coefficient and the scatter gram of residential buildings, figure 4, illustrates the results. This led to the rejection of the null hypothesis and acceptance of the alternative hypothesis that: there is a significant relationship between the magnitude of flood and the vulnerability of residential neighbourhoods.

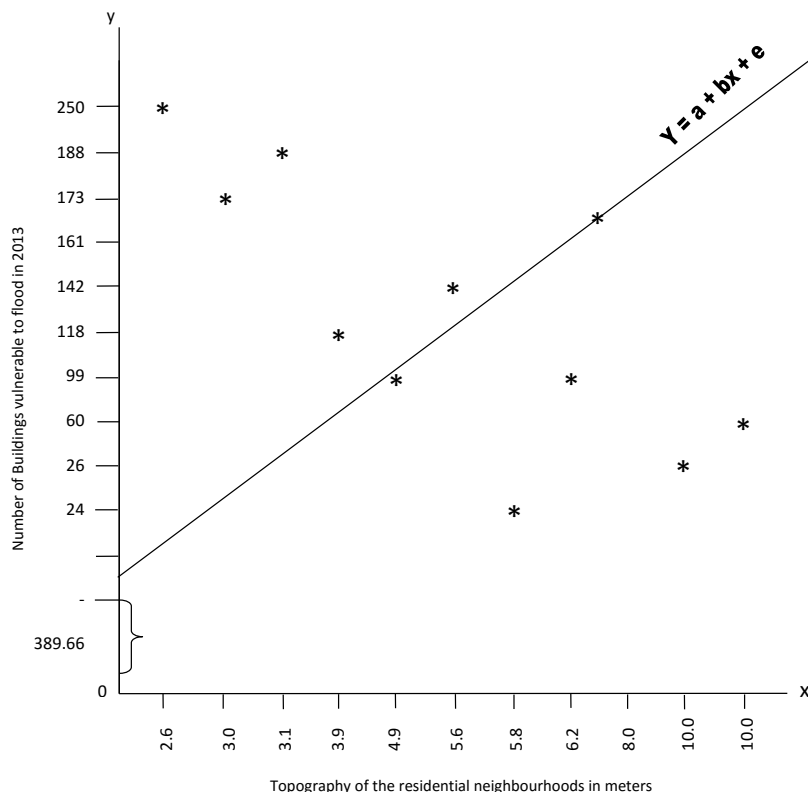


Figure 5. Scattergram of residential buildings and topography in calabar metropolis

Calculated coefficient of regression = 389.66. t-value at 0.025 significance level and degree of freedom of 10 = 2.23

SOURCE: RESEARCHERS FIELD SURVEY, 2013

Table 6. Neighbourhoods (topography) and vulnerability of residential buildings

S/N	NEIGHBOURHOOD NAME	AVERAGE HEIGHT IN METERS (X)	VULNERABILITY OF RESIDENTIAL BUILDINGS (Y)
1	IkotAnsa Town	8.0	161
2	IkotIshie Town	6.2	99
3	Ediba Qua Town	10.0	26
4	Big Qua Town	5.8	24
5	Nyahasang/Atimbo	5.6	142
6	Akim Qua Town	10.0	60
7	Mount Zion/Yellow Duke	3.1	188
8	Goldie, Target/Nelson Mandela	2.6	250
9	Mayne Avenue/Palm Street	4.9	98
10	EkpoAbasi/New Airport	3.9	118
11	Anantigha/Abitu Avenue	3.0	173
	TOTAL	63.1	1,339

Source: Researchers Field Survey, 2013.

Table 6 above was used in testing hypothesis 2 (The elements at risk to flooding in residential neighbourhoods in Calabar vary significantly according to the topography of the area.). The topography of the area (average height) is represented by 'x' (independent variable) and the vulnerability of residential buildings is represented by 'y' (dependent variable). Using regression equation and as illustrated in Figure 5 to draw the line of 'best fit', the result showed that at 0.025% significance and degree of freedom of 10, the regression coefficient was greater than the T. value and the scatter gram of residential buildings also determined the line of "best fit". This result has also rejected the null hypothesis and accepted the alternative hypothesis that: the elements-at-risk to flood in residential neighbourhoods in Calabar vary significantly according to the topography of the area.

6. Results/Findings

Findings show a significant relationship between the magnitude of flood and vulnerability of residential buildings and the elements-at-risk vary significantly according to the location and topography of the area. However, the results were in support of the reviewed literature as vulnerability is explained in terms of exposure to hazardous events and how it affects people and structures. It has also been reviewed in the literature that rapid urbanization, population increase and waste disposal habit have also inundated the magnitude of flood. Human activities such as transportation, industrial development and pavements have contributed to change in climate resulting to increase in rainfall pattern which brings about flooding affecting residential buildings and other physical features.

Findings also show that the magnitude of flood is responsible for the vulnerability of residential buildings because the larger the magnitude of flood the more residential buildings would be affected by the hazard. The topography of residential neighbourhoods expressed by the average height (in meters) also contributes to vulnerability of buildings and other physical features. This was found in Table 6 that the lowest topography (average height in meters) of 2.6 (4.12percent) has the highest number, 250 (18.67percent) of buildings vulnerable to flood and the highest average height of 10.0 meters has 26 buildings vulnerable to flood. This has resulted to variation in the elements-at-risk to flood depending on the topography of the area.

Tables 2, 3, and 4 were used in estimating residential areas of high flood risk, medium flood risk and low flood risk zones. For example, Table 2 shows the highest to be 835 (13.83percent) to 997 (16.51percent) flood diameter, Table 3 shows 118 (8.82percent) to 250 (18.67percent) buildings, and Table 4 shows 2.6 (4.12percent) to 3.1 (4.91percent) average heights. However, six residential neighbourhoods were estimated at high flood risk zone. These are Goldie/ Target / Nelson Mandela; Mount Zion / Yellow Duke; Anantigha / Abitu Avenue; EkpoAbasi / New Airport; IkotAnsa and Nyahasang / Atimbo residential neighbourhoods. The estimated medium flood risk zone has three residential neighbourhoods such as Mayne Avenue / Palm Street; Ikot Ishie and Akim Qua Town.

The estimated low flood risk zone has two residential neighbourhoods which include Ediba Qua Town and BigQuaTown.

7. Recommendations

The study recommends some regulatory approaches to reduce vulnerability; these are:

- Flood plain zoning: Laws can be passed that restrict construction of buildings and habitation of flood plains of Calabar. Instead flood plains can be zoned for urban agriculture, landscaping and recreational uses.
- Flood plain building codes: Structures that are allowed within the Flood plains of Calabar could be restricted to those that can withstand the high velocity of flood waters and are high enough off the ground to reduce risk of contact with water.
- Mortgage limitations: Lending institutions could refuse to give loans to buy or construct buildings (structures) or businesses in flood- prone areas of Calabar.

The study further recommends a proper channelization of Calabar urban drainage system, stringent flood control legislation, and development control measures should be enforced so as to discourage people from building on or near flood-prone areas of Calabar especially the estimated areas of high flood risk zones. Developers, who have to build their houses near or on flood prone areas, must present their building plans to the Ministry of Lands and Town Planning for scrutiny before building approval is granted.

There is need for adequate planning and improvement of flood prediction techniques. Planning and efficient management of the physical environment is the best way for tackling flood problems. The act of flood planning requires a team-work. This makes it mandatory for the involvement of relevant experts in specific planning projects. In the preparation of plans for coastal settlements and flood-prone areas or regions, Meteorologists and Oceanographers should be included in the planning team.

A comprehensive study of flooded settlements to determine their level of vulnerability to flood disasters should be undertaken. Residential neighbourhoods with high level of vulnerability should be relocated to inland locations that are sufficiently safe. The Nigerian Institute of Town Planners should focus on 'climate change and flood planning' in one of its Mandatory Continuing Professional Development Programmes (MCPDP) held annually in Nigeria. This would afford the practicing Town Planners opportunities to have good knowledge of flood risk planning and management.

There is high confidence that adaptation can reduce vulnerability, especially in the short term. However, adaptive capacity is intimately connected to social and economic development, but it is not evenly distributed across and within societies. There is always a distinction between the two types of adaptation measures namely: autonomous adaptation and planned adaptation.

- Autonomous adaptation action are responses that will be implemented by individuals and organizations in fighting flood disasters without any intervention or coordination by regional or state and national governments and international agreements. This is recommended for the residential neighbourhoods estimated at high flood risk zones.
- Planned adaptations are the result of deliberate policy decision that specifically take flood disaster into account. Planned adaptations, therefore, includes changes in policies, institutions and dedicated infrastructure would be needed to facilitate and maximize long-term benefits of adaptation response to flooding with the situation at hand in Calabar Metropolis within the delineated residential neighbourhoods. Planned adaptation solutions and policy coordination across multiple institutions may be necessary to facilitate adaptation to flood damage.

Finally, the following planned adaptation options would be effective for flood risk control in Calabar Metropolis.

- Environmental policy reforms, changes in urban and housing designs, removal of laws that can inadvertently increase flood vulnerability.
- Appropriate infrastructure investments:- Build-up of unblocked drainage patterns, flood defenses, increasing investments, improved health care through flood shelters and assistance shelters as part of community emergency preparedness programmes.
- Changes in water and land-use management polices:- Devising tenure markets, appropriate town planning and encouraging building of water sinking mechanisms.
- Development of flood controls and monitoring:- Capacity building for research and training to enable adaptation. Capacity building to integrate climate change and its impacts into urban development planning involving local communities, raising public awareness and education on flooding and its impacts on residential neighbourhoods of Calabar Metropolis.

8. Conclusion

The study examined the vulnerability of some residential neighbourhoods in Calabar to the menace of flooding and determined residential areas of low, medium and high flood risk zones. The significant results obtained from the regression coefficient of the least square method and the scatter gram was that the magnitude of flood predicted the vulnerability of residential buildings and other physical elements. Also the topography of the area determined the level of vulnerability of physical elements to flood.

However, through metric measurement of the diameter of flood surge to determine the magnitude of flood and counting of residential buildings affected by flood in each residential neighborhood, the study found that: the larger the diameter of flood surge the more physical elements including residential buildings are affected and the lower the topography of the area the higher the estimated level of risk of flooding in that particular area.

To stem the vulnerability of residential areas, it is imperative that a proper channelization of Calabar urban drainage system, stringent flood control legislation and development control measures be enforced so as to discourage people from building on or near flood-prone areas of Calabar especially areas of high flood risk zones.

References

- Abua, M. A., & Eze, B. E. (2002). *Environmental Hydrology*. Calabar, Ushie Printers and publishing Co. ltd.
- Bada, T. J. (1997). *The June 24th 1995 flood in Ondo, its Antecedent and Incident*. Research Publications in Geography. Ronal Press, New York.
- Chooma, B. (2006). *Surface Water Drainage in Urban Areas: The Poor Die Young* (pp. 158-168). London, Earthscan Publications.

- Cong, C., Collins, E., & Simpson, L. (2008). *The Impact of Climate Change on Insuring Flood Risk*. Institute of Actuaries of Australia, New Zealand.
- Ebong, M. O. (1983). *The Perception of Residential Quality*. Third World Planning Review.
- Few, R. M., Ahen, F., Matthies, M., & Kovats, S. (2006). *Linking Climate Change Adaptation and Disaster Management for Sustainable Poverty Reduction. Synthesis Report for Vulnerability and Adaption Resource Group (VARG)*. Retrieved from www.ec.europa.eu/development/icenter/envecvarg/adaptation_en.pdf.
- Georgakos, K. P., Guctter, A. K., & Sperflage, J. A. (1997). *Estimation of Flash Flood Potential for Long Areas* (pp. 87-100). IAHS Publication No. 239.
- Hogue, M. M., Abdullah, A., & Khan, M. S. (1997). *Storm Surge Flooding in Chittagong City and Associated Risk* (pp. 115-122). IAHS publication No. 239.
- Intergovernmental Panel on Climate Change (IPCC). (2008). *Climate Change Impact, Adaptation and Vulnerability*. Third Assessment Report.
- International Federation of Red Cross and Red Crescent Societies (IFRS). (2003). *Towards Integrated Approaches to Increase Resilience and Robustness for the Prevention and Mitigation of Flood Risk in Urban Areas*.
- Kates, R. W., & Kasperson, J. X. (1983). Comparative Risk Analysis of Technological Hazards: *Proceedings of National Academy of Science*, 80, 7027-7038.
- Mwange, T. (2006). *Kalikiliki Dam Floods: Report to the Technical Unit*. Ministry of Energy and Water Affairs, Government of the Republic of Zambia, Lusaka.
- Obongha, U. E. (2013). *Flood Assessment of Residential Neighbourhoods in Calabar Metropolis*. An unpublished undergraduate Research Project.
- Offiong, R. A. (2004). *Floral Biodiversity of the Kwafalls River Valley: A Case Study of Akamkpa L.G.A.* (unpublished Msc. Thesis). University of Calabar, Calabar.
- Ologunorisa, E. T. (2012). Climate Change Impact, Vulnerability and Adaptation in Nigeria. *Paper presented at the Mandatory Continuing Professional Development Programme (MCPDP)* Uyo April 18-19, 2012.
- Ologunorisa, E. T. (2004). An Assessment of Flood Vulnerability Zones in the Niger Delta, Nigeria. *International Journal of Environmental Studies*, 61(1), 309.
- Ologunorisa, E. T. (2006). Flood Management and Control in Nigeria. *Research Review*, 27(6), 102-203.
- Oyesiku, O. K. (2009). City Liveability: Implications and challenges, Planning for liveable Human Settlements. *Proceedings of NITP and CAP of West African Workshop Settlement held in Lagos Nigeria*, 3 & 4, 61-107
- Plate, E. J. (2002). Flood Risk and Flood Management. *Journal of Hydrology*, 267, 2-11.
- Rakodi, C., & Leduka, C. (2003). Informal land delivery processes and access to land for the Poor in six African Cities: Toward a conceptual framework. *Working paper I in the Informal land delivery processes in African cities series*. University of Birmingham, UK.
- SEMA. (2013). *Flood statistics*. Cross River State Emergency Management Agency
- Smith, D. (1996). *Environmental Hazard*. London, Routledge Publication.
- Udo, C. E. (1981). *A Morphometric Analysis of Gullies in Obatone Area of AkwaIbom State*. University of Ibadan.
- UNDP. (2005). *Baseline Report on Flooding and Erosion, Landslide in Anambra, Enugu, Lagos and Kogi states*.
- UNFCCC. (2008). *Climate Change, Impacts, Vulnerability and Adaptation in Developing Countries*. Retrieved from <http://www.wmoch/pages/prog/index.php>.
- United Nations Commission for Human Settlement (UNCHS). (1981). *Settlement Planning For Disasters*. Nairobi, World Meteorological Organization.

Copyrights

Copyright for this article is retained by the author(s) with first publication rights granted to the journal.

This is an open-access article distributed under the terms and conditions of the Creative Commons Attribution license (<http://creativecommons.org/licenses/by/3.0/>).

Valuing Urban Tropical River Recreation Attributes Using Choice Experiments

Luis Santiago¹, John Loomis², Alisa V. Ortiz¹ & Ariam L. Torres¹

¹ Graduate School of Planning, University of Puerto Rico, Río Piedras, Puerto Rico

² Agricultural and Resources Economics, Colorado State University, Fort Collins, Colorado

Correspondence: Luis Santiago, Graduate School of Planning, University of Puerto Rico, Río Piedras, Puerto Rico.
Tel: 787-764-0000 ext. 85113. E-mail: luis.santiago47@upr.edu

Received: April 26, 2016 Accepted: May 17, 2016 Online Published: May 24, 2016

doi:10.5539/enrr.v6n2p128

URL: <http://dx.doi.org/10.5539/enrr.v6n2p128>

Abstract

While providing public access to rivers in urban areas is a first step, maintaining a high quality recreation experience can be expensive. Knowing the economic benefits of high quality recreation may help recreation managers in justifying budget increases and define priorities during a time of scarce resources. To provide that information we have conducted urban river recreation valuation using Choice Experiments (CE). We value user defined recreation attribute improvements for the following: reducing the presence of trash, increasing water clarity, reducing crowds and increasing vegetation. We also tested whether pro-environmental attitudes and behaviors influence visitors' Willingness to Pay (WTP) for improvements in environmental attributes. Three of the four attribute improvements were statistically significant (marginal values are provided in parenthesis): reduction of trash (\$173), improving water clarity (\$52), and reducing crowding (\$28). The results can help managers justify improved trash removal and littering enforcement strategies, and advocate improvement of water quality by means of enacting and enforcing more strict regulations on littering, off-roading use, gravel pit discharges, and maximum visitation levels.

Keywords: Choice Experiment, environmental attribute valuation, watershed

1. Introduction and Background

Urban recreation areas are important to millions of people as the globe becomes increasingly urbanized. According to the United Nations (2015), 54% of the world's population resides in urban areas, and by 2050, this figure is expected to increase to 66%. The Americas are the most heavily urbanized in the World; 80% of the Latin American and Caribbean population is now considered urban. Puerto Rico's 2015 population density was estimated at 400 inhabitants per square kilometer, while the US mainland and Canada exhibited much lower densities; 40 and 4 inhabitants per square kilometer, respectively (The World Bank, 2015). Such rapid population growth had a direct impact on watershed resources. During the second half of the 20th century, Puerto Rico's coastal urban population grew rapidly, resulting in a reduction of forest cover along the island's coastal lowlands, and resulting in the degradation of groundwater and surface water resources (Barreto, 1997). Urban population growth was accompanied by less stringent enforcement of environmental laws compared to those of the U.S. mainland (Berman-Santana, 1996). Due to its urban character, the Manatí watershed is a location where ecosystem service degradation is evident. Its associated ecosystems have been impacted by coastal development, eutrophication, and debris disposal for decades but there have been minimal attempts to conduct formal attribute valuation studies that may help in the implementation of urban watershed management and conservation strategies.

There are two external conditions that make a recreation valuation exercise particularly relevant in Puerto Rico. A recent economic slowdown in Puerto Rico during the past five years has been so severe that it was accompanied by significant depopulation. Since economic growth and environmental protection are often seen as conflicting or competing goals, it is important to understand how residents value environmental attributes in the context of a prolonged economic downturn. Second, Puerto Rico experienced a prolonged drought during the year the study was conducted. An attribute valuation exercise of river recreation acquires more significance when water scarcity is apparent and real, not hypothetical. The former condition may diminish estimates, while the latter may have the opposite effect.

The focus of this paper will be to examine respondents' Willingness to Pay (WTP) for watershed environmental attributes as possible determinants in the context of an urban tropical watershed and a contracting economy. WTP is how economists measure economic values, and Choice Experiments are one of the standard techniques to measure it. Choice Experiments (CE) were developed from the marketing literature's conjoint analysis. The use of CE in environmental attribute valuation began in the 1990's, and its use has become prevalent (Adamowicz, Boxall, Williams, & Louviere, 1998; Boxall, Adamowicz, Swait, Williams, & Louviere, 1996). CE is a Stated Preference (SP) method designed to elicit economic responses to hypothetical scenarios that allow the estimation of preferences over attributes of environmental quality.

CE designs usually involve two or more side-by-side comparisons of several trip attribute bundles or program profiles. One of the trip attribute bundles or program profiles is generally the status quo with no added cost. To increase incentive compatibility, Carson and Grove (2007) recommend comparing only two trip profiles, one being the status quo baseline that is usually common to all of the comparisons. The overall study set of attribute bundles (including price) included in a study is usually built using an orthogonal and main effects design to keep the survey combinations manageable.

CE designs, with their several side-by-side, orthogonally designed trip profiles, can obtain a significant amount of information per respondent, particularly when respondents are asked to indicate both their best and worst alternative. This gain in statistical efficiency is accompanied by two costs: (a) a cognitive challenge that can lead to respondent fatigue, casting doubt on the quality of responses after several choice set exercises; and (b) an increased hypothetical nature of the exercise, i.e., some of the combinations presented to respondents may not match any of their previous recreation experiences.

2. Literature Review

Even though there are several examples of environmental attribute valuation in the literature, the use of Choice Experiments as a method is not as frequent. First, a brief review of studies that have summarized results of CE use in the assessment of natural or environmental resource attributes will be presented. Second, studies on the link between environmental attitudes and WTP for changes in environmental attributes will be briefly discussed.

Choice Experiments have been conducted to assess natural resource attributes in diverse contexts, many considering green areas in Europe. Some of the intervening variables included vegetation, presence of bodies of water, and presence of litter. Czajkowski, Bartczak, Giergiczy, Navrud and Zylicz (2014) found that respondents were willing to pay to reduce litter in a Polish forest, passively protect the most ecologically valuable forests, and provide more recreation and tourist infrastructure. Respondents' WTP was estimated at 6.21 Euro for a partial reduction of forest litter, and 9.14 Euro for a full reduction.

Carlsson, Frykblom and Liljenstolpe (2003) identified attributes that increased a citizen's perceived value of Swedish wetlands. In that study, surrounding vegetation was not a significant wetland attribute. Horne, Boxall and Adamowicz (2005) used CE's to assess visitors' preferences for forest management in Finland. Results showed that visitors had strong preferences for the preservation of species richness and scenic beauty. More recently, Dallimer et al. (2014) estimated WTP for the spread of plants in riparian green spaces in Sheffield, UK. WTP for a 10% increase in plant cover ranged from 0.70 British Pounds (BP) to 15.22 BP, and estimates for a 25% increase ranged from 0.37 BP to 8.09 BP. Although socio-economic attributes were not highlighted in several of the studies, Abildtrup, García, Olsen and Stenger (2013) found that a visitor's age and income has an impact on the marginal WTP associated with French forest attributes.

The literature on CE for environmental attribute improvement within the context of developing countries seems to be scarcer. Katuwal (2012) conducted a CE exercise aiming to seek natural resource attribute valuation estimates within the context of a developing country, Nepal. In that case, increases in vegetation did not register an increase in marginal WTP among participants. A CE exercise was also conducted in Costa Rica, a location more similar in climate, vegetation and economic structure to Puerto Rico, to estimate WTP for recreation attributes at forest recreation sites. One of the selected attributes was an increase in ornamental plantings at natural pool sites, which was positive and significant, with an estimated marginal WTP of \$2.81 USD to be added to current entrance fees (Vega & Alpizar, 2011).

3. Methods

The first step in a CE design is to identify the key attributes of the recreation site quality that matters to visitors. An intercept survey was used to conduct in person interviews in three watershed sites. A variation of this sampling technique has been previously used in tropical watershed studies with an underlying social-ecological framework (Santiago, Verdejo Ortiz, Santiago-Bartolomei, Meléndez-Ackerman, & García Montiel, 2014). Conducting

interviews *in situ* allows us to ensure respondents are experiencing nature while being surveyed on recreation attribute preferences.

Three one-kilometer circles defined survey sites along upstream, midstream and downstream locations (see Figure 1). Upstream survey efforts were concentrated in Toro Negro, a recreation area in the central mountainous region. It is mainly covered by forest and secondary vegetation, and includes several recreation and conservation areas where visitors can bathe in the river and enjoy picnics. Midstream, the second sampling site was the Juan A. Corretjer Linear Walkway, popular as a rest stop for people to enjoy the views, eat and exercise. The downstream survey site, the river basin outlet, is the location where the river meets the Atlantic Ocean. Alluvial and marine deposits rest over the northern limestone region where people enjoy fishing and surfing, among other recreational activities.



Figure 1. Survey Sites

Thus the first step was to identify which attributes were considered by recreationists when selecting watershed locations to visit in Puerto Rico. Forty (40) in-person interviews with open-ended questions were conducted in three Manatí watershed locations to identify attributes important to recreationists. The following were the four most frequently identified attributes: vegetation, trash, crowding, and water clarity. Pre-test results were used as input to design the CE questionnaire.

The CE design involved two side-by-side comparisons of three trip attribute bundles. Following Carson and Groves' (2007) recommendations for increasing incentive compatibility, just two trip profiles were compared, one being the status quo baseline that is usually common to all of the comparisons. The overall study set of attribute bundles (including price) included in the study was built using an orthogonal design to keep the survey combinations manageable.

The interviewer presented three subsequent trip attribute scenarios. The particular trip attribute profiles were selected randomly from twenty-four orthogonal trip attribute profiles. Each profile consisted of alternative levels of the four attributes (shown with pictures) and a pre-set bid amount. Given the orthogonal main effects design, rarely did the three combinations of trip attributes analyzed sequentially by the respondent match what was experienced the day of the interview.

The CE scenario asked the respondent to choose between two side-by-side trip attribute profiles. Thus in the CE treatment a total of eight pictures for each CE valuation choice task were shown at one time to the respondent. The baseline case was always the same in terms of the worst case level of attributes (as identified by pre-test respondents) with low vegetation, trash on the site, crowded conditions, and poor water clarity with an associated zero increase in travel cost. See Figure 2 for an example of a typical CE choice set. There were three choice sets sequentially shown to the respondent by the interviewer.









<i>Attribute</i>	<i>Base Condition</i>	<i>Condition A</i>
Vegetation		
Trash		
Crowding		
Water Clarity		
Additional Travel Cost to Visit with Condition A		\$ZZ more per trip
Would you spend the additional travel costs with these Conditions at the River?		YES NO

Figure 2. Example Choice Set for Choice Experiment

A total of 202 in person interviews were conducted during the months of June to August of 2015. Sampling was balanced by day of the week, i.e., weekdays, weekends and holidays. The on-site refusal rate for in person interviews was 5%, only 10 people out of the combined sample of 212 refused to participate. The number of interviews conducted at each site was decided according to observed visitation levels and usage during the pre-test stage. A total of 93 interviews (46% of the total) were conducted in the Toro Negro site, the most visited location for watershed recreation. The remaining two sites were not as frequently visited; 57 interviews (28%) were conducted in the JAC Lineal Walkway, and the remaining 52 (26%) at the River Outlet.

4. Hypothesis Tests

We tested whether recreation related attributes were significant factors in the valuation of a visitor's recreation experience. All data was analyzed by a logit model. The stylized version of the model is:

$$\ln\left(\frac{\text{Pr } Y}{\text{Pr}(1-Y)}\right) = B_0 + B_1(\$Bid) + B_2(\text{Vegetation}) + B_3(\text{Crowd}) + B_4(\text{Trash}) + B_5(\text{WaterClarity}) + \dots B_n X_n \quad (1)$$

where:

Y is the response to the bid amount (Yes or No).

β is the logistic regression coefficient.

\$Bid is the additional trip cost to visit the river with that scenario.

Vegetation is whether vegetation is dense or not.

Crowd is whether the river site is crowded or not.

Trash is whether trash is visible on the site or not.

Water Clarity is river water clarity, i.e., whether the water was clear or not.

Xn represents other covariates including respondent socio-demographic characteristics.

The following hypothesis test was conducted:

$$H_0: \beta_{\text{CE ATTRIBUTES}} = 0 \quad H_A: \beta_{\text{CE ATTRIBUTES}} \neq 0 \quad (2)$$

where β is the logistic regression attribute coefficient.

5. Results

A single bounded binary logistic regression model was used to estimate attribute improvement values. A full model was initially specified. The dependent variable was defined as the response to the bid amount, and the independent variables included the bid amount, river recreation attributes, and socioeconomic variables (age, gender, education and income).

The socio-demographic profile of respondents reveals a balanced sample in terms of gender, with 47% male and 53% female participants. Out of the 202 participants, nearly all respondents were residents of Puerto Rico (98%), as the sampled recreation areas attract mainly local visitors. The average respondent was 42 years old, with 2 years of college education, and an annual personal income of \$29,560. A full description of socio-demographic characteristics is provided in Table 1.

Table 1. Socio-Demographic Characteristics

	Average	Minimum Value	Maximum Value	Standard Deviation
AGE (years)	42	18	85	15
EDUCATION (years)	14	1	22	3
INCOME (US dollars)	\$29,557	\$2,500	\$75,000	\$21,981
	Women		Men	
GENDER	Count	Percentage	Count	Percentage
	107	53%	95	47%

Full regression models were run with the use of STATA statistical software. Results of the hypothesis tests are presented below (see Table 2). To conserve space and focus on the key results, we will focus on attribute coefficients in the following tables, but complete regression results are available from the lead author. Model reliability was examined by means of two key statistics, the McFadden's Pseudo-R² and the Hosmer and Lemeshow (HL) test. Our model's reported McFadden's R² was 0.27, a value that, according to guidelines

established by McFadden and Domencich (1975), falls within the range of what is considered a good fit. The reported HL chi-square value was 5.44, with a p-value of 0.71, which in logistic regression goodness of fit tests, indicates that there is no evidence the model provides a poor fit (Fagerland & Hosmer, 2012).

Table 2. Logistic Regression Results

	COEF	Standard Error	z	P(Z)	[95% Conf. Interval]		Odds Ratio
BID	-0.015	0.002	-5.95	0.000	-0.020	-0.010	0.985
VEGETATION	0.072	0.208	0.34	0.731	-0.336	0.479	1.074
CROWDING	0.407	0.208	1.96	0.050	-0.000	0.814	1.502
TRASH	2.540	0.225	11.28	0.000	2.010	2.981	12.678
WATER CLARITY	0.761	0.215	3.55	0.000	0.341	1.182	2.141
AGE	-0.007	0.007	-1.00	0.316	-0.019	0.006	0.993
EDUCATION	-0.052	0.041	-1.27	0.203	-0.131	0.028	0.950
INCOME	2.11e-06	5.37e-06	0.39	0.694	-8.41e-06	0.000	1.000
GENDER	-0.030	0.214	-0.14	0.887	-0.450	0.389	0.970

As expected, the bid amount is negative and statistically significant at the 1% level. This inverse relationship between the magnitude of the bid amount and the probability of the respondent choosing that alternative demonstrates internal validity of the application here. Specifically, this result conforms to the law of demand in which the higher the price, the less likely the product will be purchased. We measured the value attributed by respondents to an improvement in four attributes: reduction in trash, improved water clarity, reduced crowding, and increased vegetation. Results show that a reduction in trash and increased water clarity were statistically significant at the 1% level, while a reduction in crowding was significant at the 5% level. In all cases, the improved attribute condition exhibits the expected positive sign. The only statistically insignificant attribute is the reduction in vegetation at the recreation site. Socio-economic and demographic variables, specifically age, income, level of education and gender, were consistently not significant in regression results.

Table 3. Attribute Coefficients and Marginal Values

	COEF	P(Z)	MARGINAL VALUE
BID	-0.015	0.000	
VEGETATION	0.072	0.731	\$4.88
CROWDING	0.407	0.050	\$27.72
TRASH	2.540	0.000	\$172.95
WATER CLARITY	0.761	0.000	\$51.84

6. Discussion

Results for attribute statistical significance show that only one of the four watershed attributes tested, vegetation was not significant. The removal of trash and increased water clarity were both positive and significant at the 1% level. A decrease in crowding was also significant at the 5% level.

Even though it was frequently mentioned in the pre-test as one of the four most important attributes to river recreationists, the various model results consistently did show that an improvement in vegetation did not have a significant effect on the likelihood of obtaining a positive bid response. We believe enough vegetation may have been already present in the Base Condition, so visitors didn't value additional vegetation. This could also be due to the likelihood that people may want sun while swimming in the cold river water or sunbathing before and afterwards.

The estimation of the corresponding attribute marginal values allows us to understand which attribute improvements are most valued by respondents (see Table 3). Marginal values were calculated dividing the attribute coefficient by the absolute value of the bid coefficient. Trash removal was by far the most valued attribute improvement, with a marginal value of \$173. The second most valued attribute was an improvement in water clarity, with a lower marginal value of \$52. The last statistically significant attribute improvement was a reduction in the agglomeration of individuals at the recreation area. The marginal value was the lowest, estimated at \$28.

Loomis and Santiago (2013) conducted a similar Choice Experiment for a different but comparable context: beach recreation. The study was conducted in five beaches in Northeast Puerto Rico in 2010, with participation from 213 respondents. The four attributes selected by beach recreationists in a pre-test were wave height, water clarity, trash and crowding. Using a similar pre-test, river recreationists selected three of the same attributes as beach respondents: trash, crowding and water clarity. It is important to mention that in both cases, users did not select attributes from a list, but were responding to an open-ended question. Due to the differences in recreation venues, we expected to find more differences in attribute selection. The consistency in responses is evidence of the importance placed by recreationists to these particular recreation site attributes.

Comparing the significance of results in both studies, reductions of trash and water clarity were significant for both beach and river recreationists. The marginal value for water clarity improvement was nearly identical, \$51 for beach recreationists and \$52 for river recreationists. Marginal values for trash reduction differed significantly; it increased from \$98 for beachgoers to \$173 for river recreationists. Finally, crowding was not significant in the beach CE, but acquired significance in the river study, with a marginal value of \$28.

7. Conclusion

We found a consistent and statistically significant positive valuation for improvements in three of the four attributes tested: trash reduction, increased water clarity, and reduced crowding levels. Such data may inform government agencies and NGO's in proposing resource allocation strategies, either at the watershed level, or more specifically for a particular recreation site.

Trash collection efforts are not consistent in many recreation sites. The results of this study show that it should be a priority to provide adequate trash collection and enforce littering regulations at recreation sites. The Puerto Rico Department of Natural and Environmental Resources has the capacity to enforce littering regulations.

Water clarity is highly valued as well, so any efforts to improve water quality and reduce turbidity are also a priority to site users. Informal consultations with experts in the region have led us to identify two main sources of turbidity that can be regulated: the use of off-roading vehicles and gravel pit activity in the mid and upper watershed. In both instances, the Department of Natural and Environmental Resources has the capacity to regulate such activity. Resulting reductions in turbidity upstream will add value to recreational activities downstream.

Finally, reducing crowds during peak visitation periods is of value to users, so strategies to ensure maintaining an appropriate number of users while ensuring appropriate carrying capacities and sustainable practices at recreation sites should be considered. Some of these measures can include pricing strategies to control access and reduce crowding at existing recreation areas managed by the Puerto Rico Department of Natural and Environmental Resources.

Given the importance of photos to assess attribute improvements, more attention should be paid to determining whether photos are as accurate as possible in portraying attribute improvements. For instance, in future studies it may be important to make differences in vegetation between scenarios more apparent. We think that in retrospect we needed to show lower levels of vegetation in the base case scenario.

The consistency of results across Choice Experiment studies does indicate the usefulness of the method in estimating attribute valuation. Even though it was applied in different recreation contexts, result for both Puerto Rico beach and river sites show consistency. Three of the four main attributes were identical across studies (trash, water clarity and crowding), the same two attribute improvements were statistically significant in both studies (trash and water clarity), and out of those two attributes, the estimated marginal values for one (water clarity) were nearly identical. The method seems to produce robust results that may be of value to recreation site managers.

Urban recreation areas are important to thousands if not millions of people. Increasingly the world's populations are concentrated into urban areas and so the importance of managing the areas is substantial. The Choice Experiment method has the capability not only to value the recreation experience in monetary values but also inform the manager which attributes of the recreation experience are most valued. In this way managers can prioritize management strategies, allocating funding to those most important to visitors.

Acknowledgments

This is part of a NASA ROSES Interdisciplinary Research in Earth Sciences project (NASA Grant NNX14AJ23G) funded by the Ocean Biology and Biochemistry Program.

References

Abildtrup, J., Garcia, S., Olsen, S. B., & Stenger, A. (2013). Spatial Preference Heterogeneity in Forest Recreation. *Ecological Economics*, 92, 67-77. <http://dx.doi.org/10.1016/j.ecolecon.2013.01.001>

- Adamowicz, A., Boxall, P., Williams, M., & Louviere, J. (1998). Stated Preference Approaches for Measuring Passive Use Values: Choice Experiments and Contingent Valuation. *American Journal of Agricultural Economics*, 80(February 1998), 64-75. <http://dx.doi.org/10.2307/3180269>
- Barreto, M. (1997). *Shoreline changes at Puerto Rico*, 1-49 (Unpublished doctoral dissertation). University of Puerto Rico, Mayagüez.
- Berman-Santana, D. (1996). *Kicking off the bootstraps: environment, development, and community power in Puerto Rico*. University of Arizona Press.
- Boxall, P. C., Adamowicz, W. L., Swait, J., Williams, M., & Louviere, J. (1996). A Comparison of Stated Preference Methods for Environmental Valuation. *Ecological Economics*, 18(3), 243-253. [http://dx.doi.org/10.1016/0921-8009\(96\)00039-0](http://dx.doi.org/10.1016/0921-8009(96)00039-0)
- Carlsson, F., Frykblom, P., & Liljenstolpe, C. (2003). Valuing Wetland Attributes: An Application of Choice Experiments. *Ecological Economics*, 47(1), 95-103. <http://dx.doi.org/10.1016/j.ecolecon.2002.09.003>
- Carson, R. T., & Groves, T. (2007). Incentive and Informational Properties of preference questions. *Environmental and Resource Economics*, 37(1), 181-210. <http://dx.doi.org/10.1007/s10640-007-9124-5>
- Czajkowski, M., Bartczak, A., Giergiczny, M., Navrud, S., & Żylicz, T. (2014). Providing Preference-Based Support for Forest Ecosystem Service Management. *Forest Policy and Economics*, 39, 1-12. <http://dx.doi.org/10.1016/j.forpol.2013.11.002>
- Dallimer, M., Tinch, D., Hanley, N., Irvine, K. N., Rouquette, J. R., Warren, P. H., ... Armsworth, P. R. (2014). Quantifying Preferences for the Natural World Using Monetary and Nonmonetary Assessments of value. *Conservation Biology*, 28(2), 404-413. <http://dx.doi.org/10.1111/cobi.12215>
- Fagerland, M., & Hosmer, D. (2012). A generalized Hosmer-Lemeshow Goodness-of-Fit Test for Multinomial Logistic Regression Models. *The Stata Journal*, 12(3), 447-453. Retrieved from <http://www.stata-journal.com/article.html?article=st0269>
- Horne, P., Boxall, P. C., & Adamowicz, W. L. (2005). Multiple-Use Management of Forest Recreation Sites: A Spatially Explicit Choice Experiment. *Forest Ecology and Management*, 207(1), 189-199. <http://dx.doi.org/10.1016/j.foreco.2004.10.026>
- Katuwal, H. (2012). *Demand for water quality: Empirical evidence from a knowledge, attitude, behavior, and choice experiment survey about the Bagmati River in Kathmandu, Nepal* (Unpublished doctoral dissertation). The University of New Mexico, Albuquerque, New Mexico. Retrieved from <http://hdl.handle.net/1928/21046>
- Loomis, J., & Santiago, L. (2013). Economic Valuation of Beach Quality Improvements: Comparing Incremental Attribute Values Estimated from Two Stated Preference Valuation Methods. *Coastal Management*, 41(1), 75-86. <http://dx.doi.org/10.1080/08920753.2012.749754>
- McFadden, D., & Domencich, T. (1975). *Urban Travel Demand: A Behavioral Analysis*. New York, New York: North-Holland Publishing Company.
- Santiago, L. E., Verdejo Ortiz, J. C., Santiago-Bartolomei, R., Melendez-Ackerman, E. J., & Garcia-Montiel, D. C. (2014). Uneven Access and Underuse of Ecological Amenities in Urban Parks of the Río Piedras Watershed. *Ecology and Society*, 19(1), 26. <http://dx.doi.org/10.5751/ES-06180-190126>
- The World Bank, World Development Indicators. (2015). *Population Density (people per Sq. Km of Land Area)*. Retrieved from <http://data.worldbank.org/indicator/EN.POP.DNST>
- United Nations, Department of Economic and Social Affairs, Population Division. (2015). *World urbanization prospects: the 2014 revision, highlights (ST/ESA/SER.A/352)*. Retrieved from <http://esa.un.org/unpd/wup/Publications/Files/WUP2014-Report.pdf>
- Vega, D. C., & Alpizar, F. (2011). Choice Experiments in Environmental Impact Assessment: The Case of the Toro 3 Hydroelectric Project and the Recreo Verde Tourist Center in Costa Rica. *Impact Assessment and Project Appraisal*, 29(4), 252-262. <http://dx.doi.org/10.3152/146155111X12959673795804>

Copyrights

Copyright for this article is retained by the author(s) with first publication rights granted to the journal.

This is an open-access article distributed under the terms and conditions of the Creative Commons Attribution license (<http://creativecommons.org/licenses/by/3.0/>).

Modeling the Geographic Distribution of *Prosopis africana* (G. and Perr.) Taub. in Niger

Laouali Abdou¹, Abdoulaye Diouf², Maman Maârouhi Inoussa³, Boubacar Moussa Mamoudou¹,
Salamatou Abdourahamane Illiassou¹ & Ali Mahamane^{1,3}

¹ Université de Diffa, Faculté des Sciences Agronomiques, BP 78, Diffa, Niger

² Université de Maradi, Faculté d'Agronomie et des Sciences de l'environnement, Département des sciences du sol et de télédétection, BP 465, Maradi, Niger

³ Université Abdou Moumouni, Faculté des Sciences et Techniques, Département de Biologie, Laboratoire Garba Mounkaila, BP 10662, Niamey, Niger

Correspondence: Laouali Abdou, Université de Diffa, Faculté des Sciences Agronomiques, BP 78, Diffa, Niger.
E-mail: abdoulaouali2000@yahoo.fr

Received: December 19, 2015 Accepted: April 14, 2016 Online Published: May 30, 2016

doi:10.5539/enrr.v6n2p136

URL: <http://dx.doi.org/10.5539/enrr.v6n2p136>

Abstract

Prosopis africana is a species of great socio-economic importance, threatened with extinction from its natural habitat in Niger due to overexploitation. The main objective of this study is to determine the potential geographic distribution of *P. africana* in Niger. Climatic and botanical data has been collected and used to model the distribution, on the basis of principle of maximum entropy (MAXENT) using MAXENT 3.3.3k, DIVA-GIS 7.5, and ArcGIS 10.0. programs. Rainfall and temperature are the most significant variables in the distribution of *P. africana* in Niger. Thus the southern band of the country (from the sudanian zone to the sahelio-soudanian zone), the wettest, is the area conducive to the development of *P. africana* (128,692.32 km² in total, 10.16% of the territory). Given the extent of this area revealed by this study, a reforestation policy implementation of *P. africana* would allow to restore its stands in Niger.

Keywords: *Prosopis africana*, Geographic distribution, Modeling, habitat, MAXENT, Niger

1. Introduction

In the third world countries, wood plants figure prominently in the socio-economic life of the people, given the many products and services (wood, food and Pharmacoepia) that they provide (Matthias, Henri, & Félix, 2000; Larwanou, Oumarou, Laura, Dan Guimbo, & Eyog-Matig, 2010; Chidumayo, Okali, Kowero, & Larwanou, 2011; Priso, Nnanga, Etame, Din, & Amougou, 2011; Laouali, Dan Guimbo, Larwanou, Inoussa, & Mahamane, 2014). They are thus subject to overexploitation and a threat of disappearance of their natural habitats, due to high population growth and climatic conditions increasingly unfavorable to their development (Ozer, Hountondji, Niang, Karimoune, Laminou, & Salmon, 2010). Indeed, the natural range of the species is influenced, among others, by climatic variables such as precipitation, temperature and wind speed (Intergovernmental Panel on Climate Change [IPCC], 2007; Chidumayo et al., 2011). However, it should be noted that according to the quality of products supplied, woody species do not have the same importance and therefore do not have the same degree of exploitation.

In West Africa, *Prosopis africana* is distinguished from other woody plants by the exploitation and use of all its organs (leaves, bark, root ...) by the rural population. For example, its wood, very resistant, is used as building materials (sheds, attics, ...) and in the manufacture of household utensils (mortar, pestle, ...) and charcoal, judged good by blacksmiths (Agboola, 2004; Akaaimo & Raji, 2006; Laouali et al., 2014). The leaves, roots and mostly the bark are usually used in traditional pharmacopoeia. The leaves and the pods pulps are also used as fodder and the seeds in food (Larwanou, 1994; Arbonnier, 2000; Agboola, 2004; Akaaimo and Raji, 2006; Larwanou, Moustapha, Rabé & Dan Guimbo, 2012; Laouali et al., 2014).

Characterized by a low capacity of natural regeneration (Ahoton, Adjakpa, M'po Ifonti & Akpo, 2009; Niang-Diop, Sambou & Lykke, 2010; Laouali, Dan Guimbo, Youchaou, Rabiou & Mahamane, 2015a) and a low fruit production (Laouali, Dan Guimbo, Chaibou & Mahamane, 2015b), *P. africana* is represented in Niger by

generally isolated individuals whose spatial distribution across the territory remains unknown. But a good knowledge of the spatial distribution and the habitat of species helps to develop effective strategies for biodiversity planning and conservation (Scheldeman & Van Zonneveld, 2010), forecasting the effects of environmental change and zonation of plant diversity (Schmidt, König, & Müller, 2008). Among the methods that allow knowing the distribution of species, there is modeling.

The modeling of species distribution is an expanding field of science with rapidly evolving new methods (Guisan & Thuillier, 2005). This approach has been adopted by several authors throughout the world to determine suitable habitats for species development (Araújo, Pearson, Thuiller, & Erhard, 2005; Phillips, Anderson & Schapired, 2006; Doko, Kooiman, & Toxopeus, 2008; Kumar & Stohlgren, 2009; Fandohan, Gouwakinnou, Fonton, Sinsin, & Liu, 2013; Gbesso, Tente, Gouwakinnou, & Sinsin, 2013). This study aims to determine the suitable habitats for the development of *P. africana* in Niger through modeling of its potential distribution to better protect it and prevent its disappearance.

2. Material and methods

2.1 Study AREA

This study covered the entire territory of Niger, 1,267,000 km² between 11° 37' and 23° 33' north latitude and between 0° 10' and 16° 00' east longitude. Niger is bounded on the north by Algeria and Libya, to the east by Chad, to the south by Nigeria and Benin, and to the West by Burkina Faso and Mali (Figure 1).

The climate is generally warm and dry but with a variability according to a north-south aridity gradient for distinguishing a saharan zone in the north (about 2/3 of the territory) with an average annual rainfall of less than 200 mm, a sahelian zone with an average annual rainfall between 200 and 600 mm and on the south a soudanian zone whose average annual rainfall exceeds 600 mm. The passage from one zone to another is marked by a climatic transition band which implies variability in the spatial distribution of vegetation. So, from north to south, the vegetation varies from steppe to dry woodland, through savanna and Combretaceae thickets.

During the year, the mean temperature varies from 9.9 to 32.63° C in the north, from 19.44 to 32.78° C in the southeast and from 25.84 to 33.57° C in the southwest of the country.

The main types of soils in Niger are:

- raw mineral soils in the north, the least watered area of the country;
- low developed soils in the south of Tenere, in the west and center of the country;
- sub-arid soils rich in organic matter, more watered than the previous, located from west to east in the central part of the country;
- soils with sesquioxides of iron, rich in swelling clay, located in the southern part of the country;
- vertisols especially in the east in the Lake Chad basin (Saadou, 1990).

About geomorphology, Niger has a fairly wide variety of landforms: structural forms marked by the lithological and tectonic data and climatic forms related to the erosion action.

2.2 Plant Material

The genus *Prosopis* is represented by 45 species of trees and shrubs native to North America, Central America, South America, Africa and Asia (Akaaimo & Raji, 2006). The unique tropical african species of the genus is *Prosopis africana*, native to the Sahel region of West Africa. Its natural distribution covers from Senegal to Ethiopia in the north, Guinea to Cameroon in the south and Uganda to Egypt in the East (Weber, Larwanou, Abasse, & Kalinganire, 2008).

The tree, with a height of 12-15 m, sometimes even 20 m, is characterized by a straight and cylindrical trunk, sometimes up to 110 cm in diameter, an open crown and drooping light green foliage (Arbonnier, 2000). Its root system is of the tap type (Weber et al., 2008).

2.3 Data Collection

2.3.1 Presence Points of the Species

A series of botanical surveys in different regions of Niger has enabled to establish a database on the occurrence of *P. africana* in Niger. Other databases such as that of the Garba Mounkaila laboratory of Abdou Moumouni University of Niamey, and GBIF (Global Biodiversity Information Facility) (www.gbif.org, accessed on 2/11/2014) and previous works (Weber et al., 2008; Larwanou et al., 2012) have been exploited. According to all these bases, the species occurs mainly in the sahelian and sudanian climatic zones with a higher concentration in

the south-central region of the country. So, 234 presence points of the species, of which 203 in Niger and 31 distributed among eastern Burkina Faso, northern Nigeria and northern Benin were selected for this study (Figure 1). The presence points of the species have been extended beyond Niger administrative borders to improve the accuracy of the model. According to several authors (Fitzpatrick & Hargrove, 2009; Scheldeman & Van Zonneveld, 2010), it is recommended to use an area that covers to the fullest the natural distribution area of the species under the same climatic conditions.

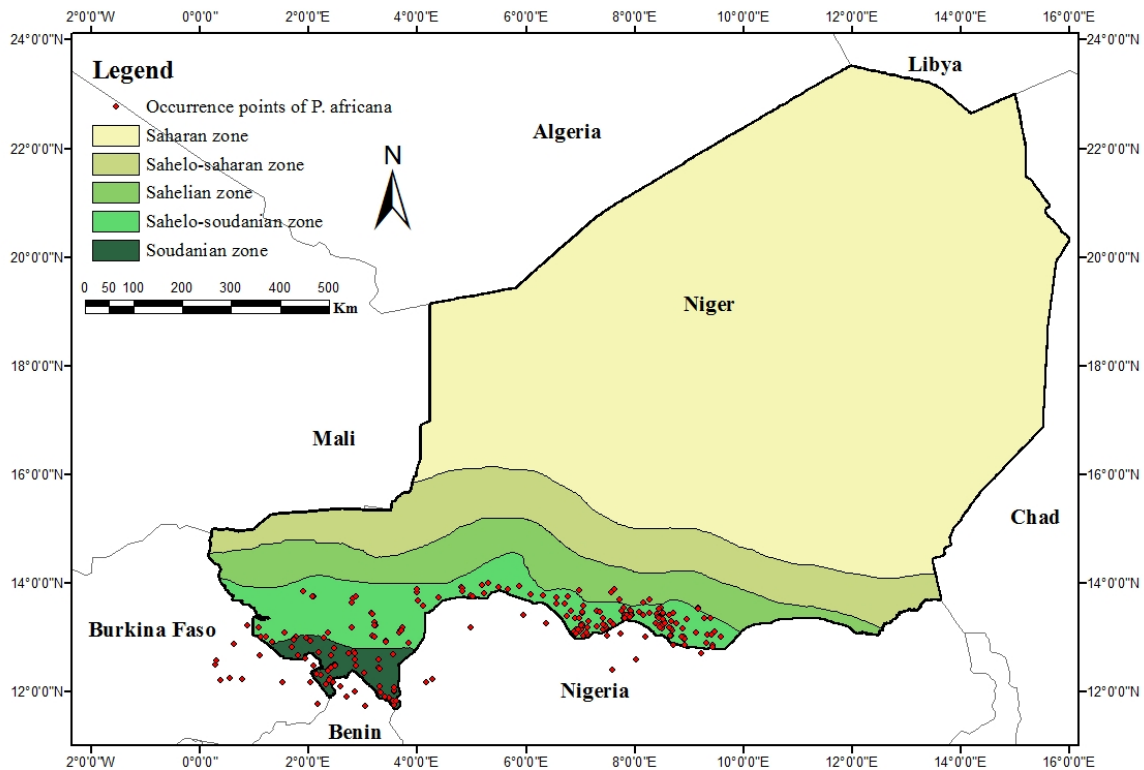


Figure 1. Presence points of *P. africana* in the study area

2.3.2 Climatic Data

As the climate is the main determinant of the ecological niche of species on a large scale (Parviainen, Luoto, Rytteri & Heikkinen, 2008), WorldClim archives have been exploited. The principle of WorldClim is to provide detailed information on the climate by interpolation of data collected around the world by more than 20,000 monitoring stations (Hijmans, Susan, Juan, Peter, & Andy, 2005).

Two types of climatic data (precipitation and temperature monthly mean, divided into 19 variables) of the 1950-2000 period were selected and used in this study. The data in raster CLM with a spatial resolution of 2.5 minutes ($5 \text{ km} \times 5 \text{ km} = 25 \text{ km}^2$ the pixel) have been downloaded from WorldClim archives (www.worldclim.org, accessed on 9/21/2014). Other environmental factors such as soil factors are decisive in the distribution of a species but at finer scales; do not take this into account in this study results from the tolerance of *P. africana* for most soil types (Weber et al., 2008).

2.4 Data Analysis

To generate the theoretical model of distribution of *P. africana*, data on the presence of the species and the 19 climatic variables were treated with DIVA-GIS 7.5, MAXENT 3.3.3k. and ArcGIS 10.0 softwares used in the same frame by several authors (Hijmans et al., 2005; Phillips et al., 2006; Scheldeman & Van Zonneveld, 2010; Young, Carter, & Evangelista, 2011).

The first step in the creation of the model consisted, using the DIVA-GIS program, to convert the CLM format of the imported climatic data in ASCII format to obtain environmental raster supported by the MAXENT modeling program. These rasters are made up of 19 climatic variables, some of which have been discarded after a Pearson correlation test. Indeed, among the variables that have a high correlation coefficient ($|r| > 0.7$, as

proposed by Dormann et al. (2013)), only one was selected based on its ecological importance for the species, because a strong correlation between these variables would introduce a bias in the model (Warren, Glor, & Turelli, 2010; Lee, Hanneman & Hackenbrook, 2011; Dormann et al., 2013; Maël, Catherine, Beatriz, & Vincent, 2014).

From the variables used and the information layer on the occurrence of *P. africana*, the MAXENT program generated a raster on the potential distribution of the species and a file containing the various statistical results of the model. Finally, the superposition of an information layer of administrative boundaries in ArcGIS, as had been done by Scheldeman and Van Zonneveld (2010), Young et al. (2011), Hijmans, Luigi, and Prem (2012), enabled to map and to locate the potential distribution areas of *P. africana*.

To determine the individual contribution of each variable, a Jackknife test (Young et al., 2011), which consists in spread by turns the variables and generating each time a model with the remaining variables then a model with the only discarded variable, was performed (Figure 2).

Cross-validation was also used in this study. Cross-validation is a process of evaluating the efficiency of a model that consists of split the presence points in two parts to calibrate and to test the model. The calibration of a model is to adjust the parameter values (climatic variables and presence points) in order for the simulated data correspond to the actual values (Guisan & Zimmermann, 2000; Dzotsi, 2002). In this study, 75% of the species' presence points were used to calibrate the model, while 25% were used to test it. These same rates have been used by Doko et al. (2008), Young et al. (2011), Fandohan et al. (2013), Gbesso et al. (2013) to calibrate and test their models. To strengthen a model, it is important to generate it from an average of multiple repetitions of cross validation (Young et al., 2011). Cross-validation was repeated 10 times in this study. About the predictive ability of the model, it was evaluated by using the parameter AUC (Area Under the Curve). The AUC is equal to the likelihood that a randomly selected presence point is located in a raster cell with a higher probability value for species occurrence than a randomly selected absence point (Phillips et al., 2006).

A model generated by MAXENT is excellent if $AUC > 0.90$, good if $0.90 > AUC > 0.80$, acceptable if $0.80 > AUC > 0.70$, bad if $0.70 > AUC > 0.60$ and invalid if $0.60 > AUC > 0.50$ (Swets, 1988). The lower value of the AUC is 0.5, corresponding to a random prediction and the highest value is 1 (Phillips et al., 2006).

3. Results

3.1 Contribution of Climatic Variables and Performance of the Model

After the correlation test, only five (5) climatic variables were selected because of their low correlations ($|r| \leq 0.7$), and used for modeling. These are BIO3 (isothermality), BIO9 (average temperature of the driest quarter), BIO10 (average temperature of the warmest quarter), BIO12 (annual precipitation) and BIO18 (precipitation of the warmest quarter). Among these variables, the study reveals that BIO12 and BIO10 have the highest levels of contribution to the model (Table 1).

Table 1. The climatic variables used and their contributions to the model

Code	Variable	Contribution (%)
BIO12	Annual precipitation	82.8
BIO10	Average temperature of the warmest quarter	8.4
BIO9	Average temperature of the driest quarter	3.9
BIO3	Isothermality (Temperature Mean Diurnal Range/Temperature Annual Range) * 100	3.3
BIO18	Precipitation of the warmest quarter	1.6

The cross-validation, with an AUC of 0.953 and the Jackknife test (Figure 2) confirm the contribution to the model of BIO12 that has the highest gain when used in isolation and decreases the gain the most when it is omitted from the analysis.

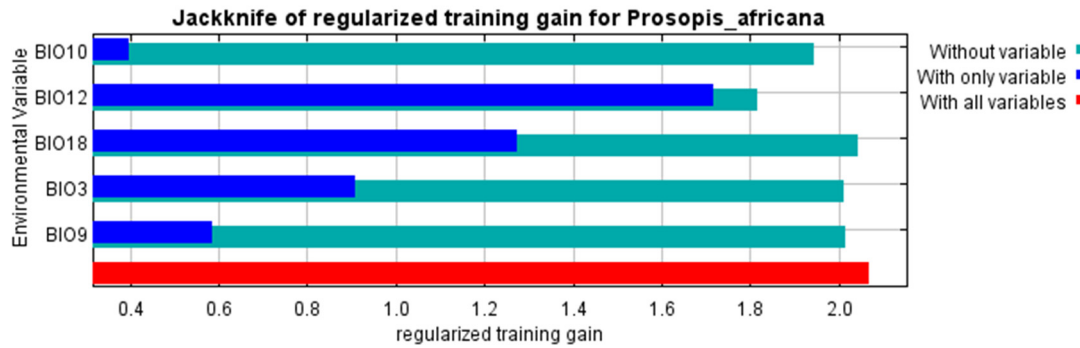


Figure 2. Jackknife test results on the 5 variables. The blue bar shows the gain obtained if a variable is used alone and the remaining variables are excluded from the analysis and the green bar shows how much the total gain is reduced if this variable is excluded from the analysis

3.2 Potential Distribution Areas of *P. africana* in Niger

The study reveals that favorable habitats for the development of *P. africana* in Niger, 128,692.32 km² in total, 10.16% of the territory, are allocated between sahelian, sahelo-soudanian and soudanian zones (Figure 3). The most favorable habitats cover an area of 41,304.32 km², 3.26% of the territory and are divided mostly between the sahelo-soudanian and soudanian zones, the wettest of the country. The averagely favorable habitats for the development of *P. africana*, with an area of 57,138 km², 4.51% of the national territory, are located mostly in the sahelo-soudanian zone. The less favorable habitats, with an area of 30,250 km², 2.39% of the territory, are mainly located in the sahelian zone.

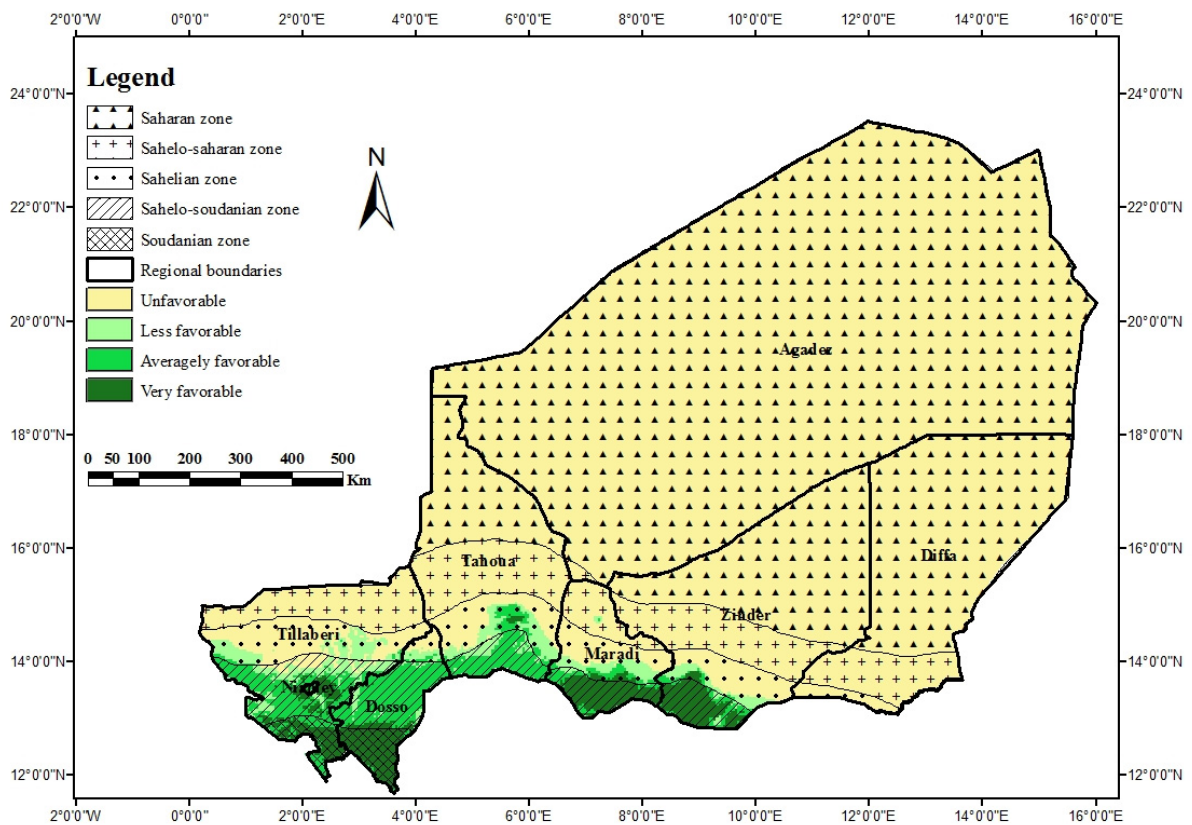


Figure 3. Potential distribution areas of *P. africana* in Niger

4. Discussion

The modeling of species distribution is very important in ecology and models can be seen as a simplified view of reality. However, the choice of data and the methodological approach affect the quality of results (Elith et al., 2006; Schmidt et al., 2008).

This study is based on a set of existing data and additional data collected in the field to fill the gaps in spatial coverage and take account of environmental variability as suggested by Hirzel and Guisan (2002) that compared the effectiveness of different sampling strategies for modeling species distribution. For these authors, systematic sampling is the best strategy for predicting the geographic distribution of species and it is the same type of sampling that was applied in this work. The low concentration of presence points of the species in neighboring countries of Niger is due to the lack of sources because field missions have not gone beyond the country's borders. Even within the country, the spatial heterogeneity of the presence points observed in the field would be partly related to the sampling effort. This could indeed vary depending on the accessibility of areas and / or the collectors' alertness, and thus constitute a limit that must be interpreted with caution, as suggested Ndayishimiye (2011). Nevertheless, the different localities surveyed cover the entire study area. The concentration of presence points of *P. africana* in the southern part, the wettest of the country, may be related to rainfall which is also one of the main factors determining the vegetation distribution in tropical zones (Saadou, 1990; Mahamane, Morou, Zaman-Allah, Saadou, Saley, Bakasso, & Jauffret, 2012). However, the spatial heterogeneity of the presence points of the species observed at the different territories in this area also suggests an influence of other factors such as human pressure, in addition to eventual sampling bias. Indeed, nearly 90% of Niger's population lives in the southern agricultural (Institut National de la Statistique [INS], 2014), the area where much of the woody vegetation is located. This demographic concentration, coupled with a shortage of farmland becoming poorer for lack of fallow could only lead to an impoverishment of the population and pressure on forest products.

The largest contribution to the model of the annual precipitation (BIO12) and the average temperature of the warmest quarter (BIO10) reflects the actual climatic conditions of the species' high concentration area that is relatively rainiest than the north part. According to Weber et al. (2008), *P. africana* prefers an annual rainfall of between 600 and 1500 mm. The effectiveness of these two direct parameters in the model, especially when the species distribution modeling covers a large spatial scale, has been noted by several authors (Guisan & Zimmermann, 2000; Fandohan et al., 2013; Gbesso et al., 2013). The type of soil is not a limiting factor in the distribution of *P. africana* because according to Weber et al. (2008), this species tolerates most soil types, although it abounds in general on land fallow or sandy clay soils. This is corroborated by the diversity of soils in the species' distribution area found in this study. Indeed, the soils are mainly sandy clay in southern Dosso region (Gavaud & Boulet, 1967), dunal to south Maradi and sandy, sandy loam, clay loam in southern Zinder (Larwanou et al., 2006; Laouali et al., 2014).

The value of AUC (0.953), closer to its maximum (1) than its minimum (0.5, corresponding to a random prediction) indicates a good model performance (Swets, 1988; Phillips et al., 2006). A high AUC value does not necessarily reflect a good performance of a model (Phillips et al., 2006; Scheldeman & Van Zonneveld, 2010) when the predicted distribution area is small compared to the total area of the study. For this study, the predicted distribution area is relatively large compared to the area of the study. In addition, the use of repetitions and cross-validation in executing MAXENT yielded a model derived from the average, most powerful.

The resulting model suggests that *P. africana* is widely distributed from the soudanian zone to the sahelo-soudanian band of the country. This potential distribution area is wider than that suggested by Bonnet, Arbonnier and Grard (2008) which is limited to a thin strip in the south of the country. It is also wider than that observed in the field through the presence points of the species. However, the probability of encountering the species is higher in the southern strip and the extreme south-west, where conditions are more favorable for its development. Indeed, a species may be absent in areas where it should be if its natural habitat has been altered by human interference (Scheldeman & Van Zonneveld, 2010). Effectively, *P. africana* is a species subject to a strong human pressure in some areas of Niger because of the domestic use of its wood and its importance in the traditional pharmacopoeia (Laouali et al., 2014), which would have contributed to the heterogeneity observed in the distribution on the field.

This study allowed estimating the distribution area of *P. africana* in Niger and revealed heterogeneity in the organization of the species in the landscape. It thus showed a theoretical distribution area wider than that observed in the field. Given the extent of the area revealed by this study and the socio-economic importance of *P. africana*, restoration operations through a reforestation policy implementation must be carried out in all

habitats favorable for its development. Other endangered species in Niger must also be the subject of similar studies to identify favorable habitats for their development and proceed to their restoration.

References

- Agboola, D. A. (2004). *Prosopis africana* (Mimosaceae): stem, roots, and seeds in the economy of the savanna areas of Nigeria. *Economic Botany*, 58(Supplement), S34-S42. Retrieved from <http://www.jstor.org/stable/4256906>
- Ahoton, L. E., Adjakpa, J. B., M'po Ifonti M'po, & Akpo, E. L. (2009). Effet des prétraitements des semences sur la germination de *Prosopis africana* (Guill., Perrot. Et Rich.) Taub., (Césalpiniacées). *Tropicultura*, 27(4), 233-238. Retrieved from <http://www.tropicultura.org/text/v27n4/233.pdf>
- Akaaimo, D. I., & Raji, A. O. (2006). Some physical and Engineering Proprieties of *Prosopis africana* seed. *Biosystems Engineering*, 95(2), 197-205. <http://dx.doi.org/10.1016/j.biosystemseng.2006.06.005>
- Araújo, M. B., Pearson, R. G., Thuiller, W., & Erhard, M. (2005). Validation of species–climate impact models under climate change. *Global Change Biology*, 11, 1504-1513. <http://dx.doi.org/10.1111/j.1365-2486.2005.001000.x>
- Arbonnier, M. (2000). *Arbres, arbustes et lianes des zones sèches d'Afrique de l'Ouest*. CIRAD - MNHN - UICN, Montpellier (France).
- Bonnet, P., Arbonnier, M., & Grard, P. (2008). *Outil graphique d'identification V.1.0*. CIRAD. CD-Rom. Ed. Quæ.
- Chidumayo, E., Okali, D., Kowero, G. & Larwanou, M. (2011). *Climate change and African forest and wildlife resources*. African Forest Forum, Nairobi, Kenya. Retrieved from <http://www.sifi.se/wp-content/uploads/2011/11/Climate-Change-Africa.pdf>
- Doko, T., Kooiman, F. A., & Toxopeus, A. G. (2008). Modeling of species geographic distribution for assessing present needs for the ecological networks. *The International Archives of the Photogrammetry, Remote Sensing and Spatial Information Sciences*, XXXVII (Part B4. Beijing), 267-276. Retrieved from http://www.isprs.org/proceedings/XXXVII/congress/4_pdf/49.pdf
- Dormann, C. F., Elith, J., Bacher, S., Buchmann, C., Carl, G., Carré, G., & Lautenbach, S. (2013). Collinearity: a review of methods to deal with it and a simulation study evaluating their performance. *Ecography*, 36, 27-46. <http://dx.doi.org/10.1111/j.1600-0587.2012.07348.x>
- Dozsi, A. K. (2002). *Application du modèle CERES-Maize de DSSAT à l'analyse des stratégies de semis pour le maïs (Zea mays L.) dans les conditions de SEVE KPOTA*. Mémoire d'ingénieur agronome, IFDC Afrique/ESA -UL, Lomé, Togo.
- Elith, J., Graham, C. H., Anderson, R. P., Dudik, M., Ferrier, S., Guisan, A., & Zimmermann, N. E. (2006). Novel methods improve prediction of species' distributions from occurrence data. *Ecography*, 29, 129-151. <http://dx.doi.org/10.1111/j.2006.0906-7590.04596.x>
- Fandohan, B., Gouwakinnou, G. N., Fonton, N. H., Sinsin, B., & Liu, J. (2013). Impact des changements climatiques sur la répartition géographique des aires favorables à la culture et à la conservation des fruitiers sous-utilisés : cas du tamarinier au Bénin. *Biotechnol. Agron. Soc. Environ*, 17(3), 450-462. Retrieved from <http://www.pressesagro.be/base/text/v17n3/450.pdf>
- Fitzpatrick, M. C., & Hargrove, W. W. (2009). The projection of species distribution models and the problem of non-analog climate. *Biodivers. Conserv.*, 18, 2255-2261. <http://dx.doi.org/10.1007/s10531-009-9584-8>
- Gavaud, M., & Boulet, R. (1967). *Carte pédologique de reconnaissance de la république du Niger*. Service cartographique de l'ORSTOM.
- Gbesso, F. H. G., Tente, B. H. A., Gouwakinnou, N. G., & Sinsin, B. A. (2013). Influence des changements climatiques sur la distribution géographique de *Chrysophyllum albidum* G. Don (Sapotaceae) au Benin. *Int. J. Biol. Chem. Sci*, 7(5), 2007-2018. <http://dx.doi.org/10.4314/ijbcs.v7i5.18>
- Guisan, A., & Thuiller, W. (2005). Predicting species distribution: offering more than simple habitat models. *Ecology Letters*, 8(9), 993-1009. <http://dx.doi.org/10.1111/j.1461-0248.2005.00792>
- Guisan, A., & Zimmermann, N. E. (2000). Predictive habitat distribution models in ecology. *Ecol. Modell.*, 135, 147-186. [http://dx.doi.org/10.1016/S0304-3800\(00\)00354-9](http://dx.doi.org/10.1016/S0304-3800(00)00354-9)

- Hijmans, R. J., Susan, E. C., Juan, L. P., Peter, G. J., & Andy, J. (2005). Very high resolution interpolated climate surfaces for global land areas. *Int. J. Climatol.*, 25, 1965-1978. <http://dx.doi.org/10.1002/joc.1276>
- Hijmans, R. J., Luigi, G., & Prem, M. (2012). *DIVAGIS Version 7.5 Manual*. Retrieved from http://www.diva-gis.org/docs/DIVA-GIS_manual_7.pdf
- Hirzel, A., & Guisan, A. (2002). Which is the optimal sampling strategy for habitat suitability modelling? *Ecological Modelling*, 157(2-3), 331-341. [http://dx.doi.org/10.1016/S0304-3800\(02\)00203-X](http://dx.doi.org/10.1016/S0304-3800(02)00203-X)
- INS. (2014). *Recensement général de la population et de l'habitat, 2012. Répertoire national des localités*. Institut National de la Statistique, Niger.
- IPCC. (2007). *Climate Change 2007: Synthesis Report*. Contribution of Working Groups I, II and III to the Fourth Assessment Report of the Intergovernmental Panel on Climate Change [Core Writing Team, Pachauri, R.K and Reisinger, A. (eds.)]. IPCC, Geneva, Switzerland. Retrieved from http://www.ipcc.ch/pdf/assessment-report/ar4/syr/ar4_syr_full_report.pdf
- Kumar, S., & Stohlgren, T. J. (2009). Maxent modeling for predicting suitable habitat for threatened and endangered tree *Canacomyrica monticola* in New Caledonia. *Journal of Ecology and Natural Environment*, 1(4), 094-098. Retrieved from http://www.academicjournals.org/article/article1379515268_Kumar%20and%20Stohlgren.pdf
- Laouali, A., Dan Guimbo, I., Chaibou, I., & Mahamane, A. (2015b). Fruit production of *Prosopis africana* (G. et Perr.) Taub., an overexploited species in the Southeastern Niger. *International Journal of Current Microbiology and Applied Sciences*, 4(5), 50-56. Retrieved from <http://www.ijcmas.com/vol-4-5/Laouali%20Abdou,%20et%20al.pdf>
- Laouali, A., Dan Guimbo, I., Larwanou, M., Inoussa, M. M., & Mahamane A. (2014). Utilisation de *Prosopis africana* (G. et Perr.) Taub. dans le sud du département d'Aguié au Niger : les différentes formes et leur importance. *Int. J. Biol. Chem. Sci.*, 8(3), 1065-1074. <http://dx.doi.org/10.4314/ijbcs.v8i3.20>
- Laouali, A., Dan Guimbo, I., Youchaou, A., Rabiou, H., & Mahamane, A. (2015a). Etude de la germination de la graine et suivi de la croissance en pépinière de *Prosopis africana* (G. et Perr.) Taub., espèce menacée de disparition au Niger. *Annales de l'Université Abdou Moumouni de Niamey, Tome XVIII-A*, 1-12.
- Larwanou, M. (1994). *Potentials of Prosopis africana (G. et Perr.) Taub leaf litter for soil nutrient enhancement and crop development*. M.Sc thesis. Department of Forest resources Management, University of Ibadan.
- Larwanou, M., Moustapha, A. M., Rabé, M. L., & Dan Guimbo, I. (2012). Contribution de la Régénération Naturelle Assistée des ligneux dans l'approvisionnement en bois des ménages dans le département de Magaria (Niger). *Int. J. Biol. Chem. Sci.*, 6(1), 24-36. <http://dx.doi.org/10.4314/ijbcs.v6i1.3>
- Larwanou, M., Oumarou, I., Laura, S., Dan Guimbo, I. & Eyog-Matig, O. (2010). Pratiques sylvicoles et culturelles dans les parcs agroforestiers suivant un gradient pluviométrique nord-sud dans la région de Maradi au Niger. *Tropicultura*, 28(2), 115-122. Retrieved from <http://www.tropicultura.org/text/v28n2/115.pdf>
- Lee, P., Hanneman, M., & Hackenbrook, D. (2011). *Cartographie des perturbations et des perspectives de rétablissement et de protection des populations de caribou des bois dans la région de la baie James du Nord québécois : Partie 2. Cartographie des perspectives de rétablissement et de protection*. Edmonton, Alberta. Global Forest Watch Canada. 5e publication de l'Année internationale des forêts. Retrieved from http://www.globalforestwatch.ca/files/publications/20111205B_QB_Caribou_Restoration_Protection_FR_HR.pdf
- Maël, D., Catherine, G., Beatriz, C., & Vincent, P. (2014). *Distribution, écologie & statut de conservation de l'Oriole de Martinique (Icterus bonana)*. DEAL Martinique. Retrieved from http://www.sosdom.lautre.net/DEAL/Carouge_Rapport_DEAL.pdf
- Mahamane, A., Morou, B., Zaman-Allah, M., Saadou, M., Saley, K., Bakasso, Y., & Jauffret, S. (2012). Climate Variability in Niger: Potential Impacts on vegetation distribution and productivity. *Journal of Environmental Science and Engineering*, 1, 49-57. Retrieved from <http://www.davidpublishing.com/davidpublishing/Upfile/2/7/2012/2012020771401153.pdf>
- Matthias, M., Henri, T., & Félix, H. (2000). Ligneux à usages multiples dans les systèmes agraires tropicaux : une étude de cas de Côte d'Ivoire. *Schweiz. Z. Forstwes*, 151(10), 355-364. <http://dx.doi.org/10.3188/szf.2000.0355>

- Ndayishimiye, J. (2011). *Diversité, endémisme, géographie et conservation des Fabaceae de l'Afrique Centrale*. Thèse présentée en vue de l'obtention du Diplôme de Docteur en Sciences. Université Libre de Bruxelles.
- Niang-Diop, F., Sambou, B., & Lykke, A. M. (2010). Contraintes de régénération naturelle de *Prosopis africana* : facteurs affectant la germination des graines. *Int. J. Biol. Chem. Sci.*, 4(5), 1693-1705. <http://dx.doi.org/10.4314/ijbcs.v4i5.65578>
- Ozer, P., Hountondji, Y.-C., Niang, A.J., Karimoune, S., Laminou, M. O., & Salmon, M. (2010). Désertification au Sahel : historique et perspectives. *BISGLg*, 54, 69-84. Retrieved from <http://popups.ulg.ac.be/0770-7576/index.php?id=942&file=1>
- Parviainen, M., Luoto, M., Rytteri, T., & Heikkinen, R. K. (2008). Modelling the occurrence of threatened plant species in taiga landscapes: methodological and ecological perspectives. *J. Biogeogr.*, 35, 1888-1905. <http://dx.doi.org/10.1111/j.1365-2699.2008.01922.x>
- Phillips, S. J., Anderson, R. P., & Schapire, R. E. (2006). Maximum Entropy Modeling of species geographic distributions. *Ecological Modelling*, 190, 231-259. <http://dx.doi.org/10.1016/j.ecolmodel.2005.03.026>
- Priso, R. J., Nnanga, J. F., Etame, J., Din, N., & Amougou, A. (2011). Les produits forestiers non ligneux d'origine végétale : valeur et importance dans quelques marchés de la région du Littoral - Cameroun. *Journal of Applied Biosciences*, 40, 2715-2726. Retrieved from <http://www.m.elewa.org/JABS/2011/40/6.pdf>
- Saadou, M. (1990). *La végétation des milieux drainés nigériens à l'Est du fleuve Niger*. Thèse de Doctorat ès - Sciences Naturelles. Université de Niamey.
- Scheldeman, X., & Van Zonneveld, M. (2010). *Training Manual on Spatial Analysis of Plant Diversity and Distribution*. Bioversity International, Rome, Italy. Retrieved from http://www.bioversityinternational.org/uploads/tx_news/Training_manual_on_spatial_analysis_of_plant_diversity_and_distribution_1431_07.pdf
- Schmidt, M., König, K., & Müller, J. V. (2008). Modelling species richness and life form composition in Sahelian Burkina Faso with remote sensing data. *Journal of Arid Environments*, 72(8), 1506-1517. <http://dx.doi.org/10.1016/j.jaridenv.2008.02.015>
- Swets, J. A. (1988). Measuring the accuracy of diagnostic systems. *Science*, 240(4857), 1285-1293. <http://dx.doi.org/10.1126/science.3287615>
- Warren, D. L., Glor, R. E., & Turelli, M. (2010). ENMtools: a toolbox for comparative studies of environmental niche models. *Ecography*, 33, 607-611. <http://dx.doi.org/10.1111/j.1600-0587.2009.06142.x>
- Weber, J. C., Larwanou, M., Abasse, T. A., & Kalinganire, A. (2008). Growth and survival of *Prosopis africana* provenances tested in Niger and related to rainfall gradients in the West African Sahel. *Forest Ecology and Management*, 256, 585-592. <http://dx.doi.org/10.1016/j.foreco.2008.05.004>
- Young, N., Carter, L., & Evangelista, P. (2011). *A MaxEnt Model v3.3.3e Tutorial (ArcGIS v10)*. Laboratory at Colorado State University and the National Institute of Invasive Species Science. Retrieved from http://ibis.colostate.edu/WebContent/WS/ColoradoView/TutorialsDownloads/A_Maxent_Model_v7.pdf

Copyrights

Copyright for this article is retained by the author(s) with first publication rights granted to the journal.

This is an open-access article distributed under the terms and conditions of the Creative Commons Attribution license (<http://creativecommons.org/licenses/by/3.0/>).

Evaluating the Competing Claims on the Role of Ownership Regime Models on International Drinking Water Coverage

Chadd Stutsman¹, Kelly Tzoumis² & Susan Bennett²

¹ International Studies, DePaul University, Chicago, IL 60614 USA

² Department of Public Policy Studies, DePaul University, Chicago, IL 60614 USA

Correspondence: Kelly Tzoumis, Department of Public Policy, DePaul University, Chicago, IL 60614 USA Tel: 1-630-306-3351. E-mail: ktzoumis@depaul.edu

Received: May 10, 2016 Accepted: May 24, 2016 Online Published: May 31, 2016

doi:10.5539/enrr.v6n2p145

URL: <http://dx.doi.org/10.5539/enrr.v6n2p145>

Abstract

While progress has been made for providing drinking water through the completion of the Millennium Development Goals and other international programs, millions of people still do not have access to clean drinking water. This study examines how drinking water coverage is impacted using three regime ownership models. Using the framework of the privately-owned, publicly-owned, and decentralized regime models, the impacts of water production, non-revenue water, and unit operation cost are evaluated for drinking water coverage. A sample of 144 utilities across 33 countries were sampled using data from the International Benchmarking Network for Water and Sanitation Utilities. Using ordinary least squares modeling, results indicate that predicting water coverage from water production, non-revenue water, and unit operational costs provided weak explanations of variation for both publicly-owned and decentralized regimes. None of the three regime models established a significant relationship between water coverage and all three independent variables. For publicly- and privately-owned water regimes, decreasing non-revenue water by plugging leaks and improving infrastructure can translate into higher rates of water coverage. For decentralized water regimes, higher levels of unit operational cost can increase water coverage. The regression analyses also showed that broad claims about regime ownership, efficiency, and improved water coverage should be suspect. None of the three regime models established a significant relationship between water coverage and all three independent variables. This suggests that the competing claims that privatized drinking water utilities as being more efficient or more able to provide water coverage as compared to other types of utilities in the literature is not supported when compared across countries.

Keywords: international drinking water, drinking water regimes, international water coverage

1. Introduction

1.1 What Impact do Ownership Regime Models of on Drinking Water Coverage?

In 2000, Cochabamba, Bolivia privatized its municipal water utility resulting in massive protests by the city's residents. Typically referred to as the 'Cochabamba Water Wars', this conflict epitomizes the long debate about the impact of ownership regime models on drinking water coverage via water utilities. How freshwater is framed as a natural resource, and managed, impacts coverage, which is vital to the human population. The World Health Organization (WHO) estimates that 842,000 people die each year from diarrhea as a result of unsafe drinking water. In addition, at least 1.8 billion people use drinking water contaminated with feces (World Health Organization, 2015). Since 1990, some progress in providing access to drinking water has been reported as part of the completion of the Millennium Development Goals in 2015. There are approximately 4.2 billion people getting drinking water through piped-connections, and another 2.4 billion people accessing water through improved sources including public taps, protected wells, and boreholes. However, in 2013, it was estimated that 783 million people still do not have access to clean drinking water (United Nations Educational, Scientific, and Cultural Organization, 2015). Academics, global leaders, and practitioners have debated for decades on the best ways to increase coverage for people across the globe.

The World Bank has taken what has been termed a 'neo-liberal' or market approach towards drinking water coverage as how it frames this critical natural resource. This argument is that privately-operated water utilities

which position water as an economic good rather than a public good are superior to other models of delivery. When framing drinking water as a commodity, it can be managed under a market-based approach that will discourage overconsumption and waste while generating much needed revenue for the infrastructure improvements of water utilities (privately-owned water coverage). Likewise, improvements to infrastructure can increase coverage by lowering the cost of piped-water delivery which may not be accessible in a widespread manner. However, if drinking water coverage is framed using an opposite approach, where coverage is a universal human right, and it is not commoditized as a private good, then ownership of water utilities would remain in the public sphere (publicly-owned water coverage). The delivery of water then would be more accessible to people, but perhaps more costly to deliver. A third approach to framing freshwater as a natural resource is having organizations of local citizens with rights to access drinking water. Of course, this framing does not give individual citizens the rights to drinking water, but in this framework, water utilities could eliminate waste from both local knowledge of natural resource management and increased accountability (decentralized water coverage). These three framing approaches serve as the foundation for the three ownership regimes for water coverage evaluated in multivariate regression modeling in this research.

Using data from the International Benchmarking Network for Water and Sanitation Utilities (2015), this research focuses on comparing three ownership regime models of water coverage (publicly-owned, decentralized, and privately-owned) for piped-water delivery provided by water utilities. The regimes are examined for the amount of water coverage predicted from water production, amount of non-revenue water (waste or seepage), and unit operational costs. The evaluation of competing claims in the literature of these three ownership regimes is the foundation of the comparison.

1.2 Literature Review

1.2.1 Publicly-Owned Regimes

Historically, for the most part, utility ownership of drinking water was the purview of states and municipalities. During the 18th and 19th centuries, states and municipalities were the only organizations capable of expanding water service to rapidly growing populations. This largely contributed to the ascendancy of states and municipalities in water delivery. States and municipalities as water providers began with European countries and expanded globally through colonialism. France was a notable exception where private companies contracted by municipalities serve as utility operators.

Publicly-owned water utilities are owned and managed by a national or state/provincial government. Water is viewed as a universal good and a “natural resource monopoly” that needs ownership and management by a publicly-owned regime for the protection of water coverage. Public water utilities in various countries are responsible for the maintenance and operation of all levels of water distribution and sanitation (Baietti, Kingon, & van Ginneken, 2006). Typically, a public water utility can be managed as a ministry or department, a statutory body, or as a public company, each with different management structures and oversight. Water utilities that are managed as a ministry or department of the government may operate under a system of direct control and oversight and do not exist as a separate legal entity. A water utility that is a statutory body is typically owned by the government and operates under public law, with a legal act establishing it as an autonomous corporate body. The publicly-owned regime is generally comprised of governments with a centralization of policymaking decisions. In this regime, water is framed as a public good that can, and should be, delivered by the state because of the critical role it has in sustaining life.

1.2.2 Privately-Owned Regimes

According to Baietti, et al. (2006), as part of a general move to market-led systems in the 1980s and 1990s, a new paradigm emerged to transform utilities into more modern service delivery organizations that emphasize operational and financial sustainability. It was thought that public-owned regimes for water coverage were costly, and not effective in maintaining affordable water delivery with maintenance of infrastructure. There was wide optimism that the private sector would resolve much of the performance problems of utilities and mobilize scarce financing to sustain growth and expand coverage. Central to this regime was a definition of water as a commodity to be privatized and managed in the market place. This “commodification” of water access took place which is the process of converting a good or service formally subject to many non-market social rules into one that is primarily subject to market rules (Gleick & Reyes, 2002).

In the privately-owned regime, private companies are thought to be better equipped at water delivery than state or municipal management (Bakker, 2007, 2010). The issue has been supported for several reasons: first, public water agencies have been unable to satisfy the most basic needs for water for all humans; second, major multinational corporations have greatly expanded their efforts to take over responsibility for a larger portion of the

water service market than ever before. Also, it is thought that commodification of water can have a positive effect on economic and social development by focusing on the implementation of public policies for the sustainable consumption of water, commercializing environmental awareness, and communicating consumers' responsibilities towards the use of water (Patsiaouras, Saren, & Fitchett, 2014).

Proponents of privatization, occasionally referred to as 'market liberals' or 'neoliberals', are characterized by the belief "that the free market is the best mechanism to maximize resource consumption, efficiency, and allocation." In essence, these theories advocate for the removal of government ownership and the liberalization of the market. Market advocates argue that public resources, such as drinking water, will not be efficiently utilized unless managed by the private sector. Privatization treats water as an economic good by establishing a price and concurrently a market. According to the advocates of this regime, priced water will be treated as a commodity giving government, industry, and society incentive to conserve and protect it. In addition, a market will bring about investment and improvements in water infrastructure and technology. Through efficiency gains and better management, private companies will be able to lower prices, improve performance, and increase cost recovery, enabling systems to be upgraded and expanded (Bakker, 2007). Market advocates often argue that publicly-owned water utilities attempt to ensure affordability by using cost subsidization schemes to keep drinking water tariffs low. Segerfeldt (2005) argues that such subsidization schemes set prices so low "that on average it only covers about 30 percent of the water supplies expenses." In essence, public water utilities are portrayed as lacking the adequate cost recovery needed to prevent infrastructure deterioration and an increase in inaccessibility of piped drinking water. Essentially, privatization proponents commonly argue that privatized water utilities' profit motive ensures cost recovery, which is used for infrastructure maintenance and expansion. While private sector involvement has indeed increased in the last decade, it has substantially fallen short of expectations that it would help turn around this sector. In essence, private financing has only accounted for less than 5 percent of the total investment in water supply and sanitation over the last 20 years (Baietti, Kingon, & van Ginneken, 2006). At the same time, some public utilities have become more autonomous and accountable. Some have improved their performance without involving the private sector and working totally within a public environment of key stakeholders and funding sources (Hall, Lobina, & de la Motte, 2005).

The privately-owned regime has encountered challenges to its use of water as a commodity. Recently there has been a shift in the ownership regime in Europe and developing countries towards re-municipalization where there is a return of water coverage to total public ownership, some from new citizen pressures for less private regime dominance of water coverage (Zamzami & Ardhianie, 2015). This trend contradicts neoliberal theorists, international financial institutions, and the expectations of superior private sector performance. Also, evidence increasingly points to re-municipalization as a credible promise of a better future for public water services and their beneficiary communities (Lobina, 2015). This shift has been also received criticism from recent austerity packages in Europe where water privatization is planned for increasing revenue for the state (Hall & Lobina, 2012). Successful public utilities are still the exception, however, and since most people in developing countries are under the jurisdiction of public utilities, the result is that much of the world's population is still not adequately served (Baietti, Kingon, & van Ginneken, 2006).

Privatization of water utilities exists on a spectrum. At one end of the spectrum a private company may have complete ownership of a water utility; while at the other end a private company may be contracted by the state to manage a utility. When a private company completely owns a water utility, they own the infrastructure for processing (plants and sanitation) with delivery (water pipes). Often they have more influence over business decisions allowing more capability to increase profits. At the opposite end of the spectrum a private company contracted to run a utility will have less influence over business decisions and will be more dependent on generating profits through efficiency gains. Despite the variability in ownership, perception of water is similar. Privatized water utilities view water as a commodity and seek to maximize profits through efficiency gains. Private utilities strive to produce more water at lower cost while decreasing non-revenue water (which is seepage or waste).

1.2.3 Decentralized-Owned Regimes

While there is a range of what constitutes publicly-, and privately-owned water regimes, there is a third type of regime separate from these other two that reflects more of a hybrid approach. Decentralized ownership regimes are operated by local entities such as city council, municipal government, drinking water association, or a water cooperative. Similar to publicly-owned water utilities, decentralized water utilities view water as a universal good. The difference is that utility governorship is handled at the local-level. Decentralization can occur in a variety of ways. The focus of this approach is that there are improvements in water coverage by increasing user influence to provide support for raising funding to support infrastructure. Moreover, in many countries, there has also been a

move to decentralize decision-making down to the lowest practical level and place greater policy and oversight responsibilities on municipal governments. For example, local entities – city council, municipal government, drinking water association, or a water cooperative – can be given decision-making ability over water utilities and the authority to collect revenue in the forms of taxes or tariffs (Ribot, 2002). The local water entity may then serve as the policymaking and regulating body. Reporting to that body in the organization is a service operator that may be set up and charged with the day-to-day operations of the water utility. Alternatively, service operations may be contracted out to a private company. Under a mixed capital model, the municipality may choose to sell a small fraction of utility ownership to smaller water associations operating in the service areas. Dickson (2006) found that in Honduras decentralization was an effective method, particularly compared to the more centralized regimes of the privately and publicly owned delivery of water coverage (Dickson, 2006). Likewise, Renzetti & Dupont (2003) reveal that there is no compelling evidence of private utilities outperforming public utilities or that privatizing water utilities leads to unambiguous improvements in performance

An increasingly popular form of decentralization is the water cooperative. Similar to publicly-owned regimes, cooperatives do not seek to create profit but to provide universal service coverage. They differ in that they are owned by the utility's consumers who are often called members. Cooperative governance structures are typically designed to allow membership voting rights, oversight, and accountability. A cooperative is an autonomous association of persons united voluntarily to meet their common economic, social, and cultural needs and aspirations through a jointly owned and democratically controlled enterprise. Utility management is accountable to member elected administrative and oversight boards, which are drawn from members. Performance of utility cooperatives varies widely. The practices and organization adopted are a determining factor in the results achieved. Well-functioning utility cooperatives provide dependable services to all members, do not discriminate, and are governed by a fair and uncorrupted management (Ruiz-Mier & Ginneken, 2006). In general, private water utilities differ from public and decentralized water utilities in its framing of water. Both public and decentralized water utilities view water as a public good, inasmuch as it's both non-competitive and non-excludable. In contrast, private water utilities treat water as an economic good and seek profit maximization.

1.3 Hypotheses Associated with the Ownership Regimes

To compare the three regimes of drinking water ownership, the effects of three independent variables are important to evaluate: water production, nonrevenue water, and unit operational costs on water coverage. These variables are fundamental in the ability to provide water coverage. Since the privately-owned regimes were expected to be more efficient in delivery of water, it is expected that there will be increased water production, lower nonrevenue water and a lower unit of operational costs for increased water coverage. For publicly-owned regimes, the expectations are increased water production, higher nonrevenue water, and higher operational costs for increased water coverage. And, decentralized regimes should exhibit increased water production, lower nonrevenue water, and higher unit operational costs for increased water coverage. Table 1 outlines the hypotheses associated with each ownership regime for drinking water.

Table 1. Regime Hypotheses

Regime	Hypothesis
Privately-Owned	
Utilities that are owned, managed, or operated by the private sector.	Increased water production, lower nonrevenue water, and lower unit operational costs should result in increased water coverage.
Publicly-Owned	
Utilities that are managed and operated by national or provincial governments as a department/ministry, statutory body, or a government company.	Increased water production, higher nonrevenue water, and higher unit operational costs should result in increased water coverage.
Decentralization-Owned	
Utilities that incorporate local entities like municipal governments, city councils, or water boards or cooperatives.	Increased water production, lower nonrevenue water, and higher unit operational costs should result in increased water coverage.

2. Research Method and Design

2.1 Sample and Data Sources

Sample utilities were identified through the World Bank's Private Participation in Infrastructure Advisory Facility (PPI, 2009) database. Samples were matched with the International Benchmarking Network for Water and Sanitation Utilities (IBNET) database, a non-governmental organization that is funded by United Kingdom's Department for International Development, The World Bank, and The United Nations Water and Sanitation Program. This organization is the world's largest performance database for water and sanitation utilities (International Benchmarking Network for Water and Sanitation Utilities, 2015). Utilities were selected based on having complete data for the three independent variables used in the model for hypothesis testing: water production, non-revenue water, and unit operational cost. This performance data is used to establish benchmarks for utility comparisons that assist practitioners, governments, and regulators in service improvement. Table 2 illustrates the criteria used for utility categorization into a regime type.

Table 1. Criteria for Utility Categorization

Regime Type	Criteria for Utility Categorization
Private	Utilities that are owned, managed, or operated by the private sector through a full divestiture sale, concession contract, lease agreement, or management contract.
Public	Utilities that are managed and operated by national or provincial governments as a department/ministry, statutory body, or a government company.
Decentralization	Utilities that incorporate local entities like municipal governments, city councils, or water boards in management process.

Using the IBNET database, 144 water utilities were identified with complete information from 33 countries which were identified by the World Bank as having "developing economies". The World Bank classifies national economies annually based on estimates of gross national income (GNI) per capita for the prior year. Economies identified as low- and middle-income economies are often referred to as developing economies. Countries with a GNI below \$976 were considered low-income and those with a GNI between \$976 and \$3,855 were considered middle income. This group included a wide variety of countries, including most of Latin America, several African countries, two Eastern European countries, and several Asian countries, including China and India. Though the sample represents a broad range in terms of size, geography, demographics, history, and politics, it is limited to countries having a similar level of economic development. This type of a sample is common in the pro-privatization literature and research. Implementation studies, of course, often emphasize the importance of context in policy considerations while the pro-privatization arguments are made from the neoliberal approach that generally argue in favor of market approaches in all circumstances. Countries such as those in the sample are often urged or even required to take a market approach by international funders such as the World Bank and the IMF. Testing the three models for water provision across a wide range of developing countries, then, seems an appropriate test of the pro-privatization model in comparison to the public, and decentralized models.

An attempt to take variations in the countries' context fully into account would require country specific analyses. Given the limited number of water utilities in each country (most had fewer than 10) and the presence of only one of the three types of water utilities in most of the countries, it would not be possible to conduct a statistical analysis to compare the three types using a country specific approach. Table 3 outlines the countries included in the sample, along with the number of utilities and regime types. The sample included 54 utilities from the privately-own regime type, 53 utilities from the publicly-own regime type, and 37 utilities from the decentralized regime type.

One critique of the sample is that it is too broad, and the scope should be limited to a specific region with similarities in geography, demographics, history, economics, and politics. It is not uncommon for studies supporting privately-owned regimes approach to drinking water coverage to use similar data sets to test claims of improved efficiency and/or water coverage. This analysis intends to engage in a similar exercise to test the significance of the regime influence on water coverage. This sample is also influenced by data availability, and most significantly, by the lack of data provided to the IBNET database. This would have some impact on external validity by not including more of countries with water coverage regimes. IBNET's data is collected by

participating water utilities self-reporting measurement data on service coverage, water consumption and production, cost and staffing, and non-revenue water. Data is reported with the use of the IBNET tool-kit, which is a collection of spreadsheets requiring specific information. The fact that data is collected through a self-reporting process does bring legitimate questions of validity to the process.

Table 3. Sample Utilities by Country

Country	# Utilities	Private	Public	Decentralized
Argentina	6	4	1	1
Armenia	2	2	0	0
Benin	1	0	1	0
Bolivia	2	0	0	2
Brazil	23	0	23	0
Burkina Faso	1	0	1	0
Chile	11	10	0	1
China	2	2	0	0
Columbia	25	13	0	12
Costa Rica	1	0	1	0
Ecuador	1	1	0	0
Gabon	1	0	1	0
India	6	0	0	6
Kyrgyz Republic	1	1	0	0
Lao PDR	10	0	10	0
Malaysia	1	1	0	0
Mali	1	0	1	0
Mauritania	1	0	1	0
Mexico	2	2	0	0
Mozambique	1	1	0	0
Niger	1	0	1	0
Panama	1	0	1	0
Paraguay	4	0	4	0
Philippines	3	3	0	0
Poland	1	0	0	1
Romania	1	1	0	0
Russia	15	13	2	0
Rwanda	1	0	1	0
South Africa	14	0	0	14
Togo	1	0	1	0
Tunisia	1	0	1	0
Uganda	1	0	1	0
Uruguay	1	0	1	0
Total	144	54	53	37

2.3 Design

Using the utilities identified from IBNET, regression models were designed using an ordinary least squares (OLS) approach. The purpose was to determine the impact of water production, nonrevenue water, and unit cost to drinking water coverage. Regression analysis will measure the strength of the relationship between an ownership model's performance in water coverage. The first independent variable, water production, provides insight into the production side of drinking water coverage. Water production is measured by liters per person per day and expresses the total annual water produced and supplied by the utility to the distribution system. Tracking and measuring this indicator will show which management models produce higher level of water and if there is an identifiable relationship between water coverage and water production.

The second independent variable, non-revenue water, will test the amount of wasted water produced by sample utilities. Non-revenue calculates the difference in water produced and water sold in order to establish how much water is lost within the distribution network before it reaches the consumer. An analysis of water lost can provide insights into the health of a distribution system. Noted earlier, a criticism of publicly-owned regime water utilities is its failure to curb waste because it is treated as a common good, whereas privatization gives water an economic value that discourages waste. Regression analysis tests the relationship between an ownership model's performance in non-revenue water and water coverage to evaluate this issue of wasting water.

The final independent variable, unit operational cost, measured the health of a utilities infrastructure. Unit operational cost takes the total operational expenses of water utilities (including staffing, infrastructure, and maintenance) and divides them by the annual volume sold to show a bottom line assessment of the mix of resources used to achieve the outputs required. This variable shows how much it costs to provide water to consumers. Lower costs could indicate a better performing water delivery system coupled with cost effective management and staffing. Regression analysis tests an ownership model's performances in unit operational cost and water coverage.

Water coverage as the dependent variable is defined as the percentage of population with coverage to water services as a percentage of the total population under utility's nominal responsibility. There are several reasons for using water coverage as a dependent variable. First, it measures the percentage of the population within the specific utility's service district that has coverage to drinking water services, including both household connections and public access water points. This makes it the best indicator of water coverage to compare across the three regimes. Second, the dependent variable of water coverage provides insight in a nation state's conception of development and its implementation through infrastructure policies. The United Nations Development Report 3, "Water in a Changing World" emphasizes how a lack of sustainable water coverage could inhibit development. Finally, water coverage as a dependent variable, unlike the three independent variables, measures distribution and not production or delivery. The three independent variables are typically used for benchmarking effectiveness and efficiency. Table 4 provides the definition of the variables used in the regression model.

Table 4. Variables for the Ordinary Least Square Regression Model

Variables	Definition
Water Coverage (y)	Percentage of the total population under utility's nominal responsibility with coverage to water services.
Water Production (x1)	Liters/person/day; Total annual water sold expressed by population served per day.
Non-Revenue Water (x2)	Difference between water supplied and water sold expressed as a percentage of net water supplied. Reflects waste and/or seepage.
Unit Operational Cost (x3)	Annual water service operational expenses/Total annual volume sold.

In sum, several predictions are made comparing the different water regime types. For instance, decentralized water systems are expected to have the most positive impacts on water allocation, infrastructure improvement and waste reduction. Non-revenue water, water production, and unit operational cost should be equal or better to privatization levels and water coverage should be equal or better to publicly managed utilities. For the privately-owned regime, utilities should perform well in non-revenue water, unit operational cost, and water production. Thus, this regime should have comparatively lower levels of non-revenue water and operational

costs while maintaining higher levels of water production. Finally, the publicly-owned regime, compared to the other two regimes, should have less infrastructure investment and higher levels of waste, and a poorer performance in water allocation. Thus, a lower level of water coverage is expected for this regime coupled with higher levels of operational cost and non-revenue water, and lower levels of water production.

To ensure the three variables used in the model to predict water coverage were independent and not overlapping in definition with each other, a multicollinearity test was run to explore possible linkages between the three independent variables- water production, non-revenue water, and unit operational cost. A weak inverse correlation of multicollinearity was found between water production and non-revenue water (Pearson's $r = -.40$; $\text{sig} = .00$). A possible explanation of this is that water production involves water moving through a utility's infrastructure. Non-revenue water measures water leaking out of a utility's infrastructure. There was no multicollinearity detected between water production and unit operational cost (Pearson's $r = -.15$; $\text{sig} = .08$). Additionally, there was no multicollinearity detected between non-revenue water and unit operational cost (Pearson's $r = -.11$; $\text{sig} = .19$). These results demonstrated the independence of these three variables with only minor multicollinearity between water production and non-revenue water which is not expected to have any impact on the regression models (Table 5).

Table 5. Regression Model Results for Privately-Owned Regime

N=144	Water Production	Non-revenue Water	Unit Operational Cost
Water Production	1	.40**	-0.15
Non-Revenue Water	0.40**	1	.11
Unit Operational Cost	-0.15	.11	1

Note* $p < 0.05$.

3. Results

OLS regression models were used to identify statistical relationships between the water coverage of water utilities (categorized as publicly-owned, privately-owned, or decentralized) and three independent variables that measure a utility's efficiency. To test the assumption that regime models impact water coverage through efficiency, regression analysis would need to establish a relationship between at least one ownership model's (private, public, or decentralized) water coverage and all three independent variables (water production, non-revenue water, and unit operational cost). The prediction included that all three regime models should show relationships between water coverage and the three independent variables.

3.1 Privately-Owned Water Utilities Regime and Impact to Water Coverage

Multiple regression analysis of privately-own regimes for water utilities was used to investigate effects of water production, non-revenue water, and unit operational cost on water coverage showed a weak and significant relationship (adjusted $R^2 = .308$, $F = 8.857$, $p < .05$). The hypothesis that there would be a significant relationship between increased water coverage from increased water production, decreased non-revenue water, and decreased unit operational cost for the privately-owned regime was partially upheld. Further analysis showed an inverse relationship between water coverage and non-revenue water (standardized $\beta = -.684$, $p = .00$) as predicted. There was no significant relationship for water production (standardized $\beta = .267$, $p = .06$) and unit operational cost (standardized $\beta = -.083$, $p = .47$) with water coverage. Thus, for the privately-owned regime, the predictor of increased water coverage was decrease of non-revenue water with the other variables not being significant (Table 6).

Table 6. Regression Model Results for Privately-Owned Regime

	Standardized Beta	Sig.
Water Production	.267	.06
Non-Revenue Water	-.684	.00
Unit operational cost	-.083	.47
(N=54)		

Adjusted $R^2 = 0.308$, $F \text{ Stat} = 8.857$, $p < 0.05$.

3.2 Publicly-Owned Utilities Regime and Impact to Water Coverage

Multiple regression analysis of public water utilities investigated effect of water production, non-revenue water, and unit operational cost on water coverage showed a weak and significant (adjusted $R^2 = .113$, $F=3.201$, $p<.05$). The hypothesis for the publicly-owned regime was that there would be a significant relationship between increased water coverage from water increased production, increased non-revenue water, and increased unit operational cost. This hypothesis was not upheld and yielded results that were not predicted. Analysis showed an inverse relationship between water coverage and non-revenue water (standardized $\beta = -.481$, $p=.01$). Meaning that as non-revenue water increased, water coverage decreased. There was no significant effect on water production (standardized $\beta = .113$, $p=.46$) or unit operational cost (standardized $\beta = -.249$, $p=.10$) on water coverage. Thus, for the publicly-owned regime, the hypothesis was not upheld for the variables of water production and unit operation cost, and the relationship predicted for non-revenue water was in the inverse direction than predicted. The results indicate that for publicly-owned regimes, decreased non-revenue water leads to increased water coverage (Table 7).

Table 7. Regression Model Results for Publicly-Owned Regime

	Standardized Beta (N=53)	Sig.
Water Production	.113	.46
Non-Revenue Water	-.481	.01
Unit operational cost	.249	.10

(N=53)

Adjusted $R^2=.113$, F Stat= 3.201, $p < 0.05$.

3.3 Decentralized Regime: Decentralized Water Utility and Impact to Water Coverage

Multiple regression analysis of decentralized water utilities was used to investigate the effect of water production, non-revenue water, and unit operational cost on water coverage (adjusted $R^2=.094$, $F=2.245$, $p<.05$). The model showed overall very weak results. For this regime, it was hypothesized that there would be a significant relationship between increased water coverage and decreased water production, decreased non-revenue water, and decreased unit operational cost which was not upheld. In fact, the analysis showed significant effect of increased unit operational cost (standardized $\beta = .383$, $p=.03$) in increased water coverage which was not predicted. There was no significant effect of water production (standardized $\beta = .288$, $p=.09$) and non-revenue water (standardized $\beta = .086$, $p=.60$) on water coverage. For the decentralized water regime, this was the weakest model, and the relationship between increased non-revenue water and increased water coverage was not expected (Table 7).

Table 7. Regression Model Results for Decentralized Regime

	Standardized (N=37)	Beta	Sig.
Water Production	.288		.09
Non-revenue Water	.086		.60
Unit operational cost	.383		.03

Adjusted $R^2=.094$, F Stat= 2.245, $p < 0.05$.

4. Discussion

The implications for this research can help guide the discussion on which regime type is best suited for providing water coverage in the most efficient manner. While there are support for all three regimes in the literature, the results show that one particular regime type did not demonstrate superiority over the others. However, some findings did give some important information when considering different regime types. For publicly- and privately-owned water regimes, decreasing non-revenue water by plugging leaks and improving infrastructure can translate into higher rates of water coverage. For decentralized water regimes, higher levels of unit

operational cost can increase water coverage. The regression analyses also showed that broad claims about regime ownership, efficiency, and improved water coverage should be suspect. Not one regime model established a significant relationship between water coverage and all three independent variables. Also, the models were not able to explain much of the variation of water coverage for the publicly-owned or decentralized regimes. According to Budds (2003), water coverage is not some inherent contradiction between private profits and the public good, because neither publicly- nor privately-owned utilities are well suited to serving the majority of low-income households with inadequate water and sanitation, and because many of the barriers to service provision in poor settlements can persist whether water and sanitation utilities are publicly- or privately-operated. This is not to say that well-governed localities should not choose to involve private companies in water and sanitation provision, but it does imply that there is no justification for international agencies and agreements to actively promote greater private sector participation on the grounds that it can significantly reduce deficiencies in water and sanitation services in the South. Future research into water coverage modeling in terms of variables that would include sociopolitical aspects of countries where the regimes are located which may yield stronger results in the decentralized and publicly-owned regimes.

Acknowledgements

A special note of acknowledgement to Dr. Kaveh Ehsani, DePaul University for working with the authors on the development of the manuscript.

References

- Baietti, A., Kingon, W., & van Ginneken, M. (2006). *Characteristics of Well-Performing Public Water Utilities*. World Bank Group. Water Supply and Sanitation Sector Board of the Infrastructure Network Note no. 9.
- Bakker, K. (2007). The 'Commons' Versus the 'Commodity': Alter-Globalization, Anti-Privatization and the Human Right to Water in the Global South. *Antipode*, 39(3), 430-455. <http://dx.doi.org/10.1111/j.1467-8330.2007.00534.x>
- Bakker, K. (2010). *Privatizing Water: Governance Failure and the World's Urban Water Crisis*. Ithaca: Cornell University Press.
- Budds, J. (2003). Are the Debates on Water Privatization Missing the Point? Experiences from Africa, Asia and Latin America. *Environment & Urbanization*, 15(2), 87-114. <http://dx.doi.org/10.1177/095624780301500222>
- Dickson, E. (2006). *Management Models of Water and Sanitation: Approaches to Decentralization in Honduras*. Canada: International Development Research Centre.
- Gleick, P. W., & Reyes, R. (2002). *The New Economy of Water: The Risks and Benefits of Globalization and Privatization of Fresh Water*. Oakland: Pacific Institute.
- Hall, D., & Lobina, E. (2012). *Water Companies and Trends in Europe 2012*. Greenwich, UK: Public Services International Research Unit.
- Hall, D., Lobina, E., & de la Motte, R. (2005). Public Resistance to Privatization in Water and Energy. *Development in Practice*, 15(3 and 4), 286-281. <http://dx.doi.org/10.1080/09614520500076126>
- Herrera, V., & Post, A. (2014). Can Developing Countries both Decentralize and Depoliticize Urban Water Services? Evaluating the Legacy of the 1990s Reform Wave. *World Development*, 64, 621-641. <http://dx.doi.org/10.1016/j.worlddev.2014.06.026>
- International Benchmarking Network for Water and Sanitation Utilities. (2015). *IBNET Database*. Retrieved from <https://www.ib-net.org/>
- Lobina, E. (2015). In S. Kishimoto, E. Lobina, & O. Petitjean (Eds.), *Our Public Water Future: The Global Experience with Remunicipalization* (pp. 6-18). Paris: Transnational Institute.
- Patsiaouras, G., Saren, M., & Fitchett, J. (2014). The Marketplace of Life? An Exploratory Study of the Commercialization of Water Resources through the Lens of Macromarketing. *Journal of Macromarketing*, 35(1), 23-35. <http://dx.doi.org/10.1177/0276146714538454>
- Pierce, G. (2014). Beyond the Strategic Retreat? Explaining Urban Water Privatization's Sallow Expansion in Low- and Middle-income Countries. *Journal of Planning Literature*, 30(2), 119-131. <http://dx.doi.org/10.1177/0276146714538454>
- Renzett, S., & Dupont, D. (2003). Ownership and Performance of Water Utilities. *Greener Management International*, 42(1), 9-19. <http://dx.doi.org/10.9774/GLEAF.3062.2003.su.00004>

- Ribot, J. (2002). *Democratic Decentralization of Natural Resources: Institutionalizing Popular Participation*. World Resources Institute.
- Ruiz-Mier, F., & Ginneken, v. M. (2006). *Consumer Cooperative: An Alternative Institutional Model for Delivery of Urban Water Supply and Sanitation Services?* Washington, DC: World Bank Water Supply and Sanitation Sector Board.
- Schiffler, M. (2015). *Water, Politics and Money" A Reality Check on Privatization*. Switzerland: Springer International Publishing. <http://dx.doi.org/10.1007/978-3-319-16691-9>
- Segerfeldt, F. (2005). *Water for Sake: How Business and the Market Can Resolve the World's Water Crisis*. Washington, DC: Cato Institute.
- The World Bank. (2009). Public Private Infrastructure Advisory Facility. "PPI Glossary - Private Infrastructure Projects - The World Bank & PPIAF." http://ppi.worldbank.org/resources/ppi_glossary.aspx
- United Nations Educational, Scientific, and Cultural Organization. (2009) World Water Development Report 3. Retrieved from http://webworld.unesco.org/water/wwap/wwdr/wwdr3/pdf/WWDR3_Water_in_a_Changing_World.pdf
- United Nations Educational, Scientific, and Cultural Organization. (2015). *United Nations World Water Day 2013*. International Year of Water Cooperation Facts and Figures. Retrieved from <http://www.unwater.org/water-cooperation-2013/water-cooperation/facts-and-figures/en/>
- World Health Organization. (2015). *Drinking Water Fact sheet no. 391*. Media Centre. Retrieved from <http://www.who.int/mediacentre/factsheets/fs391/en/>
- Zamzami, I., & Ardhianie, N. (2015). An end to the Struggle? Jakarta Residents Reclaim their Water System. In S. Kishimoto, E. Lobina, & O. Petitjean (Eds.), *Our Public Water Future: The Global Experience with Remunicipalization* (pp. 40-49). Paris: Transnational Institute.

Copyrights

Copyright for this article is retained by the author(s) with first publication rights granted to the journal.

This is an open-access article distributed under the terms and conditions of the Creative Commons Attribution license (<http://creativecommons.org/licenses/by/3.0/>).

Reviewer Acknowledgements

Environment and Natural Resources Research wishes to acknowledge the following individuals for their assistance with peer review of manuscripts for this issue. Their help and contributions in maintaining the quality of the journal is greatly appreciated.

Environment and Natural Resources Research is recruiting reviewers for the journal. If you are interested in becoming a reviewer, we welcome you to join us. Please find the application form and details at <http://www.ccsenet.org/reviewer> and e-mail the completed application form to enrr@ccsenet.org.

Reviewers for Volume 6, Number 2

Andrew Lo, Chinese Culture University, Taiwan
Debjani Sihi, University of Maryland Center for Environmental Science, USA
Robert Perry, University of Texas-Permian Basin, USA
Yi-Shiang Shiu, Feng Chia University, Taiwan
Hesham G. Ibrahim, Al-Asmarya Islamic University, Libya
Hongzhi Ma, The University of Toledo, USA
João Fernandes, National Laboratory for Civil Engineering, Portugal
Lesley Lubos, Liceo de Cagayan University, Philippines
Mohammad Valipour, Payame Noor University, Iran
Murat Eyvaz, Gebze Institute of Technology, Turkey
Shiro Horiuchi, Shibaura Institute of Technology, Japan
Srđan Kostić, University of Belgrade, Serbia
Vasilis Louca, University of Aberdeen, United Kingdom
Venkataswarup Tiriveedhi, Washington Univesrity School of Medicine in St. Louis, United States
Vikram Kapoor, US Environmental Protection Agency, USA

Call for Manuscripts

Environment and Natural Resources Research is an international, double-blind peer-reviewed, open-access journal. *ENRR* is published by the Canadian Center of Science and Education in both print and online versions. *ENRR* is striving to provide the best platform for researchers and scholars worldwide to exchange their latest findings. The scopes of the journal include, but are not limited to, the following topics: environmental assessment and management, environmental health and education, environmental science and engineering, environmental protection, ecological environment, planning and environmental design, urban and regional landscape design, environment and sustainable development, natural resources use and recycle.

We are seeking submissions for forthcoming issues. All manuscripts should be written in English. Manuscripts from 3000-8000 words in length are preferred. All manuscripts should be prepared in MS-Word format, and submitted online, or sent to: enrr@ccsenet.org

Paper Selection and Publishing Process

- a) Upon receipt of a submission, the editor sends an e-mail of confirmation to the submission's author within one to three working days. If you fail to receive this confirmation, your submission e-mail may have been missed.
- b) Peer review. We use a double-blind system for peer review; both reviewers' and authors' identities remain anonymous. The paper will be reviewed by at least two experts: one editorial staff member and at least one external reviewer. The review process may take two to three weeks.
- c) Notification of the result of review by e-mail.
- d) If the submission is accepted, the authors revise paper and pay the publication fee.
- e) After publication, the corresponding author will receive two hard copies of the journal, free of charge. If you want to keep more copies, please contact the editor before making an order.
- f) A PDF version of the journal is available for download on the journal's website, free of charge.

Requirements and Copyrights

Submission of an article implies that the work described has not been published previously (except in the form of an abstract or as part of a published lecture or academic thesis), that it is not under consideration for publication elsewhere, that its publication is approved by all authors and tacitly or explicitly by the authorities responsible where the work was carried out, and that, if accepted, the article will not be published elsewhere in the same form, in English or in any other language, without the written consent of the publisher. The editors reserve the right to edit or otherwise alter all contributions, but authors will receive proofs for approval before publication.

Copyrights for articles are retained by the authors, with first publication rights granted to the journal. The journal/publisher is not responsible for subsequent uses of the work. It is the author's responsibility to bring an infringement action if so desired by the author.

More Information

E-mail: enrr@ccsenet.org

Website: www.ccsenet.org/enrr

Paper Submission Guide: www.ccsenet.org/submission

Recruitment for Reviewers: www.ccsenet.org/reviewer

The journal is peer-reviewed
The journal is open-access to the full text
The journal is included in:

AGRICOLA
CAB Abstracts
EBSCOhost
Google Scholar
LOCKSS
NewJour (Georgetown University Library)
PKP Open Archives Havester
ProQuest
SHERPA/RoMEO
Ulrich's

Environment and Natural Resources Research Quarterly

Publisher Canadian Center of Science and Education
Address 1120 Finch Avenue West, Suite 701-309, Toronto, ON., M3J 3H7, Canada
Telephone 1-416-642-2606
Fax 1-416-642-2608
E-mail enrr@ccsenet.org
Website www.ccsenet.org/enrr

